REPUBLIC OF THE PHILIPPINES

DEPARTMENT OF AGRICULTURE AND NATURAL RESOURCES

BUREAU OF MINES

REPORT ON GEOLOGICAL SURVEY OF EASTERN MINDANAO

PHASE II

GEOLOGICAL, GEOCHEMICAL AND GEOPHYSICAL SURVEYS

SEP. 1973

METAL MINING AGENCY

OVERSEAS TECHNICAL COOPERATION AGENCY

GOVERNMENT OF JAPAN

REPUBLIC OF THE PHILIPPINES

DEPARTMENT OF AGRICULTURE AND NATURAL RESOURCES

BUREAU OF MINES

REPORT ON GEOLOGICAL SURVEY OF EASTERN MINDANAO

PHASE II

GEOLOGICAL, GEOCHEMICAL AND GEOPHYSICAL SURVEYS

SEP. 1973

METAL MINING AGENCY

OVERSEAS TECHNICAL COOPERATION AGENCY

GOVERNMENT OF JAPAN

PREFACE

The Government of Japan, in response to a request by the Government of the Republic of the Philippines, decided to investigate the potential of mineral resources in Eastern Mindanao of the Philippines, and entrusted the survey works to the Overseas Technical Cooperation Agency. The Agency, considering the importance of technical nature of the survey work, in turn sought the cooperation of the Metal Mining Agency of Japan (MMAJ) to accomplish the task.

The survey works are expected to be carried out over a period of three years, beginning in 1972. MMAJ organized a 29-man survey team headed by Mr. Hiroshi Fuchimoto, Staff of the Overseas Technical Cooperation Agency, and sent to the Philippines from January 17 to April 19, 1973. During this period, the team, with the help of the Government of the Republic of the Philippines and its various agencies, was able to complete survey work on scheduled for the current year.

This report summarizes the results of the survey, and will form a portion of the final survey reports that will be prepared with regard to the results obtained in 1972 and 1974.

Finally, I wish to take this opportunity to express my heartfelt gratitude to the officials of the Government of the Philippines for their wholehearted cooperation and support extended to the Japanese survey team.

September, 1973

Keiichi Tatsuke,
Director General,
Overseas Technical Cooperation Agency

Fig. 1 Location map of the Survey area

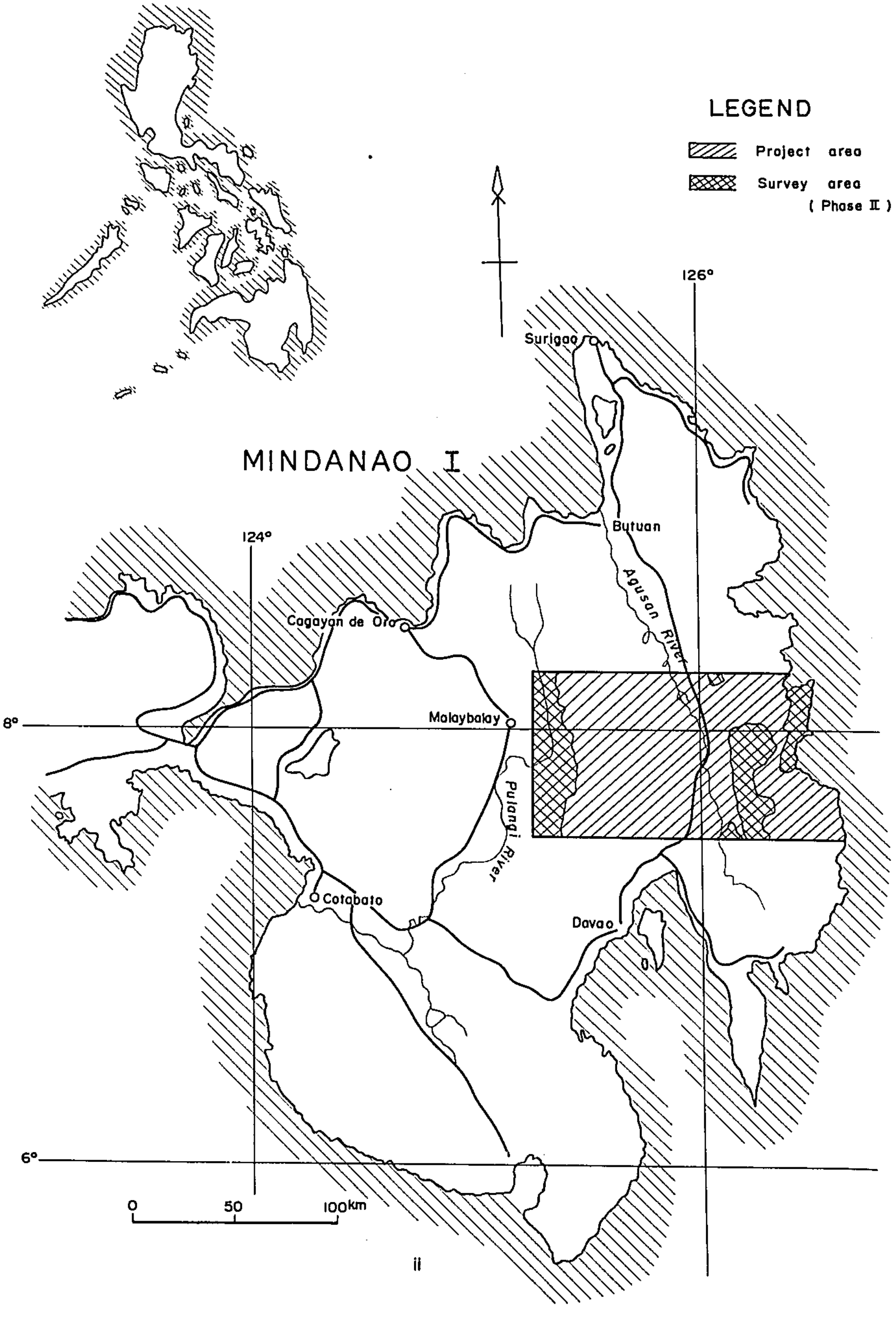

CONTENTS

PART II GEOCHEMICAL SURVEY

PART III GEOPHYSICAL SURVEY

LIST OF ILLUSTRATIONS

LIST OF TABLES

LIST OF APPENDICES

ABSTRACT

In the second Phase of the survey of eastern Mindanao, Philippines, the detailed geological, geochemical and geophysical surveys were carried out over an area of about 3,000 Km^2 selected by the Phase I survey as having high potential for mineral resources.

In the Eastern Area, geological survey disclosed the geological structures of basaltic and andesitic groups, and there was found mineralization associated with quanzdioritic rocks in the basaltic group. The mineral assemblage of the mineralization shows zonal distribution of porphyry copper type deposits, i. e., from the outside, copper-molybdenum zone, copper-hematite zone and lead-zinc zone. In the south of these zones, barite ore deposits which appear to be a sedimentary type have been recognized.

Cold-extraction analysis which was used as field spot test uncovered the same anomalous copper concentrates so that geophysical survey (IP method) was carried out on the northern half of the zoning area.

In the Western Area, the Cretaceous rocks as referred to in the Report of Phase I was divided into two groups, i.e., basaltic and andesitic volcanics and their geological structures became clear. It was proved that overlying andesitic volcanics were formed during Tertiary time.

As copper mineralization associated with diorite was found in the Tagbiga Area, geophysical survey (IP method) was conducted over the area selected by geochemical survey.

In the mineralized zone, the geophysical anomalies coincide well with the

geochemical anomalies. Further, from the geological point of view, both zones appear to be excellent indications for ore deposits. It is, therefore, desirable to carry out the follow-up work such as geological and geophysical surveys and diamond drilling for defining the ore scale and occurrence. Judging from all the results obtained, however, further surveys of the Bislig area is considered more important than that of the Tagbiga area.

GENERAL INFORMATION

1. Introduction

1-1 Purpose of Survey

The purpose of survey for the Phase II was to investigate the promising places and to make a geological map for the area of about 3,000 Km^2 selected by the Phase I survey as having high potential for mineral resources. For this purpose, the detailed geological, geochemical and geophysical surveys were carried out systematically.

1-2 Outline of Survey

There were two areas to be surveyed in Phase II; one was in the eastern area of about 1,600 Km^2 composed of volcanic rocks which is distributed in the east side area of the Philippine Fault zone, and another was in the western area of about 1,400 Km^2 composed chiefly of pyroclastic rocks which is distributed in the west side of the Pantaron Ranges dividing Davao and Bukidnon Provinces. As there had been no direct roads between these two areas, and furthermore it took more than one whole day to get from the area to the another even by plane, two base camps were set up, that is, Bislig for the east and Halapitan for the west.

It was not so easy to use helicopters as in Phase I, therefore the other means such as telegraphs, light planes and the regular air-survices were used for communications between both areas.

For geological and geochemical surveys, eight parties were organized and three of them were assigned to the Eastern Area and four parties to the Western Area. To compare both areas gelogically, the remaining party surveyed the West in twenty days and the East in ten days.

Each party consisted of one Philippino and two Japanese geologists, however, one more Philippino geologist was assigned to the detailed survey area where the mineralized zone had been found.

During the field work, it was rainy season and it rained everyday in the Eastern Area, but in the Western Area it was dry season and furthermore the public peace had been improved. Therefore the survey was carried out more smoothly than the writers had expected.

After the geological parties had defined the mineralized zones, the geophysical parties started their field work in both areas and clarified their extension by Induced Polarization method. Two geophysical parties were organized from seven members; 2 Philippino and 5 Japanese geophysists, and one party was assigned to each area.

The period of stay in the Philippines, the total length of the survey routes and the number of geochemical samples are as follows:

Table 1 Period of survey, length of survey route and number of geochemical samples

Geological team

	Stay in Philippines	Actual field work	Length of survey route	Number of samples
Eastern Area	Jan. 17 ~ Apr. 5	Feb. 10 ~ Mar. 18	510 km	3,028 pcs
Western Area	79 days	37 days	470 km	2,728 pcs
Total			980 km	5,756 pcs

Geophysical team

Eastern Area	Mar. 7 ~ Apr. 19	Mar. 10 ~ Apr. 13	18.4 km	
Western Area	44 days	35 days	16.7 km	
Total			35.1 km	

The writers are indebted to Professor Yoshio Ueda, Tohoku University on chronologizing the intrusive rocks, and Dr. Kuniteru Matsumaru of Saitama University, Dr. Kenji Kurihara of Tokyo University of Education and Dr. Hiroo Natori of Geological Survey of Japan on identifying of fossils. The writers would like to express their gratitude to these people.

All the geological data, half the rock specimens and the geochemical samples obtained by the Phase II survey have been submitted to the Philippines Bureau of Mines as well as the Phase I.

1-3 List of Members

The list of members engaged in the survey is as follows.

JUAN E. PILAC	Bureau of Mines Philippines	HIROSHI FUCHIMOTO	Overseas Technical Cooperation Agency of Japan
MAXIMO V. GARCIA	do	KYOICHI KOYAMA	Metal Mining Agency of Japan
		MAGOICHI ADACHI	do
		KAICHIRO SHIMIZU	O.T.C.A.
(Geological team)			
WENCESLAO ARGAÑO	B.O.M.	TERUYUKI TAKEDA	O.T.C.A.
NALCISO BAUTISTA	do	HARUHIKO HIRAYAMA	do
IRENEO OSCILLADA	do	YASUKICHI UEKI	do
ALBERTO ISSAC Jr.	do	YOSHINOBU WATAYA	do
DONNO CUSTODIO	do	KATSUO ARAI	do
EMIL T. AVILA, Jr.	do	TAKEOMI MIYOSHI	do
BEN ALEGADO	do	TAKASHI KATANO	do

MARIO TORRES	B.O.M.	RYOICHI SUZUKI	O.T.C.A.
TAMMY DESTACAMENTO	do	SHUSUI URAI	do
		TATSUO NIIMURA	do
		IKUHIRO HAYASHI	do
		TOKICHIRO TANI	do
		KEIJI NAKANO	do
		HIDETOSHI TAKAOKA	do
		NORIO NAGASAKI	do

(Geophysical team)

CESAR V. RAMOS	B.O.M.	ASAHI HATTORI	O.T.C.A.
MARCELINO APELO	do	ITSURO OGAWA	do
CAROL S. SAMONTE	do	OSAMU KUSAKA	do
BENERCITO BALLESTEROS	do	KATSUMI OYANAGI	do
ELIGIO ARIATE	do	HITOSHI ITO	do
		TOSHIAKI FUJIMOTO	do
		TOMIO TANAKA	do
		NAOYOSHI TAKAHASHI	do
		JUNICHI SATO	do
		SABURO TACHIKAWA	do

1-4 Reference

The references cited in this Report are almost same as those of the Report of Phase I, so that they are omitted.

2. General Discussion

Through the Phase II survey, many problems on geological, geochemical and geophysical surveys have remained, but in this chapter, only the problems on the detailed survey areas being projected in the Phase III are generally discussed.

2-1 Bislig Area

The mineralized zone found in the upper reaches of the Taon River is porphyry copper type mineralization associated with quartz diorite in the basalt group, and shows the zonal distribution of ore mineral peculiar to this type of mineralization. The detailed survey was carried out on the northern half of zoning area.

The width of quartz diorite is 800 m in the area and extends in NE direction. On the eastern side, about 400 m distant from this diorite, a diorite porphyry dike, 50 m in width, runs in same direction.

As shown in Fig. 2, geochemically anomalous zones of copper and molybdenum occur remarkably in the basalt area between the diorite and porphyry, and correspond to IP anomaly. On the grand surface of this zone nearby the intersection of the base line with line No. 9 of geophysical survey, a small exposure of quartz diorite, several meters in width, can be seen in the river. The diorite seems to be a small scale stock and a little amount of filmy or impregnated chalcopyrite and pyrite with molybdenite is recognized along the joint trending N-S. The average contents of metals present Cu 0. 15%; Mo 0. 05%, but Cu 3. 1% in part.

Rock exposure is very limited that no other mineralized zone can be seen.

1. The distribution of frequency effect values detected by IP survey is fit for porphyry copper deposits.

Fig. 2 Compilation map of detailed survey results, Bislig Area

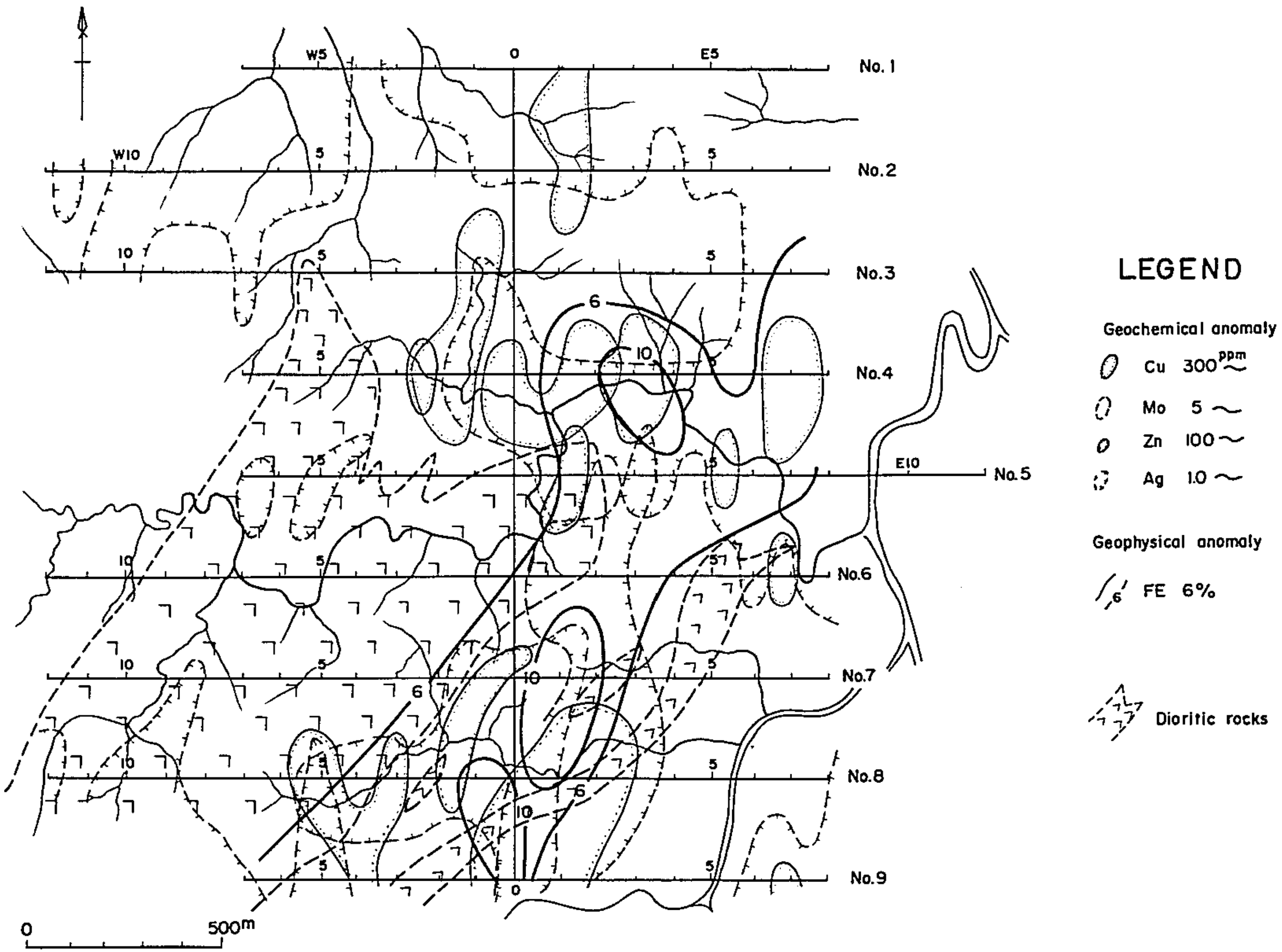

2. Between the quartz diorite and the quartz porphyry, there are some small scale dykes of 20 – 30 m in width, therefore many fissures are well developed in this zone.

From the reasons above, it can be expected that mineralization will increase at depths, though the copper content in soil is rather weak. So diamond drilling is necessary for this zone as having the highest potential for mineral resources in the detailed survey area.

Zinc anomaly extending from line No. 3 to line No. 4 on the western side of the base line of geophysical survey, should be further investigated because quartz diorite is exposed on the riverbed.

The zinc anomaly appears to be concentrated on the low land of the river but the IP anomaly does not appear, it is considered that the zinc anomaly had migrated from other places.

Furthermore, in the tributaries, running to the east nearly in the middle of the detailed survey area, and flowing into Taon River nearby the eastern end of line No. 6, joints are developed between points Nos. W2 and No. 3, and the impregnation of chalcopyrite and pyrite is found. The copper content is 0.26 – 0.37% here, but geochemical and geophysical anomalies have not been found. This fact might be due to the very small scale mineralization.

Between lines Nos. 2 and 3, many boulders of gossan composed mainly of hematite and pyrite are widely distributed on the ridge trending E–W and on its mountainside. Some gossan show more than 4.0% of copper content but geochemical and geophysical anomalies are not found. It seems to be caused by leaching and further study is desirable.

2-2 Tagbiga Area

The mineralized zone in the upper reaches of the Tagbiga River is copper deposits associated with diorite intruding mudstone and tuff of Miocene age. In the composite body consisting of pyroxenite and diorite near the western contact with sodimentary rocks mentioned above, lenticular or vein-type massive ores are found in some places. The ore consists of chalcopyrite and pyrite, and its good portion shows over 18% of Cu, but the veins are narrow and don't continue for long distances.

Geochemical anomaly by stream sediment and soil survey was found in this zone and pyritization was stronger than that of other places, so IP geophysical survey was carried out.

The results of interpretation are shown in Fig. 3. As is evident from the figure, geochemical anomalies of copper, zinc, nickel and cobalt are overlapping along the western margin of the composite body and the IP anomaly is distributed nearly corresponding to the geochemical anomalies.

It appears that diorite fills the brecciated part of pyroxenite in the composite body. Consequently, geophysical results are affected by magnetite in pyroxenite. But from the geological and geochemical points of view, IP anomaly suggests the mineralized zone of vein-type continues towards depths.

Besides, the other IP anomalous zone is found in the eastern part of the zone stated above, and shows wide and deep distribution. From the scale of anomaly, this is more interesting than that in the composite body.

This anomalous zone is in pyroxenite on the ground surface but diorite stocks are exposed nearby. Moreover, the copper anomaly coincides with IP anomaly and extends towards the NE direction. Therefore, porphyry copper deposits can be expected. The follow-up work is desirable.

Fig. 3 Compilation map of detailed survey results, Tagbiga Area

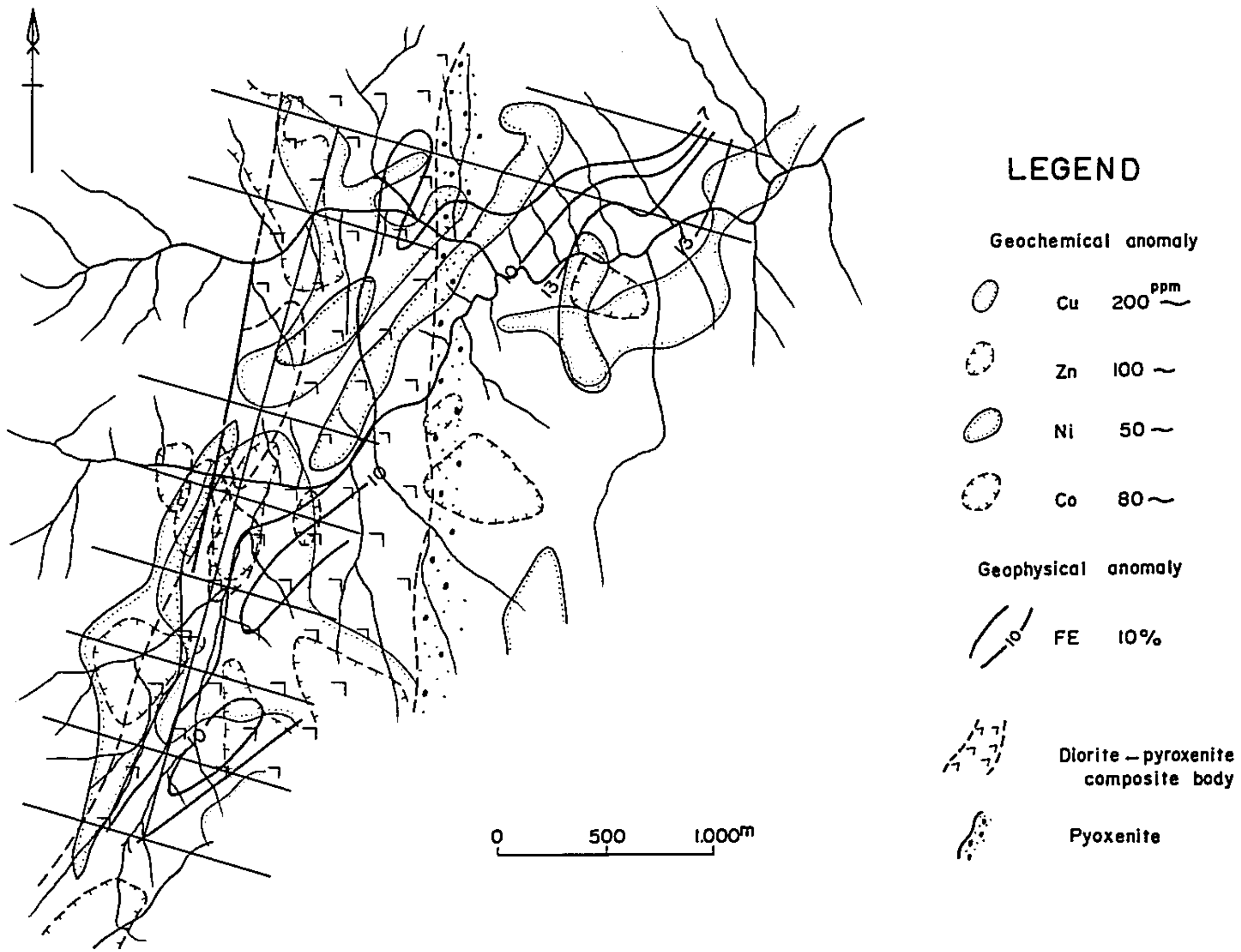

3. Conclusions and Future Problems

The detailed geological, geochemical and geophysical surveys were carried out on the area which was selected by the Phase I survey as having high potential for mineral resources.

The conclusions reached from the systematic studies based on these surveys are as follows:

1. In the Eastern Area composed chiefly of basaltic rocks, it was discovered that quartz diorite stock has intruded along the anticlinal axis trending northeast. The mineralization of copper, lead, zinc and molybdenum associated with the stock shows a typical zonal distribution of porphyry copper deposits. From geological evidence, the intruding time of quartz diorite appears to be middel or late Miocene.

2. Det ailed survey on the northern half of mineralized zone showed that the geochemical anomalous zone on the eastern rim of the stock coincided with the geophysical anomalous zone, indicating the existance of porphyry copper deposits there. As both anomalous zones trend to extend toward the south, the follow-up work will be desirable. For this purpose, several methods such as geological and geophysical surveys and diamond drilling should be used for this area.

3. East side area of the Philippine Fault zone composed mainly of andesitic rocks were divided into five formations by the difference of volcanic activities, and geological structure of the formations were also elucidated. A larg scale altered zone with weak geochemical zinc anomaly stretching in NS direction was found along the upstream of the Bahayan River. Consequently, it will be desirable to carry out the follow-up program later on.

4. In the Western Area, the volcanic rocks referred to as Cretaceous rocks in the Phase I report can be divided into two groups — basaltic and andesitic. It is found that a large amount of volcanic rocks in the andesite group distributed on the other group had been formed in Oligocene to middle Miocene time. Many rock fragments of schists considered to be basement rocks are found in the conglomerate and sandstone of andesitic group. In the uplifted zone intruded by large scale periodolite, therefore, the depth of basement is more shallow than the writers had expected.

5. Vein or lens type copper mineralization associated with diorite is discovered in the West Tagbiga Area. Geophysical anomalies corresponding to geochemical anomalies are likewise recognized there. In addition, there are more promising indications in the northeast of these anomalies so that the follow-up work will be necessary. But in respect to exploration to be carried out, the Bislig Area in the east will be synthetically more important than the Tagbiga Area in the west.

6. Geochemical survey using spot test, i.e. rubeanic acid method, in the field has proved effective for defining a copper mineralized zone. However, there has been some slight difference between the anomalous zone as shown by spot test and that under atomic absorbtion method. The difference might have been caused by chemical decomposition of the sample, which could mean, in other word, the spot test showing cold extractable copper and the other, total copper. So that in seeking promising areas by geochemical field test, the fusion method such as biquinoline method capable of determining copper content quantitatively is probably better than spot test.

7. It has been proved that the use of application of IP method is most effective to approximate the horizontal and vertical distribution of mineralized zones. So

that IP method is recommended in the case of conducting further survey to determine the extension of anomalous zones. However, it is very difficult to analize the IP results in case the rocks are accompanied by mineralization of primary sulphides or oxides. The other geophysical methods such as the self-potential and magnetic methods will make analysis easier with information on types of minerals and shapes of intrusive rocks.

PART I GEOLOGICAL SURVEY

1. General Remarks

The volcanic and normal sedimentary rocks referred to as the Cretaceous system in the Report of Phase I spread widely in the surveyed area. Since the Phase I survey was a reconnassance survey to select the area of high potentiality for mineral resources, the detailed geologic structure obscurely remained.

In the Phase II survey, therefore, a great emphasis was placed on the elucidation of the detailed geologic structure of this area and on finding out the intrusive bodies accompanied by mineralization.

Some important conclusions obtained from the survey are summarized below.

Eastern Area

1. Some quartz diorite bodies are observed in Bislig-Lingig region intruding basaltic lava flows, and a porphyry copper type mineralization associated with the bodies was disclosed.

2. The strip stretching along the Philippine Fault is chiefly composed of andesitic lava flows and is divided into some formations by sedimentary rocks intercalated within them. The geologic structure was also made clear by tracing those sedimentary rocks.

Western Area

1. The tuff previously lumped together as the Cretaceous system was roughly divided into two groups. It was proved that the upper section is formed during Oligocene to middle Miocene time.

2. The geologic structure was made clear by tracing some characterlistic sedimentary key beds.

3. A diorite body with copper mineralization was discovered.

2. Geology

The rocks in the surveyed area belong to the Cretaceous to Paleogene period. Basaltic or andesite lava flows and their pyroclastic rocks spread widely in the Eastern Area and basaltic and andesitic pyroclastic rocks in the Western Area.

In the Western Area a large sclae peridotite dyke and a diorite stock intruded into the above-mentioned volcanic rocks. The Miocene limestone and the Pliocene to Pleistocene Molasse type sedimentary rocks are also observed in the Western Area.

The names of place printed on the 1:250,000 scale topographical map were given to the formations which had been lumped together as the Cretaceous system in the Phase I.

2-1 Stratigraphy

A generalized stratigraphic section of the surveyed area is shown in the Table I-1.

The Eastern Area consists of the Barcelona group, the Kaban group, the Mangagoy formation, the Bislig formation, the Dacongbonwa formation, the Kapalong formation, the Agtuuganon formation and the Aluvium in the ascending order.

The Barcelona group composed of basaltic rocks is exposed in the hills facing the Philippine Sea.

The Kaban group consists of andesitic rocks and extends narrowly adjacent to the eastern side of the Philippine Fault. This group can be divided into five formations on the basis of their lithologic characteristics. The correct age of this group, as well as the Balcolona group, is unknown because of lack of fossils.

Table I-1. Generalized stratigraphic section in the survey area

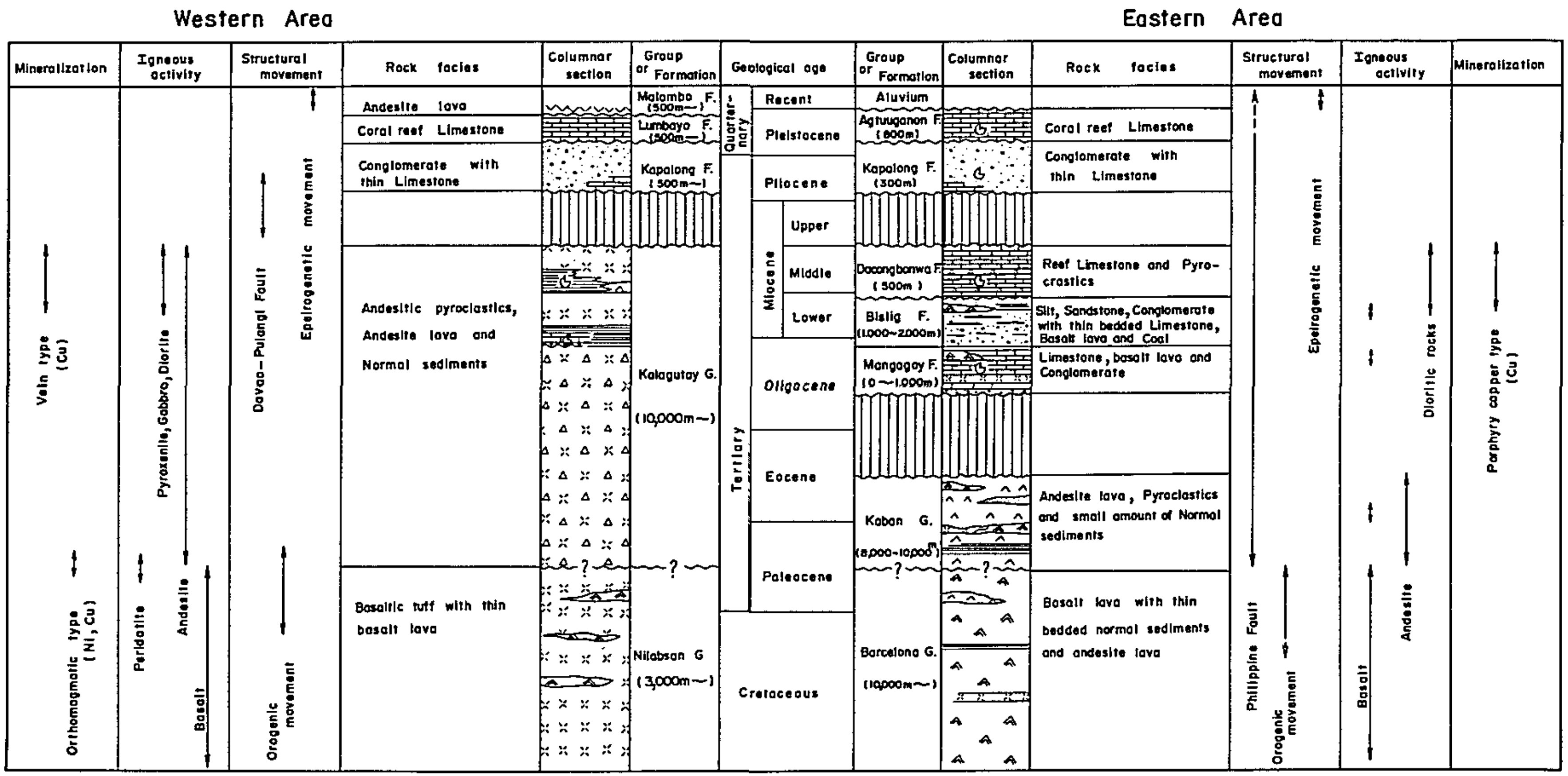

The Mangagoy formation is a sequence of conglomerate, sandstone, shale and limestone. The formation is observed from Mangagoy to Boston and unconformably overlies the Barcelona and the Kaban groups. It was formed by the marine transgression which started at the middle Oligocne epoch.

The Bislig formation overlies the Mangagoy formation conformably. It consists of shallow-sea sedimentary rocks filling up the basin between the Barcelona and the Kaban groups. Therefore, the direct relation between the two groups is not known.

The Dacongbonwa formation unconformably overlying the Bislig formation consists of the middle Miocene coral reef limestone.

The Kapalong formation composed of Molasse sediments is observed narrowly along the foot of mountains within the Philippine Fault zone. The age of this formation is upper Pliocene to Pleistocene on the basis of fossils.

The Agtuuganon formation is chiefly composed of coral reef limestone and formed in Pleistocene time.*

The Western Area consists of the Nilabsan group, the Kalagutay group, Kapalong formation, Lumbayo formation and Malanbo volcanics.

The Nilabsan group composed chiefly of basaltic pyroclastic rocks spreads in the drainage basin of the Nilabsan and Sita Rivers.

The Kalagutay group occupies the greater part of this area and covers the Nilabsan group uncomformably. This group consists chiefly of andesitic pyroclastic rocks and lavas intercalating limestone and mudstone of Oligocene to

---

*The Agtuuganon formation referred to as late Miocene in the Report of Phase I is divided into two formations. The one is the Dacongbonwa formation and the other is the Agtuuganon formation overlying the former unconformably.

middle Miocene. Nevertheless, subdivision of this group could not be accomplished at this time since the nature of the igneous activities is the same throughout the sequence.

The Kapalong formation is Molasse type sediments and spreads at the foot of mountains east of the Pilangi- Davao fault. It is locally observed also in the west side of the fault. This formation was formed in Pliocene to Pleistocene.

The Lumbayo formation composed of coral reef limestone and overlying Malambo andesite lava are attributed to the Quarternary period. Both of them are observed on the top of mountains ranging along the western rim of the surveyed area.

2-2 Eastern Area

A large amount of volcanic rocks composes the main part of this area, and the local characteristics of the volcanic activities can be recognized. Namely basaltic lava flows develop in the east coast and are intruded by dioritic bodies. In the east side area adjacent to the Philippine Fault, however, there are developed a large amount of andesitic volcanic rocks.

Pyroclastic rocks and normal sedimentary rocks are poorly observed in the two areas.

2-2-1 Barcelona Group

This group spreads along the east coast from Sanco point to San Roque through Lingig in the belt-shops of 7 to 8 Km in width and about 35 Km in length.

Basaltic lava flows and dolerite intrusives account for more than 80% of this group and andesitic lava flows, basaltic pyroclastic rocks and normal sedimentary rocks are intercalated.

The basalt crops out typically at the cliff behind the PICOP factory and the Taon River flowing west of Barcelona. It is a compact and massive rock which is dark grey, grey or dark green in colour. Texture of the basalt flows vary from glassy to porphyritic. The presence of pillow and columnar stractures is proof that they are marine and terrigenous lava flows.

Under the microscope, twinned or zoned plagioclase and augite phenocrysts scatters in the ground mass of plagiolase laths, augite, glass and magnetite without olivine, and shows basaltic or ophitic texture. Chloritization is generally recognized.

Some andesite lava flows are observed in the upper reaches of the Taon River with 100 – 1250 meters in thickness. Most of them show grey colour and porphyritic texture macroscopically. Under the microscope, twinned or zoned plagioclase and augite phenocrysts are in the groundmass composed of plagioclase laths or needles, ore minerals and augite. All augite crystals are altered to chlorite or carbonate minerals.

The alternation of black shale and sandstone with less than 100 meters in thickness and basic tuff are intercalated in this group.

As there are few key beds, it is difficult to make clear the structure of this group. Generally the group inclines gently southwest. The anticlinal structure with the axis of NE-SW direction along the Taon River and the synclinal structure with the axis parallel to the hill behind PICOP factory are presumed.

The age of the Barcelona basalt is not clear due to lack of fossils within the intercalated clastic rocks. Therefore, in this Report the age is tentatively placed as Cretaceous to Palaeocene because this group is overlain unconformably by the Oligocene Mangagoy formation composed of conglomerate, tuff and limestone.

Near Boston about 10 Km south of San Roque, hornblende andesite, andesitic tuff, sandstone and mudstone are observed. From the fact that they show a dip of SE-NW direction, which is discordant with that of the above mentioned basalt, either unconformity or fault is presumed between them but it is not sure because both of them are overlain by the Mangagoy formation unconformably. Judging from the general geological structure, the andesitic rocks seem to be younger than the basaltic rocks and may belong to the Kaban group mentioned in the next section.

2-2-2 Kaban group

The Kaban group spreads along the east side of the Philippine Fault with 5 to 20 kilometers in width and about 50 kilometers in extention. It is observed typically in the Kaban mountain range about 5 kilometers northwest of Monkayo.

By lack of key beds such as lava flow or sedimentary rocks continuing for long distances, the detailed structure of the group is not so clear. But from the lithologic characteristics, the Kaban group can be divided into the following five formations.

Formation I — This is observed at the south end of the surveyed area and consists of hornblende-andesite, altered andesite and tuff breccia or lappili tuff of the same composition, intercalating thin beds of limestone and mudstone. General strike trends NW or EW and dips 20^{o} - 30^{o} towards N.

The uppermost horizon of this formation is characterized by the lapilli tuff exposed in the upper reaches of the Cateel River, and is overlain unconformably by the Formation II. The bottom of the formation can not be confirmed in this area. The thickness of the Formation I is over 4,000 meters.

Formation II — the Formation II spreads in the northern side of the Formation I, and has a concordant relation to the latter. It consists of glassy andesite, augite andesite and tuff breccia or tuff of the same compositon intercalating sandstone, mudstone and limestone in the upper horizon of this formation. It shows a strike of E-W and a dip of 20^{o} - 30^{o} N as well as the Formation I. The Formation II is conformably overlain by the Formation III at the Ngan River, where pyroxene basalt, tuff and normal sedimentary rocks expose narrowly.

The glassy andesite shows purplish gray and other volcanic rocks, dark green or pale green in colour. Chloritization, albitization and epidotization are commonly observed.

The andesite with augite cropped out along the crest of dome in the upper reaches of the Bahyan River is correlated to the Formation II, and is affected remarkably by silisification, argillization and pyritization. The thickness of this formation is about 1,500 meters.

Formation III – The Formation III spreads from the Ngan River to the Mamunga River overlying conformably the Formation II. It is also observed in the headwaters of the Bahoyan River surrounding the Formation II, which forms the core of the dome structure. Both of them are composed chiefly of altered andesite with intermediate plagioclase. Two-pyroxene andesite with porphyritic texture is also observed.

From the occurrences, almost all of andesite are lava flows and greenalization of this formation is weaker than that of the Formation II. The top of the Formation III is a pumiceous tuff. The thickness of this formation is about 1,000 meters.

Formation IV – The Formation IV spreads from the Mamunga River to the Sukod River. In the drainage basin of the Bahayan River, the same formation takes part in the dome structure surrounding the Formation III. It has a pumice bed on the base and consists of two-pyroxene andesite, augite andesite, augite basalt and their pyroclastic rocks. Tuff-breccia, tuff, sandstone and mudstone pile up in the ascending order.

Augite andesite and mudstone are at the top of this formation. The formation overlie conformably the Formation III and attains about 1,000 meters in thickness.

Formation V — The Formation V is the youngest of the Kaban group and constitutes the outermost rim of the Bahayan River dome. It occupies the north end of survey area adjacent to the Philippine Fault.

The formation consists of altered andesite and its pyroclastics, and is unconformably overlain by the Mangagoy or the Biolig formation.

As described above, the Kaban group is divided into five formations and each characteristic of volcanic rocks is roughly stated. From the change of nature of the igneous activities, three cycles can be recognized in this group.

The first cycle is characterized by the igneous activities changing andesitic to basaltic, followed by the sedimentation of sandstone, mudstone and limestone. Formations I and II correspond to this cycle.

The second cycle begins with andesitic volcanic activities, ending with basaltic one in the subaquatic environment. It was explosive in the early stage and became calm later. Tuffacious sandstone, mudstone and tuff deposited in the later stage. Formations III and IV were formed throughout this cycle.

The third cycle corresponding to the Formation V is characterized by the explosive andesitic volcanic activities.

The igneous activities of the Kaban group are schematically shown in Fig. I-1.

Fig. I-1 Igneous activity of Kaban group

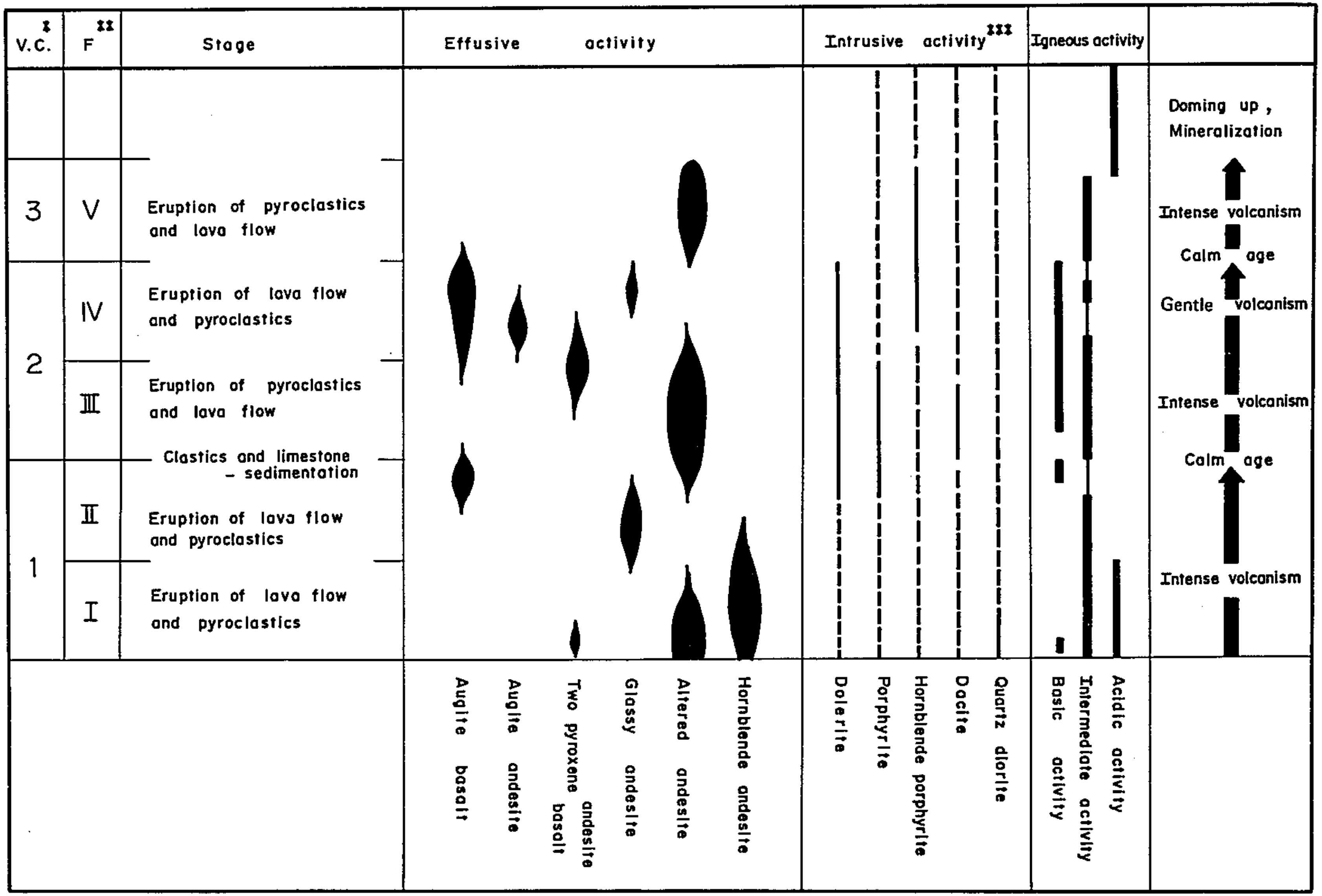

Remarks. V.C.* : Volcanic cycle
F** : Formation
*** —— Field evidence
---- Estimation

2-2-3 Igneous Rocks

(1) Gabbro

The Gabbro are exposed in the porphyry copper type mineralization area located in the upper reaches of the Taon River.

They are small in scale. One of them has a long shape stretching NE direction and cuts the diorite body which will be mentioned later.

Macroscopically it is grayish black holocrystalline rock. Under the microscope, plagioclase laths, augite, biotite and opaque minerals embed the gap among large crystals of plagioclase and augite.

Little alteration can be recognized.

(2) Dolerite

The narrow dolerite dykes are observed not only in the same mineralized area but also in the Kaban group. All of them are grayish black in colour and holocrystalline rock. Microscopically, phenocrysts of plagioclase and augite (5 - 7 mm in length) occur in a groundmass of plagioclase laths, augite and opaque minerals showing ophytic texture.

Secondary minerals such as chlorite, calcite and zeolite are recognized without exception.

From the evidence that the dolerite with same appearance and same mineral composition cuts the Bislig formation, the age of intrusion is probably the late Miocene.

(3) Porphyrite

The porphyrite dykes intrude into the Balcelona and the Kaban groups. Large phenocrysts (maximum 1 cm in diamter) of plagioclase are characteristic of these rocks. Macroscopically it shows dark gray or dark green in colour and porphyritic texture. Under the microscope, phenocrysts of plagioclase, pyroxene or hornblende are in a matrix of plagioclase and pyroxene microlites.

Sericite, chlorite, zeolite, calcite and clay minerals are commonly observed in this rock.

(4) Quartz Diorite

The quartz diorite is well exposed along the upper reaches of the Taon River and the Agsan River. The Taon River's diorite intrudes into the Barcelona basaltic rocks with about 1 Km in width and 3 Km in length trending NE. Rock facies of diorite vary from place to place. They are quartz diorite, quartz diorite porphyry, granophyre and diorite porphyry.

Typical quartz diorite is grayish white, medium grained rock. Microscopically, it is mainly composed of quartz, plagioclase, biotite and amphibole with accessory sphene and apatite. Usually plagioclase is subhedral and rimmed by alkali feldspar. Sericite, chlorite, epidote and others are commonly observed as secondary minerals in this rock.

The absolute alterration age of quartz diorite is 129×10^6 years by K/Ar method. The alteration would probably be due to mineralization, therefore, if assuming that the mineralization had occurrred in the wake of diorite intrusion, the age of diorite would be early Cretaceous. As there still remains some problems, they will be discussed in the section 3-2.

The Agsan River's diorite crops out at the southern end of the surveyed area as a platy dyke with 5 to 10 meters in width. It suffers remarkably from pyritization. Macroscopically it is leucocratic, medium grained holocrystalline rock. It consists mainly of quartz, plagioclase, amphibole and biotite. Sericite and epidote are much observed.

The absolute age of this rock is 60 x 10^6 years by K/Ar method.

2-3 Western Area

Basic to intermediate volcanic rocks are distributed in the greater part of this area. They were referred to as the Cretaceous system as a whole without confirmations in the Phase I survey. But this time, it has been made clear that they can be divided into two groups and that the upper section belongs to the Oligocene epoch.

2-3-1 Nilabsan Group

The Nilabsan group is the lowest section in this area and spreads in the western side of the Davao River. It is typically exposed along the Sita River and the Nilabsan River.

This group has been formed by basic igneous activity. It consists of pyroclastic rocks such as dark green or greenish gray fine tuff, sandy tuff, lapilli tuff, tuff breccia and reddish brown fine tuff intercalating black mudstone and gray fine-grained sandstone.

All the fragments in the pyroclastic rocks are andesitic volcanic rocks and no sedimentary rock fragments can be recognized. Microscopically, lithic fragments of porphyritec or aphyric andesite and chips of plagioclase and augite are embedded by clay minerals or glass.

The reddish brown fine tuff which characterized this group is a compact rock with traces of stratification. It is usually within 10 meters in thickness. Under the microscope, a few crystals such as amphibole, plagiolase and clinopyroxene occur in reddish brown volcanic glass. Some of them contain colourless spherulites.

Along the Sita River, a unit of well sorted bedding consists of lapilli tuff, coarse tuff and fine tuff in the ascending order is observed repeatedly. The thickness of a unit is 10 to 20 meters.

The features of the Nilabsan group as mentioned above resemble closely that of the formation distributed in the east side of the peridotite body surveyed in the Phase I. Therefore the former is probably the upper sequence of the later. In spite of no paleontological evidences, the age of this group seems to be the Cretaceous to the early Paleocene because it is intruded by the peridotite which has been considered as late Cretaceous to early Paleocene in age.

Small scale synclinal and anticlinal structures are observed from place to place, but generally speaking, the Nilabsan group has a strike of NNE – NS and inclines westward.

It is about 3,000 m in thickness.

2-3-2 Kalagutay Group

The Kalagutay group is typically exposed along the Kalagutay River and spreads widely from the upper reaches of the Sita River and the Nilabsan River to the mountain area west side of the Pulangi River. It is also distributed narrowly in the east side of the Plungi-Davao fault.

The group consists of pyroclastic rocks such as andesitic volcanic breccia, tuff breccia, lapilli tuff and fine tuff with subordinate normal sedimentary rocks such as mudstone, sandstone and conglomerate. Andesitic and basaltic lava flows are also intercalated.

The volcanic breccia typically crops out in the middle course of the Sita River and the upper reaches of the Kalagutay River. It is dark green or dark gray in colour and contains rounded breccias with more than 10 centimeters in diameter. In places, it shows auto-brecciated structure. Under the microscope, the breccia contains phenocrysts of plagioclase, green amphibole and augite. Groundmass is composed of plagioclase microlite and glass. A large amount of chlorite, calcite and pumpellyite are recognized as alteration products.

This volcanic breccia often contains accidental breccias and gradually changes to tuff breccia or fine tuff laterally.

Lapilli-tuff, tuff breccia and fine tuff are distributed widely from the upper reaches of the Nilabsan River to the Malicapan River. They are also observed in the eastern side of the Davao-Pulangi fault. They are dark green to dark gray in colour, and because of the strong alteration, it is difficult to discern the kind of breccias in them even under the microscope.

But the lapilli tuff exposed along the upper reaches of the Nilabsan River is rather fresh, and contains characteristically chromite and serpentine fragments which were probably derived from peridotite. From the evidence that chromite and serpentine are not contained in the Nilabsan group, it is conceivable that the sedimentary environment changed conspicuously between the two groups.

The normal sedimentary rocks such as mudstone, sandstone and conglomerate spread widely in the eastern side of the Davao-Pulangi fault and other areas.

Along the Bamoayo River, these rocks abut to the peridotite body. Sandstone or conglomerate contains characteristically a large amount of granules of sericite schist and quartz-mica schist which are presumed to compose the basement of this area.

Some limestone beds, which are each 2 to 10 meters in thickness, are distributed in the middle coarse of the Sita River alternating with sandstone and conglomerate. The age of the limestone beds as determined from fossils is upper Oligocene to lower Miocene.

Though intermittently, one of them can be traced about 40 kilometers from the Sita River to the Babonawan River through the Nilabson and the Kalagutay Rivers.

In the upper reaches of the Babonawan River, smaller foraminiferas were found out from the mudstone about 1,000 meters above this limestone.

The Kalagutay group has a strike of N-S and a dip of W generally. But the anticlinal structure with axis trending E-W is observed near San Fernand, and the synclinal structure is near Silae to Paradise and in the upper reaches of the Tigua River.

The thickness of this group attains 10,000 meters although the top is not confirmed.

2-3-3 Kapalong Formation

The Kapalong formation is distributed mainly in the eastern side of the Davao-Pulangi fault and partly in the upper reaches of the Sita River. It consists of conglomerate, sandstone and siltstone accompanying with thin limestone bed in the lowest horizon. This formation is Molasse type of Plioce to Pleistocene.

It is observed typically along the Kiulom River, southern part of the surveyed area. The Kapalong sedimentary basin was formed in Pliocene as the result of subsidence of the eastern block of the Davao-Pulangi fault and contemporaneous uplifting of the peridotie zone. The existence of synclinal structure located at northern end of the Kapalong formation is one of evidences of the historical development on the basin.

2-3-4 Lumbayo Formation

The Lumbayo formation consists of conglomerate with limestone pebble, sandstone, mudstone and limestone, and overlies the Kalagutay group clinounconformably. It is observed at the top of the mountains about 400 – 900 meters in height, such as the Mt. Merui, the upper reaches of the Sita River and Little Baguio.

2-3-5 Malambo Andesite

The Malambo andesite is hornblende andesite lava and crops out typically in the upper reaches of the Tigua River. It is distributed in the elevation higher than 1,000 meters. The geological age is probably the end of Pleistocene.

2-3-6 Intrusive Rocks

(1) Peridotite, Gabbro

Peridotite forms the Pantaron Ranges dividing Bukidnon Province and Davao Province. It is a large scale dyke with 2 – 5 kilometers in width stretching in N–S direction. It is compact and is yellowish dark green in colour. Under the microscope, ultramafic minerals are almost serpentinized and mesh structure is remarkable. The relict minerals are usually clino-pyroxene and rarely olivine. It contains a small amount of chromite without exception.

Dark greenish gray gabbro with large crystals of diallage accompanies this periodotite. It is composed of plagioclase, olivine, diallage and a few opaque minerals. Olivine is mostly serpentinized.

In the headwaters of Balahayo River, amphibole schist, which is probably the basement rock of this area, was found in the peridotite body as xenolith. Some small scale dykes of serpentinized peridotite also intrude into the Kalagutay group and stretch in the N-S direction.

(2) Pyroxenite, Gabbro, Diorite

Igneous composite body which is composed of pyroxenite, gabbro and diorite with 5 kilometers in width and 15 kilometers in length, crops out from the upper reaches of the Nirobsan River to the Tigua River by way of the Locawan River in NNE direction. It has intruded into mudstone and sandstone of middle Miocene belonging to the Kalagutay group.

Pyroxenite occupies the eastern part of this body, diorite the southern and the western parts. Gabbro intrudes into pyroxenite as stocks at two places.

Mutual relation among these rocks suggests that intrusions took place in the order of pyroxenite, gabbro and diorite. But they are probably comagmatic from resemblance of their mineral assemblage.

The geological age of gabbro is 11×10^6 years by K/Ar method.

Macroscopic and microscopic characters of these rocks are as follows.

(a) Pyroxenite

Pyroxenite is dark green or gray holocrystalline rock and is composed chiefly of augite and magnetite with a few amphibole, biotite and apatite.

(b) Gabbro

Gabbro is dark yellowish green, compact rock. Plagioclase and augite are main consituents and biotite, sphene and apatite are accessories.

(c) Diorite

Diorite is grayish black holocrystalline rock. It consists of potash-feldspar, plagioclase, augite and biotite accompanying with a few magnetite, sphene and apatite.

2-4 Geological Structure and Geological History

2-4-1 Geological Structure

The geological structure of the project area was generally mentioned in the Phase I Report. In this section, therefore, description will be made only about the detailed structure which has been made clear by the Phase II survey.

In the Eastern Area, the folding structure and faults trending NE-SW are prominent. Especially along the anticlinal axis near the Taon River, there is seen an intrusion of the quartz dioritic bodies. The Oligocene Mangagoy formation also takes part in this folding structure. In the lower Miocene Bislig formation, however, structural direction of E-W system takes the place of the NE-SW system.

In the Mangagoy formation, at the southern part of the Barcelona group, synclinal structure with the axis trending NE system is observed. As described before, there are some geological discordances between the northern basalt and the southern andesite so that either unconformity or fault may be presumed.

The NE-SW system was probably formed in middle to late Miocene contemporaneous with the quartz diorite intrusion.

The Kaban group adjoining to the Philippine Fault forms monoclinal structure dipping northwards in the southern to the central region, but forms dome structure in the upper reaches of the Bahayan River. Contrasting to the Balcelona group, E-W system structure is rather prominent in the Kaban group.

The Philippine Fault can be actually observed at the foot of mountain southeast of Jaguimitan, where it looks like the normal fault falling down the west-side block.

Some minor faults trending N-S which are parallel to the Philippine Fault are assumed in the Kaban group. Their throws, however, are not clear due to lack of key beds.

In the Western Area, N-S system structures are prominent. Especially in the Nilabsan group, there are developed anticlinal and synclinal structures in a small scale. On the contrary, the structure of Kalagutay group is relatively simple dipping westwards monoclinically.

The Davas-Pulangi fault running through the central part of the surveyed area probably moved in early Pliocene. The sedimentary basin formed by accumulation of the Molasse type sediments spreading widely in the southern area of the Pantaron peridotite body was probably generated simultaneously with this fault.

Pyroxenite observed in the drainage basin of the Tagbiga River, namely in the Western detailed survey area of the Phase II, intrudes as sheet without disturbing the host rock. The western rim of this body, however, is in contact with Kalagutay group with N-S trending fault.

2-4-2 Geological History

The Eastern Area is separated from the Western Area with about 60 kilometers in this Phase. Besides, the Central Lowland Area with few geological data spreads widely between these two areas, and the stratigraphical correlation is more difficult than that of the Phase I.

The tendency of change of volcanic activities, from basaltic to andesitic with the passing of time, is very resemble between the both areas, so that assuming the activities occurred in the same period, the geological history referred to in the Report of Phase I will be partially correct by the facts obtained in the Phase II survey.

At the end of Jurasic, the sedimentary basin was formed by the orogenic movements. Marine transgression began in Cretaceous and in the Eastern Area the vigorous volcanic activities produced a large amount of basaltic lava. In the Western Area, on the contrary, basaltic pyroclastic rocks with more than 10,000 meters in thickness were deposited.

At the end of Cretaceous period, uplifting occurred in the Western Area accompanying the peridotite intrusion and the crystalline schist of the basement rock in this area is presumed to be exposed.

The volcanic activity changed to the andesitic in late Cretaceous to Paleocene or Eocene period. In the Eastern Area, a large amount of lavas and pyroclastic rocks with a few normal sedimentary rocks were deposited in this period. After the temporary uplifting in early Oligocene, the Mangagoy formation and the Bislig formation were formed in the neritic environment.

In the Western Area, the Kalagutay group composed of andesitic pyroclastics, lavas and normal sediments was deposited during the late Cretaceous to middle Miocene time a few rock fragments of peridotite were supplied to this group.

Since the peridotite body mentioned above was exposed above the sea level at that time; a few rock fragments of peridotite were supplied to this group.

In the late Miocene time, diorite intruded into both areas and accompanied porphyry coppor type and vein type mineralizations.

After that the Davao-Pulangi fault was made by the sudden uplifting of the peridotite zone in the Western Area. Consequently the sedimentary basin of the Kapalong formation was formed.

The Kaban group in the Eastern Area was elevated above sea level in this period and the hollow formed by the Philippine Fault was burried with Molasse type sediments. In Pleistocene a thick pile of limestone was deposited. Thereafter, the continuing marine regression caused the limestone cliffs to be made at high places. In the Western Area, there followed andesitic volcanic activities.

3. Economic Geology

By the surveys of Phase II, the porphyry copper type mineralization was found in the Bislig-Lingig Area and the vein type of copper in the Tagbiga Area. In these areas, geochemical coppor anomalies had been found by stream sediment survey of Phase I.

3-1 Mineralized Zone

3-1-1 Bislig-Lingig Area

The basalt in the upper reaches of the Taon River is intruded by quartz diorite trending NE, accompanied by porphyry copper type mineralization.

In this area, there are two old mines which were operated for gold and silver by the Surigao Colorado Mining Association and the Southern Investment and Development Corporation before World War II, but the porphyry copper type mineralization has not been reported before.

As shown in Plate II-3A, in the neighborhood where the upper reaches of the Taon River curves to the west, a small stock of quartz diorite with about 50 meters in width is exposed, and filmy or disseminated chalcopyrite and pyrite with molybdenite can be observed along joints trending N-S in the stock.

The same mineral assemblage as chalcopyrite–molybdenite–pyrite is found in the tributary of the river about 1 kilometer north of this place. Metal contents are Cu: 0.1 – 0.3%, Mo: 0.02 – 0.05% but Cu is partially over 3%.

In the mineralized zone with molybdenum, potash alteration on the host rock of quartz diorite is recognized remarkably, and secondary biotite and potash feldspar occur. Besides, under the microscope, plagioclase alters into an aggregate of feathery sericite, and mafic minerals to chlorite and epidote partially.

Surrounding this copper-molybdenum zone, there is the mineralized zone having the mineral assemblage of chalcopyrite-pyrite. A small hill forming the divide between the Bahayan and the Taon Rivers takes part of this zone. Because of gentle slope, rock exposure is very limited and a large number of gossan boulders cover the whole hill. Most of the boulders consist of chalcopyrite, specularite, pyrite and quartz.

They have been dissolved away and changed into reddish brown or yellowish brown limonite. Consequently the gossans do not show their original contents, but the analysis of some comparatively fresh boulders is shown in Table 4 for reference. The copper content ranges mostly from 0.1 to 0.5% but some as much as 4%. The host rock in this zone is affected by strong chloritization so that its original texture is not clear, but it is presured to be andesite from the geology of neighboring area.

In the upper reaches of the Taon River, several quartz veins with 0.50 – 1.00 meters in width occur in strongly argillized porphyrite. These veins were prospected by drift (the length of cross cut : 25 meters, drift : 5 meters), and contain low grade of gold and silver (Au: 0.2 g/T, Ag 2 - 4 g/T). In the host rock, however, many tiny pyrite-quartz veinlets accompanied by sphalerite are fairly observed.

In white-argillized basalt about 300 m east of these veins, the old shaft and 5 tons of ore stockpile are seen. The ore consists of chalcopyrite, galena, sphalerite and pyrite showing high contents such as Cu: 0.85%, Pb: 17.6%, Zn 28.9%.

It seems that vein type or lens shape ore body was prospected. The Surigao Colorado Mining Association which is reported to have operated a gold and silver mine, probably had its mine site on this deposit judging from the location.

This zone characterized by lead and zinc are located on the outside of the above-mentioned copper-hematite zone, as well as the zinc impregnation found on the road along the Taon River.

In the upper reach the Haguimitan River south of this area, are two mine sites. The one is Lepanto Mine and the other, Soriano Mine. Both mines were reportedly explored for barite.

In the Lepanto mine area, mineralized zone occurs in a strongly silicified rock which seems to be shale originally, and five drilling holes could be recognized (See PL II-4A). The black colored, strongly silicified rock contains a few acicular barite with fine grained pyrite and white clay mineral (montmorillonite or kaoline). Enduring erosion, small five ridges consisting of the silicified rock extend in N50W direction.

The Soriano mine was explored for lenticular barite body with 8 meters in length, 8 meters in width and 2 meters in thickness. The body occurs in the contact between dacite and dacitic tuff and both rocks are strongly argillized. From its occurrence, it seems to be sedimentary type. Analysis of some composition gives the following percentage.

Au: 0.3 g/T, Ag: 512 g/T, Cu: 0.12%, Pb; trace, Zn; 0.06%, $BaSO_4$: 59.3%, S; 25.2%.

As stated above, the porphyry copper type mineralization in this Bislig Area, shows zonal distributions, that is, from the center to the outside, copper-molybdenum zone, copper-hematite zone and (gold-silver-) lead-zinc zone. And corresponding to these zones, the alterations of the host rock have been changed, namely, from the center, biotite-potash feldspar-quartz zone, chlorite-biotite-quartz zone, and chlorite-montmorillonite zone.

The zonal distribution in this area is somewhat schematically shown in Fig. I-2.

The zoning area extends 4 kilometers in E-W direction and 7 Km in N-S direction.

3-1-2 Bahayan-Mamunga Area

In the andesite area adjoining to the Philippine Fault, a large scale pyrite impregnated zone accompanying argillization and silicification in the upper reaches of the Bahayan and Mamunga Rivers. It was pointed out in the Report of Phase I, but its occurence was made more clear by the Phase II survey. It was ascertained that the mineralized zone extends over 14 kilometers in N-S direction with 1 kilometer in width.

Although copper content is very low, judging from the geological structure, strong montmorillonitization kaolinitization and sericitization suggest a shallow igneous intrusion accompanied by ore deposits.

3-1-3 Tagbiga Area

In the Tagbiga Area at the headwaters of the Tigua River, pyroxenite and composite body of pyroxenite and diorite spread widely. Mineralization is observed along the joints developed in the composite body or in the sheared zone as vein.

The direction of veins mainly shows two systems, NW-SE direction with pyrite-clay veins and NNE-SSW direction with chalcopyrite-pyrite veins. The former veins are 0.20 – 0.50 meters in width and their contents are Au: 6 g/T, and Cu: 0.5%. Accompanied clay minerals are composed of zeolite, chlorite and sericite.

The latter ones are lenticular massive ores with 0.10 – 0.20 meters in width and are accompanied by sericite and chlorite as well. The contents are very high,

Fig. I-2 Zonal distribution in the Bislig Area

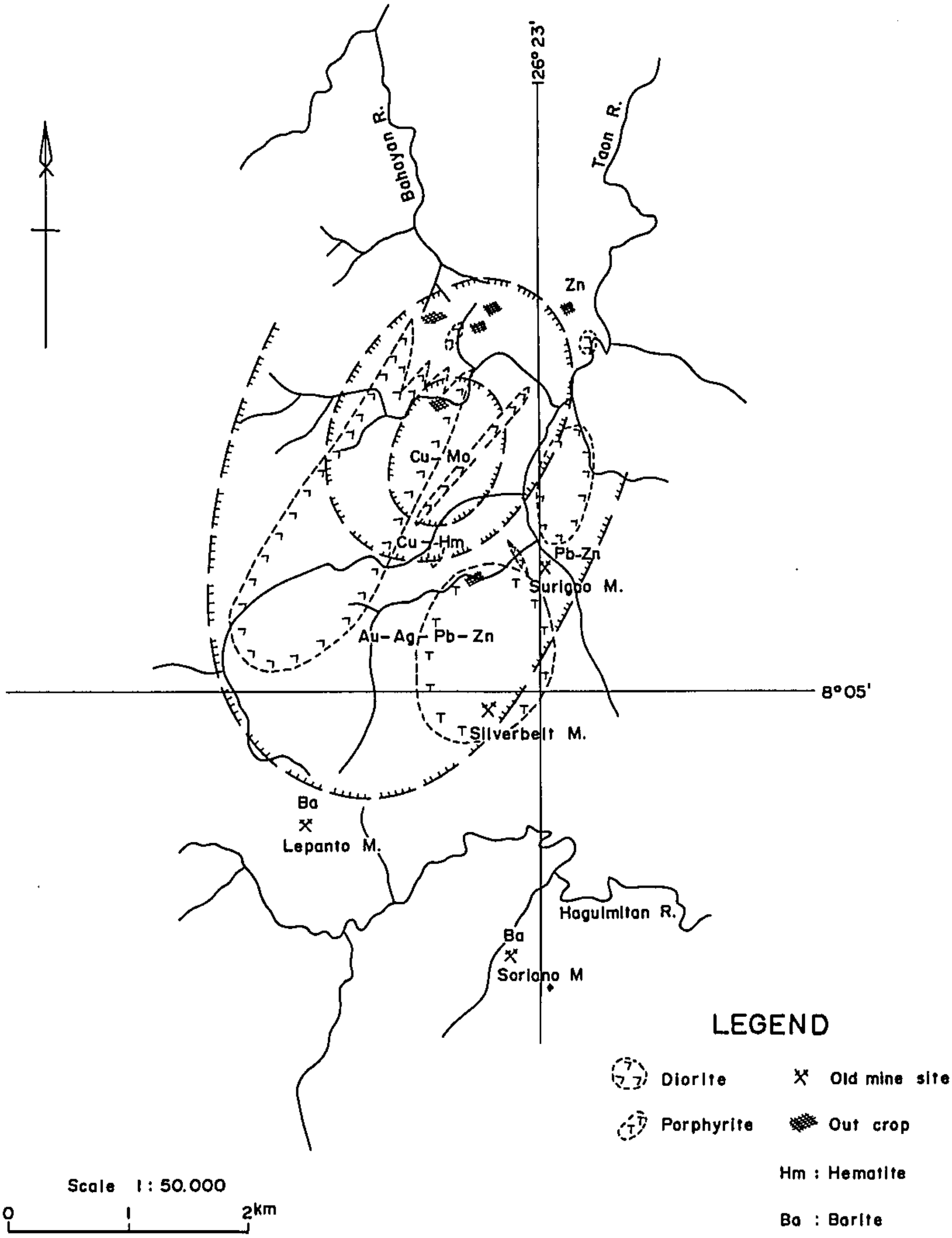

varying from 6 to 15 g/T of gold and from 12 to 18% of copper but the veins do not continue for long distances.

All of the veins do not contain molybdenum.

Besides, there are found pyrite impregnation at places but as a whole the mineralized zone trend to concentrate on the western margin of the composite body.

3-2 Mineralization Age

As shown in Table 2 of Appendices, the absolute alteration age of quartz diorite in the eastern mineralized area is 129 x 10^6 years (early Cretaceous period) by K/Ar method.

According to F.C. Gervacio (1966), the igneous activity of dioritic rocks in Mindanao Island is recognized in the early Cretaceous period, thereafter spilitic volcanic activity is followed. And andesitic volcanic activity continus to the Oligocene time through the orogenesis in the end of Cretaceous period. He stated also that in the Jurassic period before the activity of dioritic rocks, sedimentary rocks with a few spilite are chiefly formed and they are more or less altered to schist.

From the evidences described below, the writers consider the age of diorite intrusion accompanied by mineralization to be late Miocene.

1. The igneous character changes from basaltic to andestic in both Eastern and Western Areas.
2. In the Eastern Area, the Oligocene formation overlying the basaltic rock is intruded by the diorite having a strong resemblance to that in mineralized area.

3. Measured datum is only one.

The age of mineralization in the Western Tagbiga Area is late Miocene because diorite cuts the mudstone of middle Miocene and absolute age (11×10^6 years) by K/Ar method gives also support to this estimation.

PART II GEOCHEMICAL SURVEY

1 General Remarks

The geochemical survey of the Phase II by stream sediment and soil sampling was carried out over an area of about 3,000 Km^2 selected by the Phase I in order to define the most promising area for mineral resources.

In this Phase II, geophysical survey (IP method) was to be carried out after geological and geochemical surveys. Therefore, it was necessary to know the geochemically anomalous zone in the field.

From the results of the Phase I survey, there were expected porphyry copper deposits associated with diorite and nickel (accompanying copper) with peridotite in the survey area. So, rubeanic acid and dimethylglyoxime solution were prepared for detecting copper and nickel semi-quantitatively in the field and analytical results were plotted on the map in order to establish the geophysical survey lines.

Thus, two copper mineralized zones were found, the one was in the Eastern Area and the other, in the Western Area. Geophysical lines were set up from the viewpoints of shape of geochemical anomalous zones and geology.

The quantitative analyses of samples collected by the geologists were done in Japan after finishing the surveys. From geological characteristics, silver, copper, zinc and molybdenum were chosen for analytical element in the Eastern Area and copper, zinc, nickel and cobalt, in the Western Area. In the vicinity of barite deposits in the Eastern Area, lead and barium were analysed instead of copper and molybdenum because copper anomaly did not appear by rubeanic acid field test.

The following became clear from the rubeanic test and the quantitative analysis.

1. There are little areal differences on the pH values of running water in the survey area ranging 6.2 to 6.8.

   Therefore, it is not necessary to consider the effect of pH on metal contents when interpretation of the results are made statistically.

2. Copper anomalous zone detected by rubeanic method coincides with the quantitative analytical results as a whole. That method has proved efficient to defined the mineralized zone but a few problem still remained.

3. Colorimetric method using acetic acid (pH 4. 0) prepared for rubeanic acid field test and dimethylglyoxime solution, was ineffectual for determination of nickel contents in stream sediments.

2 Field Operations

Geochemical survey was carried out with geological survey. The survey routes were set up along streams to cover all drainage systems.

As a rule, stream sediment samples were taken every 500 m in the main streams and at the meeting are sample from each side of the stream was also collected. Generally 10 — 20 grams of very fine-grained silty sediments (under 80-mesh fraction) were sampled by hand. Care was taken to avoid overlap of the Phase I routes. In case that it was forced to take the same routes, the samples were collected every 1,000 m for checking of metal contents. The amounts of metal deposition on stream sediments are much controlled by pH, so that pH values of all main streams were measured using pH test paper in order to make the following interpretation easier.

The total area is covered by 3,463 samples which represents an average of 1.15 pcs/Km^2.

These stream sediments were dried in the sun and analyzed for copper and nickel by the simple methods in the field. According to the results, copper anomolies occurred in the same places as those of Phase I, i. e., in the upper reaches of the Taon River, east of Bislig in the Eastern Area, and in the upper reaches of the Tigua River, south of Halapitan in the Western Area. In both areas, veinlets or impregnations of chalcopyrite were recognized, so that these areas were selected for survey in detail.

Stream sediment sampling with higher sampling density and also soil sampling with ridge-and-spur pattern were carried out on the most promising parts in the selected areas.

Soil was turned up about 20 cm in depth with hammer, and yellow soil samples below humus (so-called B-horizon) were collected. 100 m sampling interval was taken in the Western Area, but 25 m in the Eastern Area. Because the amount of gossan in the East was much larger than that in the West, and the mineralization appeared to be stronger also.

The area of detailed survey and the number of geochemical samples are as follows.

Table II-1 Area and number of geochemical samples of detailed survey

	Area	Number of samples	Density of samples
Bislig Area	19 km^2	893 pcs	47 pcs/km^2
Tagbiga Area	20	539	27
Total	39	1,432	37

The soil samples were sieved by 30-mesh screen and -30-mesh fractions were analyzed for copper in the field.

Although both the survey routes and the number of samples were enough to establish the geophysical survey lines, 826 of additional samples were taken along the geophysical lines in order to use these data for interpretation of geophysical results and to define the area of Phase III survey.

The geochemical sample sites are shown in PL. II-2. Different letters were assigned to each party, i. e., from A to H and the serial number was also used on the sample. When three or four geologists of one party surveyed different creeks separately, a capital letter was given to the party chief and small letter to other members. A Philippino geologist was requested to use the combination letters such as a capital letter and his initials. The samples taken by geophysical team in the Western Area, the another combination letters of initial "P" and survey line's names from A to K (for example PB-3) were used to distinguish geological team's samples from geophysical ones.

3. Analytical Technique

Samples dried in the sun and prepared under 80-mesh fraction were analyzed semi-quantitatively for copper and nickel in the field. Finally, all samples were carried back to Japan and analyzed to a unit of ppm by atomic absorption spectrometry, colorimetry and X-ray fluorescence analysis.

Each analytical procedure is as follows.

3-1 Field Test

3-1-1 Copper

1. Scoop 1 g into test tube.
2. Add 2 ml of extracting solution (disolve 5 g of hydrated sodium acetate with 100 ml of acetic acid and adjust with distilled water exactly to 450 ml).
3. Shake 1 minute vigorously.
4. Pour the resultant mixture of soil and extractant into the tip of the filter (Place a piece of filter paper on the bottom of a breaker. Lay a strip of the filter paper. Fold a filter paper into cone. Let the tip of the filter touch the reagent paper).
5. Compare the darkening of the reagent paper with a standard series.

3-1-2 Nickel

1. Scoop 1 g into test tube.
2. Add 2 ml of the same extracting solution.
3. Add a few drop of 1% dimethylglyoxime solution after vigorous shaking.
4. Compare with a standard series.

3-2 Atomic Absorption Spectrometry

The same analytical method as the Phase I was used for the determination of copper, lead, zinc, nickel and cobalt. But the following was the procedure followed for sample decomposition for silver.

1. Weigh 1 g into Pyrex beaker.
2. Add 10 ml of aqua regia and heat on a sandbath till near-dryness.
3. Add 10 ml of HCl (1 + 1) and solve.
4. Add 20 ml of ammonium citrate (50%) and adjust with distilled water exactly to 50 ml.

The content of 6 elements stated above was measured by atomic absorption spectrophotometer.

Measuring wave lengths are as follows:

Cu	:	3247 Å
Pb	:	2833 Å
Zn	:	2139 Å
Ni	:	2320 Å
Co	:	2407 Å
Ag	:	3281 Å

3-3 Colorimetry

Molybdenum was determined by handy procedure of I. L. Elliot's zinc-dithiol method.

1. Weigh 0. 25 g of samples into Pyrex beaker.
2. Add 2 ml of aqua regia, 1 ml of perchloric acid and 2 ml of sulfuric acid (1+1) and heat till white vaper goes up.

3. Add dilute sulfuric acid and solve by heating.

4. Transfer to a test-tube calibrated at 10 ml, and adjust to this volume with 2 – 3 ml of ammonia water and distilled water.

5. Pipette 2 ml of the clear solution into a test-tube. Add 2 ml of hydroxylamine hydrochloride solution (2.5%) and shake gently.

6. Add 0.5 ml of zinc-dithiol solution (1%) and shake gently at frequent intervals over a period of 20 min.

7. Compare with a standard series.

3-4 X-ray Fluoresence Analysis

Barium was analyzed by X-ray fluorescence analysis.

Pulverized sample into test-tube and apply X-rays. Measure the intensity of Ba-Ka line picked up by spectroscope from fluorescent X-rays by scintillation counter and compare with standards.

4 Compilation and Interpretation of the Results

4-1 Statistical Treatment

5,756 geochemical samples consisting of stream sediment and soil, as stated above, were collected. It become clear as the survey progressed that they included some samples from the area of younger volcanic or sedimentary rocks, and for making sampling pattern homogeneous, some samples were omitted to be analyze.

Consequently 4,234 geochemical results, i.e., 2,560 of stream sediment and 1,665 of soil sample were finally accumulated.

On treating these data statistically, available 728 samples of the Phase I were included, so that, 19,120 analytical results of about 5,000 samples were obtained.

The graphical methods have a great advantage of being quick and effective to treat a large amount of date. Therefore C Lepeltier's method as well as the Phase I has been used to determine the mean background values and the treshold values.

The surveyed area can be divided into the following four areas chalacterized by different rock facies.

I. Bislig Area — the area from Mangagoy to Lingig, mainly composed of basalt.

II. Kaban Mountainous Area — the strip extending from north to south along the Philippine Fault, mainly composed of andesite.

III. Pantaron Mountainous Area — the area on the western side of the Davao-Pulangi fault, mainly composed of peridotite.

IV. Tigua River Area — the area on the western side of the Davao-Pulangi fault, mainly composed of andesitic pyroclastic rocks, and can be subdivided into IV-a (pyroxenite-diorite area) and IV-b (the rest).

In the detailed survey areas of I and II, high sampling densities were obtained. Therefore, the local mean background and the threshold values of these areas were calculated in addition to the above regional values. The assay contour lines in the Western Area were drawn from "raw" data. But in the Eastern Area, three point's moving average method was employed in order to seek the trend of geochemical anomalies. Because the sampling interval is much shorter than the space interval and it is difficult to draw the lines in some places where the metal contents are remarkably different at adjoining sample sites.

The coefficients of correlation and of deviation were also determined by graph. Some samples of the former are shown in the Fig. 2 of appendices.

4-2 Interpretation of the Results.

The mean background and the threshold values of stream sediments were determined by Lepeltier's method and geochemical anomalies were divided into the following three ranks. They are 1) (t-10%) — t, 2) t — 2 t and 3) 2t — in the Eastern Area and 1) t — 2t, 2) 2t — 4t and 3) 4t — in the Western Area because of large range, where "t" is the threshold value.

The results are shown in PL. II-1 (in pocket).

The mean background and the threshold values of stream sediments in the surveyed area are shown in Table II-2.

Table II-2 Regional mean background and threshold values of stream sediment samples

(ppm)

		Number of Samples	Ag		Cu		Zn		Mo		Ni		Co		Characteristic rocks
			b	t	b	t	b	t	b	t	b	t	b	t	
Eastern Area	I	449	1.7	3.5	88	270	110	380	0.68	3.2	–	–	–	–	Basalt, Quartz diorite
	II	1,046	1.3	3.6	75	170	82	160	0.52	1.5	–	–	–	–	Andesite
Western Area	III	552	–	–	40	58	50	76	–	–	330	1,200	33	70	Peridotite
	IV -a	157	–	–	80	220	35	80	–	–	12	17	13	18	Pyroxenite, Diolite
	IV -b	678	–	–	36	60	55	90	–	–	30	150	18	25	Pyroclastic rocks

Remarks b: mean back ground value
t: threshold value

What is evident from the Table is as follows.

1) Silver ---------- The mean background and the threshold values are about the same in the Areas I and II.

2) Copper --------- Both mean background and threhold values in the Area I and IV-a are somewhat higher than those in the Areas III and IV-b. This fact may have been caused by mineralization associated with diorite. The differences of regional mean background values probably depend upon the distinction of rock facies.

3) Zinc ----------- The background values in the Areas I and II which are composed of volcanic rocks are 2 — 3 times larger than the other areas. The high treshold value of Area I may be due to mineralization.

4) Molybdenum --------- The high threshold value of Area I is surely related to the porphyry copper type mineralization.

5) Nickel and cobalt ----- Both background and threshold values are very high. This will be due to peridotite without doubt.

As is obvious from PL. II-1, several geochemical anomalous zones by stream sediment survey were found.

In the upper reaches of the Taon River in Area I, there is a place where three elements of copper, zinc and molybdenum exceed the threshold values by far. Here, the highest values are Cu: 739 ppm, Zn: 1,138 ppm and Mo: 10.2 ppm. This anomalous zone coincides well with the porphyry copper type mineralized zone. In the lower reaches of the Lingig River, silver anomaly ranging from 2.3 to 4.0 ppm is recognized, and in the main stream of the Haguimitan 3 Km north of the Lingig River, there is a spot showing 80 ppm of silver. But no conclusion can be reached because of few samples, so that more detailed survey will be desirable.

In the Area II composed of andesitic rocks, the geochemical anomalies of silver, copper and zinc were found as did the Phase I survey at the headwaters of the Bahayan River. Pyritization and silicification are remarkable and they appear to have been caused by mineralization.

Many results of each element show about the same value as each threshold one and trend to disperse widely.

In the upper reaches of the Agusan River, the high copper content of stream sediment samples ranging from 300 to 500 ppm is considered to be related to the Sabena and the Manat Mines. Both mines have been under exploration for pophyry copper deposits by drifting or drilling.

In the Area III chiefly composed of peridotite, there were many sites showing higher values than the threshold one in every water system.

In the uppermost reaches of the Davao River, nickel content ranging from 1,500 to 1,800 ppm was recognized in the peridotite body. The copper anomaly in the small branch of about 3 Km lower reaches, shows from 200 to 250 ppm. It occurs in the andesitic tuff and could probably have some relations to the Bonacao mineralized zone which was found about 5 Km north from here in the Phase I survey.

Copper and zinc anomalies located 5 Km northeast of Paradise, are in the Molasse type formation of Pleistocene. It is difficult to explain their causes geologically, but logging road runs through nearby, so artificial pollution may be considered.

In the tributary of the Pulangi River north of the survey area, copper anomaly with nickel, cobalt and zinc is found. Its content is nearly the same as the threshold value (60 ppm). This is presumed to have been caused by partial concentration in the peridotite body.

In the Area IV, west of the Davao and the Pulangi Rivers, the background and the threshold values were approximated by the preliminary interpretation. After careful discussions, it became clear that the values in pyroxenite-diorite body were much higher than those in pyroclastic rocks, nevertheless the interpretation was made on the complex populations so that strange values as mentioned above were obtained.

Therefore, interpretation have been done on two areas, IV–a and IV–b.

As to Area IV–a, two remarkable copper anomalies were recognized in the composite body of pyroxenite and diorite where diorite looked to have intruded into pyroxenite as filling fissures developed at the margin of pyroxenite. One of anomalies is in the upper reaches of the Tagbiga River, the tributary of the Tigua River, and the other, at the headwaters of the Locawon River, the tributary of the Davao River.

There are some sites showing over 200 ppm of copper, and a few sites, more than 400 ppm.

In the upper reaches of the Tagbiga River, copper mineralized zone of vein type occurs in a composite body and rubeanic acid field test showed high copper concentration. Therefore, this place was selected as an area for the detailed survey without hesitation. But according to atomic absorption spectrometry the other anomaly, was better than the Tagbiga Area.

These opposite results are due to the difference of decomposition of samples, that is, cold leaching and hot leaching methods. It proves that soluble copper is low but total copper is rather high in the Locawon River.

In the upper reaches of the Nilabsan River, diorite is exposed about 3 Km along the river. Although weak zinc anomaly was found but copper anomaly did not appear.

In the Area IV composed mainly of pyroclastic rocks, nickel anomalies with relatively high content of cobalt were found at the places where dykes of peridotite were recognized.

Copper anomalous zone accompanied by zinc was obtained in the drainages on the west side of the lower reaches of the Bodonawan River. Copper contents ranging from 200 to 325 ppm are equivalent to 3 to 5 times of the regional mean backbround value. Numerically speaking, these contents are not so high but they are concentrated, so it is desirable to carry out follow-up works such as detailed geological and geochemical surveys. This area is composed of andesite lava or its tuff.

5 Description of the Anomalies

5-1 Bislig Area

5-1-1 Porphyry Copper Area

This area lies in the upper reaches of the Taon River, 10 Km south of Mangagoy where PICOP factory is in operation. As a roadway runs through from Bislig to Lingig on the eastern side of the detailed survey area, accessibility is very well.

The mineralized zone is of porphyry copper type associated with diorite intruded into basalt lava and andesite lava. Outcrops of mineralized rock and floots of gossan are found everywhere. Among them chalcopyrite and copper oxide were commonly recognized, and a fairly strong reaction of copper was carried out at intervals of 25 — 50 m along the river and ridge. The soil sampling along the geophysical survey lines was also carried out every 25 m, because this area appeared to be the most promising area from the geological and geochemical points of view and to be taken up as a target in Phase III Survey.

The mean background and threshold values of this area are shown in Table II-3. In PL II-3C two assay contour lines are drawn so as to catch easily the trend of each element. The one is a line of threshold value, the other, a line of the mean value of threshold and mean background values.

Copper —— The most remarkable anomalous zone extends in NNE direction from the intersecting point between base line and line No. 9 of geophysical survey. Near the point E. 3 of Line No. 4, a small scale anomaly is also found. The former is in diorite. For example, at the bank of Taon River near the interset-

Table II-3 Local mean background and threshold values of soil samples, Bislig Area

(ppm)

	Ag	Cu	Zn	Mo	Number of samples
b	0.9	110	30	1.0	829 pcs
t	1.8	550	215	10.0	
s	2.6	4.3	4.4	5.1	

b: mean background value
t: threshold value
s: coefficient of deviation

ing point, there is the impregnation of chalcopyrite, pyrite and molybdenite extending towards north. The latter is in basalt, and the floats of hematite and quartz are scattered. In parallel to these anomalous zones, another anomaly with copper content from 300 to 500 ppm is found on the western side. This anomaly coincides well with the eastern boundary of diorite.

Molybdenum —— The eastern anomaly overlaps the copper one. Besides weak indication is also recognized in the center part of quartz diorite body.

As shown in PL. II-3C, both anomalies of copper and molybdenum trend to extend towards south over the soutern limit of the detailed survey area.

Zinc —— Somewhat concentrated anomaly is obtained between line No. 3 and line No. 4 on the western side of the base line, and another one appears near the eastern end of line No. 4. The former concentrated on the low land, such as creek, looks to have been migrated from other places. The fact that IP anomaly does not appear supports this estimation.

The latter is at the top, so it shows true anomaly.

Silver —— Being different from other three elements silver contents do not concentrate at one place but disperse in a wide area. This may be a result from the facts that the contents are generally low and that it is difficult to classify them because of small range. In another wards, it may be said that silver mineralization in this area is not so strong. id that silver mineralization in this area is not so strong.

The silver anomalous zone which is tentatively decided by usual way, corresponds to the copper anomalous zone in the southern part, but it is rather closely related to zinc anomalous one. As a whole, it is located on the outside of copper -molybdenum zone, and seems to show a geochemical zoning.

In this area, the floats of gossan are distributed on the hills or the hillsides. Some of them run 4% in copper content; nevertheless copper content in soil is lower than expected. The climate of this area is tropical-forest-type so it might have been caused by leaching and further study is desirable.

The coefficients of correlation among each element are shown in Table II-4.

Table II-4 Coefficient of correlation, Bislig Area

	Mo/Cu	Mo/Ag	Mo/Zn	Cu/Zn	Cu/Ag	Zn/Ag
ρ	0.375	– 0.208	– 0.309	0.120	0.242	0.620

ρ: coefficient of correlation

It is obvious that silver has close relation with zinc but no correlation can be seen among other elements.

5-1-2 Silver Belt Mine Area

The Mine Area is situated in the uppermost reaches of the Taon River and very close to the PICOP logging road.

The impregnation of chalcopyrite, pyrite and sphalerite is seen in the porphyrite with large phenocrysts of plogioclase. Argillization is generally observed and locally sillicification is strong. Trench prospecting for the impregnated zone and quartz veins had been carried out in many places. Therefore, soils were collected along the creeks and the ridges.

The mean background and threshold values calculated from the 95 samples of this area are shown in Table II-5.

Table II-5 Local mean background and threshold values of soil samples, Silver Belt Mine Area

(ppm)

	Ag	Cu	Zn	Mo	Number of samples
b	0.7	42	27	1.1	95
t	1.6	210	120	2.9	
s	1.9	3.4	3.2	2.1	

Comparing these values with those of the Porphy Copper Area (Table II-3), copper is about a half of the latter in the mean background value, and silver, zinc and molybdenum almost approximate. In the threshold value, only silver approximates, on the other hand, and other elements less than a half.

As is evident from PL. II-4B of geochemical map, each element does not trend to concentrate. Considering the mean background and threshold values it is presumed that the mineralization in this area is not so strong.

5-1-3 Lepanto Mine Area

The Lepanto Mine Area lies in the upper reaches of the Haguimitan River, 3 Km south of the Porphry Copper Area.

In the silicified shale, pyrite and barite were impregnated.

As this was an area where drilling-prospecting had been carried out before, soil samples were collected in anticipation of there being the sedimentary type ore deposite, and four elements of silver, lead, zinc and barium were analyzed. Copper was not detected by rubeanic acid fild test from these samples.

Through the sampling pattern was irregular, the mean background and threshold values calculated from the analytical data, are as follows.

Table II-6 Local mean background and threshold values of soil samples, Lepanto Mine Area

(ppm)

	Ag	Pb	Zn	Ba	Number of samples
b	0.9	25	28	115	86 pcs
t	3.5	230	120	290	
s	2.8	3.3	3.2	1.8	

As far as the writers can judge from the Table, four elements do not show much high values. With no data available on barium in the Porphyry Copper Area, it cannot compare these values with others. According to B. Mason, the mean barium content in shale is 580 ppm and in igneous rock, 425 ppm. It can be said, therefore, barium mineralization is not worthy of special mention.

As shown PL. II-4B, anomaly of each element is not concentlated, and a little silver anomaly is only observed at the site where prospecting had been done.

5-2 Western Tagbiga Area

The copper anomalous area detected by rubeanic acid field test lies in the upper reaches of the Tigua River about 10 Km south of Halapitan. The anomaly exists in pyroxenite and diorite intruding into pyroxenite.

The mean background and threshold values are shown in Table II-7, but in PL. II-5C of geochemical map, two contour lines, the one is the threshold value and the other is the mean value of threshold and mean background values, are drawn as well as PL. II-3C.

Table II-7 Local mean background and threshold values of soil samples, Tagbiga Area

(ppm)

	Cu	Zn	Ni	Co	Number of samples
b	105	50	36	53	394 pcs
t	420	105	70	120	
s	3.9	1.6	1.8	2.3	

b: mean background value
t: threshold value
s: coefficient of deviation

Anomalies of each element are as follows.

Copper —— Anomalies appear widely near the western contact between the composite body and sedimentary rock, and in the northeast part of detailed survey area. In the former zone, vein type or lenticular massive ores composed of chalcopyrite, pyrite and quartz are recognized at some places, so geophysical survey was carried out.* The highest content of copper is 600 ppm. The latter anomaly is in pyroxenite but mineralization can not be seen along the creeks. As both stream sediment and soil samples were weak in reaction of rubeanic acid test, geophysical survey was not carried out. From the result of atomic absorption spectrometry, the latter shows better concentration than that of the former. Though the exposure is limited, further study is desirable.

Zinc —— Anomaly corresponds well to that of copper. The contents are relatively low. The highest value is 145 ppm.

Nickel —— In the western part adjacent to the western copper concentration, nickel anomaly extends narrowly.

This location coincides perfectly with the boundary of composite body. Besides the anomaly extending in the NE direction from this place and another one near the meeting point of Tigua and Tagbiga Rivers are found although these anomalies are overlapping partially copper and zinc ones, coefficient of correlation between nickel and copper or nickel and zinc is very low. Therefore, nickel as well as cobalt is probably included as primary mineral of pyroxenite. Even though they are same ultrabasic rocks, nickel content in pyroxenite is about 1/10 to 1/20 times of that in serpentine.

Cobalt —— The main anomaly is located in the northweastern part of this area and corresponds well to nickel one. Also, there is a small scale concentration overlaping the western copper, zinc and nickel anomalies. The highest value in this area is 166 ppm.

Compiling the geochemical results of four elements stated above, there is a clear concentration of these elements in the same western margin of pyroxenite-diorite composite body. Other than this, the concentrations of copper and nickel or cobalt are found widely in the northeastern part of the area.

The coefficients of correlation among each element are as follows.

Table II-8 Coefficient of correlation, Tagbiga Area

	Cu/Zn	Cu/Ni	Cu/Co	Zn/Ni	Zn/Co	Ni/Co
ρ	0.450	0.191	0.559	0.259	0.525	0.438

As is evident from Table II-8, copper and zinc or cobalt, cobalt and zinc, and cobalt and nickel are closely related each other but there is few connection between nickel and copper or zinc.

Generally speaking, pyrite usually contains cobalt; therefore, copper, zinc and cobalt anomalies seems to have been caused by the same mineralization. On the other hand, nickel as well as cobalt (partly) is presumed to be contained in pyroxinite as primary mineral.

PART III GEOPHYSICAL SURVEY

1. ABSTRACT

According to the results of the Phase I geological and geochemical surveys and the Phase II detailed geological surveys, the eastern area, Bislig and the western area, Tagbiga were selected as high potential areas for mineral resources.

The purposes of the geophysical investigations reported here are to know electrical property, distribution and scale of the mineralized zone and to discuss the possibility of finding ore deposits and to select the best drilling points, by applying electrical survey (Induced Polarization Method) in those areas.

As IP methods indicate a remarkable anomaly for the porphyry copper type deposit and its surrounding mineralized zone which are expected to be found in those areas, it has made remarkable development of finding mineralization in tropical jungles where outcrops are hard to find.

In this project, IP survey was conducted over 18.4 Km of survey lines in the eastern area and of 16.7 Km in the western area, and the total survey lines are 35.1 Km.

These geophysical survey lines were planned from the informations of the mineral outcrops of copper, the distribution of geochemical anomalies and from geological standpoints.

Judging from the results of the geophysical survey, additional IP lines were also run.

Results of these surveys indicate IP anomalous zones in both areas.

In the eastern area, the width of the anomalous zone is about 400 m and the length is more than 1,500 m extending to a N-S direction accompanied by a low

resistivity zone due to hydrothermal alteration. Together with the results of geochemical anomalies, hopeful drilling points were selected in this area.

In the western area, an anomalous belt more than 3,500 m in length in a NNE direction was found and was expected to extend to a NE direction, but some anomalies seem to be due to primary magnetite and pyrite, therefore further surveys are recommended hereafter.

2. Induced Polarization Method

2-1 Principle

Although the phenomenon of IP is extremely complex, certain insight has been gained into its mechanism as a results of recent researches. It now seems well established that two principal effects must be distinguished; an electrode polarization and a membrane polarization.

Electrode polarization or Over voltage

The electric current in the ground is normally carried by ions in the electrolytes present in the pores of rocks. If the passage of these ions is obstructed by certain mineral particles (which, like common metals, transport the current by electrons,) ionic charges pile up on the surface of the mineral particle. The accumulated charges create a voltage that tends to oppose the flow of electric current across the interface and the particles are said to be polarized.

When the current is interrupted a residual voltage continues to exist across the particle but it decreases continuously as the ions slowly diffuse back into the pore-electrolytes.

With the change of frequency of the supplied current, the resistance of the metallic minerals vary due to the motion of the charged ions.

These phenomena are the combined effect of ionic conductivity and electronic conductivity and these processes give the IP effect.

Foremost among the ore minerals having an electronic mode of conduction and therefore exhibiting strong IP are ;

Sulfides:	Pyrite, Pyrrhotite, Marcasite, Galena, Chalcopyrite, Molybdenite, Pentlandite, Cobaltite, Algentite
Oxides:	Magnetite, Pyrolusite, Cassiterite
Others:	Native Copper, Graphite, Arsennide, Clay mineral

Normal Effect or Background

This phenomenon is due to electrochemical change such as membrane polarization, diffusion potential and flow potential by supplying electrical current into the ground where no metallic minerals are present. Ionic movement is the cause of this phenomenon.

For example, the surface of a clay particle is negatively charged and this attracts positive ions from the electrolytes. An electric double-layer is therefore formed at the surface of the particle somewhat as sketched in Fig. III-1, the concentration of positive ions being greatest at the surface of the clay particle.

When an electric current is forced through the clay, the positive ions are displaced and upon interruption of the current, the positive charges redistribute themselves in their former equilibrium pattern. The movement of the ions is detected as IP effect.

Fig. III-1 Induced polarization phenomenon

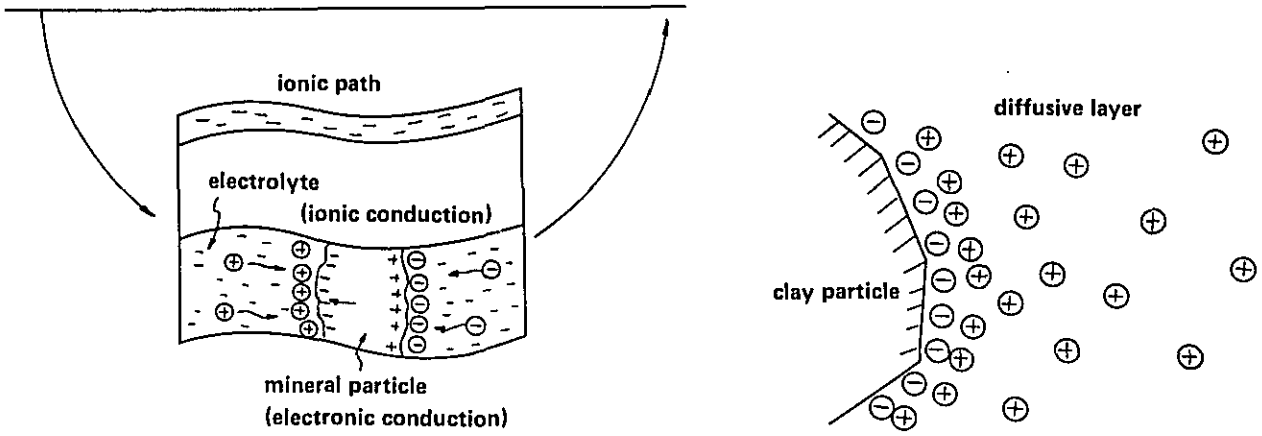

A. Electrode polarization phenomenon at mineral-electrolyte interfaces.

B. Membrane polarization phenomenon in clays.

Polarization is essentially a surface phenomenon. Hence the greater the surface presented by sulfides or clays to an electric current, the stronger are the polarization effects.

From the nature of the IP effect, it follows that impregnation-type ores such as porphyry copper type deposit which have a large effective surface of mineral particles, are particularly suitable targets for exploration by IP method.

Condenser Model

This is a simple but far-reaching and useful analogy to the polarization phenomena in rocks.

Consider an electric circuit consisting of a condenser and a high resistance in parallel (Fig. III-2).

Fig. III-2 Electric circuit analogy to IP phenomenon

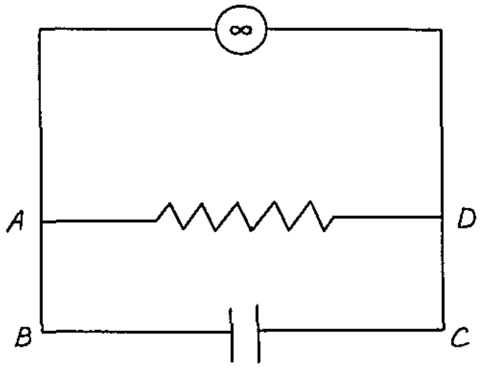

The circuit in Fig. III-2 has the property that if the battery is replaced by a source of alternating electromotive force, the amplitude of the alternating voltage in the circuit decreases with the frequency for constant magnitude of the circuit.

In other words, the effective electrical resistance (impedance) of the circuit decreases as the frequency of the applied current increases. The reason for the decrease is that, although a condenser presents an infinite resistance to a direct current, it allows alternating current to pass across it (circuit B–C), so that when the current alternates, an extra path B–C becomes available to it.

If the polarization phenomenon in the ground where due to the ore-electrolyte interfaces acting as condensers, the resistivity of rocks should be expected to decrease as the frequency of the current passing through them increases. This is indeed found to be the case. (Fig. III-3)

Fig. III-3 Decrease of the electric resistivity of rocks with the frequency of the current through them.

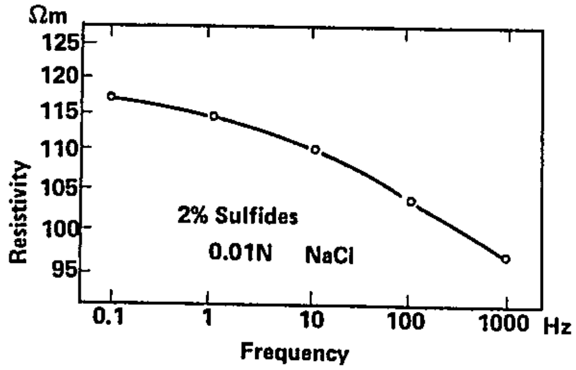

Thus each electrolyte-mineral grain interface in the ground may be likened to a tiny condenser storing ionic charges whose diffusion in the electrolytes, after the cessation of the current, corresponds to the leakage through the resistance A–D in Fig. III-2, giving rise to a steadily decreasing voltage between two potential electrodes on the surface. This is the time domain IP effect.

And as the frequency domain IP effect adopted in this survey a ratio of two kinds of resistivity for low (0.1 — 0.3 Hz) and high (3 — 10 Hz) frequencies are measured directly on the deviation meter.

2-2 Measurement of IP Effect

The methods of IP effect are divided into two main groups as mentioned above.

In time domain method, IP effect is expressed as a parameter of chargeability which is a residual voltage Vs at a definite time after the current cut off or time integrated voltage divided by the voltage Vp just before the current cut off. (Fig. III-4)

Fig. III-4 Current wave form supplied from current electrodes

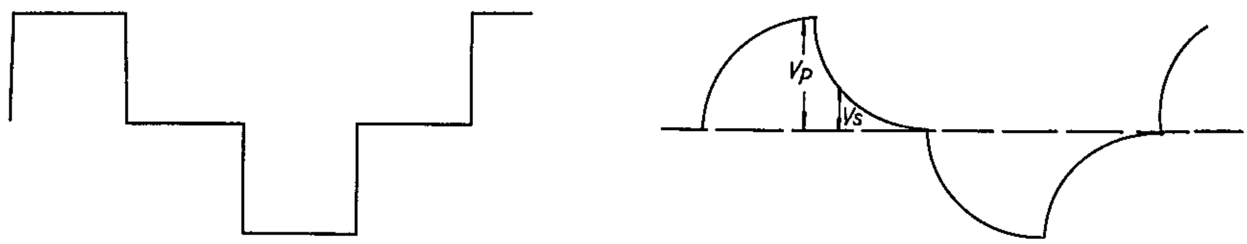

$$\text{Chargeability}; \quad m = \frac{Vs}{Vp} \times 100 \ (\%)$$

$$\text{or} \quad = \frac{\int_{t_1}^{t_2} Vs \, dt}{Vp} \quad (\text{mV-sec})$$

The practice in frequency-domain methods is to determine the apparent resistivity of the ground at two frequencies with almost ten times variation.

But it is mathematically proved that those methods are two different aspects of one and the same phenomenon.

Let ρdc be the resistivity of a rock for direct current and ac that for an alternating current of high frequency.

Then the frequency effect FE is defined as:

$$\rho ac = \frac{\rho dc}{1 + FE \dfrac{Fac}{Fdc}}$$

When Fac = 10x Fdc,

$$FE = \frac{\rho dc - \rho ac}{\rho ac}$$

In the field work, FE can be read directly in % on the deviation meter.

Conception of two frequencies are shown on Fig. III-5.

Fig. III-5 Comparison between long and short cycles of measurement

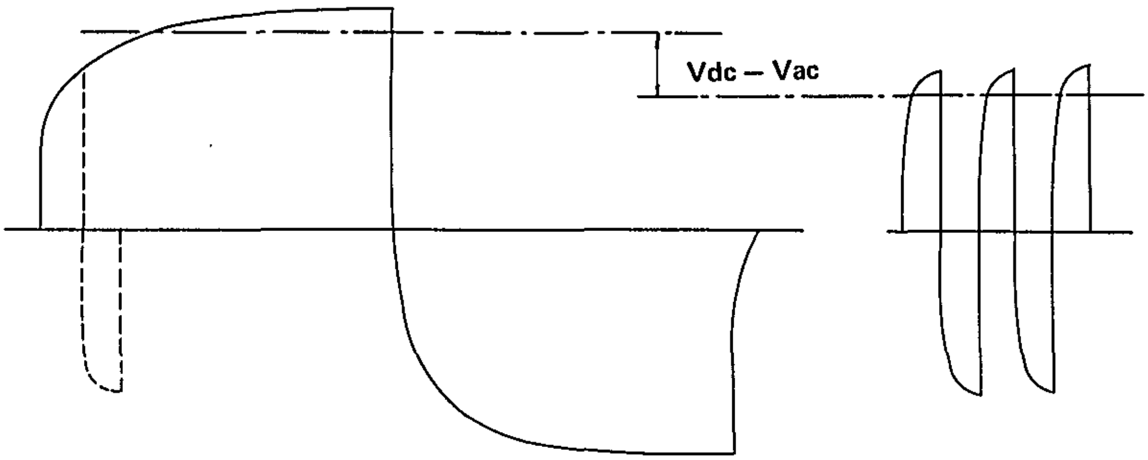

In this survey of Phase II frequency of ρac was 2.5 Hz in the eastern area, 3 Hz in the western area because of the difference of IP measuring system. ρdc was both 0.3 Hz, then only 1.08 times of FE in the eastern area have to be corrected to compare with the results of the western area.

2-3 Indication of Results

Three kinds of sections are indicated as IP results such as Frequency Effects (FE %), Apparent Resistivity ($\rho\Omega$ –m) and Metal Conduction Factor (MCF ℧ /m).

The electrode configuration is dipole-dipole which together with the method of plotting results, are shown on Fig. III-6.

As illustrated, the current is applied at two points (5, 6) a distance (a)= 100 m apart.

The receiver is located at two other points (1, 2) on the same line and measures the potential between these points which are also a distance (a) apart.

The distance (a) is commonly called the "electrode spread length".

The distance between the nearest current and potential electrodes is (na), where (n) is a variable integer commonly between 1 and 3 or 4.

The depth of penetration (h) is increased by increasing (n),

$$h = \frac{a(n+1)}{2} = 50\ (n+1) \quad \text{(meters)}$$

Fig. III-6 Method used in plotting dipole-dipole IP results

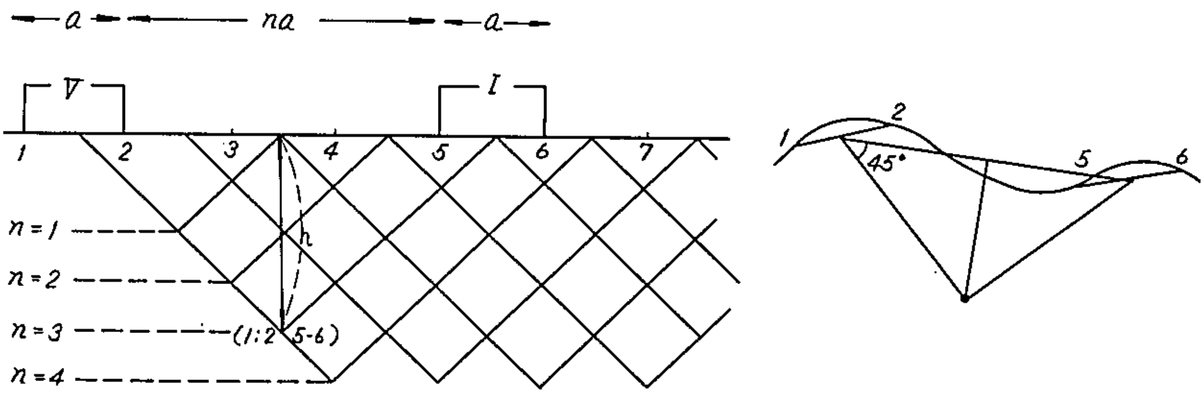

The values from each measurement are plotted at the intersection of 45 degree lines from the center point of the current electrodes and the center points of the potential electrodes.

Apparent Resistivity

The equations to be used in calculation of apparent resistivity is;

$\rho = F \cdot V/I,$

where V is a measured potential

I is a constant current at 3 Hz

and F is expressed as below in any electrode configurations

$$F = 2\pi / \left(\frac{1}{c_1 p_1} - \frac{1}{c_1 p_2} - \frac{1}{c_2 p_1} + \frac{1}{c_2 p_2} \right)$$

In this survey, all survey lines are straight (except D-line in Tagbiga), then

$$F = \pi a n(n+1)(n+2)$$

$$= 314 n(n+1)(n+2)$$

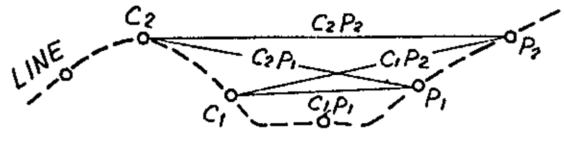

Apparent resistivity measured by dipole-dipole configuration tends to be influenced by steep topography.

If the topography should continue infinitely in perpendicular direction, corrections could be calculated by electronic computer or using analog carbon paper corrections could be done experimentally. But it is expensive and three dimensional effects may not be rejected. So topographical corrections have been done referring to many model sections calculated by computer. (Fig. III-7)

Fig. III-7 Topographic influence ($\tan^{-1}(2/5)$, $a = 2$, $\rho_0 = 1$)

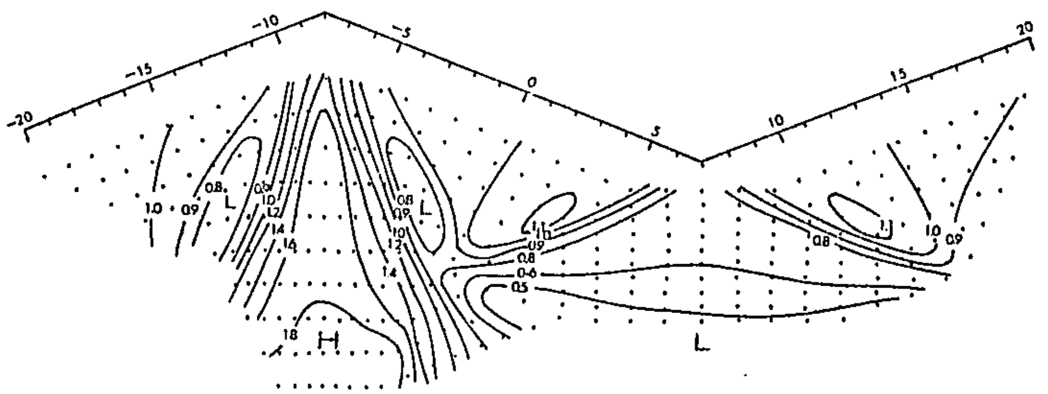

Metal Conduction Factor

The theory of electrode-polarization effects shows that IP is greatly influenced by the resistivity of the electrolytes in the country rock.

The parameter known as metal conduction factor (MCF) was devised by MADDEN to correct (partially) for the resistivity of the country rock. In principle, it is defined simply as the frequency effect divided by the lower frequency apparent resistivity.

However, as the number thus obtained is inconveniently small, it is multiplied by 1,000 so that the practical definition of the metal factor becomes;

$$MCF = \frac{FE}{\rho\, dc} \times 1,000 \quad (\mho/m)$$

If the resistivity is expressed in Ω −m, the dimension of the metal conduction factor is $\Omega^{-1}\ m^{-1}$, that is, those of the electric conductivity.

Under ideal circumstances big metal conduction factor are detected by low resistivity and high FE due to ores and alterations, but the topographic influence to the apparent resistivity must be considered to interpret it.

On each section, contours are drawn in moderate interval, but it is important to appreciate that these contour plots cannot be considered as vertical sections of the electrical properties of the ground.

For example, contours for some models are shown on Fig. III-8, but the anomalous sources do not coincide with high anomaly but actually lie in the shallower zone.

Fig. III-8 FE Model curve

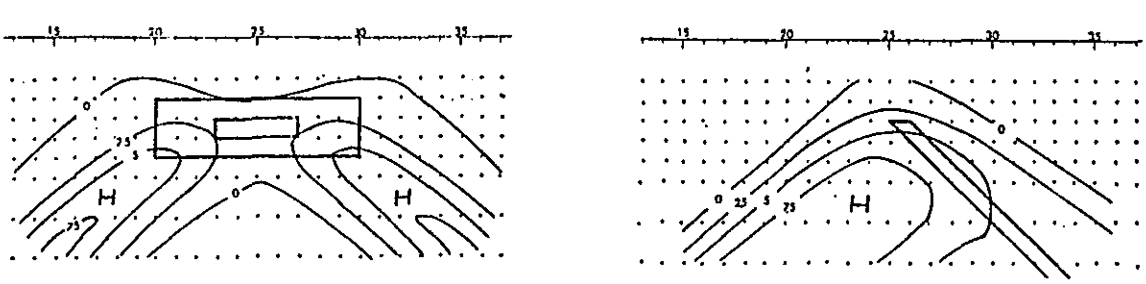

2-4 Physical Property of Rock Samples

To make analysis easy, electrical property of the collected rock samples were measured. Typical rock samples in both areas were collected, 32 in the eastern area and 25 in the western area and frequency effect and resistivity were measured in each rock. As the rock samples were collected from the surface of the ground, change in resistivity was unexpectedly wide because of the porosity and the weathering effect so that the resistivity of rock samples are generally higher than that underground. (Table III-1, III-2)

A small current supplied from an ultra low frequency oscillator was 1 or 5 micro-amperes and the measuring equipments were Model YMO-412A and P-660 which were used in the field survey, getting the same results.

$$R = \frac{V}{I} = \rho \cdot \frac{\ell}{s}$$

$$\rho = \frac{s}{\ell} \cdot \frac{V}{I}$$

R	:	Resistance (Ω)
I	:	Current (A)
V	:	Potential (V)
ρ	:	Resistivity (Ω-m)
ℓ	:	Length (M)
s	:	Section (M^2)

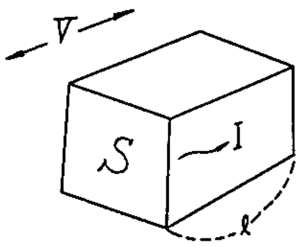

3. Result of Induced Polarization Survey in the Eastern Area

3-1 Surveyed Area

The area surveyed is situated in the province of Surigao del Sur in Mindanao Island, south of the municipality Bislig between Barrio Mangagoy and The Municipality Lingig, around the valley of Taon.

It is bounded by

Latitude 8° 5'40" and 8° 7' 0" N (2.0 Km north to south), and

Longitude 125° 22' 0" and 126°23'30" E (2.0 Km east to west).

The base station lies approximately at

Latitude 8° 6'30" N and Longitude 126°22'38" E.

3-2 Period of the Survey

The survey started March 7, 1973 and concluded on April 18, 1973 with 30 days of actual work during the 41 days of stay in the area.

3-3 Members of the Survey Team

CAROL S. SAMONTE	ITSURO OGAWA
CESAR V. RAMOS	KATSUMI OYANAGI
NARCISO BAUTISTA	NAOYOSHI TAKAHASHI
BENERCITO BALLESTEROS	JUNICHI SATO
ALBERTO ISSAC	SABURO TACHIKAWA

3-4 Place and Transportation

The area of survey is about 100 Km northeast of Davao City. A domestic flight of Philippine Airlines connecting Davao City and Bislig in 30 minutes is available as a means of transportation.

The base camp was set up at PICOP Station Office of Barrio Mangagoy, 8 Km east of Bislig. From this camp to the area of survey, it takes about 20 minutes by car using a logging road from Mangagoy.

Well developed logging road network over this area provided a very convenient access to the area. All the eastern end of each survey line intercept the road going to Linging from where one can easily enter the survey area.

3-5 Geological Features

The rocks of this area composed of basalt and andesite lavas of late-Cretaceous Barcelona basalt group, dioritic rocks such as quartz diorite, diorite and diorite porphyry, which are products of igneous activity during the last Miocene, and gabbro and porphyrite.

The basalt lava occupies the largest portion of the surveyed area. Andesite lava intercalated in the basalt lies mainly in the northeastern part of the area. They extend northeastward striking NW-SE and dipping $20^{\circ} - 30^{\circ}$ to the south.

The dioritic rocks are distributed in several areas all extending northeastward at right angles to the lavas.

The biggest dioritic body lies southwest of the area stretching over 2,000 m in length and about 700 m in width.

All the dioritic rocks are probably the facies of a single intrusive mass occuring in a comparatively shallow depth.

The basalt and andesite lavas mentioned above are hydrothermally altered by the post-igneous activity of the dioritic rocks. Hydrothermal alteration such as silicification, sericitization, argilization and potasium alteration are commonly seen. Accompanying these alterations, impregnations or veinlets of pyrite, chalcopyrite, molybdenite, magnetite, hematite, or zincblende, etc. are observed everywhere.

In the northern part, small bodies of gabbro which are late intrusions, are distributed. Small scale dykes of porphyrite lies between the two main bodies. Both of them are intruded after mineralization. They look fresh and are not affected by hydrothermal alteration.

3-6 IP Instruments

IP Transmitter

Model P 660 made by McPHAR Co., CANADA

Maximum output power	5A, 700V
Engine Generator	3.5 Kw, 400 Hz, 110 V

IP Receiver

Model P 660 made by McPHAR Co., CANADA

Fullscale 100 Microvolt

Transceiver

Model CH-1330 made by HITACHI Co., JAPAN

Maximum output power 500 mW, 10 sets

3-7 The Survey

Determination of the survey lines were based primarily on the results of the geological and geochemical survey. The final survey lines were decided considering the limitation and restrictions of the induced polarization survey method. From an expected distribution of IP anomalies, some additional survey lines were also planned.

The base station was not determined by solar observation as usually done in the Philippines but simply by locating the intercept point between survey line No. 3

and the base line on the 1/50,000 scale topographic map.

The barometer reading (164.70 m above the sea level) was employed as the elevation of the base station.

The surveyed area is situated between 100 m and 300 m above sea level. Because of the thick vegetation, fully grown plants were cut along all the surveyed lines.

The directions of the survey lines were referred from the magnetic north. The base line is in the direction of north-south and the survey lines are east-west.

The total length of the survey lines is 18.4 km, where the base line is 2 km and the total of the other survey lines including some additional lines is 16.4 km.

Survey lines are 250 m apart and measuring points were established every 100 meters. Along the eastern part of survey line No. 3, however, distance between measuring points is 50 m with additional complementary points introduced because of detected anomalies.

Instruments and Accuracy (Common with the Western Area)

Instruments used for the survey were USHIKATA handy compass S-25 and measuring tape of 50 m made by eslon and the accuracy of survey was more than 1/50.

Specifications are shown below;

A. USHIKATA handy compass S-25

Angle of inclination	Full circle divided into one degree scale division
Angle of declination	Zero back method

Telescope	X12 reversible
Fine adjust	Adjustable horizontally and vertically
Weight	1.3 Kg

B. Measuring tape (Eslon tape)

Factory inspected error	50 m - - - -26mm, +52mm
Tension Pull	150 Kg for 12 – 16 m tape width
Expansion	0.25 mm for 1 meter

3-8 Interpretation of Results of Survey

The results of induced polarization method (IP) survey are shown in PLIII-E2 to E11 as frequency effect (FE), apparent resistivity and metal conduction factor contours along a vertical section of each survey line.

Equi-FE map and equi-apparent-resistivity maps correspond to 100 M (N=1) and 200 M (N=3) under the surface are shown in PLIII-E12 to E17.

Remarkable anomalies shown in profiles along each survey lines are described in the following section.

3-8-1 Result of Survey along Each Line

Line No. 1 (PLIII-E2)

Apparent resistivity shows two layer structures with the upper layer of 150-400ohm-M and the lower layer of 400-800ohm-M. The upper layer seems to show the low resistivity of andesite. The lower layer is considered to be diorite.

Frequency effect (FE) shows only a slight anomaly of 4% at measuring point E-6.

Line No. 2 (PLIII-E3)

The andesite layer extended from survyy line No. 1 (150-400ohm-M) is dominant here. A high resistivity zone distributed at measuring points W-3 and 4 near surface seems to be the same diorite extending from survey line No. 1 as shallow intrusive bodies.

FE is almost as low as the back ground level everywhere except a weak anomaly near point W-1 where mineralization was observed at the surface.

Line No. 3 (PLIII-E4)

In the eastern part of Line No. 3, outcrops of andesite (150-400ohm-M) is probably the extension of the same andesite layer from survey line No. 1 and No. 2. The low resistivity zone reflects the existence of andesite layer. In the western part, only near points W-5 and W-6, a high resistivity zone due to diorite, is observed.

This might be the same body extended from measuring points W-3 and 4 of line No. 2.

FE shows only a weak anomaly at the east end of the line.

Line No. 4 (PLIII-E5)

The resistivity profile is separated in two parts, namely the western low resistivity (50-100ohm-M) zone and the eastern high resistivity (higher than 400ohm-M) zone. The geological map shows the low resistivity zone being basalt and the high resistivity zone being dioritic intrusives.

A remarkable FE anomaly of 10% is found in the low resistivity zone at E-3, which coincides well with the observed outcrops and geochemical anomalies. From the characteristic of this anomaly, any deep mineralized zone is not expected. Concerning the shape and properties of mineralized zone, see the result of the Model Calculations (PLIII-E18)

Line No. 5 (PLIII-E6)

As seen in the case of survey line No. 4, east of the base line is the low resistivity zone of basalt and west of it is the high resistivity zone of diorite. Under measuring point 0 (intercept with the base line), basalt is supposed to have diorite intrusion.

In the low resistivity zone, west of the small valley near point E-7, widely distributed FE anomaly is seen. As in the case of line No. 4, probable existence of a shallow mineralized zone is indicated.

Line No. 6 (PLIII-E7)

Now the high resistivity diorite zone is found in the central part between W-9 and E-1. And both ends of the line are in the low resistivity zone.

Near the surface between W-5 and W-6 which are in the high resistivity zone, FE anomaly of a probable mineralized zone is shown. FE anomaly extended from line No. 5 found at points E-2, 3 could have been due to the strong mineralization of pyrite.

Line No. 7 (PLIII-E8)

Near points W-2, 3, 6 and 7, the high resistivity zone recognized from the low resistivity basalt zone, indicates the existence of diorite very clearly.

The observed FE anomalies are expected to be in basalt zone and at the interface between the basalt and the diorite zones on this survey line.

Line No. 8 (PLIII-E9)

Basalt in the middle of this survey line shows a lower resistivity (less than 200 ohm-M) than that found in the northern area of line No. 7, and the intrusion of diorite is inferred to be very deep.

The remarkable anomalies of FE between points W-3 and E-2 are in basalt or diorite intruded into basalt. No anomaly of FE was observed in basalt and gabbro in the eastern part of E-8 where mineralization of pyrite and chalcopyrite is exptected.

Line No. 9 (PLIII-E10)

East of the base line, where basalt and gabbro occur, wide spread low resistivity zone is observed.

No FE anomaly was detected east of a mineralized zone in the small valley between points 0 and E-1, where 12 – 13% FE anomaly in this valley is due to mineralization of pyrite and chalcopyrite which appears to incline sharply to the east.

Anomalies of FE (6-9%) are widely found west of the base line where basalt and diorite might be extensively mineralized.

Base Line (PLIII-E11)

High resistivity zone observed between measuring point 10 and 13 is caused by a south dipping diorite which penetrates the surrounding basalt (of lower resistivity than 200 ohm-M).

A 8-9% FE anomaly is observed near the interface between this diorite and the basalt distribured in the southern area. Both seem to be very strongly mineralized. FE anomaly was not observed in the northern extension of andesite.

3-8-2 Equi-Frequency-Effect and Equi-Apparent-Resistivity Maps

Equi-Frequency-Effect Map

N=1 (depth 100 M) (PLIII-E12)

The remarkable anomalies seen in the middle of the surveyed area extending northeast which corresponds to the near surface occurrences of basalt are due to pyritization at shallow depths. The copper outcrops found near E-3 of line No. 4 and 0 of No. 9 also belong to this most prospective area of 6% FE.

The western portion of the diorite area does not show any anomaly except the 5-8% FE anomaly observed near its interface with andesite.

Andesite and micro diorite occur along the Taon River in the southeastern part of the surveyed area, where no significant anomaly is observed.

N=3 (depth 200 M) (PLIII-E13)

The anomaly caused by the shallow mineralized zone at E-3 of survey line No. 4 weakened in this map. Most features of the distribution of FE anomalies, however, do not change, since the sources of anomalies lie very deep.

Equi-Apparent-Resistivity Map

N=1 (depth 100 M) (PLIII-E14)

Apparent resistivity varies 50 to 1,000ohm-M and is divided into two zones, namely a high resistivity (higher than 500ohm-M) zone and a low resistivity (lower than 250ohm-M) zone.

The high resistivity zone surrounded by 500ohm-M equi-resistivity contour roughly coincides with the occurrence of diorite and porphyrite.

In the eastern part of the surveyed area, the low resistivity zone lies north and south. The low resistivity zone in the north reflects andesite and gabbro occurrences; the southern low resistivity zone reflects the basalt occurrences. The extremely low resistivity (less than 100ohm-M) zone seen around the measuring points E3 - E5 of survey lines No. 4, 5, 6 may be considered the area of hydrothermally altered basalt.

The fine grain diorite in the southeastern part of the surveyed area show low resistivity due to their high porosity.

N=3 (depth 200 M) (PLIII-E15)

The extension of the high resistivity zone observed in this map is wider than that of the map of N=1. The high resistivity zones around measuring points E-1, E-4 of survey line No. 1 and W-1 of line No. 2 are due to intrusions of diorite, emanating from a common rock body at depth.

The low resistivity zone lying north and south in N=1 map lies now south of survey line No. 3 in this map, suggesting the deep extension of hydrothermally altered basalt.

The andesite and gabbro in the northern part of the surveyed area correspond to the distribution of the resistivity of 250 - 500ohm-M in the northern part of the survey line No. 3.

The topographical effect is generally not observed except in the high resistivity zone at E-3 of the survey line No. 6.

3-9 Physical Properties of Collected Rock Samples

Physical properties of 32 rock samples collected in the surveyed area are shown in Table III-1.

Except ore samples, FE is under 4% similar to the background value measured in the field. In rock samples of comparatively high FE, pyrite mineralization is observed, indicating the anomalies being mainly due to pyrite.

Even the resistivity of rock samples of same material ranges 100ohm-M to several 10kohm-M. This large fluctuation of resistivity is mainly due to the degree of weathering of the sample taken in the field and also due to variation of the physical property during the transportation. Therefore the remarkable differences of apparent resistivity observed from place to place in the field was not confirmed in the laboratory.

3-10 Model Calculations

The shape and properties of source of observed remarkable IP anomalies were studied using an analogue computer.

The results are shown in PLIII E-18, E-19. These were calculated based on the anomalies observed at measuring points E-3, E-4 of survey line No. 4 and E-1, E-2 of line No. 7 from an assumed geological structure. A background value of 200ohm-M was assumed for the resistance network of survey line No. 4 and 400ohm-M for line No. 7.

Even though it is extremely difficult to find a real structure from thousands of possible combinations of shape and properties of the source of anomaly, the assumption of a shallow source for survey line No. 4 and a deep source for line No. 7 is very plausible.

Table III-1 Physical properties of the rock samples, Bislig Area

Sample No.	Rocks	Section (cm^2)	Length (cm)	Current (μA)	Potential (mV)	Resistivity (Ωm)	F E (%)
OW-1	Andesite	11. 65	2. 11	5 1	982. 0 192. 0	10, 700	1. 8
OW-2	Basalt	6. 08	1. 31	5 1	876. 0 178. 4	8, 210	1. 5
OW-3	Micro Diorite	5. 58	1. 44	5 1	1, 200. 0 334. 0	11, 100	0. 8
OW-4	Diorite	10. 71	3. 54	5 1	703. 6 151. 2	4, 420	0. 5
OW-5	Quartz Diorite	5. 62	1. 59	5 1	920. 0 202. 0	6, 820	1. 0
OW-6	Basalt	5. 79	3. 55	5 1	3, 382. 0 692. 0	11, 200	3. 5
OW-7	Micro Diorite	11. 27	3. 45	5 1	1, 198. 0 416. 7	10, 700	4. 2
OW-8	Micro Diorite	5. 67	2. 20	5 1	4, 185. 0 845. 0	21, 700	2. 4
OW-9	Micro Diorite	3. 85	2. 79	5 1	126. 0 25. 5	13, 400	1. 3
OW-10	Diorite	8. 39	2. 47	5 1	1, 434. 0 504. 2	13, 400	1. 3
OW-11	Micro Diorite	5. 83	2. 06	5 1	3, 440. 0 772. 0	20, 700	2. 3
OW-12							
OW-13	Silicified Lapilli Tuff	6. 21	1. 50	5 1	23. 28 4. 63	190	8. 8
OW-14	Andesite	4. 13	1. 63	2. 7 1	3, 110. 0 1, 230. 0	30, 200	-0. 1
OW-15							
OW-16	Micro Diorite	3. 38	3. 48	5 1	894. 0 196. 0	1, 820	1. 1
OW-17	Ore (origin: Basalt)	4. 44	1. 55	5 1	35. 3 7. 7	210	39. 8
OW-18	Andesite	7. 77	1. 90	5 1	264. 0 52. 0	2, 140	3. 4
OW-19	Andesite	9. 44	3. 80	5 1	902. 0 212. 5	4, 880	3. 7
OW-20	Basalt	6. 55	2. 46	5 1	435. 0 89. 2	2, 350	1. 8
OW-21	Andesite	2. 25	2. 80	5 1	1, 018. 0 245. 5	1, 800	1. 9
OW-22	Basalt	8. 02	1. 95	5 1	1, 118. 0 279. 0	10, 300	1. 3

Sample No.	Rocks	Section (cm^2)	Length (cm)	Current (μA)	Potential (mV)	Resistivity (Ωm)	F E (%)
OW-23	Basalt	8.58	1.99	5 1	4,982.0 984.0	42,700	2.3
OW-24	Basalt	9.25	1.70	5 1	82.42 17.82	930	0.5
OW-25	Basalt	14.17	2.19	5 1	653.0 122.9	8,200	3.8
OY-1	Micro Diorite	7.22	1.79	5 1	410.0 86.8	3,400	4.9
OY-2-2	Quartz Diorite	9.53	2.96	5 1	311.1 73.5	2,200	-0.1
OY-2-3	Diorite	5.97	1.63	5 1	131.4 25.98	960	1.9
OY-3	Basalt	7.98	2.45	5 1	6,230.0 1,311.0	41,200	1.5
OY-4	Diorite	9.69	2.10	5 1	627.8 149.4	6,340	1.5
OY-5	Andesite	9.91	1.61	5 1	199.1 39.7	2,450	2.9
OY-6	Micro Diorite	7.38	2.53	5 1	812.0 222.7	5,620	1.3
OY-7	Quartz Diorite	12.95	2.33	5 1	364.5 84.4	4,370	1.7
OY-8	Quartz Diorite	8.55	2.80	5 1	619.0 137.0	3,980	0.0

4. Result of Induced Polarization Survey in the Western Area

4-1 Surveyed Area

The surveyed area is situated 150 Km southeast of Valencia, in Bukidnon Province in MINDANAO Island.

It is bounded by

Latitude 7° 46' 41" and 7° 48' 34" N (3.5 Km north to south),

and

Longitude 125° 17' 04" 125° 19' 00" E (1.2 Km east to west).

The base station lies approximately at

Latitude 7° 47' 38" N and Longitude 125° 17' 23" E

K-Line No. 35

4-2 Period of the Survey

The survey started March 7, 1973 and concluded on April 18, 1973 with 30 days of actual work during 41 days of stay in the area.

4-3 Members of the Survey Team

WENCESLAO ARGAÑO	ASAHI HATTORI
MARCELINO APELO	OSAMU KUSAKA
EMIL T. AVILA, Jr.	HITOSHI ITO
ELIGIO ARIATE	TOSHIAKI FUJIMOTO
	TOMIO TANAKA

4-4 Place and Transportation

Valencia is situated about 130 Km south of Cagayan de Oro City along the national high way Route 3, and San Fernando, where the base camp for food supply was settled, is about 20 Km East of Valencia.

Barrio Katipunan is the terminal village for the transportation of members and surveying goods by logging trucks, from where all the equipments and foods were carried by human power for about two hours along Tigua river and its upstream Tagbiga.

The base camp was settled beside Tagbiga river in the middle of the surveyed area, but the area was so extensive and rugged that it took about half an hour on foot to reach the nearest line and one and one half hour to the farthest line.

More than 40 laborers always lived in the camp, so that a few laborers went to and from San Fernando every day to replenish their food supplies in the camp.

4-5 Geological Features

Geology of the surveyed area is comparatively simple. Normal sediments such as conglomerate, sandstone and mudstone belonging to the Kalagutay group of early to middle Miocene age, are intruded by pyroxenite and diorite during late Miocene.

Quaternary andesite lava covers partially the rocks mentioned above.

Pyroxenite and diorite occupy more than half of the surveyed area.

The trend of these intrusive rocks coincide with the general strike ($N5^{o}W$) of sedimentary rocks.

About 500 ~ 1,000 m eastwards from the contact between intrusive rocks and the normal sediments, diorite intrude into pyroxenite in dyke and network form, and it appears to be a composite body.

Further eastward, the composite body changes gradually to pyroxenite with few diorite dykes.

Pyroxenite in this area is dark green or dark gray holocrystalline rock composed of augite, hornblende, biotite and magnetite. 5% ~ 10% of magnetite grains are included in the pyroxenite.

Diorite is fine grained holocrystalline rock consisting of biotite, plagioclase, augite and a few magnetite.

Thermal metamorphism of the sedimentary rock is not recognized. Impregnations of pyrite are observed in some places of the intrusive rocks. Further more a few veinlets of chalcopyrite and other ore minerals are also found mainly in the composite body.

4-6 IP Instruments

IP Transmitter

Model 506 made by CHIBA Electronic Laboratory, JAPAN

Maximum output power 2.5A, 800 V

Engine Generator Model MK-2 2.0 Kw, 400 Hz, 115 V

IP Receiver

Model YMO-412 made by YOKOHAMA Electronic Laboratory, JAPAN

Fullscale 10 Microvolt

Transceiver

Model CH-1330 made by HITACHI Co., JAPAN

Maximum output power 500 mW, 10 sets

4-7 Survey

Lines and Bench Mark

The IP survey lines were planned by the geological team based from the results of the geological and geochemical surveys. The base line was brushed along the general direction of copper outcrops and geochemical anomalies.

Ten IP survey lines were planned including one base line but one additional line was surveyed considering the results of IP survey, namely A Line, B Line, -----, J Line from the north and K Line as the base line. The direction of the base line is N15^{o}E (magnetic north) and the other lines intercept it at right angle each 400 m apart.

The base station was selected at the intercept of F Line and K Line (K-33) using the elevation of 800 m from the enlarged map of 1/10,000, for lack of an established bench mark in this area.

The length of every survey lines are as follows,

A, C — J Line	9 lines each 1,200 m	total	10,800 m
B Line			2,600
K Line			3,300
		Total	16,700 m

Actual Survey

As thick vegetation covers the area and the topography is very steep, the compass and tape traverse survey was conducted.

Measuring instruments were USHIKATA handy compass S-25 and eslon measuring tape with an accuracy of more than 1/50.

Measuring points were established 100 m interval and complementary points at 50 m interval. Circular calculator and a table of horizontal distances were used in the field.

Elevation of the measuring points ranges from 640 m to 1,250 m.

Average inclination of the surveyed line is generally from 25^{o} ~ 35^{o}. In the southern part of the area, more than 50^{0} slope was recorded between two points.

4-8 Interpretation of Results of Survey

The results of survey were interpreted by two dimensional analysis of their profile along each survey line and three dimensional analysis of their plane distribution over the surveyed area.

Two typical anomalies (line A and I) were further studied quantitatively by model calculations.

Profiles of frequency effect (FE), apparent resistivity and metal conduction factor are shown in PLIII-W2 ~ W12 together with the topographical profiles. Their horizontal plane sections are shown in PLIII-W13 ~ W18 for the depths N=1 and N=3.

4-8-1 Interpretation of Profiles at Each Survey Line

Line A (PLIII-W2)

A typical anomaly of over 10% FE was detected in the eastern part of the survey line at measuring points 18–21. According to the model calculations later described, this anomaly is considered to be caused by a 150 M wide mineralization with a westward dip. It might be due mainly to disseminated pyrite.

An anomaly of 4~5% FE was observed at 100 M under measuring point 10, which indicates nearly 200 M of extension of a mineralization with a width of about 100 M.

Except the high resistivity of topographical influence observed at both ends of this survey line, the resistivity is low especially at measuring point 8 (lower than 50ohmM) where the late andesite lava cover exists.

Line B (PLIII-W3)

The wide and strong FE anomaly is found in the eastern portion of the survey line. Anomalies of over 6% FE are all located within pyroxenite area to the east of the small valley around measuring point 20. Notably, the remarkable anomaly zone seen around point 45 east of point 36, indicate that pyroxenite is mineralized from shallow to deeper places. The nanomaly is due to magnetite in the pyroxenite and partly due to pyrite mineralization.

The apparent resistivity varies from several 10 to 600ohmM divided into two zones, namely that of andesite west of point 11 with resistivity value of about 600ohmM, and that of diorite and pyroxenite in the east with about 150ohmM resistivity.

The large scale topographical unevenness influenced very much the apparent resistivity, so that one third to four times as much as the true resistivity are observed at points 18, 24, 32 and 43 as high resistivity and at points 28, 40 and 46 as low resistivity.

Line C (PLIII-W4)

6-8% FE anomaly observed at points 20-22 should correspond to a shallow mineralization in pyroxenite and extends over the north gully to the anomaly of measuring point 22 of line B.

In the west side of the valley at point 12, resistivity is low (under 100ohmM), showing a high porosity of sedimentary rocks. FE is also low (-0.5 to 1.0%) there indicating absence of mineralization.

Line D (PLIII-W5)

This line was additionally surveyed along the valley of Tagbiga and its branch to study the very extensive anomaly zone discovered on survey line B. FE anomaly as much as 10% was observed all over this additional survey line. As in the case of line B, the anomaly seems to be of magnetite or pyrite mineralization of pyroxenite and near point 20, it coincides with the low resistivity zone and the mineralized zone is expected to extend at depth.

The resistivity of pyroxenite was estimated from the average resistivity along this line as 150ohmM where topographical influence is negligible.

Line E (PLIII-W6)

No remarkable anomaly was observed except the slight anomaly of FE 5% about 150 M under point 19 which is considered to be the west edge of the mineralized zone extending northward by northwest.

No clear contrast of apparent resistivity was obtained becuase of topographical fluctuations.

Line F (PLIII-W7)

FE anomalies found in the eastern part of the survey line are owing to mineralization of pyroxenite shown at the surface or point 16 and east of point 19. As observed on rock samples R-1 ~ R-3, pyroxenite is mineralized strongly in the area even at the surface.

The anomaly extends to great depth and the resistivity is considerably low so that an additional survey is recommendable in the eastern part of this line.

Low resistivity of sedimentary rocks was observed west of point 9.

Line G (PLIII-W8)

Very clear FE anomaly whose centre is at point 18 is in an area of pyrorenite-diorite composite body. A source of anomaly about 200 M wide (point 16 ~ 20) and more than 150 M deep with a westward dip can be supposed.

The rock samples collected at the surface has high content of pyrite as well as magnetite and the FE anomaly higher than 13% must have originated from the pyrite.

Line H (PLIII-W9)

The wide distribution of FE anomaly east of the gully at point 16 was confirmed by measurements every 50 M. The rock samples collected at the surface showed strong mineralization of magnetite and pyrite in the pyroxenite-diorite composite body. The resistivity being comparatively low, point 16 can be a prospective boring point.

Line I (PLIII-W10)

A result of model calculations based on the result of survey along this line is shown in PLIII-W20. According to that, the source of anomaly is at the depth of about 150 M and about 200 M wide with a westward dip. FE was assumed 20%. As seen in the case of rock sample R-9, the mineralization might be partially intensive.

Line J (PLIII-W11)

From now on the centre of the anomaly is in the western part of line K. Typical shape of a couple of anomalies extending with 45^{o} inclination as shown in the profile indicates a strong mineralization localized near the surface around points 11~13.

West of these couple of anomalies, resistivity is so low that a distribution of porous rocks is expected.

Line K (PLIII-W12)

In the resistivity profile after the removal of topographical fluctuations, a uniform distribution of resistivity of 100-200ohm-M of pyroxenite is seen.

In the FE profile, south of point 45, a north by northeast extension of mineralization is indicated by a widely distributed anomaly of 5.0%.

The 6-8% anomaly at point 46 was also recognized by some outcrops and a copper anomaly observed in the geochemical survey. Its size is not large but it is clearly a shallow anomaly.

Also at point 54 near the surface, a small source of anomaly is seen. South of this point is the extension of the anomaly described in relation to line I and line J.

4-8-2 Interpretation of Plane Maps of Each Depth

Equi-Frequency-Effect Map

N=1 (depth 100 M) (PLIII-W13)

The anomaly was detected on point 11 of line J and extend to point 13 to 19 on line I, point 15 to 23 on line G and point 19 to 25 on line F. The anomaly was not detected on line E but reappeared strongly all over on line D, extending to point 36 to 53 on line B and point 16 to 21 on line A. Although there is lack of information about this anomalous zone in the area between line C and line E, which are 700 meters apart, the area surrounded by 7% FE contour almost agrees with the distribution of mineralized zone.

2% FE contour defines well the geological borderline between sedimentary rocks and pyroxenite.

N=3 (depth 200 M) (PLIII-W14)

Main features of the map are almost the same as the map N=1. The shallow anomaly at point 11 of line J, however, has disappeared, on the contrary, the anomaly extending north by northeast is now more distinct by the deep anomaly under point 18 of line H.

The anomaly zone of line I – line F extends almost due north and due south along the east of the gully at point 16 of line G. This might show that mineralization occurs along the sheared zone and the source of anomaly varies in width and depth as the scale of the sheared zone as seen in the shallow anomaly of line J or the deep anomaly of line H.

<u>Equi-Apparent-Resistivity Map</u>

<u>N=1 (depth 100 M)</u> (PLIII-W15)

Apparent resistivity measured by dipole method involves not only topographical influence but also an erroneous resistivity of the surface in 45° directions. To avoid it, the average resistivity of three nearest neighboring point

$$\rho_c = (\rho_1 + \rho_2 + \rho_3) \ / \ 3$$

is employed in the maps.

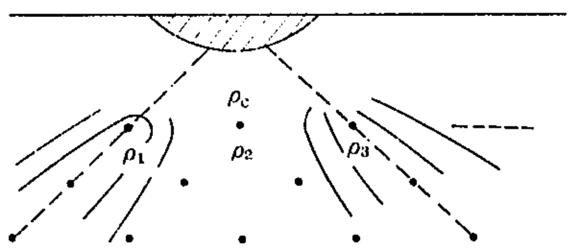

The 100ohmM equi-resistivity contour parallel to line K agrees very well with the borderline between pyroxenite and sedimentary rocks shown in the geological map, and the resistivity of the pyroxenite and the sedimentary rocks are estimated to be 150ohmM and 60ohmM respectively. Pyroxenite has a resistivity of 200ohmM in the high resistivity zone on the hill at the eastern end of lines G, H, I and J.

On the other hand the contour of 50ohmM at line A shows moist andesite exist there.

The variation of resistivity described above are considered to be due to real geological differences and the contours are expressed in thick lines. The other contours which might be due to topographical influence or very local variation and have little meaning with the inter-survey-line distance of 400 M are expressed in broken lines.

N=3 (depth 200 M) (PLIII-W16)

The geological variation of the distribution of resistivity shown in the map of N=1 has dissappeared in this map.

Since topographical effect is strong and it is very difficult to relate the results of survey of neighboring lines, the contours in this map are all expressed in broken lines.

Equi-Metal-Conduction-Factor Map (PLIII-W17, W18)

The distribution of metal conduction factor (MCF) over 50mho/M agrees with that of the mineralized zone. At some places as point 14 of line G and point 8 of line J, however, MCF is high due to low apparent resistivity caused by topographical irregularity and the detail of the structure cannot be observed.

It should be necessary to survey further the anomaly extending northeast by southwest between point 20 of line D and the eastern end of line E, since the anomalous source extends persistently at depth in line D.

4-9 Physical Properties of Collected Rock Samples (Table III-2)

Resistivity of rock samples collected at the surface varies considerably with the degree of weathering, chemical change and other conditions after their collection.

The resistivity of the collected rock samples measured in the laboratory cannot be correlated with resistivity obtained in the field. Resistivity of the rocks in the laboratory is usually higher than that measured in the field.

In all the samples with FE higher than 3%, magnetite and pyrite are clearly visible to the naked eye.

Sedimentary rocks have less FE than 2%, which agrees with the value of the low FE zone in the western part of the surveyed area.

From the observation of external appearance and thin section under the microscope, it is concluded that the rocks of high FE contains considerable amount of magnetite which forms strong source of FE anomaly together with pyrite.

4-10 Model Calculations

In the course of quantitative study of the observed IP anomalies, many precedent model calculations were applied. For the two remarkable anomalies at lines A and I, model calculations were carried out by an IBM360 Model J/195 computer.

As shown in PLIII-W19, W20, the underground was divided hypothetically into about 1,400 grids each named with a 'code number'. The values of resistivity and FE were given as parameters to each grid and the two-dimensional resistance networks were solved by Gaus-Seidel iteration.

The combination of resistivity and FE and the shape of the source of anomaly was changed several times so as to find an optimum solution by which the result of calculation comes closest the observed value.

Table III-2 Physical properties of the rock samples, Tagbiga Area

Sample No.	Rocks	Section (cm^2)	Length (cm)	Current (μA)	Potental (mV)	Resistivity (Ωm)	F E (%)
R-1	Feldspar vein	4. 10	1. 58	5 1	55. 2 10. 6	280	12. 3
R-2	Pyroxenite	4. 07	1. 40	5 1	56. 4 10. 6	320	9. 7
R-3	Pyroxenite	10. 21	1. 15	5 1	46. 2 8. 91	810	18. 0
R-4	Conglomerate	10. 07	2. 38	5 1	224. 0 49. 56	2, 050	0. 7
R-5	Pyroxenite	12. 83	1. 96	5 1	223. 2 52. 05	3, 160	2. 7
R-6	Pyroxenite with diorite net	11. 65	1. 80	5 1	75. 5 14. 92	970	8. 3
R-7	Micro Diorite	9. 63	1. 39	5 1	603. 2 118. 2	8, 270	4. 1
R-8	Pyroxenite	11. 84	1. 81	5 1	207. 0 41. 7	2, 720	13. 4
R-9	Pyroxenite	5. 30	2. 15	5 1	137. 6 27. 5	680	28. 8
R-10	Pyroxenite with diorite net	4. 90	3. 48	5 1	23. 04 4. 58	65	18. 4
R-11	Pyroxenite	8. 60	1. 22	5 1	67. 8 13. 4	950	0. 6
R-12	Sandy Tuff	12. 08	1. 68	5 1	4. 37 . 82	61	0. 5
R-13	Pyroxenite	8. 52	3. 86	5 1	866. 6 176. 2	3, 860	11. 0
R-14	Pyroxenite	7. 13	1. 53	5 1	50. 2 9. 8	460	58. 0
R-15	Pyroxenite	5. 76	1. 55	5 1	83. 1 15. 7	600	27. 4
R-16	Pyroxenite	11. 53	1. 45	5 1	24. 7 4. 84	390	6. 9
R-17	Andesitic Tuff	7. 85	2. 26	5 1	101. 1 20. 7	710	1. 6
R-18	Taffaceous shale	6. 93	1. 58	5 1	42. 4 8. 48	370	0. 1
R-19	diorite net with diorite net	11. 39	1. 93	5 1	124. 0 24. 86	1, 470	22. 5
R-20	Pyroxenite with diorite net	7. 15	1. 31	5 1	92. 6 18. 5	1, 010	3. 0
R-21	Pyroxenite with diorite net	4. 85	1. 30	5 1	104. 5 20. 6	770	29. 9

Sample No.	Rocks	Section (cm^2)	Length (cm)	Current (μA)	Potential (mV)	Resistivity (Ωm)	F. E (%)
R-22	Pyroxenite	8.75	1.33	5 1	223.2 52.05	3,180	2.7
R-23	Pyroxenite	9.88	1.65	5 1	82.4 16.34	980	1.2
C-58	Red Tuff	6.48	1.33	5 1	54.6 10.7	530	0.2

5. Conclusion and Future Prospect

5-1 Eastern Area

The apparent resistivity varies widely from 50ohmM to 100ohmM and the contrast between the low and the high resistivity zone is considerably clear.

Dioritic rocks in southwestern part of the surveyed area have high resistivity ranging from 500-1,000ohmM. From this property the distribution of dioritic rocks was well interpreted at the surface as well as in depth.

Basalt showed low resistivity from 100 to 250ohmM, and less than 100ohmM in the hydrothermally altered zone which coincides with a high FE zone.

As for FE anomaly which indicates mineralization, a remarkable anomalous zone extending to the northeast was detected in the middle of the surveyed area. The anomalies at point E-3 of line No. 4 and point 0 of line No. 9 should be at or near the surface, and outcrops of pyrite and chalcopyrite were discovered by the geological survey at those particular points.

The other FE anomaly extending to the east of point E-1 of line No. 5 and to the west of point 0 of line No. 9 could be due to basalt in dioritic rocks and mineralization from the surface to the depth of dioritic rocks in the western part of the surveyed area. According to the geological survey, the FE anomaly conforms mainly with the pyritized zone. Since this zone coincides with the low resistivity zone with alterations, it should be the most prospective area.

The ore deposit which is expected in this area lies probably at the interface between basalt and diorite. From 6 to 8% FE anomaly is considered to be the most promising zone of copper deposit extending to the southwestern part of point E-1 of line No. 6, point 0 to W-1 of line No. 7 and point W-2 of line No. 8

In this zone, point E-1 of line No. 6 is recommended as the interesting boring site.

To investigate further the anomaly found in the basalt, a bore hole site within the vicinity of point E-3 on line No. 4 is highly recommended.

As a future plan, an additional IP survey is necessary to study further the distribution of the well defined anomaly observed on survey lines No. 8 and No. 9 which might be considered extending to the southwest of this area.

5-2 Western Area

Since this broad survey of IP over an area 3,300 M long from the north to the south and width varying from 1,200 - 2,600 M from the east to the west was planned well and taking into consideration the results of geological and geochemical surveyes, we could get a significant information about the distribution of mineralized zone from well defined IP anomalies.

Equi-FE contour of 7% shown in PLIII-W13, 14 corresponds very well to the distribution of mineralization. This anomaly zone is observed only in the pyroxenite and the composite body of pyroxenite and diorite in the eastern portion of the surveyed area. No anomaly is detected in the sedimentary rocks in the western portion of the area.

The strong and deep anomaly observed in the eastern part of line B and the whole part of line D is considered to be due to fresh magnetite grains in pyroxenite or mineralization of diorite intrusive at depths.

Having partially low resistivity, this area is most interesting shown by the result of the geophysical survey.

The shape and source of anomalies distributed in the direction of north-south in the southern part of the surveyed area varies from survey line to survey line. This variation of shape of anomalous zone is probably due to the effect of the distribution of intrusive bodies and the concentration distribution of magnetite and/or due to the magnetite grain distribution over the sheared zone along the gully passing point 16 on line G.

Along line F and line H, a wide and deep anomaly was observed.

Although topographical elevations vary considerably and the results of the apparent resistivity is influenced much by the topographical irregularity, the low resistivity sedimentary rocks and andesite are well distinguished from the high resistivity pyroxenite and composite body of pyroxenite and diorite.

Despite the fact that the copper anomaly is weak in the geochemical survey, the strong FE anomalous zone described in the IP survey is recommended to be surveyed hereafter as it might be the halo of a porphyry copper deposit.

Furthermore the gap between the anomaly zones striking NE-SW, that is east of line E and F and to the south of line D, is desired to be investigated.

According to the results of the geophysical survey, point 20 of line D shows the most consistent IP anomaly. This point is recommended as the most prospective boring site.

Point 16 of line H, where a comparatively broad N-S extension of IP anomaly is expected, might be the secondary proposal site of boring.

In the future surveys, application of the magnetic observation as well as the self potential method (SP) is desired as a complementary survey to the IP method, since the IP anomaly detected in the survey is considered to be due mainly to fresh magnetite.

Magnetic measurements could be very effective in the identification of ore and the determination of the distribution of igneous rocks.

APPENDICES

Table 1. Fossils

1. Smaller Foraminifera

In the 14 foraminiferous samples, benthonic foraminifera is more common than planktonic foraminifera. Among them samples G-35 and G-52 consist of a few species of benthonic forms which indicate shallow water environment of inner-bay condition. Samples b-102 and E-0 contain also shallow water benthonic species. Planktonic foraminifera is common in four samples (CN-11, D-35, E-5 and B-68), which consist of Middle Miocene planktonic fauna associated with benthonic foraminiferal assemblage indicating deep-water environment. It is noteworthy that two species of Ostracoda are commonly found in samples E-56A and h-59.

Sample No.	Locality	Group or Formation	Benthonic Foraminifera	Planktonic Foraminifera	Geological age	Paleoecology
B-68 (Mudstone)	Halapitan	Kalagutay G.	Nodosaria longiscata Sphaeroidina bulloides Stilostomella lepidula Uvigerina cf. proboscidea Cassidulina subglobosa	Globorotalia cf. menardii G. mayeri G. praemenardii Globigerina sp. Globoquadrina altispira Globigerinoides ruber G. trilobus Globigerinita glutinata Orbulina bilobata O. suturalis O. universa	Middle Miocene	Deep water
b-102 (Limy sandslone)	do	Lumbayao F.	Pseudorotalia (?) sp. Elphidium sp. Operculina sp. Amphistegina sp. Cibicides sp. Hanzawaia nipponica		Younger age	Shallow water
CN-11 (Mudstone)	Tagbiga C.	Kalagatay G.	Nodosaria longiscata Globobulimina sp. Uvigerina cf. proboscidea Amphistegina sp. Cibicides (?) sp.	Globigerinita cf. glutinata Globoquadrina cf. venezuelana Orbulina suturalis O. universa	Early or Middle Miocene	Deep water

Sample No.	Locality	Group or Formation	Benthonic Foraminifera	Planktonic Foraminifera	Geological age	Paleoecology
D-35 (Siltstone)	Nilabsan R.	Kalagatay G.	Eggerella sp. Amphistegina sp. Gyroidina sp.	Globigerina spp. Globigerinoides sacculifer G. cf. trilobus Orbulina suturalis	Early or Middle Miocene	Deep water
E-5 (Andesitic tuff)	Davao R.	do	Calcarina sp. Elphidium cf. craticulatum E. crispum Operculina sp. Poroeponides cribrorepandus Amphistegina sp. Cibicides pseudoengerianus C. sp.	Globorotalia mayeri Globigerinoides ruber subquadratus G. sacculifer Orbulina universa	Early or Middle Miocene	Shallow
E-56A (Mudstone)	Dacongbonwa R.	Barcelona G.	Pyrgo sp. Uvigerina sp. Ammonia beccarii Pararotalia sp. Elphidium craticulatum Operculina sp. Cibicides sp. Florilus sp.		Not clear	Shallow water
E-56B (Mudstone)	do	do	Elphidium craticulatum		Not clear	Not clear
E-59 (Calca)	do	do	Pyrgo sp. Triloculina sp.		Not clear	Not clear
E-0 (Limestone)	Sanco Point	Agtunganon F.	Ammonia beccarii Elphidium cf. advenum E. sp. Nonionella sp.		Younger age	Shallow
G-35 (Mudstone)	Simulaw R.	Kapalong F.	Elphidium advenum E. craticulatum E. sp. Ammonia beccarii A. sp.		Pliocene~ Pleistocene	Shallow water

Sample No.	Locality	Group or Formation	Benthonic Foraminifera	Planktonic Foraminifera	Geological age	Paleoecology
G-52 (Mudstone)	Pasian R.	Kapalong F.	Ammonia beccarii Elphidium craticulatum		Piocene-Pleistocene	Shallow water
G-313 (Mudstone)	Pagtitaan R.	Mangagoy F.	Uvigerina sp. Melonis cf. pacificus	spp. (indeterminable)	Not clear	Not clear
G-313 (fine sandstone)	do	do	Bolivinopsis sp. Textularia spp. Dorothia sp. Martinottiella sp. Melonis cf. pacificus	Globigerinoides spp. spp. (indeterminable)	Not clear	Not clear
h-59 (Mudstone)	Ngan R.	Kaban G.	Elphidium craticulatum E. sp.		Not clear	Not clear

2. Larger Foraminifera

Larger Foraminiferal Fauna \ Sample No. and Formation	(Eastern Area)	E-I (Mangagoy F.)	E-P (do)	E-V (do)	E-W (Float)	P-27 (Mongagoy F.)	P-28 (do)	P-29 (do)	f-498 (do)	P-512 (do)	P-522 (Agtuuganon F.)	P-538 (Dacongborwa F.)	P-555 (do)	P-564 (Agtuuganon F.)	P-575 (Dacongbonwa F.?)	P-578 (Mangagoy F.)	G-307 (Agtuuganon F.)	G-315 (Mangagoy F.)	G-316 (Agtuuganon F.)	H-14 (Mangagoy F.)	H-260 (Float)	Sabena Mine	(Western Area)	BT-2 (Kalagutay G.)	C-55 (do)	C-58 (do)	C-10 (do)	E-13 (do)	E-14 (do)	E-15 (do)	E-25 (do)	E-26 (do)	E-28 (do)
Nummulitidae																																	
Nummulitinae																																	
Nummulites sp.			○													○																	
Operculina ammonoides (Gronovius)				○				○																									
O. venosa?				○										○																			
O. sp.					○														○		○						○						○
Heterosteginae																																	
Heterostegina borneensis van der Vlerk		○					○	○		○												○		○									
Spiroclypeus tidoenganensis van der Vlerk										○																							
S. margaritatus Schlumberger								○		○												○											
S. leupoldi van der Vlerk						○	○			○																							
S. cf. higginsi Cole																				○													
S. sp.						○																											
Cycloclypeinae																																	
Cycloclypeus communis Yabe and Hanzawa				○	○	○		○	○																						○		
C. eidae Tan							○	○		○															○		○						○
C. posteidae Tan				○																													
C. carpenteri Brady				○																							○						
C. cf. carpenteri Brady																											○						
Lepidocyclinidae																																	
Nephrolepidina sumatrensis (Brady)				○																	○						○						
N. inflata Provale					○													○								○	○				○		
N. angulosa Provale									○									○		○	○					○							
N. japonica Yabe																		○								○					○		
N. cf. cebuensis Yabe and Hanzawa																				○							○						
N. inornata Rutten									○						○						○			○		○						○	○
N. ferreroi Provale																					○						○						
N. verbeeki Newton and Holland																					○											○	
N. parva Oppenoorth				○					○	○					○			○			○					○	○					○	○
N. sp.			○															○															
Eulepidina planata Oppenoorth				○																											○		
E. formosa Schlumberger				○						○																							
E. favosa Cushman									○																								
E. sp.																																	
Miogypsinidae																																	
Miogypsinoides abunensis (Tobler)															○																		
M. dehaarti van der Vlerk															○						○					○					○	○	
M. formosensis Yabe and Hanzawa																					○					○						○	
Miogypsina thecidaeformis Rutten				○														○			○					○	○				○	○	
M. polymorpha Rutten																		○			○			○			○					○	○
M. inflata Yabe and Hanzawa																										○							
M. globulina (Michelotti)				○														○			○			○		○	○				○	○	
M. sp.				○	○													○							○		○						
Amphisteginidae																																	
Amphistegina radiata (Fichtel and Moll)				○	○						○	○				○	○	○			○			○		○	○		○	○	○	○	○
Alveolinidae																																	
Borelis pygmaeus (Hanzawa)						○	○											○															
B. sp. A.							○					○																					
Flosculinella bontangensis Rutten																														○	○		
F. globulosa Rutten																										○							
Miliolidae																																	
Fabulariinae																																	
Austrotrillina howchini (Schlumberger)							○								○			○								○	○				○	○	○
Miliolinae																																	
Kanakaia cf. marianensis Hanzawa													○																			○	
Peneroplidae																																	
Soritinae																																	
Sorites martini Verbeek				○									○		○			○						○		○					○		○
Marginopora vertebralis Blainville															○						○					○							
Planorbulinidae																																	
Planorbulinella larvata (Parker and Jones)															○	○					○			○		○	○					○	
P. sp. B.													○								○												
Homotrematidae																																	
Homotrematinae																																	
Homotrema rubrum (Lamarck)													○												○	○	○						
Sporadotrema cylindricum (Carter)								○										○			○			○					○			○	○
Victoriellinae																																	
Carpenteria utlicularis (Carter)																												○				○	
C. proteiformis Goes															○									○		○		○					
C. sp.						○												○				○		○	○	○	○				○	○	
Acerbulinidae																																	
Acerbulina inhaerens Schultze				○									○								○					○	○				○	○	○
A. linearis Hanzawa																		○						○									
A. (Ladoronia) vermicularis Hanzawa																					○					○					○		
Gypsina globulus Reuss		○				○	○	○	○							○	○									○	○					○	○
G. vesicularis (Parker and Jones)												○				○					○						○			○		○	
Cymbaloporidae																																	
Halkyardia minima (Liebus)																																	
Geological age: Pleistocene (Th)*											○			○			○			○													
Geological age: Middle Miocene (Tf)												○	○												◌		○			○			◌
Geological age: Lower Miocene (Upper Te ~ lower Tf)					○										○						○				○	○					○	○	○
Geological age: Upper Oligocene (Te ~ Upper Te)		○		○		○	○	○	○	○						◌		○		○		○		○									
Geological age: Middle Oligocene (Td)			○													○																	

Remarks * West Pacific Standard

Table 2. Potash-Argon ages on some intrusive rocks

Sample No.	Location	Rock	Mineral	Potash content %	Air contamination %	Age year	Remarks
B-44	*Locawon* R.	*Hornblende-biotite-clinopyroxene* gabbro	*Biotite*	4.47	35.53	11×10^6	Late Miocene
E-20	Sita R.	Altered dioritic rock	Plagioclase	0.17	89.81	20×10^6	Early Miocene
E-27	do	Hornblende andesite (dike)	Feldspar & Homblende	2.08	19.79	21×10^6	do
F-409	*Taon* R.	*Altered quartz diorite*	*Colorless mineral*	0.49	40.62	129×10^6	Early Cretaceous
H-84	Ngan R.	Hornblende andesite (dike)	Hornblende	0.77	47.92	21×10^6	Early Miocene
H-9	Agusan R.	Altered biotite-hornblende granodiorite	Hornblende	0.54	23.11	60×10^6	Late Paleocene

Explanation:

From the field observation, B-44 and E-20 rocks seem to be intruded at the same time. *The potash content of E-20 sample shows very low* and the air contamination is very high so that the measured age is not so reliable.
Therefore, the intruding age of both rocks is surely Late Miocene.

F-409 quartz diorite is too old in absolute age. This datum does not coincide with the field evidences. Though the writers think its age as to be Late Miocene tentatively, it is desirable to carry out more detailed geological survey in Phase III.

Table 3. Microscopic observations

Sample No.	Location	Group or Formation	Rock	Macroscopic features	Microscopic observations	Remarks
	(Thin Section)					
A-3	Koburocanan C.	Kalagutay G.	Andesite	Pale gray, coarse-grained rock.	Crystals of plagioclase (0.5 mm ~ 1 mm in length) and chloritized biotite occur in a less clearly defined glassy matrix. Lithic fragments can not be observed. Secondary minerals are chlorite, calcite, epidote, prehnite, sericite, quartz and sphene.	
A-4	do	do	Andesite	Dark gray, compact rock.	Composition is quite similar to A-3, although crystals are fine and there are a small amount of lithic fragments. Secondary minerals are chiefly calcite, chlorite and opaque minerals.	
A-5	do	do	Altered andesite	Grayish green, coarse-grained rock with white veinlets.	Lithic fragments of porphyritic augite andesite and phenocrysts of augite, plagioclase and hornblende are in a argillaceous matrix. Chlorite, epidote, calcite, prehnite and laumontite occur as secondary minerals.	
B-13	Mampilo C.	do	Basic conglomerate	Grayish green rock with many kinds of pebbles (diameter is up to 1 cm).	Pebbles of serpentinite, dolerite and gabbro are cemented by radiated zeolite (thomsonite?). Fragments of pyroxene and chlorite are also present.	
B-17	do	Intrusives	Serpentinite	Yellowish dark green rock.	Mafic minerals are completely serpentinized and show mesh structure. A few opaque mineral is recognized along small cracks.	
B-24	do	do	Dolerite	Dark gray, compact rock.	Microphenocrysts of twinned plagioclase are in a matrix of twinned plagioclase laths, clinopyroxene, sphene and opaque minerals. Matrix shows intergranular texture.	
B-25	do	do	Cataclastic clinopyroxene gabbro	Grayish white rock with black spots.	Holocrystalline. Twinned plagioclase, clinopyroxene, clinozoisite (aggregate of small crystals) and serpentine are the main constituents. Plagioclase and clinopyroxene crystals are crushed by cataclasis. Clinozoisite is interstitial to plagioclase.	
B-26	do	do	Olivine-clinopyroxene gabbro	Medium-grained holocrystalline rock.	Plagioclase, clinopyroxene and olivine are the principal minerals. Plagioclase shows carlsbad or albite twinning and partly altered to clay minerals. Clinopyroxene and olivine are almost serpentinized. Opaque minerals are recognized also.	See PL-1A

Sample No.	Location	Group or Formation	Rock	Macroscopic features	Microscopic observations	Remarks
B-32	Kalakangon R.	Kalagutay G.	Argillaceous tuff	Greenish gray, compact rock with white veinlets.	Many volcanic fragments (chiefly feldspar and augite) are welded by volcanic glass and chlorite. Feldspar is fresh and rarely twinned. White veinlets are composed of barite.	
B-37	do	Intrusives	Clinopyroxene serpentinite	Dark yellowish green, compact rock.	Serpentine is principal mineral. Clinopyroxene, chromite and opaque minerals are observed.	
B-38	do	do	Serpentinized pyroxenite	Dark gray, compact rock.	Pyroxene is almost clinopyroxene which is partly serpentinized.	
B-46	Locawon R.	do	Biotite-clinopyroxene diorite	Gray, compact rock with dark greenish gray xenolith (pyroxenite).	Medium-grained, holocrystalline. Zoned plagioclase partly altered to sericite, clinopyroxene, biotite, opaque minerals and apatite make up this rock. Xenolith is composed of clinopyroxene, hornblende, biotite, opaque minerals, zoisite and apatite.	
B-49	do	do	Hornblende-biotite pyroxenite	Grayish green, medium-grained, holocrystalline rock.	Principal minerals are clinopyroxene and opaque minerals. A small amount of hornblende and biotite is present interstitially to the clinopyroxene (prismatic augite).	See PL-1B
B-50	do	do	Biotite-clinopyroxene dolerite	Gray compact rock with pyrite inpregnation.	Holocrystalline and poikilitic texture. Feldspar crystal encloses abundant small crystals of pyroxene, hornblende and ore mineral.	
B-51	do	do	Biotite-clinopyroxene diorite	Gray, medium grained, holocrystalline rock with dark gray xenolith.	Clinopyroxene, biotite, plagioclase, alkali feldspar, ore mineral, sphene and apatite are the principal minerals. Xenolith is ultrabasic, holocrystalline rock, composed of clinopyroxene, biotite, ore mineral and apatite.	
B-52	do	do	Hornblende-biotite-clinopyroxene diorite	Gray, medium-grained, holocrystalline rock.	Potash feldspar showing perthite texture, twinned plagioclase altered to sericite, biotite, hornblende and clinopyroxene are main constituents. Accessories are ore minerals, apatite and sphene. Large crystals of secondary epidote are recognized. Quartz is absent.	See PL-1C
B-53	do	do	Biotite-clinopyroxene porphyrite	Dark gray, compact rock.	Holocrystalline rock with porphyritic texture. Phenocrysts of augite and biotite occur in a matrix of plagioclase laths, acicular or granular clinopyroxene, biotite and opaque mineral.	

Sample No.	Location	Group or Formation	Rock	Macroscopic features	Microscopic observations	Remarks
B-62	Locawon R.	Kalagutay G.	Porphyritic augite basalt	Gray, compact rock with a few green spot.	Phenocrysts of euhedyal augite (0.6 mm in size) occur in a matrix of plagioclase laths, clinopyroxene and opaque mineral. Secondary epidote occures in druses as radial aggregates. Carbonate minerals are also present in druses and fissures.	
B-67	San Fernand	Intrusives	Potash feldspar-plagioclase pegmatite	Leucocratic, pegmatitic rock.	Holocrystalline and pegmatitic rock. Principal minerals are potash feldspar and plagioclase. Potash feldspar shows graphic intergrowth with plagioclase and is altered to sericite perfectly. Plagioclase has polysynthetic albite twinning.	
BT-6	Kalagutay R.	Kalagutay G.	Augite-hornblende andesite	Gray, porphyritic, compact rock.	It shows porphyritic texture. Phenocrysts of euhedral hornblende, augite, anhedral plagioclase and opaque minerals are in a matrix of plagioclase laths, granular pyroxene, cristobalite and opaque minerals.	See PL-2A
b-2	Balacayo Co.	do	Sandstone	Dark gray, bedded, sandy rock.	Rounded to subrounded fragments (1 ~ 5 mm in size) are composed of volcanic, plutonic, metamorphic and sedimentary rocks. Compositions which make up each fragment are as follows. Volcanic rock: porphyritic, aphyric and glassy andesite. Plutonic rock: serpentinite, granite and hornblende diorite. Sedimentary rock: chert, limestone and tuff. Metamorphic rock: mica schist, quartz-mica schist and amphibolite.	See PL-2B
b-6	do	Intrusives	Diallage-olivine gabbro	Dark greenish gray, holocrystalline rock with a few large phenocryst.	Subhedral to anhedral plagioclase (partially altered to sericite), olivine (showing mesh structure), diallage (having clear parting) and a few opaque minerals are the main constituents of this rock. Olivine is replaced by serpentine partly or wholly.	
b-8	Kalakangon R.	Kalagutay G.	Basic sandstone	Greenish gray,coarse-grained rock.	Grains are made up of angular to subrounded rock and mineral fragments. Mineral fragments are chiefly composed of muscovite, clinopyroxene, hornblende, calcite, plagioclase, apatite and chromite. Rock fragments are dolerite, serpentinite and gabbro.	
b-17	Locawon R.	Intrusives	Biotite-augite gabbro	Dark gray, medium-grained, holocrystalline rock.	The essential minerals are plagioclase, clinozoisite altered from pyroxene and biotite. Sphene, apatite and opaque minerals are present.	
b-20	do	do	Lamprophyre	Melanocratic, coarse-grained, holocrystalline rock.	Subhedral to anhedral clinopyroxene, biotite and opaque minerals are the principal minerals. Felsic minerals are absent.	

Sample No.	Location	Group or Formation	Rock	Macroscopic features	Microscopic observations	Remarks
b-101	Babonawan R.	Nilabsan G.	Pyroxene basalt	Gray, compact rock with amygdaloidal druses.	It shows porphyritic texture. Microphenocrysts of euhedral pyroxene (maximum size is 1 mm) altered to chlorite are scattered in a matrix of plagioclase laths, granular augite, altered pyroxene and granular opaque minerals. Some plagioclase have twinning and are altered to carbonate minerals. Amygdaloidal druses are filled with carbonate mineral, opal and plagioclase.	
C-3	Tagbiga C.	Intrusives	Two pyroxene andesite	Gray, compact rock.	Phenocrysts of augite and hypersthene are in a matrix of plagioclase laths and opaque mineral. Abundant carbonate altered from plagioclase and clay mineral are present.	
C-4	do	do	Pyroxenite	Dark green to gray rock with epidote spots.	Hornblende, biotite, magnetite and augite are main components. Epidote and apatite are commonly observed. Mafic minerals are replaced by chlorite and actinolite.	
C-10	do	do	Biotite-hornblende-augite diorite	Granitic, compact rock.	Augite, hornblende, biotite, plagioclase and opaque minerals are the principal constituents. Plagioclase are altered to calcite and clay minerals.	
C-11	do	do	Altered pyroxenite	Yellowish green rock.	Original texture does not remain. Pyroxene is altered to aggregates of epidote, chlorite, calcite and opaque mineral. Anhedral plagioclase is also changed to sericite, calcite and clay minerals.	
C-14	do	Ore	Ore		Ore minerals fill the fissures with quartz grains. Mafic mineral (probably pyroxene) is completely altered to fibrous chlorite.	
C-15	do	Intrusives	Augite microdiorite	Fine-grained, compact rock.	Holocrystalline. Augite altered to chlorite, epidote, plagioclase and a few potash feldspar are present. Opaque mineral and calcite are commonly found.	
C-18	do	Kalagutay G.	Mudstone	Black, fine-grained rock.	Grains are composed of angular quartz, plagioclase and lithic fragments. Lithic fragments are almost acidic volcanic rock. Chlorite, calcite and zircon are observed. It shows clear graded bedding.	
C-22	do	do	Clayey mudstone	Gray, laminated rock.	Chips of plagioclase and quartz are embedded in a nearly opaque matrix that also contains a few specks of calcite.	
C-24	do	do	Altered conglomerate	Green conglomerate.	Lithic fragments of andesite and microdiorite and chips of augite, plagioclase, quartz and calcite are in a matrix of white mica, quartz and plagioclase.	

Sample No.	Location	Group or Formation	Rock	Macroscopic features	Microscopic observations	Remarks
C-26	Tagbiga C.	Kalagutay G.	Hornblende andesite	Porphyritic rock.	Euhedral green hornblende (1 ~ 5 mm in size) and twinned and zoned plagioclase are in a matrix of plagioclase laths and glass. Accessories are apatite, magnetite and chlorite.	
C-28	do	do	Augite andesite	Black, compact rock.	Phenocrysts of plagioclase and augite (both are 0.1 ~ 0.5 mm in size) are enclosed in smaller crystals of plagioclase, magnetite, chlorite, hematite and sericite with some interstitial glass.	
C-31	do	do	Hornblende andesite	Porphyritic rock.	Texture and mineral compositions are same to C-25.	
C-33	do	Intrusives	Biotite microdiorite	White, fine-grained granitic rock.	Holocrystalline. The main minerals are plagioclase (altered to sericite, epidote and clay mineral) and biotite. Potash feldspar, magnetite and chlorite are fairly present.	
C-37	do	do	Pyroxenite	Pale green rock with pyrite veinlets.	Augite, green hornblende and biotite are major constituents. Secondary chlorite and serpentine are also observed.	
C-47	do	Molambo andesite	Andesitic tuff-breccia	Pale green, compact rock.	Chips of biotite, augite, plagioclase and magnetite are distributed through a glassy matrix.	
C-49	Tagbiga R.	Intrusives	Biotite-clinopyroxene microdiorite	Granitic, compact rock.	Principal minerals are plagioclase, biotite and augite (some of them are aegirine augite). A few small grains of magnetite, apatite and epidote are commonly observed.	
C-50	do	Kalagutay G.	Andesitic tuff-breccia	Gray, compact rock with lithic fragments.	Fragments of glassy and microcrystalline andesites and chips of plagioclase, hornblende and magnetite are cemented by chlorite, sericite and clay minerals.	
C-54	Pulangi R.	do	Sandstone	Green, massive rock.	Abundant chips of plagioclase and hornblende and magnetite are welded by clay mineral. There are some andesitic rock fragments.	
C-60	Balakayo R.	Basement rock?	Amphibole schist	Schistose rock with silky brightness.	.The foliation is very clear in this section, which is made up of amphibole, anthophyllite, garnet and zoisite.	
CU-1	Tigua R.	Intrusives	Augite andesite	Black, compact rock with many amygdales.	Phenocrysts of plagioclase (altered to calcite and quartz) and augite are in a intersertal matrix which is composed of plagioclase laths, augite and glass. Amygdales are filled with secondary zeolite, calcite and quartz.	

Sample No.	Location	Group or Formation	Rock	Macroscopic features	Microscopic observations	Remarks
CN-9	Tigua R.	Kalagutay G.	Andesitic tuff	Dark gray, compact rock.	Essential rock fragments, that is, amygdaloidal glassy andesite, porphyritic augite andesite and pilotaxitic andesite occur in a matrix of argillaceous material.	
CN-15	do	Intrusives	Andesite	Glassy, compact rock.	Phenocrysts of euhedral and zoned plagioclase are in a matrix of plagioclase laths and glass. A few grains of apatite is observed.	
D-5	Takamile R.	Nilabsan G.	Andesitic tuff-breccia	Gray rock with lithic fragments.	Volcanic rock fragments are composed of porphyritic andesite, glassy andesite and chloritized tuff.	
D-7	do	do	Augite basalt	Gray, spherulitic rock.	Many spherulites occur in a matrix of plagioclase laths which are intergranular to augite and ore mineral. Spherulites are filled with carbonate, chlorite and feldspar.	
D-8	do	Intrusives	Augite dolerite	Dark grayish green, compact rock.	Holocrystalline and porphyritic texture. Phenocryst is subhedral to euhedral plagioclase altered to chlorite and clay mineral. Twinned plagioclase laths, chlorite, fresh granular augite and ore mineral make up this groundmass.	
D-10	do	Nilabsan G.	Red tuff	Gray, compact, banded rock.	Holocrystalline rock which is composed of anhedral feldspar (replaced by carbonate or chlorite), carbonate, chlorite and ore mineral. The rock shows traces of foliation.	See PL-2C
D-12	do	do	Augite basalt	Grayish black, compact rock.	Phenocrysts of twinned and zoned plagioclase (altered to sericite and clay mineral), augite and green hornblende are in a intergranular matrix of plagioclase laths, augite, chlorite and ore mineral.	
D-14	do	Intrusives	Augite dolerite	Grayish black, compact rock.	Subhedral twinned plagioclase, subhedral augite (partly altered to chlorite) are phenocrysts. Groundmass is composed of plagioclase laths, augite, chlorite and opaque mineral. It shows doleritic texture.	
D-18	Panganan R.	Nilabsan G.	Brecciated augite andesite	Grayish black rock with breccia.	Andesitic rock fragments are cemented by porphyritic andesite. They are composed of phenocrysts of twinned plagioclase and augite in a matrix of plagioclase laths, chlorite and ore mineral.	
D-21	do	do	Augite basalt	Gray, spherulitic rock.	Similar to D-7. Spherulites are filled with carbonate, feldspar and quartz. Phenocrysts of altered plagioclase occur in a matrix of feathery augite, devitrified mineral and chlorite.	

Sample No.	Location	Group or Formation	Rock	Macroscopic features	Microscopic observations	Remarks
D-22	Panganan R.	Nilabsan G.	Hornblende andesite	Gray, porphyritic rock.	Phenocrysts consist of plagioclase, hornblende, augite and opaque mineral. Matrix is made up of plagioclase laths, microlite or crystallite and opauqe mineral.	
D-23	Lobong C.	do	Augite-hornblende andesite	Gray, compact rock.	Phenocrysts of twinned plagioclase, hornblende and augite are in a matrix of many tiny plagioclase and hornblende microlites.	
D-28	Nilabsan R.	do	Spherulite-bearing tuff	Reddish brown, compact rock.	Colourless spherulites filled with amorphous material and chips of plagioclase regularly arrange in reddish brown tuff which might be composed of fine volcanic glass.	
D-33	do	Kalagutay G.	Andesitic tuff-breccia	Grayish black rock.	Fragments of andesite and chloritized rock make up this rock. The latter is composed of euhedral plagioclase phenocrysts and yellowish green groundmass. There are many cavities filled with chlorite, a small amount of plagioclase laths and augite in the chloritized rock.	
D-37	do	Intrusives	Hornblende-biotite diorite	Micro-holocrystalline rock.	Main constituents are twinned plagioclase, green hornblende, biotite, augite and epidote (altered from plagioclase). A few grains of apatite and ore mineral are accessories.	
D-39	do	do	Hornblende andesite	Gray, porphyritic rock.	Phenocrysts of euhedral hornblende rimmed with opacite and zoned plagioclase are scattered in a groundmass of plagioclase laths (rimmed with potash feldspar), hornblende and opaque mineral.	
D-40	do	do	Biotite-augite diorite	Grayish black, fine-grained, holocrystalline rock.	Large crystals of anhedral biotite (2 mm in size) and zoned and twinned plagioclase occur in small crystats of plagioclase, augite, biotite, sphene, apatite and ore mineral.	
D-44	do	do	Biotite-augite diorite-porphyry	Gray, porphyritic rock.	Phenocrysts of zoned and twinned plagioclase (rimmed with alkali feldspar), biotite, apatite and ore mineral are enclosed in a fine-grained mixture of plagioclase, quartz, biotite, augite, ore mineral and zoisite.	
D-46	Locawon R.	Intrusives	Augite-hornblende andesite	Gray, porphyritic rock.	Phenocrysts are euhedral augite. Matrix consists of plagioclase laths, green hornblende, chlorite, epidote and ore mineral.	
D-47	do	Nilabsan G.	Augite andesite	Gray, porous, volcanic rock.	Many vesicles (filled with plagioclase, pyroxene and chlorite) and a few phenocrysts of plagioclase and augite are in a matrix of plagioclase laths, granular augite and small vesicles.	

Sample No.	Location	Group or Formation	Rock	Macroscopic features	Microscopic observations	Remarks
D-48	Locawon R.	Intrusives	Hornblende andesite	Gray, porphyritic rock.	Phenocrysts of plagioclase altered to clay mineral, fresh hornblende and augite are in a matrix of plagioclase laths, quartz, chlorite, epidote and ore mineral. Sphene, apatite and opaque mineral are accessories.	
D-50	do	Nilabsan G.	Hornblende andesite	Gray, porphyritic rock.	Phenocrysts of twinned plagioclase and mafic minerals (altered completely to carbonate, chlorite and epidote) are distributed in a poikilitic matrix of plagioclase laths with chlorite patches and ore mineral.	
d-5	Pailuman R.	do	Andesitic tuff-breccia	Dark gray, brecciated rock.	Fragments of porphyritic andesite and chips of plagioclase and augite are cemented by chlorite and clay mineral.	
d-10	Nilabsan R.	Kalagutay G.	Hornblende andesite	Gray, porphyritic rock.	Phenocrysts of twinned and zoned plagioclase, hornblende, augite, biotite and quartz are present in a matrix of plagioclase laths, granular augite, brown biotite and opaque mineral.	
d-16	do	do	Altered tuff-breccia	Pale green rock with vesicles.	Fragments of hornblende andesite, augite andesite and shale and chips of chromite are welded by chlorite and clay mineral. Abundant tremolite and a few epidote are alteration products.	
d-17	do	Malambo andesite	Hornblende-biotite andesite	Gray, volcanic rock.	Phenocrysts of twinned and zoned plagioclase, green hornblende, biotite and augite are scattered in a pilotaxitic matrix of plagioclase laths, hornblende and ore mineral. Apatite is also observed.	
E-6	Sita R.	Nilabsan G.	Andesitic coarse tuff	Dark green, coarse-grained rock with white veinlets.	Fragments of porphyritic andesite, pilotaxitic andesite and glassy andesite and crystal chips of plagioclase occur in a matrix of less clearly defined glassy fragments. Secondary minerals are clay minerals with zeolite and pumpellyite.	
E-8	do	do	Andesitic lapilli tuff	Dark green rock cemented by white minerals.	Lithic fragments of porphyritic augite andesite and chips of augite and plagioclase are cemented by laumontite and clay mineral. There are many cavities (0.2 mm in size) which are filled with analcite and clay mineral.	
E-9	do	Kalagutay G.	Augite basalt (pebble of volcanic breccia)	Dark grayish green rock with vesicles filled by dark green minerals.	Microphenocrysts of augite occur in a matrix of plagioclase laths arranged regularly, granular augite, magnetite and brown glass. The matrix shows intergranular texture. Calcite, pumpellyite and clay mineral replace the glass.	

Sample No.	Location	Group or Formation	Rock	Macroscopic features	Microscopic observations	Remarks
E-11	Sita R.	Kalagutay G.	Hornblende andesite	Dark green, compact rock.	Phenocrysts of zoned plagioclase, green hornblende, and a few grains of augite occur in a matrix of plagioclase microlite and glass. Generally this rock has many phenocrysts and shows porphyritic texture. Pumpellyite and calcite are associated with much chlorite.	
E-16	do	do	Augite basalt	Dark green, compact rock.	Phenocrysts of augite occur sporadically or glomeroporphyritically. Groundmass consists of plagioclase laths arrenged regularly, granular augite, glass and opaque mineral. Saponite and calcite are recognized as secondary minerals.	
E-22	do	Intrusives	Serpentinite	Yellowish dark green rock.	This rock is serpentinized completely and original constituents are not clear. Pale green to colourless antigorite and considerable opaque mineral are present.	
E-23	do	do	Diorite	Pale gray, holocrystalline rock.	The main minerals are twinned plagioclase and green amphibole (cummingtonite). There are much actinolite or uralite.	
E-24	do	do	Gabbro	Yellowish green, holocrystalline rock.	Medium-grained, holocrystalline texture. Principal minerals are plagioclase enclosed augite grains poikilitically, amphibole (probably cummingtonite) and augite. Secondary actinolite or uralite and calcite are commonly observed.	
E-29	do	Kalagutay G.	Augite basalt (pebble of tuff-breccia)	Dark greenish gray rock.	Phenocrysts of plagioclase and augite are distributed sporadically in a matrix of plagioclase microlite, granular augite and brown glass. Secondary calcite and chlorite partly replace pyroxene.	
E-31	Nilabsan R.	do	Crystal tuff	Dark gray rock accompanied with large white minerals.	Euhedral or crushed crystals of hornblende, plagioclase and biotite occur in a matrix of volcanic glass. Hornblende is green to pale brownish green and has strong pleochroism.	
e-5	Davao R.	Intrusives	Dolerite	Reddish gray rock with a few small spherulites.	Plagioclase laths and ophitic augite laths, with secondary calcite, quartz, epidote and some ilmenite. Albitization of plagioclase is remarkable.	
e-6	Sita R.	Kalagutay G.	Calcareous fine tuff	Gray, fine-grained, soft rock.	Tiny fragments of andesite, basalt, augite and hornblende are cemented by aggregates of secondary calcite, clay minerals and pumpellyite. Some smaller fossils are also present.	

Sample No.	Location	Group or Formation	Rock	Macroscopic features	Microscopic observations	Remarks
F-24	Lingig R.	Barcelona G.	Augite andesite	Gray, porphyritic rock.	Phenocrysts of plagioclase altered to clay mineral and augite with opaque mineral are embeded in a groundmass of plagioclase laths, acicular augite and chlorite.	
F-31	Haguimitan R.	do	Shale	Black, compact rock with pyrite impregnation.	Prismatic barite crystals and numerous opaque mineral are scattered in a argillaceous matrix.	
F-41	Taon R.	do	Vesicular basalt	Gray, compact rock with many spherulites.	Spherulites filled with calcite, quartz and chlorite occur in a matrix of plagioclase laths, chlorite, secondary quartz and calcite.	
F-42	do	Intrusives	Biotite quartz diorite	Grayish white, holocrystalline rock.	Principal minerals are composed of anhedral quartz, twinned and zoned plagioclase and brown biotite. Opaque mineral, augite and apatite are accessory minerals.	See PL-3A
F-98	do	do	Augite gabbro	Grayish black, holocrystalline rock.	The essential minerals are twinned plagioclase (7 mm in size) and augite (5 mm in size). Smaller plagioclase, augite, biotite and ore mineral are also observed.	See PL-3B
F-411	do	do	Hornblende-biotite quartz diorite	Grayish white, holocrystalline rock.	Anhedral quartz, subhedral, zoned and twinned plagioclase, biotite altered to chlorite and hornblende are dominant minerals. Accessories are epidote, apatite and sphene.	
F-412	do	do	Hornblende-biotite quartz diorite	Grayish white, holocrystalline rock.	Graphic quartz, euhedral, zoned and twinned plagioclase partially altered to sericite, green hornblende and biotite (altered completely to chlorite and epidote) are principal minerals. Black opaque mineral is present in the altered biotite and hornblende.	
F-422	do	do	Biotite quartz diorite	Gray, holocrystalline, altered rock.	Main constituents are quartz, plagioclase altered to aggregates of sericite and chlorite, biotite which is also altered to chlorite, ore mineral and a few epidote.	
F-432	do	do	Biotite quartz diorite	Gray, holocrystalline rock with pyrite impregnation.	Similar to F-422. There is a little more epidote.	
F-433	do	do	Porphyritic granophyre	Gray, porphyritic rock.	Large crystals of zoned and twinned plagioclase and mafic mineral altered to chlorite perfectly are embeded in a grandmass with micrographic texture.	

Sample No.	Location	Group or Formation	Rock	Macroscopic features	Microscopic observations	Remarks
F-487	Taon R.	Intrusives	Vesicular dolerite	Dark gray, compact rock with many spherulites.	Many spherulites filled with microcrystals of quartz, feldspar and calcite and phenocrysts of zoned and twinned plagioclase are enclosed in a matrix with doleritic texture. A few opaque mineral is present.	
F-526	Simulaw R.	Bislig F.	Basic volcanic rock	Reddish brown, porphyritic rock.	This rock is altered entirely. Plogioclase crystals are decomposed to clay minerals and olivine(?) to reddish brown opaque mineral. A mixture of tiny opaque minerals and clay mineral makes up the groundmass.	
F-551	Tangmoan R.	Mangagoy F.	Crystal tuff	Dark gray, compact rock.	Lithic fragments of porphyritic andesite and aphyric andesite and chips of plagioclase, hornblende, augite and opaque mineral are cemented by carbonate and clay mineral. A few fragments of microfossil is present.	
F-626	Taon R.	Intrusives	Augite-biotite diorite-porphyry	Dark gray, holocrystalline rock.	Large crystals of euhedral, zoned and twinned plagioclase (rimmed with alkali feldspar) and prismatic augite are enclosed by small crystals which are composed of zoned and twinned plagioclase, granular augite, opaque mineral, biotite and chlorite.	
F-681	Kabasagan R.	do	Augite andesite	Gray, porphyritic rock.	Phenocrysts of zoned and twinned plagioclase, augite partially altered to chlorite and opaque mineral occur in a matrix of plagioclase laths, augite and opaque minerals. A small amount of sphene is present also.	
F-2723	Haguimitan R.	Barcelona G.	Dacitic tuff	Grayish green, soft rock.	Chips of quartz (with rounded and corroded edges), plagioclase altered to clay mineral, opaque mineral and sphene and rock fragments of porphyritic andesite and pumice are separated by argillaceous material.	
f-24	Taon R.	Intrusives	Augite diorite-porphyry	Dark gray, porphyritic rock.	Main phenocrysts are euhedral, twinned and zoned plagioclase enclosing augite and opaque mineral poikilitically. Groundmass consists of plagioclase laths, granular to irregular augite, hornblende and biotite. The texture is porphyritic.	
f-41	do	do	Altered dolerite	Greenish white, compact rock.	Abundant epidote and chlorite are produced by strong alteration. Plagioclase showing glomeroporphyritic texture has carlsbad and albite twinning and is altered to chlorite and epidote. A groundmass of plagioclase laths, opaque mineral, chlorite and epidote shows intersertal texture.	See PL-3C

Sample No.	Location	Group or Formation	Rock	Macroscopic features	Microscopic observations	Remarks
f-46	Taon R.	Barcelona G.	Augite dolerite	Gray, compact rock.	Phenocrysts are very rare. Prismatic augite (2 mm in size) is altered to actinolite and chlorite. Groundmass consists of plagioclase laths, actinolite, chlorite, epidote and ore mineral and shows doleritic texture.	
f-50	do	Intrusives	Augite quartz diorite	Gray, porphyritic rock.	Phenocrysts of zoned and twinned plagioclase and euhedral augite occur in a holocrystalline matrix of plagioclase laths, granular augite, hydromica, chlorite and opaque mineral. Alkali feldspar rims on the plagioclase.	
f-75	do	do	Augite gabbro	Dark gray, compact rock.	Zoned and twinned plagioclase and augite are the principal constituents. Biotite, chlorite and opaque mineral also occur. A small quartz vein penetrates this rock.	
f-653	do	do	Altered dolerite	Dark green, compact rock.	Medium-grained, holocrystalline rock with intergranular texture. Plagioclase, actinolite after augite, opaque mineral and sphene make up this rock.	
G-1	Simulaw R.	Kaban G.	Augite basalt	Dark green, compact rock.	Phenocrysts of plagioclase and augite occur in a matrix of plagioclase laths arranged sporadically, augite and magnetite. The texture is intergranular. Secondary mineral is very few.	
G-5	do	do	Augite andesite	Greenish gray, compact rock.	A few phenocrysts of plagioclase and augite are observed in a hyalopilitic matrix of plagioclase laths and glass. Plagioclase laths are arranged regularly and partially altered to saponite.	
G-18	do	do	Augite basalt	Dark green, compact rock.	Phenocrysts are composed of tiny augite (0.2 mm in size) and plagioclase. The texture is glomeroporphyritic. Matrix is holocrystalline and consists of regularly arranged plagioclase laths, microgranular aguite and opaque minerals. Saponite replaces the phenocrysts partially.	See PL-4A
G-45	do	do	Augite andesite	Bluish gray rock.	Phenocrysts of plagioclase and augite occur in a matrix of plagioclase laths and magnetite. Sphene and calcite are accessories. Strong chloritization and albitization affect this rock.	
G-60A	Pasian R.	Kaban G.	Andesite	Bluish gray rock.	Abundant plagioclase phenocrysts occur in a pilotaxitic matrix which is composed of plagioclase microlite. Calcite and chlorite are commonly observed. A little laumontite, prehnite and epidote are present also. Albitization of plagioclase is notable.	

Sample No.	Location	Group or Formation	Rock	Macroscopic features	Microscopic observations	Remarks
G-60B	Pasian R.	Kaban G.	Fine andesitic tuff	Greenish gray rock.	Fine fragments of plagioclase and porphyritic andesite (1 ~ 2 mm in size) are cemented by clayey mineral. Much opaque mineral, chlorite and calcite are accompanied with sphene.	
G-69	do	do	Augite basalt	Dark green, compact rock.	There are some plagioclase phenocrysts containing augite grains poikilitically in a matrix of plagioclase laths arranged regularly, granular augite, magnetite and brown glass. Clay mineral and zeolite partially replace the glass.	
G-71A	do	do	Augite basalt	Grayish green rock with vesicles filled with white minerals.	Phenocrysts of plagioclase and augite occur in a matrix of plagioclase laths, granular augite, magnetite and glass. A few calcite is associated with much saponite.	
G-71B	do	do	Andesitic tuff-breccia	Brownish gray rock showing flow structure.	Rock fragments are all andesitic. In a groundmass composed of plagioclase microlite, brown glass and opaque minerals, there are some phenocrysts of plagioclase and pseudomorph of microphenocrysts of mafic minerals. The matrix enclosed the phenocrysts shows a brecciated texture. Pale green chlorite (some are brown) occur secondarily. A few pumpellyite and acicular ilmenite are present.	
G-73A	do	do	Basaltic fine tuff	Dark gray, compact rock.	Lithic fragments of andesite showing intergranular and pilotaxitic textures and chips of plagioclase and augite are in a matrix of glass and opaque mineral. Calcite and chlorite are produced partially.	
G73B	do	do	Andesite	Dark gray, compact rock.	Phenocrysts of plagioclase are scattered sporadically in a groundmass of plagioclase laths arranged regularly and glass. The texture shows porphyritic.	
G-76	do	do	Augite basalt	Yellowish gray, compact rock.	Phenocrysts are composed of much plagioclase and a little aguite. Plagioclase laths arranged at random, augite and magnetite make up the groundmass. A large amount of secondary clay mineral are present.	
G-85	Lungsad C.	do	Andesite	Bluish gray, compact rock.	Similar to G-60. Microphenocrysts of plagioclase are distributed sporadically in a ground mass of plagioclase laths and magnetite. The groundmass shows pilotaxitic texture. Calcite, chlorite and albite after plagioclase are recognized. There are some hematite veins.	
G-90	do	do	Lapilli tuff	Greenish yellow rock.	Rock fragments of basalt, andesite with various texture and altered pumice are embeded by secondary zeolite and clay mineral.	

Sample No.	Location	Group or Formation	Rock	Macroscopic features	Microscopic observations	Remarks
G-96	Lungsad C.	Kaban G.	Augite basalt	Dark green, compact rock.	Phenocrysts are plagioclase and a little augite. Groundmass consists of plagioclase laths, granular augite and magnetite with holocrystalline texture.	
G-103	do	do	Augite basalt	Pale gray rock accompanied with many cavities filled with white minerals.	Phenocrysts of plagioclase and a few microphenocrysts of augite are enclosed in a groundmass of plagioclase laths and intergranular augite. Many cavities filled with zeolite and saponite are developed in the rock.	
G-111	do	do	Augite basalt	Dark green, compact rock.	A matrix composed of plagioclase laths, granular augite, magnetite and glass contains abundant phenocrysts of plagioclase and a few augite phenocrysts. Greenish brown clay mineral replace the glass but alteration is weak.	
G-115	do	do	Two-pyroxene basalt	Yellowish gray, porphyritic rock.	Phenocrysts of plagioclase and orthopyroxene are scattered sporadically in a groundmass of plagioclase laths, small grains of clinopyroxene, orthopyroxene and glass. Texture is intergranular.	
G-127	Lungsad C.	Kaban G.	Augite andesite	Reddish dark green, compact rock.	Similar to G-291. Phenocrysts of plagioclase and glomeroporphyritic augite occur in a groundmass of plagioclase microlite, glass and opaque mineral. The texture is porphyritic. Saponite and hematite are present.	See PL-4B
G-134	do	do	Augite andesite	Dark green rock.	Similar to G-291. Phenocrysts of plagioclase containing augite poikilitically and augite are in a matrix of plagioclase microlite and glass. Abundant saponite is secondary mineral.	
G-136	do	do	Two-pyroxene basalt	Dark green rock.	A matrix composed of plagioclase microlite, granular augite and opaque mineral encloses phenocrysts of plagioclase, augite and orthopyroxene with reaction rim of granular augite. Secondary saponite and hematite are present.	See PL-4C
G-226	Buhay R.	do	Augite basalt	Dark green, compact rock.	Phenocrysts of abundant plagioclase and a few augite are in a matrix of plagioclase laths arranged at random, granular augite and magnetite. Clay mineral is seen as a secondary mineral but alteration is weak.	
G-232	do	do	Basaltic andesite	Black, compact rock.	Phenocrysts of plagioclase and augite are scattered sporadically in a matrix of plagioclase laths, granular aguite and glass. Plagioclase laths arrange regularly and the texture is trachytic.	

Sample No.	Location	Group or Formation	Rock	Macroscopic features	Microscopic observations	Remarks
G-246	Buhay R.	Kaban G.	Basic coarse tuff	Pale green, polycolored rock.	Fragments are composed of basalt to andesite (2 ~ 3mm in size) and plagioclase. Secondary minerals are brownish green clay mineral, calcite, zeolite and sphene.	
G-251	do	do	Basaltic andesite	Reddish gray, compact rock.	Phenocrysts of plagioclase occur in a groundmass of plagioclase microlite and glass. The texture shows porphyritic. Occurrences of chlorite, laumontite and calcite suggest this rock is affected by thermal alteration. The rock becomes red by hematite.	
G-255	Buhay R.	Kaban G.	Basaltic andesite	Grayish green, compact rock.	Phenocrysts of plagioclase in a matrix of plagioclase laths, micrograined augite and magnetite are altered to albite. The texture is intergranular. Chlorite and calcite are commonly observed.	
G-269	do	do	Augite basalt	Greenish gray, compact rock.	In a holocrystalline matrix of plagioclase laths and augite, phenocrysts of zoned plagioclase and augite are scattered sporadically. It shows glomeroporphyritic texture. A small amount of greenish clay mineral and glass replace the phenocrysts partially.	
G-271	do	do	Basaltic andesite	Dark green, compact rock.	Phenocrysts of plagioclase (1 ~ 2 mm in size) and rare augite (0.5 mm in size) are in a holocrystalline matrix of plagioclase laths (0.1 mm in size), fine augite and magnetite. Alteration is weak.	
G-272	do	do	Augite basalt	Yellowish dark green, compact rock.	Similar to G-271. Phenocrysts of plagioclase enclosing some augite grains poikilitically and augite occur sporadically in a groundmass of plagioclase laths, augite and opaque mineral. The texture is intergranular.	
G-278	Sukod R.	do	Basaltic andesite	Grayish black, compact rock.	A matrix composed of plagioclase laths (more or less 0.1 mm in size), fine augite and opaque mineral enclose some phenocrysts of plagioclase. This rock shows porphyritic texture and has many irregular cavities.	
G-285	do	do	Andesite	Gray, porphyritic rock.	Abundant plagioclase phenocrysts are found in the groundmass of plagioclase microlite and brown glass. Occurrences of calcite, chlorite, laumontite and sphene show this rock is affected by hydrothermal alteration.	
G-291	Wagas C.	Kaban G.	Two-pyroxene basalt	Reddish gray, compact rock.	Phenocrysts of zoned plagioclase and glomeroporphyritic augite occur in a matrix of plagioclase laths and glassy material. The texture is porphyritic. Calcite, saponite and hematite are also present.	

Sample No.	Location	Group or Formation	Rock	Macroscopic features	Microscopic observations	Remarks
G-292	Wagas C.	Kaban G.	Two-pyroxene andesite	Yellowish dark green, compact rock.	Phenocrysts are composed of zoned plagioclase with poikilitic augite, augite and orthopyroxene which has reaction rim of augite. Groundmass is a mixture of plagioclase microlite and glass. Xenoliths of gabbro are observed in this section.	See PL-5A
G-305	Sanco point	Intrusives	Dolerite	Yellowish dark green rock.	Plagioclase laths and subhedral or interstitial augite show ophitic texture. Opaque mineral, brownish green clay mineral, calcite and laumontite are commonly found.	
G-308	Pagtilaan R.	Dacongbanwa F.	Limestone	Brownish gray rock.	It mainly consists of calcite grains with chips of smaller fossils.	
G-314	do	Mangagoy F.	Two-pyroxene basalt	Dark green, compact rock.	Small phenocrysts of plagioclase occur in a groundmass of plagioclase laths (altered to albite), clinopyroxene, orthopyroxene and magnetite. There is much saponite.	
g-1	Bahayan R.	Kaban G.	Andesitic coarse tuff	Pale green rock.	Lithic fragments of porphyritic andesite and chips of plagioclase are cemented by glassy material. By the strong alteration, a large amount of chlorite, calcite, sericite and eipdote occur secondarily. Albitization of the plagioclase is notable.	
g-11	do	do	Andesitic coarse tuff	Pale reddish green rock.	A matrix of brownish red glass and plagioclase laths encloses fragments of andesite, plagioclase and augite. Laumontite and pale brownish green clay mineral are rich in this rock.	
g-32A	Buhay R.	Intrusives	Gabbro	Melanocratic, medium-grained rock.	Principal minerals are plagioclase, amphibole (cummingtonite) and augite. Abundant actinolite, uralite and sericite replace them.	
g-32B	do	Kaban G.	Augite dolerite	Dark gray, compact rock.	Euhedral to subhedral, zoned plagioclase, augite enclosing plagioclase grains interstitially or poikilitically, and opaque mineral show subophitic texture. Saponite is predominant.	
g-40	Sukod R.	do	Augite andesite	Reddish gray rock.	Abundant phenocrysts of plagioclase and augite are in an altered matrix. Zeolite (probably laumontite) and chlorite replace the matrix. Acicular hematite is common.	
g-58	Kaban R.	do	Augite andesite	Dark green, compact rock.	Phenocrysts of zoned plagioclase and augite are embeded by plagioclase and pyroxene microlites and glassy material.	

Sample No.	Location	Group or Formation	Rock	Macroscopic features	Microscopic observations	Remarks
g-68	Simulaw R.	Kaban G.	Augite basalt	Dark green, compact rock.	Groundmass is holocrystalline and shows basaltic texture. Plagioclase laths, granular augite and magnetite make up the groundmass. Phenocrysts are composed of a few crystals of plagioclase and abundant augite which show sometimes glomeroporphyritic texture.	
g-72	Pasian R.	Kapalong F. ?	Andesitic tuff-breccia .	Pale greenish gray rock.	Fragments of andesite showing various textures, plagioclase, augite and hornblende are welded by volcanic glassy material.	
g-73	do	Kaban G.	Silicified rock.		The rock is altered to aggregates of secondary quartz. A few relic mineral of albite and much magnetite are present.	
g-74	Jaon R.	Intrusives	Augite dolerite	Dark green rock.	Phenocrysts of plagioclase and augite occur in an ophitic matrix of plagioclase laths, augite and magnetite. Secondary saponite is commonly observed.	
H-16	Maposo R.	Kaban G.	Porphyritic andesite	Dark blue, porphyritic rock.	All mafic minerals (chiefly orthopyroxene) are replaced by chlorite, calcite and quartz. Many plagioclase crystals (1 ~ 1.5 mm in size) change to saussurite. Groundmass is composed of altered plagioclase, opaque minerals and secondary quartz.	See PL-5B
H-23	do·	do	Two-pyroxene andesite	Dark blue rock.	This rock is affected by greenerization. Phenocrysts of plagioclase, altered orthopyroxene and clinopyroxene are in a groundmass of tiny plagioclase laths, pyroxene and opaque minerals. Especially, alteration of orthopyroxene is strong which changes to chlorite perfectly.	
H-24	do	do	Fine andesitic lapilli tuff	Green rock with well sorted breccia.	Breccias of aphanitic and porphyritic andesites are cemented by plagioclase crystals, glassy material and their fine fragments. By the strong alteration, original minerals are replaced by chlorite, quartz and calcite. There are some veinlets of quartz and calcite.	
H-45	Kinayan R.	do	Fine lapilli tuff	Grayish white rock with tiny fragments.	Strongly silicified. Fragments are composed of mud and igneous rocks (intensely altered). Matrix is made up of their smaller fragments and fine tuff which are altered to microcrystalline quartz or calcite.	
H-54	Ngan R.	do	Two-pyroxene andesite	Dark blue rock with large phenocrysts of pyroxene and plagioclase.	Phenocrysts of twinned plagioclase, orthopyroxene and clinopyroxene are embeded by a matrix of plagioclase laths, spherical pyroxene, opaque minerals and glass. Plagioclase is altered to saussurite and some pyroxene to chlorite. There are some green-coloured minerals.	

Sample No.	Location	Group or Formation	Rock	Macroscopic features	Microscopic observations	Remarks
H-58	Tingari R.	Kaban G.	Aphanitic andesite	Bluish rock with plagioclase crystals.	By strong silicification, secondary quartz grains showing equigranular texture are formed. Some plagioclase laths are recognized in a matrix which is almost replaced by quartz and clay minerals.	
H-61	do	do	Andesitic lapilli tuff	Purplish, brecciated rock.	Lapilli is composed of aphyric andesite with pilotaxitic texture and tuff. The matrix made up of volcanic ash, lithic fragments and plagioclase chips is replaced partially by clay minerals.	
H-68	Maenitu R.	do	Andesitic lapilli tuff	Green, compact rock with polycoloured, essential rock fragments.	Quartz, carbonates, chlorite and clay minerals replace all parts of the rock. From the existence of plagioclase and pyroxene pseudomorphs, the original composition seems to be andesitic.	
H-75	Ngan R.	Kaban G.	Hornblende andesite	Polycoloured (reddish brown to green) rock with mosaic texture.	Phenocrysts of plagioclase, green hornblende and opaque minerals occur in a matrix of plagioclase laths and green coloured minerals. Some plagioclase are altered to chlorite and clay minerals.	See PL-5C
H-86	do	do	Fine tuffaceous sandstone	Black, compact rock.	Grains (0.2 mm in mean size) consist of plagioclase altered to zeolite, quartz, hornblende and augite. Cementing materials are replaced by clay minerals, quartz, zeolite and calcite.	
H-92	Bango R.	do	Pyroxene andesite	Gray, porphyritic rock.	Phenocrysts of plagioclase (altered to chlorite partially) and pyroxene (altered to chlorite or zeolite) occur in a groundmass of plagioclase laths, opaque minerals, microlite and glass. Secondary minerals are chlorite, zeolite, calcite and clay minerals.	
H-107	Naboc R.	do	Andesitic lapilli tuff	Gray, pyrite impregnated rock.	Breccias of porphyritic andesite are in a crystalline matrix. Secondary minerals are calcite, zeolite and clay mineral.	
H-138	do	do	Augite basalt	Black, compact rock.	Phenocrysts of twinned and zoned plagioclase and augite are embeded in a groundmass of plagioclase laths, granular augite and opacite. It shows intergranular texture.	
H-140	do	do	Porphyritic andesite	Dark blue, porphyritic and compact rock.	Phenocrysts of plagioclase and augite which are altered to epidote or chlorite occur in a micro-grained groundmass relaced by clay mineral and chlorite.	

Sample No.	Location	Group or Formation	Rock	Macroscopic features	Microscopic observations	Remarks
H-143	Naboc R.	Intrusives	Porphyrite	Pale green rock.	This rock contains large crystals of plagioclase and augite in a fine-grained, altered plagioclase and augite. It has microholocrystalline and porphyritic texture. Chlorite, clay minerals, zeolite and calcite replace plagioclase partially.	See PL-6A
H-147	do	Kaban G.	Andesitic sandy tuff	Well bedded, pale blue rock.	Only plagioclase phenocrysts are distinguished as original mineral. Other minerals are strongly altered to microgranular quartz, calcite and dusty opaque minerals.	
H-153	do	do	Andesitic tuff-breccia	Pale blue, compact rock.	Alteration of this rock is strong. A few plagioclase and pyroxene remain fresh in a altered matrix composed of chlorite, epidote, calcite, quartz and clay minerals.	
Hi-47	do	do	Dacite	Blue, porphyritic rock with xenoliths.	Phenocrysts of twinned plagioclase, quartz and hornblende pseudomorphs occur in a granular microcrystalline to glassy groundmass. Abundant chlorite is derived from hornblende. Calcite veinlets penetrate the field.	
h-17	Maa R.	do	Andesite	Black rock with prismatic plagioclase.	Phenocrysts of twinned and saussuritized plagioclase and pyroxene psuedmorphs occur in a groundmass of plagioclase laths and glass. Chlorite, calcite and zeolite are secondary minerals. A few aragonite is present also.	
h-25	Karamakan R.	do	Hornblende andesite	Dark blue, compact rock.	A groundmass of plagioclase laths, pyroxene and glass contains phenocrysts of twinned plagioclase, hornblende and opacite. It shows felty texture. Chlorite, zeolite and clay minerals are secondary minerals.	
h-26	Hagibana R.	do	Glassy andesite	Purplish, glassy, porphyritic rock.	Phenocrysts of plagioclase, augite and orthopyroxene (altered to chlorite perfectly) are enclosed in a groundmass of glass, plagioclase laths and opacite. Considerable chlorite is present.	
h-29	do	do	Glassy andesite	Purplish, glassy rock with hematite veinlets.	Phenocrysts of plagioclase and pyroxene are scattered in a groundmass of glass and plagioclase laths. By the strong alteration, a large amount of chlorite, hydromica and clay minerals are produced.	See PL-6B
h-39	Ambawon R.	do	Glassy andesite	Purplish, glassy rock with flow banding.	Phenocrysts of plagioclase and pyroxene in a glassy matrix of plagioclase and glass (changed to hydromica and chlorite) are altered strongly by hydrothermal solution. There are some hematite veinlets.	

Sample No.	Location	Group or Formation	Rock	Macroscopic features	Microscopic observations	Remarks
h-45	Canobi R.	Intrusives	Altered porphyrite	Pale green, compact rock.	Phenocrysts of plagioclase and clinopyroxene are embeded by microphenocrysts of plagioclase, pyroxene and opacite. Abundant chlorite, clay minerals, zeolite and a few epidote are observed.	
h-51	Cow R.	Kaban G.	Hornblende andesite	Gray rock with large plagioclase and hornblende crystals.	Phenocrysts of oxyhornblende, plagioclase and augite occur in a matrix of plagioclase, oxyhornblende and opacite. Oxyhornblende is characteristic mineral of this rock.	
h-67	Ngan R.	do	Tuffaceous sandstone	Blueish gray, medium-grained rock.	Well sorted grains of quartz, plagioclase, mafic minerals (altered to chlorite or clay mineral) and opacite. Secondary quartz, chlorite and clay minerals are observed.	
h-74	Magtonob C.	do	Two-pyroxene andesite	Bluish gray, porphyritic texture.	Phenocrysts of twinned plagioclase, augite and a few orthopyroxene occur in a glassy matrix of clay minerals, plagioclase microlite and opacite. Chlorite replaces plagioclase and pyroxene.	
h-76	Naboc R.	do	Lapilli tuff	Bluish gray, porphyritic rock.	Chips of plagioclase and hornblende are recognized and altered strongly.	
h-107	do	do	Altered andesite	Gray, porphyritic rock.	A matrix showing intersertal texture is composed of plagioclase laths and glass. Phenocrysts of twinned plagioclase, augite, hypersthene and opacite are altered to epidote, chlorite, quartz and hydromica.	
h-110	do	do	Lapilli tuff	Dark green rock with lithic fragments.	Lithic fragments are composed of porphyritic, two-pyroxene andesite. A matrix is altered to clay mineral, micro-opacite and chlorite. Alteration is relatively strong.	
	(Polished Section)					
b-23	Locawon R.	Intrusives	Pyroxenite		Pyrite veinlet (1 ~ 2 mm) penetrates a large amount of primary magnetite and a few small chalcopyrite crystals disseminate irregularly.	
c-14 c-37	Tagbiga R.	do	do		Chalcopyrite, pyrite and magnetite are main constituents. Magnetite is enclosed by chalcopyrite. Pyrite has irregular shape.	See PL-7A
F-31	Lepanto Mine	Barcelona G.	Mudstone		Numerous tiny pyrite grains (0.03 ~ 0.08 mm in diameter) are scattered in dark gray, muddy, compact matrix (probably mudstone). Some of pyrite show colloform or framboidal texture.	See PL-7B

Sample No.	Location	Group or Formation	Rock	Macroscopic features	Microscopic observations	Remarks
F-75	Surigao Mine	Intrusives	Porphyrite		Corroded galena, with some trace of cubic form, partially replaced by enclosing sphalerite. The sequence of deposition of minerals is, from the older to the younger, galena, chalcopyrite and sphalerite. These minerals are penetrated by quartz veins with a few pyrite.	See PL-7C
F-689 F-2474	Taon R.	Barcelona G.	Andesite		Acicular hematite is associated with pyrite. There is a small amount of chalcopyrite replaced by chalcocite partially.	See PL-8A
f-73 f-61 f-100 f-691	do	Intrusives	Quartz diorite		Chalcopyrite, pyrite and gangue minerals. Pyrite is replaced by chalcocite along grain boundaries and fractures. Chalcopyrite is also replaced partly by chalcocite and covellite.	See PL-8B

PL-1

A: Olivine-clinopyroxene-gabbro (Sample No. B-26)

Plagioclase (pl), clinopyroxene (cp) and olivine (ol) are the principal minerals. Clinopyroxene and olivine are almost serpentinized.

X–nichols

x 50

B: Hornblende-biotite-pyroxenite (Sample No. B-49)

Clinopyroxene (cp), biotite (bi), hornblende (hb) and abundant magnetite (m) make up this rock.

// –nichols

x 50

C: Hornblende-biotite-clinopyroxene-diorite (Sample No. B-52)

Twinned plagioclase (pl), biotite (bi), hornblende (hb) and clinopyroxene (cp) are main constituents.

X–nichols

x 50

PL-2

x 50

A: Augite-hornblende-andesite
(Sample No. BT-6)

Phenocrysts of hornblende (hb), augite (au), plagioclase (pl) and opaque minerals (o) are in a matrix of plagioclase laths, granular pyroxene and so on.

// –nichols

x 50

B: Sandstone
(Sample No. b-2)

Many kinds of rock fragments make up this rock. In this photograph, the biggest one with a distinct schistosity is quartz-mica-schist (sch).

// –nichols

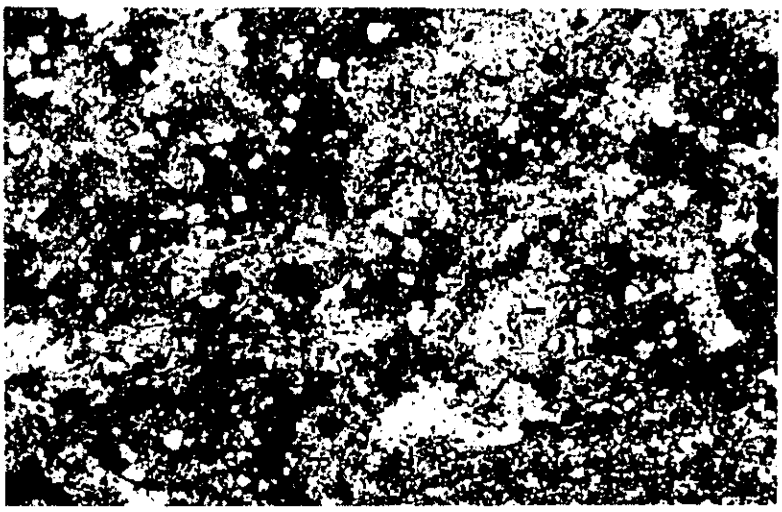

x 50

C: Red tuff
(Sample No. D-10)

Feldspar, chlorite, carbonate minerals and opaque minerals make up this rock.

X–nichols

PL-3

A: Biotite-quartz-diorite
(Sample No. F-42)
Twinned plagioclase (pl) partially altered to sericite, quaetz (q) and brown biotite (bi).
X–nichols

x 50

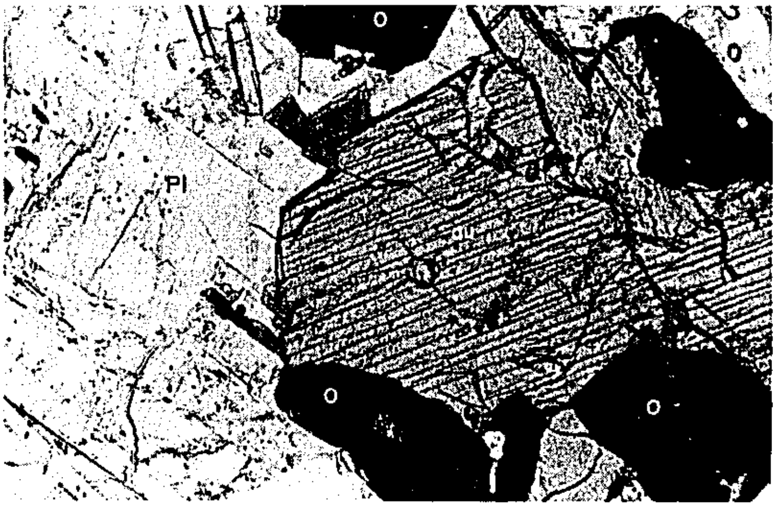

B: Augite-gabbro
(Sample No. F-98)
Twinned plagioclase (pl), augite (au) and opaque minerals (o) are main constituents.
//–nichols

x 50

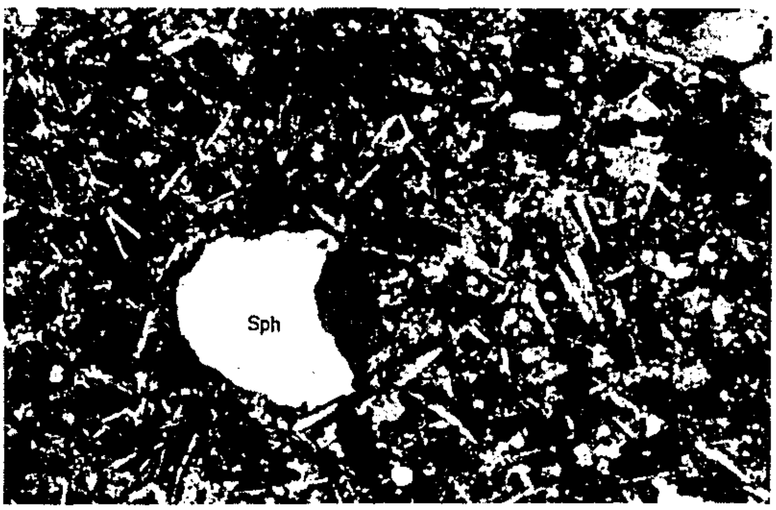

C: Altered basalt
(Sample No. f-41)
Spherulite (sph) composed of quartz occur in a groundmass. The groundmass consists of abundant epidote, chlorite and plagioclase lanths.
X–nichols

x 50

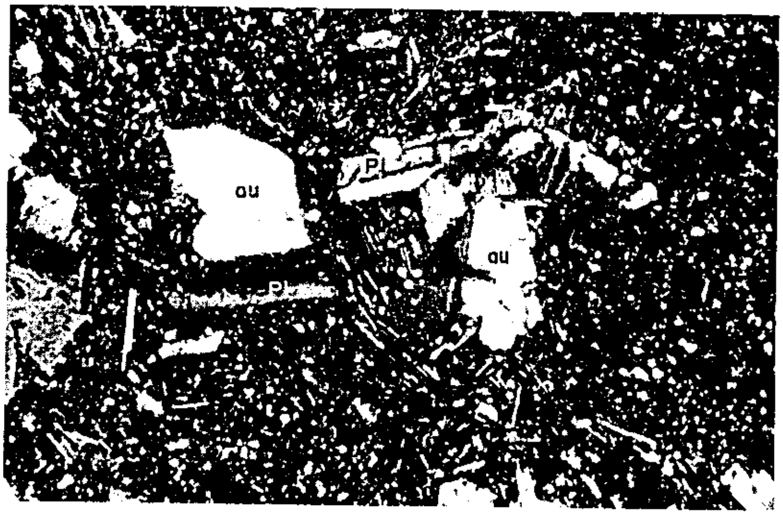

A: Augite-basalt
(Sample No. G-18)
Augite (au) and plagioclase (pl) make up phenocrysts showing glomeroporphyritic. The matrix consists of plagioclase laths and micro-granular augite and opaque minerals.
X—nichols

x 50

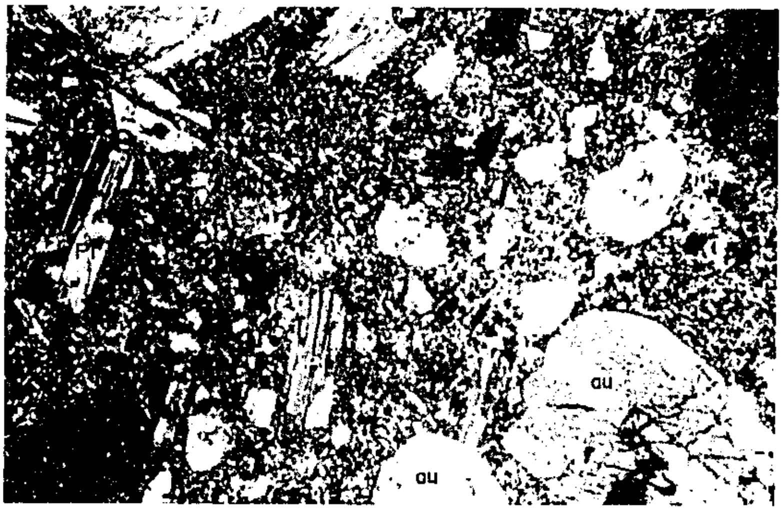

B: Augite-andesite
(Sample No. G-127)
Phenocrysts of twinned plagioclase (pl) and augite (au) occur in a matrix of plagioclase microlite, glass and opaque minerals.
X—nichols

x 50

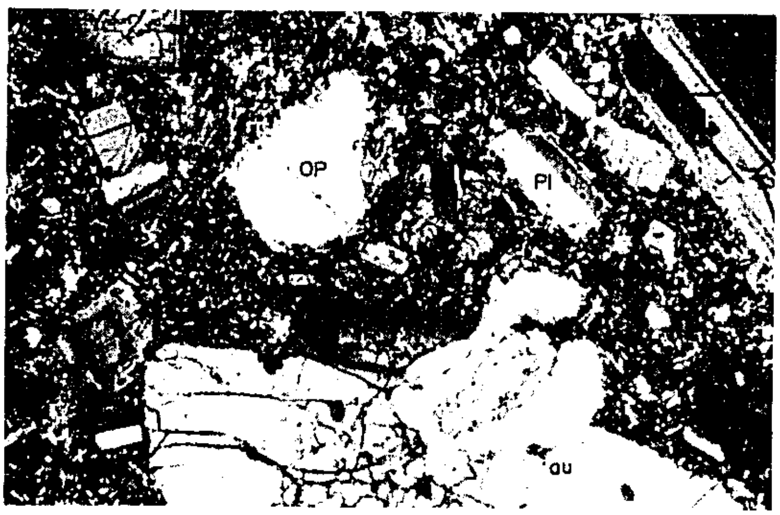

C: Two-pyroxene-basalt
(Sample No. G-136)
Phenocrysts of plagioclase (pl), augite (au) and orthopyroxene (op) with reaction rim (rr) of granular augite occur in a matrix of plagioclase laths, granular augite and opaque minerals.
X—nichols

x 50

A: Two-pyroxene-andesite
(Sample No. G-292)
Phenocrysts of plagioclase (pl), augite and orthopyroxene (op) with reaction rim (rr) of granular augite, are in a matrix of plagioclase microlite and glass.
X–nichols

x 50

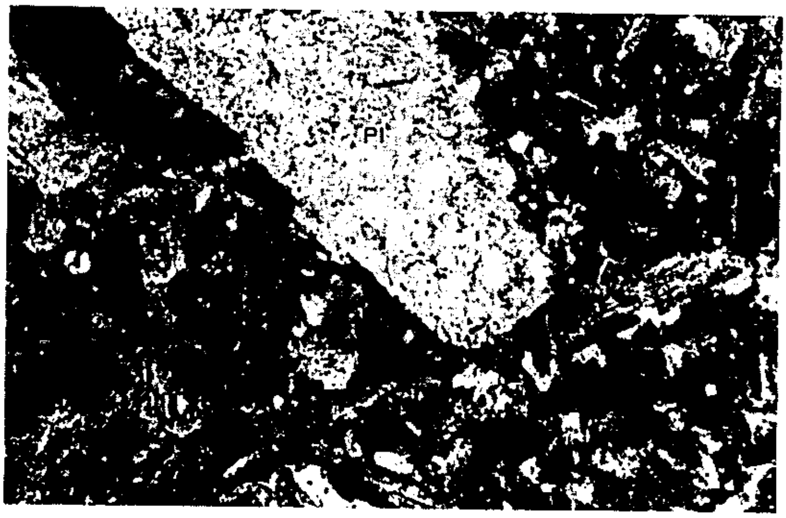

B: Porphyritic andesite
(Sample No. H-16)
Large crystals of plagioclase (pl) altered to saussurite are phenocrysts. A matrix is composed of altered plagioclase, secondary quartz and opaque minerals.
X–nichols

x 50

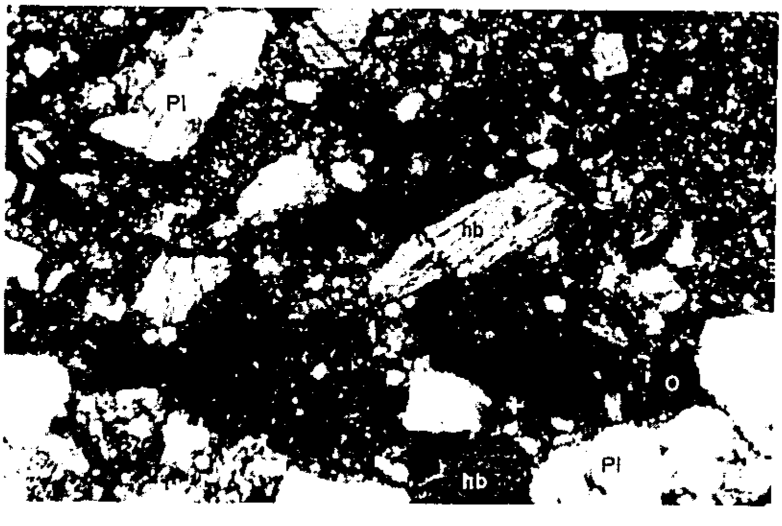

C: Hornblende-andesite
(Sample No. H-75)
Phenocrysts of plagioclase (pl), green hornblende (hb) and opaque minerals (o) occur in a matrix of altered plagioclase and green colored minerals.
X–nichols

x 50

PL-6

A: Porphyrite
(Sample No. H-143)
Large crystals of augite (au) and plagioclase (pl) partially altered to calcite, and small crystals of altered plagioclace and augite make up this rock.
X–nichols

x 50

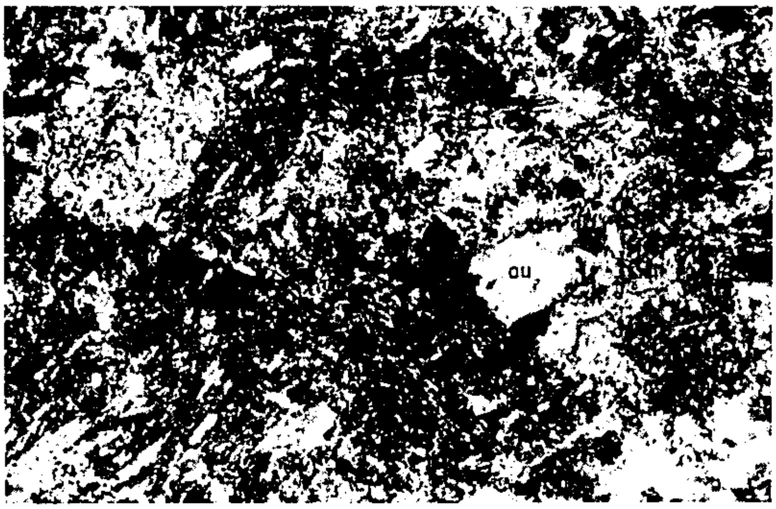

B: Glassy andesite
(Sample No. h-29)
In this photograph, it is observed that a small crystal of augite (au) is in a groundmass of altered glass and plagioclase laths.
X–nichols

x 50

PL-7

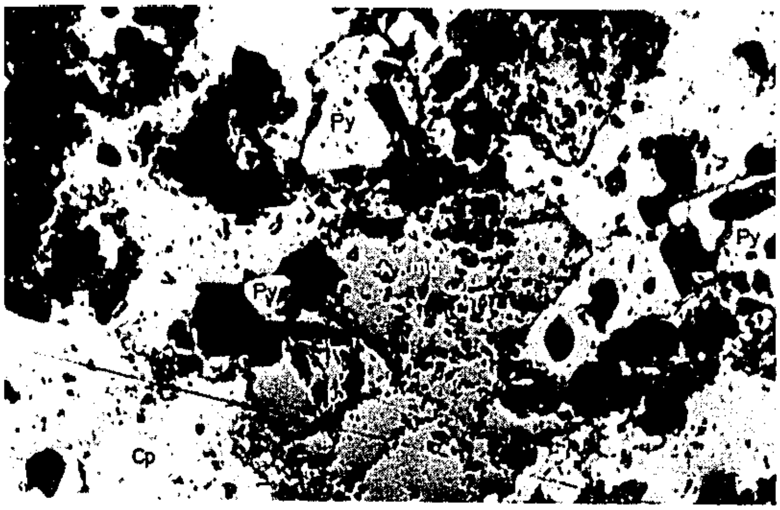

A: Chalcopyrite (cp)-pyrite (py) -magnetite
(Sample No. C-14)

Chalcopyrite, pyrite and magnetite are constituents. Magnetite and pyrite are enclosed by chalcopyrite.

// —nichols

x 25

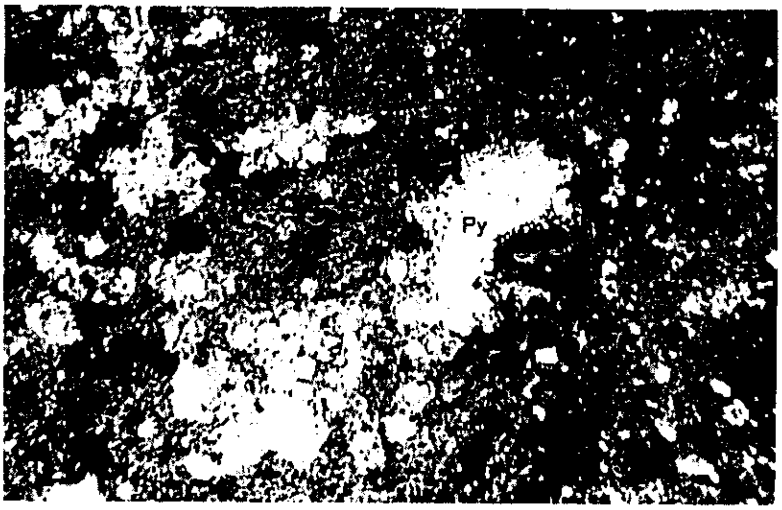

B: Coloidal pyrite in muddy compact rock
(Sample No. F-31)

Numerous tiny pyrite is scattered in muddy compact matrix (probably mudstone). Some of pyrite show coloform of framboidal texture.

// —nichols

x 25

C: Chalcopyrite (cp)-galena (ga) -sphalerite (sph)
(Sample No. F-75)

Chalcopyrite and galena show intergrowth, and they are enclosed by sphalerite.

// —nichols

x 25

PL-8

A: Disseminated specularite (sp) -Pyrite (py)
(Sample No. F-689)

Acicular specularite is associated with pyrite.

// —nichols

x 25

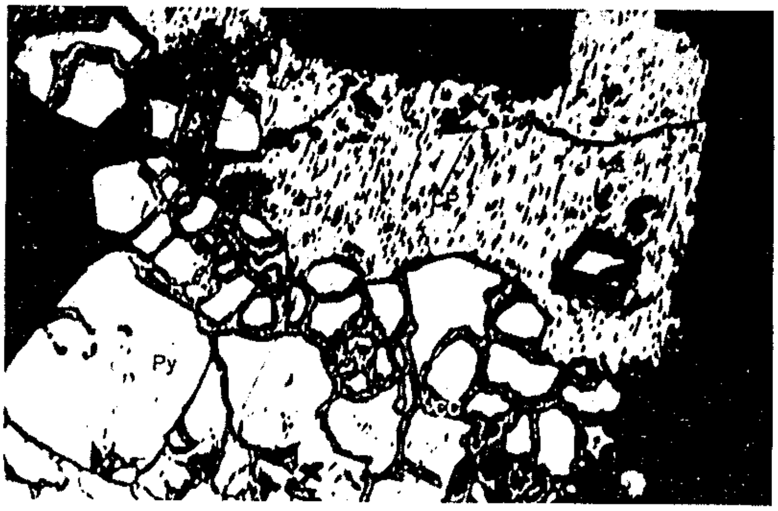

B: Disseminated chalcopyrite (cp) -pyrite (py)-secondary copper minerals
(Sample No. f-73)

Chalcopyrite and pyrite are main constituents. Pyrite is replaced by chalcocite along grain boundaries and fractures.

// —nichols

x 25

Table 4. Chemical analysis of rock samples

Sample No.	Location	Country rock	Au g/T	Ag g/T	Cu %	Pb %	Zn %	Mo %	$BaSO_4$ %	S %	Remarks
C-6	Tagbiga R.	Pyraxenite	6	-	0.53	-	-	<0.01	-	-	Pyrite-clay vein. Width: 0.30m
C-8	do	do	<1	-	18.05	-	-	<0.01	-	-	Chalcopyrite-pyrite-clay vein, Width: 0.02m
C-9	do	do	<1	-	<0.01	-	-	<0.01	-	-	Pyrite-clay vein, Width: 0.20m
C-11	do	do	6	-	11.69	-	-	<0.01	-	-	Malachite stain, Width: 0.20m
C-14	do	do	15	-	16.62	-	-	<0.01	-	-	Chalcopyrite-pyrite vein, Width: 0.15m
F-31	Lepant Mine	Silicified Shale?	-	-	0.11	tr	0.06	-	4.4	7.6	Silicified rock sampling, Width: 5.70m
F-42	Taon R.	Diorite	0.1	2	0.15	-	tr	0.046	-	1.7	Chalcopyrite-pyrite-*molybdenite veinlets*
F-42-1	do	do	1.2	20	3.10	-	0.01	0.036	-	17.6	do (best part)
F-75	Surigas Mine	Porphyry?	-	-	0.85	17.6	28.9	-	-	17.0	Ore stockpile (5T)
F-82	do	do	0.2	4	0.01	-	0.06	-	-	-	Quartz vein, Width: 1.00m
F-83	do	do	0.2	2	0.03	-	0.04	-	-	-	do Width: 1.00m
F-84	do	do	0.2	2	0.16	-	0.07	-	-	-	do Width: 0.25m
F-87	do	do	-	-	0.24	-	-	0.027	-	2.9	Altered porphyry
F-88	do	Andesite	0.1	2	0.04	-	0.09	-	-	3.2	Altered andesite
F-102	Silver Belt Mine	Porphyrite	-	-	0.01	-	0.11	-	-	-	Silicified & pyrite impregnated rock
F-158	Lepanto Mine	Silicified shale?	-	-	-	-	-	-	tr	2.6	do sampling Width: 5.00m
F-160	do	do	-	-	-	-	-	-	tr	0.85	do
F-162	do	do	-	-	-	-	-	-	tr	0.24	do
F-190	do	do	-	-	-	-	-	-	tr	0.61	do
F-202	do	do	-	-	0.02	tr	0.03	-	77.8	6.3	Barite lens
F-411	Taon River	Quartz diorite	0.4	-	0.18	-	-	0.021	-	1.5	Chalcopyrite-pyrite-magnetite impregnation
F-422	do	do	tr	-	0.26	-	-	0.022	-	-	do
F-425	do	do	0.3	-	0.37	-	-	0.019	-	-	do
F-432	do	do	0.2	-	0.20	-	-	0.024	-	-	do
F-2040	do	Andesite	0.2	-	2.5	-	-	0.030	-	-	Float (Chalcopyrite-pyrite-quartz)
F-2055	do	do	0.2	-	0.14	-	-	0.024	-	-	Float (. do)
F-2721	Soriano Mine	Dacite ~ Dacitic tuff	0.3	512	0.12	tr	0.06	-	59.3	25.2	Barite lens (barite-pyrite)

Sample No.	Location	Country rock	Au g/T	Ag g/T	Cu %	Pb %	Zn %	Mo %	$BaSO_4$%	S %	Remarks
f-45	Taon River	Basalt	-	-	0.57	-	-	0.025	-	37.9	Pyrite-barite impregnation
f-73	do	do	0.2	-	4.0	-	-	0.053	-	9.7	Float
f-81	do	do	0.2	-	0.22	-	-	0.023	-	-	do
f-100	Silver Belt Mine	Porphyrite	0.5	188	1.9	tr	tr	0.038	-	12.6	Chalcopyrite-pyrite impregnation
f-101	do	do	1.0	-	0.14	2.1	5.9	0.019	-	-	Chalcopyrite-sphalerite-galena impregnation
f-638	Taon River	Basalt	0.4	-	1.07	-	-	0.026	-	-	Float (pyrite-chalcopyrite-quartz) Width:0.50m
f-657	do	Andesite	0.1	-	tr	-	-	0.026	-	-	do (hematite-quartz)
f-658	do	do	0.2	-	0.24	-	0.91	0.023	-	5.6	Float
f-659	do	do	0.2	-	0.01	-	0.17	0.023	-	0.33	Sphalerite-pyrite impregnation
f-678	do	Basalt	0.1	-	0.01	-	-	0.030	-	-	Float
f-689	do	Andesite	0.2	-	0.54	-	-	0.023	-	-	do
f-691	do	do	0.2	-	0.50	-	-	0.021	-	-	Pyrite-hematite-chalcopyrite-Quartz vein
f-686	do	do	0.2	-	0.35	-	-	0.023	-	-	Float

Table 5. X-ray diffractive analysis

Sample No.	Location	Group or Formation	Rock	Clay mineral									Qz	Felds	Sulfate		Cal	Sulfide			Apa	Remarks
				Kao	Pyro	Halloy	Mont	Seri	Mus	Chl	Laum	Talc			Gyp	Bar		Cp	Py	Sph		
C-6	Tagbiga C.	Intrusives	Pyroxenite						O	O	O			O			O					Clay associated with ore
C-11	do	do	do						O	O			O					O			O	do
C-14	do	do	do							O				O				O	O			do
H-28	Cateel R.	Kaban G.	Andesite				O						O	O				O				Strongly argillized
H-29	do	do	do	O									O	O					O			do
H-31	do	do	do	O			O						O						O			do
H-33	do	do	do				O						O	O					O			do
Hi-10	Agusan R.	do	do	O			O	O					O	O								Weak argillized
Hi-11	do	do	do				O	O					O					O				do
Hi-16	Ngan R.	Intrusives	Porphyrite				O						O	O								Strongly argillized
Hi-19	do	do	do	O	O		O					O		O								do
Hi-24	do	Kaban G	Andesite					O					O		O							Silicified
Hi-29	do	do	do	O									O						O			Pyrite-impregnation
Hi-34	do	do	do			O							O	O	O				O			do
h-47	Batutu R.	do	Basalt	O			O						O	O								Strongly argillized
h-57	Ngan R.	do	Andesite				O						O	O					O			do
h-60	do	do	Sandstone	O			O						O						O			do
h-98	Mamunga R.	do	Andesite				O			O			O	O								do
h-104	do	do	do					O					O						O			do
F-31	Lepant M.	Barcelona G.	Shale	O												O						
P-42	Taon R.	Intrusives	Quartz diorite							O	O		O	O								Mineralized diorite
P-88	do	Barcelona G.	Andesite					O					O									Silicified
F-202	Lepant M.	do	Shale										O			O						Barite-lens
F-411	Taon R.	Intrusives	Quartz diorite					O		O	O		O	O								Weak argillized
F-422	do	do	do					O		O			O							O		do
F-425	do	do	do					O		O			O									do
F-432	do	do	do					O		O			O									do
F-2720	Sariano M.	do	Dacitic tuff	O				O					O									Strong argillized
P-2722	do	do	Dacite	O				O					O									do
F-2723	do	do	Dacitic tuff	O			O						O	O								do
f-41	do	do	Dolerite							O			O	O								Green, compact
f-71	do	Barcelona G.	Andesite										O									Float
f-96	do	do	do					O					O						O			do

Remarks:

Kao : Kaoline	Seri: Sericite	Talc : Talc	Bar : Barite	Sph : Sphalerite
Pyro : Pyrophyllite	Mus : Muscovite	Qz : Quartz	Cal : Calcite	Apa : Apatite
Halloy: Halloysite	Chl : Chlorite	Felds: Feldspar	Cp : Chalcopyrite	O : Present
Mont : Montmorillonite	Laum: Laumontite	Gyp : Gypsum	Py : Pyrite	

Table 6. Metal content of geochemical samples

(A) Stream sediment (−80-mesh fraction)

(ppm)

Ser.No.	Sample No.	Cu	Zn	Ni	Co	Ser.No.	Sample No.	Cu	Zn	Ni	Co	Ser.No.	Sample No.	Cu	Zn	Ni	Co
1	A - 2	39	87	182	23	56	A - 107	33	56	585	38	111	A - 194	36	44	165	28
2	8	39	49	45	18	57	110	33	57	585	39	112	196	51	60	590	37
3	13	30	43	39	15	58	113	46	70	558	40	113	197	41	40	173	27
4	14	34	43	32	14	59	116	34	51	438	34	114	198	67	63	237	32
5	17	83	45	55	17	60	118	71	93	418	39	115	200	58	55	151	25
6	19	35	50	45	16	61	119	59	99	656	44	116	202	73	57	219	31
7	20	43	68	39	20	62	120	49	62	540	42	117	204	60	53	265	47
8	22	36	45	52	18	63	121	41	70	444	35	118	205	35	42	216	29
9	24	41	57	132	31	64	124	26	45	468	35	119	206	30	31	99	21
10	26	41	57	55	19	65	125	31	43	695	44	120	208	32	33	146	32
11	27	35	58	43	14	66	126	81	108	393	39	121	210	60	74	159	29
12	28	43	55	41	14	67	128	40	81	903	41	122	211	52	53	193	25
13	30	38	51	44	13	68	129	56	74	466	40	123	212	46	38	121	23
14	31	33	47	42	19	69	130	19	42	1018	47	124	217	33	41	274	33
15	33	45	59	52	17	70	131	29	59	1125	51	125	218	50	62	212	33
16	35	36	52	49	12	71	133	57	65	323	43	126	219	34	40	273	33
17	37	35	44	33	10	72	134	48	60	380	44	127	220	43	59	98	20
18	44	26	36	22	9	73	136	24	33	582	46	128	221	37	45	232	28
19	46	29	42	27	13	74	137	32	36	455	49	129	222	43	79	61	15
20	47	39	44	29	11	75	139	44	44	660	53	130	224	35	47	226	26
21	48	37	57	31	15	76	140	22	34	609	45	131	225	51	58	293	23
22	49	33	49	29	14	77	141	37	48	747	61	132	226	40	54	253	26
23	50	33	53	42	15	78	142	28	42	690	52	133	227	28	45	493	36
24	51	21	41	25	10	79	143	44	60	938	76	134	230	32	54	420	28
25	55	37	65	55	20	80	144	44	50	484	35	135	231	52	58	593	44
26	57	35	64	45	19	81	151	61	85	303	35	136	232	40	54	574	42
27	58	31	62	43	19	82	155	41	69	504	43	137	233	47	51	223	36
28	59	28	63	41	19	83	157	108	128	431	40	138	234	27	33	277	29
29	60	30	59	39	16	84	158	43	55	613	49	139	235	61	54	202	27
30	61	40	76	45	19	85	159	80	129	576	50	140	236	55	50	253	26
31	62	41	63	49	23	86	160	52	88	267	33	141	237	98	87	635	53
32	64	43	62	51	20	87	161	37	53	444	40	142	238	60	60	283	32
33	67	38	62	51	21	88	162	143	162	1514	118	143	239	31	46	413	36
34	68	40	60	52	21	89	165	75	106	301	35	144	242	27	40	366	31
35	70	35	49	30	15	90	166	40	68	137	24	145	244	29	64	60	10
36	71	38	56	51	19	91	167	45	80	372	40	146	246	124	98	279	22
37	73	38	54	52	19	92	168	34	52	417	41	147	248	32	45	338	26
38	74	39	59	54	19	93	169	41	60	537	47	148	250	65	71	298	27
39	75	38	55	48	20	94	170	54	74	493	46	149	251	16	36	221	16
40	77	21	48	601	35	95	174	41	58	520	49	150	252	48	68	199	18
41	80	24	44	817	42	96	175	32	64	482	44	151	254	37	48	522	32
42	84	27	46	800	43	97	176	53	62	543	48	152	255	49	66	163	18
43	85	16	55	62	15	98	177	39	58	534	47	153	257	57	61	131	20
44	86	25	44	838	42	99	178	31	49	530	46	154	258	30	46	161	23
45	87	28	57	774	42	100	180	29	43	504	46	155	259	42	50	151	19
46	90	29	44	755	40	101	181	29	47	428	42	156	262	36	66	276	20
47	91	31	46	778	40	102	185	38	48	198	32	157	264	142	166	421	24
48	95	30	73	588	38	103	186	49	51	207	32	158	265	51	68	268	21
49	99	31	69	515	35	104	187	84	104	90	26	159	268	35	49	449	24
50	100	33	93	98	24	105	188	40	43	173	28	160	271	60	76	314	24
51	101	35	66	643	42	106	189	61	59	151	25	161	273	36	55	458	24
52	102	44	72	600	38	107	190	53	49	184	29	162	274	37	62	574	26
53	103	34	61	637	41	108	191	48	66	138	27	163	276	50	45	615	27
54	104	49	71	528	38	109	192	30	40	130	21	164	278	35	56	546	25
55	106	35	60	506	34	110	193	36	42	163	26	165	279	33	54	650	29

(ppm)

Ser.No.	Sample No.	Cu	Zn	Ni	Co
166	A - 280	62	78	240	20
167	283	25	53	718	27
168	284	37	60	733	29
169	286	38	51	456	18
170	289	42	66	401	20
171	290	29	67	807	73
172	292	38	61	903	82
173	294	50	60	1389	212
174	296	94	98	522	57
175	297	40	56	439	39
176	298	41	79	642	60
177	299	65	73	703	68
178	300	71	74	723	57
179	303	76	84	60	18
180	304	36	72	35	16
181	307	90	92	55	21
182	311	59	66	51	22
183	316	130	99	52	18
184	317	158	137	63	21
185	318	100	94	70	19
186	319	80	93	42	19
187	322	61	75	85	19
188	323	95	129	114	24
189	326	222	149	60	17
190	330	275	183	55	16
191	331	99	121	34	12
192	335	136	112	81	16
193	338	41	63	48	24
194	339	41	60	27	13
195	341	49	64	16	13
196	342	51	59	17	11
197	343	325	190	44	13
198	344	294	236	62	16
199	346	76	102	21	19
200	348	29	66	15	20
201	349	102	129	25	22
202	350	81	122	29	13
203	351	203	152	28	14
204	354	188	171	47	12
205	356	122	114	25	12
206	359	217	146	708	64
207	306	255	157	693	64
208	361	26	47	584	51
209	362	188	303	513	37
210	a - 3	61	50	450	31
211	6	42	43	520	35
212	8	34	37.8	557.9	36.8
213	11	38	42.8	840.0	68.8
214	12	91	71	497	33
215	13	59	53	271	30
216	14	35	35	596	39
217	15	33	509	181	24
218	16	62	74	150	23
219	17	47	50	214	32
220	19	53	61	210	32
221	20	53	95	194	27
222	22	80	145	103	24
223	23	46	127	244	31
224	28	40	71	270	41
225	27	57	147	313	33
226	28	50	85	275	48
227	29	81	89	488	59
228	30	68	83	397	46
229	31	73	105	558	53
230	32	43	63	566	62
231	a - 33	69	107	602	61
232	37	57	76	431	52
233	38	67	96	503	50
234	39	54	83	555	57
235	42	46	70	177	32
236	43	40	111	83	19
237	44	54	76	361	50
238	45	32	66	147	25
239	51	41	74	296	26
240	53	50	43	163	27
241	54	48	61	108	20
242	55	42	65	202	29
243	56	57	48	146	27
244	57	30	47	144	29
245	58	31	53	181	30
246	59	39	65	83	20
247	60	22	38	193	35
248	64	62	70	120	27
249	65	49	58	170	31
250	66	36	48	107	19
251	68	76	50	142	27
252	69	42	55	231	39
253	70	46	50	186	40
254	73	33	40	181	34
255	74	31	39	320	54
256	75	31	45	174	36
257	77	22	43	300	35
258	78	35	49	338	40
259	79	42	48	203	29
260	80	29	49	303	39
261	82	33	42	377	46
262	83	80	88	464	57
263	86	48	68	292	34
264	88	25	50	302	36
265	90	51	71	177	36
266	92	40	61	291	44
267	96	45	67	263	37
268	102	48	85	277	44
269	103	34	52	285	37
270	104	47	61	286	39
271	108	34	48	496	41
272	109	42	63	242	33
273	113	46	63	237	36
274	114	40	57	137	37
275	115	31	50	156	21
276	120	38	47	104	23
277	124	60	47	64	16
278	130	77	72	65	19
279	133	36	56	68	28
280	134	36	55	61	25
281	140	36	57	76	17
282	141	39	47	64	23
283	143	57	56	124	30
284	B - 6	33	48	369	28
285	7	37	43	349	27
286	9	33	48	401	31
287	10	77	56	284	32
288	13	70	70	390	28
289	15	34	44	460	32
290	17	40	48	452	33
291	18	45	49.2	464.0	32
292	19	28	33	232	24
293	20	43	58	482	34
294	21	36	45	641	37
295	23	24	34	312	30
296	B - 25	58	61	302	26
297	26	32	37	330	25
298	27	69	77	330	32
299	28	41	42	310	26
300	29	40	49	317	27
301	30	88	102	306	26
302	31	45	43	360	31
303	32	40	50	282	27
304	34	53	56	312	30
305	35	39	49	408	31
306	36	27	37	640	39
307	42	38	44	282	36
308	46	51	47	274	29
309	48	85	48	310	32
310	49	42	46	296	34
311	50	46	48	277	30
312	54	25	33	442	32
313	57	27	32	449	33
314	58	31	32	162	22
315	59	27	33	509	34
316	61	19	30	726	39
317	62	59	50	493	34
318	64	268	137	353	28
319	66	26	35	970	42
320	68	29	43	408	35
321	71	47	43	918	55
322	72	14	25	889	54
323	82	16	30	819	44
324	83	25	36	657	41
325	84	230	134	693	46
326	85	104	91	360	31
327	87	35	44	585	41
328	88	247	143	371	32
329	90	42	53	335	31
330	91	49	59	310	29
331	93	38	41	302	27
332	95	199	121	437	33
333	96	33	42	420	33
334	97	163	66	14	12
335	98	135	29	24	23
336	99	190	73	8	12
337	100	52	19	7	9
338	101	84	35	9	12
339	102	78	30	8	11
340	103	77	17	7	9
341	104	42	19	9	9
342	105	138	49	7	8
343	107	101	21	6	10
344	108	183	68	10	11
345	109	194	55	11	10
346	110	106	21	6	9
347	111	119	35	7	11
348	113	60	31	6	6
349	114	69	24	10	9
350	115	117	34	8	9
351	121	52	26	10	10
352	122	106	31	10	13
353	123	82	39	9	9
354	124	83	40	11	9
355	125	405	217	14	14
356	126	22	18	9	10
357	128	67	25	10	10
358	129	215	100	17	13
359	130	48	40	16	13
360	131	52	20	15	17

(ppm)

Ser.No.	Sample No.	Cu	Zn	Ni	Co
361	B - 132	68	25	8	12
362	133	79	15	7	9
363	134	93	27	10	11
364	135	51	69	11	12
365	136	84	21	9	10
366	137	117	24	6	11
367	138	49	24	7	11
368	139	53	15	4	8
369	141	140	56	5	19
370	142	78	20	7	10
371	143	64	24	6	11
372	144	70	27	7	10
373	145	29	29	10	11
374	147	54	16	11	12
375	148	100	39	9	15
376	150	29	45	12	16
377	151	36	48	14	18
378	152	40	19	9	17
379	153	16	15	13	16
380	154	48	42	8	13
381	155	62	43	8	15
382	156	38	38	7	10
383	157	55	69	10	17
384	160	37	25	10	10
385	163	24	50	22	16
386	165	31	76	34	22
387	166	19	56	20	15
388	167	29	62	40	25
389	168	26	60	25	21
390	169	35	74	44	27
391	171	34	67	41	26
392	174	32	55	20	15
393	175	28	50	24	16
394	177	34	23	13	12
395	178	44	60	53	33
396	181	38	29	20	18
397	182	54	32	21	20
398	186	23	43	736	43
399	187	19	32	691	42
400	188	15	45	861	55
401	189	22	37	755	45
402	190	19	36	600	36
403	192	23	40	1142	83
404	193	19	38	520	33
405	194	12	32	1220	71
406	196	18	36	762	62
407	197	13	37	920	56
408	198	22	40	713	68
409	199	8	30	984	60
410	200	22	51	1111	62
411	201	12	28	1028	36
412	203	26	47	560	69
413	205	11	37	771	43
414	206	24	45	626	37
415	207	33	44	511	42
416	209	27	45	513	28
417	210	25	45	297	98
418	211	17	66	826	31
419	212	39	56	324	69
420	213	23	27	520	39
421	221	23	24	420	31
422	222	38	39	201	18
423	223	18	36	1016	52
424	224	18	21	438	31
425	226	16	41	979	57
426	B - 227	16	34	1120	58
427	228	31	36	324	25
428	229	9	18	881	54
429	231	15	22	875	65
430	232	28	34	302	22
431	234	29	36	427	29
432	236	21	59	93	19
433	237	24	55	45	17
434	238	77	52	10	14
435	240	27	60	44	17
436	242	41	63	122	19
437	243	30	57	81	15
438	244	22	55	79	15
439	245	30	51	43	13
440	249	30	63	83	17
441	252	24	117	40	29
442	253	73	50	23	13
443	254	25	68	19	15
444	255	28	88	20	24
445	b - 2	29	36	319	28
446	4	35	38	186	27
447	5	32	51	153	23
448	6	34	50	85	19
449	8	37	42	414	42
450	9	36	27	199	31
451	10	36	35	294	33
452	13	32	31	219	31
453	17	34	27	233	32
454	18	24	27	472	37
455	19	31	30	51	22
456	20	13	23	772	42
457	21	59	50	83	27
458	22	47	51	264	32
459	24	34	33	406	33
460	26	27	40	342	31
461	27	30	38	399	34
462	28	27	36	331	30
463	32	27	43	86	15
464	33	28	43	125	20
465	34	28	44	89	15
466	36	32	43	104	17
467	37	28	45	60	12
468	38	25	38	102	16
469	39	28	44	56	15
470	41	30	41	59	12
471	42	38	30	177	25
472	45	34	31	285	29
473	46	38	41	224	29
474	47	43	46	166	30
475	48	47	52	181	31
476	49	22	26	150	17
477	50	32	32	216	23
478	51	29	34	125	18
479	52	24	31	152	18
480	53	27	31	168	20
481	54	24	25	224	22
482	55	27	21	159	17
483	56	26	23	146	18
484	57	18	31	27	10
485	58	20	34	22	9
486	59	17	28	14	5
487	60	17	31	25	8
488	61	18	40	33	9
489	62	17	38	19	10
490	66	18	55	14	14
491	b - 68	50	17	15	10
492	69	56	15	9	9
493	72	71	17	8	13
494	74	75	30	71	28
495	75	62	16	14	10
496	76	66	91	46	26
497	77	39	58	140	27
498	78	49	50	45	24
499	81	53	58	45	23
500	83	53	65	55	27
501	84	76	64	53	25
502	85	102	71	67	30
503	87	60	76	53	29
504	88	65	110	69	33
505	89	41	55	27	19
506	96	47	37	34	22
507	97	62	14	4	9
508	98	89	15	9	14
509	99	76	24	9	13
510	100	95	20	12	15
511	101	159	25	15	16
512	102	90	18	10	16
513	103	78	16	10	12
514	104	109	22	9	14
515	106	244	21	15	20
516	107	51	20	6	22
517	110	118	26	10	13
518	111	99	22	14	15
519	113	67	17	5	9
520	114	69	14	5	9
521	116	204	26	27	26
522	120	72	15	10	12
523	123	69	30	29	22
524	124	83	14	5	7
525	125	105	46	27	26
526	129	241	22	12	[illegible]
527	130	90	12	10	12
528	131	254	18	10	13
529	132	79	10	7	12
530	133	168	10	9	12
531	134	59	18	9	17
532	136	85	11	8	15
533	137	124	12	7	12
534	138	158	17	7	15
535	139	196	18	6	12
536	141	74	18	8	12
537	142	230	19	6	11
538	143	113	15	8	13
539	144	82	16	6	8
540	145	68	15	6	9
541	146	88	8	5	5
542	149	44	15	7	11
543	150	35	12	7	9
544	151	67	26	10	13
545	154	100	31	10	13
546	155	100	32	12	14
547	161	25	33	11	9
548	164	20	62	18	18
549	165	25	78	40	14
550	169	21	60	23	13
551	180	29	52	148	25
552	181	16	49	28	16
553	182	30	53	215	31
554	183	38	68	103	19
555	186	41	59	18	14

(ppm)

Ser.No.	Sample No.	Cu	Zn	Ni	Co
556	b - 187	27	71	67	18
557	188	16	62	27	18
558	190	77	74	20	17
559	191	24	54	21	15
560	192	69	68	16	16
561	193	30	59	20	14
562	194	30	56	12	13
563	195	29	65	17	16
564	196	33	66	35	16
565	197	42	77	12	17
566	BT - 4	45	70	572	47
567	5	34	60	491	50
568	7	34	54	146	28
569	9	22	61	451	39
570	10	26	58	298	30
571	12	15	53	337	28
572	13	29	43	148	24
573	14	22	62	642	55
574	16	17	56	529	44
575	19	20	52	327	39
576	21	22	59	332	33
577	22	40	55	352	33
578	23	29	59	427	42
579	24	36	79	355	56
580	26	36	89	23	22
581	27	35	71	15	17
582	28	40	81	15	21
583	29	57	63	25	16
584	30	35	69	22	16
585	C - 341	35	24	8	8
586	344	37	51	10	15
587	346	32	68	31	20
588	348	41	53	12	15
589	350	36	73	29	17
590	351	35	52	30	14
591	353	44	59	27	22
592	354	42	50	5	11
593	356	36	61	28	18
594	357	21	92	23	24
595	359	41	67	8	14
596	362	33	74	14	16
597	363	49	58	8	13
598	364	55	72	7	16
599	365	41	73	5	16
600	368	44	55	18	11
601	369	42	40	3	8
602	371	60	77	7	15
603	372	36	65	3	14
604	375	18	32	10	8
605	376	39	60	47	24
606	378	29	58	62	25
607	380	24	40	14	12
608	386	25	50	72	19
609	387	25	46	50	14
610	388	30	54	102	24
611	391	20	42	72	20
612	392	25	42	7	9
613	393	33	50	67	17
614	394	29	54	38	15
615	395	36	51	104	23
616	396	33	41	23	11
617	397	27	43	34	13
618	398	34	48	214	24
619	408	36	53	233	26
620	409	31	43	631	34
621	C - 411	44	84	214	31
622	412	33	44	641	36
623	413	43	55	414	33
624	414	34	44	547	33
625	416	36	41	619	34
626	417	40	54	201	24
627	418	33	54	660	36
628	420	33	47	192	22
629	421	34	49	659	36
630	422	35	46	539	31
631	423	40	58	421	27
632	429	48	73	104	24
633	CU - 1	42	53	13	11
634	3	66	28	9	10
635	4	50	33	9	9
636	5	123	67	18	17
637	6	32	55	14	13
638	7	61	86	24	20
639	8	31	104	29	24
640	9	46	47	11	11
641	10	56	47	9	11
642	12	43	94	23	22
643	13	41	87	21	19
644	19	46	31	9	10
645	CA - 141	108	57	24	18
646	143	91	58	20	17
647	144	67	71	28	19
648	146	67	79	38	22
649	147	63	56	20	14
650	162	34	70	113	21
651	164	36	61	183	38
652	165	25	52	61	14
653	166	23	47	57	16
654	168	32	49	71	17
655	169	17	51	46	13
656	170	22	58	31	12
657	171	26	53	67	15
658	172	15	47	29	9
659	173	25	47	56	15
660	176	26	57	48	15
661	177	23	39	11	9
662	179	19	39	99	8
663	180	13	49	22	11
664	181	21	55	91	18
665	182	22	69	47	16
666	190	33	60	87	23
667	192	45	77	32	24
668	193	22	59	67	30
669	197	31	44	241	24
670	198	29	66	89	20
671	199	30	47	242	26
672	200	27	44	225	24
673	202	26	46	540	36
674	203	35	52	363	27
675	204	40	51	518	34
676	205	35	54	163	22
677	206	35	36	409	27
678	207	45	65	161	23
679	209	32	31	493	31
680	CN - 212	37	73	7	12
681	213	39	73	31	16
682	214	22	57	26	11
683	216	47	50	26	10
684	217	46	81	41	19
685	219	61	80	26	18
686	CN - 220	39	75	40	19
687	221	30	79	27	17
688	222	38	79	43	20
689	223	68	80	41	20
690	224	281	79	56	22
691	230	54	61	24	16
692	232	56	49	17	13
693	233	59	39	22	12
694	234	57	32	13	10
695	236	36	72	81	22
696	237	38	74	93	24
697	238	27	64	97	21
698	239	22	71	104	22
699	241	27	79	120	24
700	242	19	53	54	15
701	243	43	54	78	24
702	244	33	55	56	21
703	245	16	44	29	12
704	CE - 117	36	51	25	12
705	127	51	65	102	22
706	132	19	49	10	8
707	133	47	49	18	12
708	135	20	42	81	20
709	137	25	57	67	17
710	138	24	54	102	20
711	139	24	48	148	21
712	140	29	52	110	20
713	141	24	50	656	50
714	142	28	53	92	20
715	143	29	65	40	18
716	144	29	67	93	21
717	147	25	66	60	19
718	148	31	65	108	20
719	150	38	66	59	21
720	D - 21	30	51	50	17
721	22	32	57	55	16
722	23	40	61	68	23
723	26	34	50	60	20
724	27	48	49	81	23
725	28	31	50	39	15
726	32	26	57	32	16
727	34	28	54	31	16
728	38	20	51	18	9
729	39	22	49	18	9
730	40	25	48	21	12
731	43	23	70	20	12
732	44	38	53	55	19
733	45	39	60	30	17
734	46	35	50	47	16
735	50	37	47	55	16
736	53	49	46	79	22
737	54	39	50	56	19
738	55	49	50	180	33
739	56	39	59	52	19
740	59	49	57	163	29
741	60	38	54	41	17
742	61	48	34	74	19
743	63	30	64	29	17
744	64	40	62	31	16
745	65	28	51	33	15
746	71	40	55	27	17
747	74	26	49	15	15
748	75	38	62	25	16
749	77	39	52	30	17
750	78	38	63	25	15

(ppm)

Ser.No.	Sample No.	Cu	Zn	Ni	Co
751	D - 82	38	61	29	16
752	83	39	74	32	17
753	85	39	65	31	17
754	86	39	67	31	17
755	88	32	50	28	13
756	89	51	50	41	24
757	94	41	64	42	19
758	97	42	65	31	19
759	98	25	63	20	13
760	100	38	55	28	17
761	101	31	57	21	14
762	102	29	52	21	15
763	106	31	40	21	12
784	111	45	34	23	12
765	115	42	53	21	13
766	116	45	46	24	11
767	118	33	39	13	9
768	119	46	47	28	13
769	121	44	58	29	15
770	122	40	49	23	12
771	123	29	75	21	15
772	124	45	57	28	16
773	125	33	63	21	14
774	126	33	68	19	13
775	127	31	62	15	11
776	129	37	58	25	14
777	130	36	75	27	16
778	131	33	103	22	14
779	132	25	58	44	16
780	133	34	63	46	17
781	136	35	71	45	21
782	137	51	50	27	12
783	138	77	53	32	13
784	141	35	56	51	13
785	142	35	51	53	14
786	143	43	70	46	19
187	144	26	48	44	11
788	145	24	50	77	20
789	151	66	45	13	10
790	152	65	46	15	11
791	153	30	25	7	9
792	154	59	43	13	10
793	155	45	30	10	10
794	157	162	27	11	11
795	158	75	36	8	10
796	162	81	61	15	13
797	163	100	32	7	13
798	164	178	29	7	10
799	165	100	30	7	12
800	166	102	29	6	12
801	167	107	28	8	11
802	170	56	52	35	18
803	171	71	47	35	19
804	172	44	40	25	16
805	173	43	62	26	20
806	176	38	66	23	17
807	178	32	65	21	16
808	179	35	63	24	16
809	d - 2	42	54	69	21
810	8	53	59	48	23
811	15	35	56	63	20
812	16	53	55	186	39
813	17	36	60	38	20
814	21	38	62	32	21
815	22	40	61	54	21
816	d - 23	33	63	116	21
817	24	23	65	75	17
818	25	29	58	87	20
819	26	40	67	32	17
820	27	36	48	30	18
821	28	34	66	26	11
822	30	42	68	75	23
823	33	23	61	19	10
824	34	31	63	32	13
825	35	37	60	51	17
826	39	34	56	34	16
827	43	11	39	10	8
828	44	28	50	20	14
829	45	39	42	21	11
830	46	40	39	19	10
831	49	56	42	28	12
832	50	38	45	22	11
833	53	39	44	21	13
834	57	83	53	38	16
835	61	55	42	19	12
836	63	61	38	20	11
837	64	28	55	29	14
838	67	44	37	14	10
839	68	57	44	31	13
840	70	78	43	24	13
841	71	20	57	105	19
842	72	40	43	128	16
843	73	46	34	13	10
844	74	39	32	10	8
845	75	51	31	13	8
846	76	49	45	13	12
847	77	37	70	78	19
848	80	61	39	13	10
849	84	57	39	11	10
850	85	57	35	13	8
851	86	27	70	85	19
852	87	59	41	10	9
853	88	54	43	14	11
854	90	55	50	26	14
855	91	47	44	9	9
856	94	61	39	12	10
857	95	58	40	11	11
858	98	122	25	15	14
859	99	56	25	7	7
860	100	85	78	48	18
861	104	27	73	19	15
862	105	37	74	33	15
863	106	25	78	20	14
864	107	18	90	14	16
865	108	42	92	127	24
866	109	27	86	23	15
867	110	22	101	20	21
868	111	32	69	26	15
869	113	71	55	16	10
870	114	40	47	16	10
871	116	39	90	32	18
872	117	31	76	23	16
873	118	29	57	18	11
874	119	33	61	23	13
875	122	39	60	35	18
876	123	37	70	38	19
877	124	34	62	31	15
878	125	44	81	68	27
879	126	41	64	41	21
880	127	33	102	20	15
881	d - 130	43	68	30	21
882	132	46	90	31	20
883	133	38	86	29	21
884	Dd - 4	24	41	19	11
885	6	39	63	31	19
886	7	22	44	17	10
887	8	34	52	29	15
888	9	54	57	40	20
889	10	40	59	32	18
890	13	31	59	27	15
891	E - 21	28	63	57	18
892	22	32	59	47	16
893	23	36	49	38	18
894	24	31	48	44	15
895	25	27	51	31	14
896	26	29	58	32	17
897	27	24	41	31	13
898	28	38	43	49	12
899	29	26	50	40	15
900	30	27	47	60	17
901	31	31	43	64	18
902	32	27	55	41	17
903	33	20	52	24	12
904	34	24	48	27	14
905	35	28	42	51	18
906	36	23	51	55	16
907	37	19	47	23	10
908	38	27	49	40	16
909	39	18	50	23	11
910	40	20	49	25	12
911	41	19	56	17	10
912	42	16	74	22	13
913	43	33	46	16	15
914	44	28	61	86	19
915	45	17	56	23	11
916	46	25	51	[illegible]	10
917	47	27	58	85	16
918	48	27	69	63	17
919	49	27	56	53	16
920	50	13	73	17	10
921	51	27	53	493	39
922	52	15	58	24	11
923	53	25	73	44	19
924	54	20	71	26	15
925	55	14	31	186	51
926	56	29	47	720	52
927	57	12	108	42	21
928	58	16	54	134	22
929	59	16	61	221	29
930	80	33	59	157	24
931	61	27	56	289	40
932	62	29	68	82	20
933	63	17	54	184	26
934	64	23	73	92	18
935	65	22	66	144	28
936	66	19	59	141	23
937	67	33	71	39	20
938	68	31	82	57	19
939	69	57	81	33	31
940	70	33	86	68	22
941	71	35	125	35	34
942	72	31	95	64	21
943	73	21	98	37	19
944	74	25	97	85	20
945	76	67	68	53	19

(ppm)

Ser.No.	Sample No.	Cu	Zn	Ni	Co
946	E 77	108	59	19	16
947	78	103	46	16	13
948	79	44	77	105	23
949	80	33	69	37	18
950	83	23	60	14	14
951	84	28	63	37	13
952	85	18	31	14	6
953	e - 21	30	55	83	21
954	22	15	54	15	7
955	23	21	72	27	13
956	24	15	39	16	7
957	25	40	57	43	20
958	26	13	57	16	9
959	27	14	68	16	13
960	30	15	45	17	9
961	EM - 9	23	48	31	14
962	10	20	78	22	14
963	11	21	48	27	12
964	12	27	55	28	15
965	13	20	46	25	13
966	14	21	70	26	16
967	15	19	104	24	17
968	16	22	50	28	14
969	17	16	55	19	11
970	18	36	41	67	21
971	C - 1	96	75	53	33
972	2	50	43	30	15
973	3	75	67	44	29
974	4	77	63	48	30
975	5	44	57	46	29
976	6	92	115	54	52
977	7	64	60	42	33
978	8	75	65	46	33
979	9	104	130	104	39
980	10	74	65	41	35
981	11	75	72	16	38
982	12	148	60	13	42
983	13	119	70	15	35
984	14	173	35	16	41
985	15	160	63	14	33
986	16	171	65	14	33
987	17	133	47	8	36
988	18	169	37	7	29
989	19	111	35	6	27
990	20	92	25	7	30
991	21	52	55	13	29
992	22	142	43	6	28
993	23	108	40	8	27
994	24	146	63	12	33
995	25	100	30	6	29
996	26	133	57	6	30
997	27	94	41	9	29
998	28	83	40	6	17
999	29	96	41	9	17
1000	30	68	33	6	33
1001	31	103	31	10	17
1002	32	196	75	7	38
1003	33	102	48	10	30
1004	34	118	50	7	27
1005	35	100	50	7	23
1006	36	129	43	5	27
1007	37	106	43	10	27
1008	38	208	55	7	29
1009	39	94	37	9	27
1010	40	108	37	6	27
1011	C - 41	108	42	7	27
1012	42	216	120	12	61
1013	43	102	48	9	30
1014	44	90	44	7	27
1015	45	137	31	6	27
1016	46	119	27	11	33
1017	47	392	68	10	46
1018	48	73	30	5	26
1019	49	100	40	7	26
1020	50	358	51	9	42
1021	51	81	35	5	26
1022	52	135	35	6	27
1023	53	83	39	9	33
1024	54	83	41	6	24
1025	55	54	28	7	36
1026	56	58	42	8	36
1027	57	78	30	6	23
1028	58	168	32	6	26
1029	59	103	40	8	30
1030	60	144	40	12	45
1031	61	52	50	7	18
1032	62	35	43	6	15
1033	63	111	79	16	42
1034	64	119	75	14	36
1035	65	92	70	15	30
1036	66	146	75	16	45
1037	67	39	62	11	15
1038	68	71	76	34	45
1039	93	57	23	5	26
1040	94	42	20	5	26
1041	95	65	20	5	20
1042	96	58	22	6	27
1043	97	63	35	6	30
1044	98	90	23	6	29
1045	99	60	23	5	24
1046	100	97	42	6	29
1047	101	52	15	4	16
1048	102	83	30	6	30
1049	103	47	29	6	30
1050	113	46	54	11	26
1051	114	225	54	30	38
1052	115	44	56	12	30
1053	116	92	80	24	42
1054	117	38	51	12	30
1055	118	73	70	23	30
1056	119	46	60	14	27
1057	120	71	65	14	30
1058	121	46	54	10	24
1059	122	61	74	19	30
1060	123	44	60	13	26
1061	124	46	58	12	24
1062	125	17	25	5	15
1063	126	46	60	13	30
1064	127	50	70	16	21
1065	128	54	70	15	23
1066	129	44	65	15	15
1067	130	54	60	16	23
1068	131	37	65	11	18
1069	132	57	75	15	30
1070	133	60	67	13	30
1071	134	54	78	46	44
1072	135	45	82	43	37
1073	136	44	85	44	49
1074	137	45	85	45	43
1075	138	41	80	40	37
1076	C - 139	49	80	43	30
1077	140	49	98	36	36
1078	141	49	75	53	30
1079	142	66	67	68	36
1080	143	33	67	37	21
1081	144	30	72	58	25
1082	145	25	55	16	16
1083	146	25	49	18	19
1084	147	131	45	33	39
1085	148	125	45	33	24
1086	149	105	49	37	30
1087	150	84	42	36	37
1088	151	254	50	31	37
1089	152	63	28	32	27
1090	153	93	43	37	41
1091	154	115	69	42	50
1092	155	91	40	31	37
1093	156	112	50	29	37
1094	157	76	30	23	30
1095	158	129	73	86	47
1096	159	94	35	28	33
1097	160	74	79	63	44
1098	161	56	65	56	30
1099	162	39	30	26	15
1100	163	49	68	55	30
1101	164	66	79	69	47
1102	165	49	54	51	26
1103	166	63	65	63	32
1104	167	57	50	37	18
1105	168	49	55	54	30
1106	194	98	50	37	31
1107	195	184	38	37	40
1108	196	85	58	37	35
1109	197	78	35	36	26
1110	198	152	57	36	42
1111	199	90	44	28	25
1112	200	89	45	25	25
1113	201	80	44	31	26
1114	202	59	39	26	25
1115	203	80	35	25	26
1116	204	57	44	31	25
1117	205	126	28	31	30
1118	206	118	40	38	31
1119	207	78	158	29	29
1120	208	78	45	54	60
1121	209	67	44	37	39
1122	210	74	43	33	36
1123	211	177	50	40	44
1124	212	95	37	26	23
1125	213	84	38	26	28
1126	214	72	63	36	37
1127	215	78	30	18	21
1128	216	98	39	25	25
1129	CA - 1	154	76	48	47
1130	2	123	113	85	50
1131	3	139	54	31	35
1132	4	197	70	36	44
1133	5	115	40	23	28
1134	6	186	62	38	47
1135	7	227	105	61	71
1136	8	181	135	55	77
1137	9	98	95	61	43
1138	10	120	118	74	59
1139	19	115	35	15	24
1140	20	71	43	23	38

(ppm)

Ser.No.	Sample No.	Cu	Zn	Ni	Co
1141	CA - 21	61	62	25	35
1142	22	61	47	25	30
1143	34	284	50	22	35
1144	35	56	61	45	32
1145	36	51	67	42	32
1146	37	30	73	36	24
1147	38	49	55	39	32
1148	39	49	52	41	34
1149	40	46	49	33	22
1150	41	52	62	33	28
1151	42	39	50	36	28
1152	43	35	48	34	16
1153	44	36	70	46	32
1154	66	168	35	24	24
1155	70	254	95	33	60
1156	73	87	83	79	45
1157	74	90	75	82	39
1158	75	93	79	55	41
1159	76	89	80	68	46
1160	77	93	82	70	43
1161	78	93	65	66	46
1162	90	260	53	25	48
1163	93	66	40	31	25
1164	94	77	49	38	32
1165	95	254	85	28	39
1166	96	129	53	31	28
1167	97	66	39	36	28
1168	98	85	65	25	28
1169	99	92	45	43	34
1170	100	115	44	61	36
1171	101	36	23	16	20
1172	102	32	29	31	29
1173	103	39	29	36	29
1174	104	36	34	26	27
1175	105	44	34	20	26
1176	106	43	36	29	33
1177	134	82	39	47	83
1178	CE - 1	119	92	63	45
1179	2	129	58	38	45
1180	7	50	59	41	37
1181	8	108	42	53	53
1182	9	240	35	31	31
1183	10	278	36	28	27
1184	11	126	40	28	35
1185	12	62	63	69	44
1186	13	78	62	38	38
1187	14	61	82	37	59
1188	15	61	71	43	59
1189	16	48	72	47	33
1190	17	74	81	40	54
1191	18	34	86	49	59
1192	19	95	74	40	49
1193	20	86	60	27	36
1194	21	103	41	63	38
1195	22	74	43	38	46
1196	23	94	54	81	44
1197	24	132	44	85	48
1198	25	87	47	81	45
1199	26	132	52	54	45
1200	27	46	52	95	50
1201	CE - 28	103	52	78	52
1202	29	102	120	87	49
1203	30	98	92	109	54
1204	31	97	98	103	53
1205	34	96	37	25	33
1206	63	56	38	32	38
1207	64	78	51	47	48
1208			37	39	38
1209	76	100	43	26	32
1210	77	80	47	27	33
1211	78	110	44	29	33
1212	79	83	51	25	35
1213	80	50	49	48	27
1214	81	29	49	39	33
1215	93	167	35	39	45
1216	94	233	35	33	34
1217	95	198	45	33	51
1218	96	333	37	43	51
1219	105	337	43	24	37
1220	106	102	37	33	52
1221	107	104	40	37	45
1222	CN - 1	188	69	30	45
1223	2	83	92	40	49
1224	3	146	37	23	31
1225	4	271	75	31	48
1226	5	104	60	30	40
1227	6	333	49	29	47
1228	7	69	48	28	38
1229	8	146	57	29	45
1230	9	115	52	23	38
1231	10	158	46	35	45
1232	11	129	37	19	36
1233	12	169	60	35	48
1234	13	104	54	23	36
1235	14	105	66	28	42
1236	15	127	150	21	38
1237	16	50	68	38	85
1238	22	204	58	32	69
1239	33	92	49	27	36
1240	34	96	37	25	33
1241	35	112	40	24	33
1242	36	71	46	27	39
1243	37	177	60	30	43
1244	38	63	40	25	34
1245	39	37	29	18	22
1246	40	73	58	31	44
1247	41	25	32	17	19
1248	42	20	27	38	21
1249	43	17	28	29	26
1250	44	29	35	31	33
1251	45	13	17	29	15
1252	46	13	35	25	37
1253	63	79	58	24	36
1254	64	35	52	43	27
1255	65	20	50	38	22
1256	66	10	40	23	12
1257	67	17	48	32	21
1258	68	20	46	30	21
1259	69	25	46	29	21
1260	70	20	55	29	23
1261	CN - 71	25	55	32	22
1262	72	31	52	29	23
1263	73	25	56	26	26
1264	74	29	53	30	25
1265	75	20	46	18	18
1266	76	10	41	16	13
1267	89	167	32	19	26
1268	90	254	37	17	30
1269	91	38	43	22	26
1270	92	83	17	24	38
1271	93	354	55	21	35
1272	94	329	43	18	26
1273	95	171	35	21	32
1274	113	38	64	55	35
1275	114	46	66	28	38
1276	115	38	40	32	27
1277	116	62	33	29	32
1278	117	208	46	26	38
1279	118	135	52	43	33
1280	119	125	33	26	28
1281	120	156	35	26	27
1282	121	62	66	40	43
1283	122	56	63	40	39
1284	123	52	58	42	36
1285	124	83	62	31	38
1286	132	73	17	19	27
1287	133	69	17	20	28
1288	139	104	46	27	32
1289	142	90	46	24	31
1290	143	38	40	29	20
1291	145	31	32	25	18
1292	157	21	58	24	30
1293	158	29	63	31	38
1294	159	22	56	29	36
1295	160	146	33	23	26
1296	161	131	29	13	23
1297	162	104	22	18	24
1298	163	146	28	17	20
1299	165	166	29	19	25
1300	196	96	21	14	20
1301	197	33	29	20	17
1302	198	46	37	26	23
1303	199	31	39	20	19
1304	200	46	37	23	20
1305	201	33	37	18	16
1306	202	33	35	22	19
1307	203	62	29	20	19
1308	211	8	47	16	14
1309	CU - 35	71	18	56	20
1310	49	67	20	14	26
1311	50	62	17	12	20
1312	51	67	19	16	26
1313	52	48	17	16	20
1314	53	46	18	16	20

(ppm)

Ser.No.	Sample No.	Ag	Cu	Zn	Mo
1315	E - 91	1.0	93	123	0.9
1316	92	1.5	139	167	0.9
1317	94	1.5	90	164	0.9
1318	96	1.5	154	166	1.4
1319	97	1.0	81	155	1.1
1320	98	1.0	90	152	1.0
1321	99	1.0	148	134	0.4
1322	100	1.0	101	77	0.5
1323	101	2.0	81	154	0.9
1324	102-1	1.5	133	93	0.2
1325	" -2	2.0	108	166	0.7
1326	103-1	1.5	146	139	0.6
1327	" -2	2.0	104	135	1.0
1328	104	1.5	128	157	0.5
1329	105	1.5	105	119	0.7
1330	106	1.0	146	121	0.6
1331	108	1.5	128	192	0.6
1332	109	1.5	148	126	0.6
1333	110	1.5	128	158	0.6
1334	114	1.0	121	186	0.6
1335	115	1.0	67	108	0.5
1336	116	1.5	78	158	0.6
1337	118	1.5	113	183	0.7
1338	119	1.0	79	134	0.6
1339	F - 3	3.4	151	104	0.7
1340	5	2.8	92	140	0.5
1341	7	3.4	127	109	0.3
1342	8	3.4	157	104	0.4
1343	9	4.0	187	168	0.4
1344	10	3.4	128	96	0.8
1345	11	2.8	96	93	0.7
1346	12	2.8	137	102	0.5
1347	13	3.4	95	183	0.4
1348	17W	3.4	87	224	0.5
1349	18	2.8	79	169	0.7
1350	21	4.0	86	131	0.8
1351	22W	3.4	69	267	0.7
1352	23W	2.8	87	248	0.9
1353	27	2.8	74	81	0.6
1354	28	2.8	64	51	1.3
1355	467	2.3	147	187	0.9
1356	468	2.3	126	67	0.5
1357	469	2.8	125	88	0.4
1358	470	2.3	143	103	0.5
1359	471	2.3	172	96	0.4
1360	472	2.8	121	186	0.9
1361	473	2.3	181	105	0.8
1362	479	3.4	129	86	0.2
1363	480	2.8	135	98	0.3
1364	481	2.5	132	107	1.4
1365	482	2.0	94	111	1.1
1366	483	2.0	118	82	0.6
1367	484	2.0	157	80	0.5
1368	485	2.0	125	90	0.7
1369	488	2.0	80	93	0.5
1370	489	2.0	101	84	0.6
1371	490	1.5	138	67	1.2
1372	491	1.5	186	94	1.1
1373	492	1.5	130	81	0.8
1374	493	1.5	143	72	0.9
1375	494	1.5	141	85	1.0

Ser.No.	Sample No.	Ag	Cu	Zn	Mo
1376	F - 495	1.5	191	142	1.0
1377	496	2.0	194	75	1.7
1378	497	2.0	236	105	1.0
1379	499	1.5	169	83	1.1
1380	503	1.5	114	79	0.6
1381	505	2.0	103	57	0.6
1382	506	2.0	177	104	1.7
1383	507	2.0	147	83	1.0
1384	508	2.0	131	77	0.6
1385	509	1.5	202	84	0.7
1386	510	1.5	142	82	0.9
1387	511	1.5	125	87	0.7
1388	512	1.5	170	235	1.2
1389	513	1.6	157	145	0.4
1390	514	1.6	81	121	1.3
1391	515	1.6	176	145	0.5
1392	516	2.1	164	218	0.7
1393	517	1.6	94	80	0.4
1394	518	1.6	162	114	0.3
1395	521	1.0	66	75	0.4
1396	523	2.1	47	94	0.2
1397	525	1.0	69	48	2.9
1398	527	2.1	128	141	0.4
1399	528	2.1	83	98	0.5
1400	529A	2.1	73	123	0.6
1401	529B	2.6	115	81	0.8
1402	530	2.6	86	47	0.3
1403	531	3.1	107	134	0.5
1404	532	2.6	109	139	0.4
1405	533	3.1	100	184	0.4
1406	534	2.6	91	115	0.2
1407	535	2.1	94	171	0.3
1408	540	3.1	104	217	0.7
1409	541	2.6	81	100	0.3
1410	543	2.6	101	104	0.8
1411	545	2.6	56	95	1.4
1412	546	2.1	50	135	0.4
1413	549	1.6	86	101	0.3
1414	550	2.0	64	110	1.1
1415	552	1.5	80	137	0.5
1416	553	1.5	53	100	0.4
1417	554	1.0	90	82	1.1
1418	556	1.5	59	105	1.5
1419	558	2.0	36	61	1.2
1420	559	1.0	164	57	3.6
1421	561	2.0	22	20	0.8
1422	562	2.0	106	52	1.4
1423	565	1.5	120	81	3.2
1424	566	1.5	106	65	2.0
1425	567	1.5	53	72	0.8
1426	569	1.0	186	94	9.6
1427	570	1.5	67	52	3.6
1428	571	1.0	103	62	2.9
1429	572	1.0	105	86	2.8
1430	574	2.0	65	53	2.0
1431	576	1.0	130	73	1.1
1432	577	1.5	101	74	1.0
1433	580	1.5	58	58	0.7
1434	581	1.5	144	70	0.5
1435	582	2.0	36	66	0.3
1436	583	1.5	50	86	0.8
1437	584	1.5	101	67	0.8
1438	585	2.0	110	78	1.1
1439	586	1.5	83	90	0.3
1440	587	3.1	77	94	0.2

Ser.No.	Sample No.	Ag	Cu	Zn	Mo
1441	F - 588	2.1	93	141	0.9
1442	589	2.6	91	68	0.4
1443	590	2.6	167	66	0.8
1444	591	2.1	40	95	0.6
1445	596	1.5	144	38	0.7
1446	29	1.0	54	120	2.3
1447	f - 1	2.1	158	153	2.1
1448	4	2.6	155	112	1.4
1449	6	3.1	162	115	0.9
1450	11	1.5	176	129	1.1
1451	12	2.1	153	137	0.3
1452	18	1.5	253	84	0.5
1453	19	1.0	106	125	0.4
1454	24	1.5	155	135	0.7
1455	29	2.1	140	129	0.6
1456	33	1.0	109	126	0.5
1457	500	1.5	55	83	1.5
1458	501	2.1	86	65	2.2
1459	504	2.1	77	36	0.3
1460	505	1.5	73	74	1.2
1461	506	1.0	53	121	1.4
1462	508	1.0	40	92	0.6
1463	511	1.5	100	96	0.5
1464	513	1.5	51	47	1.3
1465	515	1.6	54	42	0.4
1466	516	1.0	130	74	0.2
1467	521	1.0	72	51	4.2
1468	522	1.0	48	71	0.6
1469	524	1.0	73	92	0.4
1470	525	1.0	43	177	0.7
1471	526	1.0	133	71	0.4
1472	527	1.0	61	100	0.6
1473	529	1.0	59	52	0.4
1474	530	1.6	143	80	0.3
1475	532	1.0	61	72	0.3
1476	533	1.0	47	58	0.3
1477	534	1.6	73	91	0.3
1478	535	1.0	71	72	0.5
1479	536	1.6	91	132	0.4
1480	537	1.6	38	117	0.7
1481	538	2.1	44	129	0.6
1482	539	1.0	103	73	1.8
1483	540	2.1	151	86	1.2
1484	544	1.6	86	87	0.3
1485	550	1.0	77	76	0.5
1486	552	1.6	242	160	1.3
1487	553	1.0	59	126	0.3
1488	554	1.0	55	111	0.7
1489	555	0.5	104	76	0.3
1490	556	2.5	118	173	0.7
1491	557	2.0	95	109	0.8
1492	558	2.0	46	78	0.6
1493	559	2.5	86	167	0.7
1494	560	3.0	34	135	0.8
1495	561	3.0	94	171	0.9
1496	562	1.5	121	106	0.5
1497	564	1.5	149	105	0.5
1498	565	2.0	131	102	0.5
1499	566	2.0	221	119	0.6
1500	571	1.5	50	106	1.5
1501	573	2.0	111	191	0.9
1502	574	1.5	76	132	1.4
1503	576	1.5	64	107	0.8
1504	578	2.0	59	111	1.0
1505	579	2.5	55	120	1.0

(ppm)

Ser.No.	Sample No.	Ag	Cu	Zn	Mo	Ser.No.	Sample No.	Ag	Cu	Zn	Mo	Ser.No.	Sample No.	Ag	Cu	Zn	Mo
1506	f - 583	2.0	38	77	3.0	1571	G - 48	2.1	34	141	0.3	1636	G - 132	1.1	111	90	0.9
1507	584	1.5	74	172	0.9	1572	49	1.5	52	136	0.5	1637	133	2.2	193	236	1.1
1508	585	1.0	21	94	1.0	1573	51	1.5	118	53	0.4	1638	135	2.2	127	128	0.7
1509	586	1.0	40	81	9.2	1574	53	1.0	67	59	0.5	1639	136	2.2	94	76	0.6
1510	587	1.5	51	84	2.2	1575	55	1.0	60	57	0.4	1640	137	5.0	62	46	0.5
1511	588	2.5	20	62	1.0	1576	56	1.5	40	52	0.4	1641	139	3.3	81	86	0.9
1512	589	1.5	43	84	3.6	1577	57	1.5	58	59	0.3	1642	140	3.3	105	109	0.7
1513	590	1.5	162	141	1.9	1578	58	1.5	55	61	0.5	1643	141	2.8	103	69	0.5
1514	591	1.5	65	124	1.0	1579	59	2.6	57	52	0.7	1644	142	3.3	68	37	0.5
1515	592	3.5	10	21	0.1	1580	60	2.1	44	54	0.6	1645	143	3.9	156	171	1.0
1516	593	2.5	184	69	0.7	1581	62	2.6	54	59	0.7	1646	145	5.0	84	108	0.7
1517	595	2.0	28	54	0.4	1582	63	3.1	57	66	0.4	1647	146	3.9	103	46	0.4
1518	597	1.5	43	56	1.1	1583	64	2.6	55	66	0.7	1648	147	3.3	113	85	0.6
1519	598	2.5	85	107	1.5	1584	65	3.1	55	51	0.7	1649	149	3.3	55	49	0.7
1520	600	2.0	75	60	1.2	1585	66	3.6	38	60	0.5	1650	150	4.4	144	77	0.4
1521	601	2.0	66	157	0.2	1586	69	3.6	151	55	0.4	1651	151	3.3	59	74	0.7
1522	602	2.0	64	56	0.4	1587	70	3.1	144	60	0.3	1652	152	3.9	92	72	0.7
1523	603	2.0	53	58	0.3	1588	72	3.1	182	64	0.3	1653	154	3.3	59	73	0.5
1524	604	2.0	75	64	0.2	1589	73	1.5	108	57	0.3	1654	155	2.8	73	86	0.8
1525	605	1.5	78	79	0.5	1590	74	1.5	82	67	0.2	1655	156	2.8	55	53	0.9
1526	606	2.5	71	63	0.1	1591	76	1.5	83	80	0.2	1656	157	3.9	73	43	0.6
1527	G - 1	2.5	133	156	0.4	1592	77	1.0	104	76	0.3	1657	158	2.2	62	74	1.1
1528	2	2.0	81	143	0.4	1593	79	1.5	76	62	0.0	1658	159	3.3	59	103	0.7
1529	3	1.5	137	97	0.3	1594	81	1.5	131	76	0.2	1659	160	2.8	59	68	0.6
1530	4	2.0	129	80	0.2	1595	82	2.1	81	66	0.3	1660	161	2.8	43	65	0.4
1531	5	2.0	119	145	0.5	1596	83	1.5	116	118	0.3	1661	162	3.3	51	53	1.6
1532	6	2.5	137	110	0.4	1597	84	3.1	69	154	0.7	1662	163	4.4	45	64	0.4
1533	7	2.5	92	98	0.2	1598	85	3.1	98	99	0.3	1663	165	3.3	51	64	0.7
1534	8	2.0	135	100	0.3	1599	87	3.1	123	119	0.4	1664	166	2.2	61	53	0.4
1535	9	1.5	117	74	0.2	1600	88	2.6	82	55	0.2	1665	167	4.4	114	61	0.3
1536	10	2.0	133	109	0.4	1601	90	3.6	93	121	0.7	1666	168	4.4	79	67	0.6
1537	11	2.0	137	108	0.4	1602	91	3.6	130	112	0.2	1667	169	4.4	89	74	1.0
1538	12	1.5	117	85	0.2	1603	92	3.6	79	96	0.3	1668	170	3.9	60	69	0.6
1539	13	2.5	134	121	0.4	1604	93	4.1	109	167	0.5	1669	171	3.3	69	91	0.7
1540	14	2.6	89	167	0.5	1605	94	4.1	122	174	0.5	1670	172	3.3	65	69	0.6
1541	15	1.0	106	93	0.3	1606	96	3.6	81	106	0.6	1671	173	3.3	81	56	1.7
1542	17	1.6	132	92	0.2	1607	97	3.1	78	100	0.5	1672	174	2.8	67	70	0.5
1543	18	1.0	141	59	0.4	1608	98	3.1	79	113	0.7	1673	175	2.8	95	45	0.3
1544	19	1.6	97	80	0.2	1609	99	2.1	103	119	0.3	1674	176	2.8	91	163	1.1
1545	20	1.6	87	58	0.1	1610	100	2.6	92	108	0.6	1675	177	3.3	98	53	0.3
1546	21	2.1	95	147	0.3	1611	101	2.1	105	63	0.3	1676	178	2.2	99	49	0.0
1547	22	2.6	87	93	0.2	1612	103	2.1	93	56	0.2	1677	179	2.2	92	48	0.2
1548	23	3.6	100	92	0.3	1613	104	2.1	148	139	0.3	1678	180	2.2	64	54	0.6
1549	24	2.1	105	80	0.3	1614	105	2.1	154	104	0.3	1679	182	3.3	158	37	0.1
1550	25	1.6	101	71	0.3	1615	106	3.8	151	108	0.6	1680	183	3.9	95	54	0.3
1551	26	1.0	102	88	0.2	1616	107	3.3	138	83	0.6	1681	184	3.9	71	56	0.4
1552	27	2.1	85	79	0.2	1617	109	2.7	126	72	0.9	1682	185	4.4	72	61	0.0
1553	28	1.6	86	114	0.3	1618	110	3.3	116	53	0.5	1683	186	3.3	65	112	0.8
1554	29	2.1	132	53	0.2	1619	111	2.7	123	70	0.4	1684	187	3.3	56	108	0.8
1555	30	1.0	125	61	0.2	1620	112	2.7	125	76	0.6	1685	188	2.8	65	105	0.8
1556	32	1.0	89	63	0.7	1621	113	4.3	101	91	0.8	1686	189	3.3	85	155	1.0
1557	34	1.6	85	84	0.7	1622	115	3.3	114	115	0.8	1687	190	2.2	91	177	1.1
1558	35	3.1	44	82	0.8	1623	116	3.3	95	86	0.8	1688	191	1.7	43	118	0.9
1559	36	2.1	63	81	0.6	1624	117	3.3	127	84	0.4	1689	192	1.7	68	124	1.0
1560	37	2.1	48	76	0.6	1625	118	2.7	101	136	0.5	1690	193	3.1	75	92	0.5
1561	38	2.1	52	69	0.5	1626	119	3.8	96	68	0.2	1691	194	3.1	103	253	0.5
1562	39	2.1	81	97	1.0	1627	121	3.8	98	108	0.5	1692	197	2.6	84	179	0.8
1563	40	2.6	47	73	0.6	1628	122	2.7	86	46	0.7	1693	198	2.6	83	183	0.7
1564	41	1.6	51	84	0.5	1629	123	2.2	112	75	0.2	1694	199	2.1	66	80	0.3
1565	42	3.1	57	95	0.6	1630	124	2.7	113	100	0.5	1695	200	2.1	110	237	0.7
1566	43	2.6	41	147	0.3	1631	125	2.2	99	80	0.7	1696	201	1.5	153	107	0.5
1567	44	2.1	50	118	0.5	1632	126	2.2	105	84	0.6	1697	202	2.1	98	115	0.8
1568	45	1.5	37	110	0.5	1633	127	2.2	127	77	0.8	1698	203	1.0	160	56	0.6
1569	46	1.0	61	100	0.6	1634	129	2.2	105	96	1.0	1699	204	1.0	103	118	0.7
1570	47	1.5	38	129	0.5	1635	130	1.6	120	70	0.4	1700	205	1.0	121	95	0.2

(ppm)

Ser.No.	Sample No.	Ag	Cu	Zn	Mo
1701	G - 206	1.0	104	60	0.4
1702	207	2.1	133	74	0.5
1703	208	2.1	104	62	0.5
1704	209	1.5	112	83	0.3
1705	210	1.5	116	98	0.5
1706	211	1.0	101	93	0.4
1707	212	1.5	110	95	0.6
1708	213	1.0	113	58	0.4
1709	214	1.0	116	99	0.8
1710	215	1.5	98	82	0.5
1711	216	1.0	116	74	0.7
1712	217	1.0	136	100	0.6
1713	218	1.0	124	195	0.9
1715	219	1.0	133	60	0.4
1715	220	3.6	130	103	0.6
1716	221	3.1	89	130	0.5
1717	222	3.1	93	101	0.5
1718	223	2.6	97	120	0.5
1719	224	3.1	111	73	0.4
1720	225	3.1	82	117	0.7
1721	226	3.6	108	75	1.0
1722	227	3.1	79	102	0.3
1723	228	2.1	106	63	0.5
1724	229	1.5	107	74	1.0
1725	230	1.5	108	76	0.5
1726	231	1.5	165	85	0.5
1727	232	3.1	107	93	0.6
1728	233	2.6	118	62	0.3
1729	234	2.6	119	58	0.3
1730	235	2.1	114	103	0.6
1731	236	2.6	109	64	0.5
1732	237	1.5	117	51	0.2
1733	238	1.5	111	48	0.3
1734	239	1.5	125	76	0.4
1735	240	1.5	109	50	0.4
1736	241	2.1	78	96	0.3
1737	242	2.1	119	175	0.4
1738	243	1.5	106	110	0.3
1739	244	1.5	119	85	0.4
1740	245	2.4	88	147	0.5
1741	246	1.5	133	86	0.3
1742	247	2.4	128	80	0.4
1743	248	1.9	127	65	0.3
1744	249	2.4	142	107	0.4
1745	250	1.9	168	148	0.6
1746	251	1.9	140	72	0.3
1747	252	2.4	152	81	0.3
1748	254	1.9	97	69	0.3
1749	255	1.9	135	127	0.4
1750	256	2.9	132	128	0.4
1751	257	1.5	150	61	0.3
1752	259	1.5	142	82	0.4
1753	260	1.9	141	96	0.6
1754	261	1.5	128	77	0.5
1755	263	1.5	150	98	0.3
1756	265	1.5	153	50	0.4
1757	266	1.5	152	133	0.4
1758	267	1.5	91	97	0.7
1759	270	1.5	100	109	0.6
1760	271	1.5	113	78	0.5
1761	272	1.0	108	64	0.5
1762	274	1.5	101	82	0.4
1763	276	1.0	141	61	0.2
1764	277	1.0	101	83	0.4
1765	278	2.4	105	94	0.9
1766	G - 279	1.9	111	133	0.8
1767	280	1.9	102	158	0.8
1768	282	1.5	75	112	0.6
1769	283	1.0	93	77	0.7
1770	284	1.0	69	82	0.6
1771	285	2.4	119	86	1.2
1772	288	1.9	112	86	1.2
1773	289	2.4	113	102	1.9
1774	g - 1	1.5	74	69	0.5
1775	3	1.9	115	304	0.9
1776	4	1.9	83	106	0.5
1777	5	1.5	74	59	0.1
1778	7	1.5	59	64	0.2
1779	9	1.5	115	74	0.7
1780	10	1.0	116	106	0.6
1781	11	1.9	143	134	0.8
1782	12	1.9	120	87	0.7
1783	13	1.5	131	132	0.8
1784	14	1.9	132	99	0.7
1785	15	1.5	98	118	0.4
1786	16	1.5	122	75	0.7
1787	17	1.0	110	99	0.8
1788	18	1.9	138	135	0.8
1789	19	1.9	140	176	1.3
1790	20	1.0	122	83	0.7
1791	21	1.0	124	70	0.5
1792	22	1.0	127	87	0.4
1793	23	1.5	126	73	0.5
1794	24	1.5	127	76	0.4
1795	25	2.5	126	106	0.3
1796	26	1.0	157	128	0.3
1797	27	1.5	123	102	0.3
1798	28	1.0	129	155	0.3
1799	29	1.0	143	91	0.3
1800	30	1.5	135	75	0.3
1801	31	1.5	127	79	0.3
1802	32	2.0	130	88	0.3
1803	33	2.5	114	102	0.3
1804	34	1.5	141	84	0.3
1805	35	1.0	74	107	0.6
1806	36	1.5	78	108	0.7
1807	37	1.0	83	135	0.5
1808	38	1.0	64	136	0.6
1809	39	1.0	78	115	0.5
1810	40	1.0	103	157	0.7
1811	41	1.5	87	126	0.7
1812	42	2.0	76	105	0.8
1813	43	1.5	100	118	1.8
1814	44	1.0	90	192	0.9
1815	45	1.0	104	139	0.7
1816	46	1.5	72	125	0.6
1817	47	1.5	122	186	0.9
1818	48	1.0	86	81	0.5
1819	49	2.0	100	168	1.3
1820	50	1.5	89	82	0.5
1821	51	2.0	165	242	2.8
1822	52	1.5	116	208	1.1
1823	54	1.5	103	110	0.4
1824	55	1.5	132	131	0.5
1825	56	3.0	94	136	0.7
1826	57	2.5	137	114	0.5
1827	H - 1	1	138	45	< 2
1828	3	1	91	63	< 2
1829	4	1	89	77	< 2
1830	5	1	242	49	< 2
1831	H - 6	< 1	54	49	< 2
1832	7	< 1	35	45	< 2
1833	8	1	72	90	< 2
1834	9	< 1	109	100	< 2
1835	10	1	72	37	< 2
1836	11	1	86	34	< 2
1837	12	1	53	75	< 2
1838	13	1	72	77	< 2
1839	14	1	77	83	< 2
1840	15	1	72	71	< 2
1841	16	1	72	63	< 2
1842	17	1	72	86	< 2
1843	18	1	62	67	< 2
1844	19	1	48	76	< 2
1845	20	1	72	66	< 2
1846	22	1	53	77	< 2
1847	23	1	62	71	< 2
1848	24	1	45	212	< 2
1849	25	1	86	75	< 2
1850	27	1	62	95	< 2
1851	28	1	72	78	< 2
1852	29	1	91	71	< 2
1853	30	1	100	75	< 2
1854	31	1	86	73	< 2
1855	32	1	132	73	< 2
1856	33	1	86	77	< 2
1857	34	1	35	84	< 2
1858	35	1	77	74	< 2
1859	36	1	118	77	< 2
1860	37	1	118	83	< 2
1861	38	1	77	85	< 2
1862	39	1	62	98	< 2
1863	40	1	53	93	< 2
1864	41	1	50	94	< 2
1865	42	1	137	84	< 2
1866	43	1	72	78	< 2
1867	44	1	36	51	< 2
1868	45	1	62	107	< 2
1869	46	1	72	96	< 2
1870	47	1	45	75	< 2
1871	48	1	45	116	< 2
1872	49	2	62	93	< 2
1873	50	1	100	96	< 2
1874	51	1	77	80	< 2
1875	52	1	45	100	< 2
1876	53	1	96	86	< 2
1877	54	1	72	106	< 2
1878	55	1	53	107	< 2
1879	56	1	53	143	< 2
1880	57	1	53	123	< 2
1881	58	1	36	96	< 2
1882	59	1	62	105	< 2
1883	60	1	53	136	< 2
1884	61	2	45	76	< 2
1885	62	2	62	86	< 2
1886	63	3	58	87	< 2
1887	64	1	72	93	< 2
1888	65	1	72	90	< 2
1889	66	1	45	77	< 2
1890	67	1	62	93	< 2
1891	68	1	30	76	< 2
1892	69	1	72	90	< 2
1893	70	1	62	77	< 2
1894	71	1	72	108	< 2
1895	72	1	58	78	< 2

(ppm)

Ser.No.	Sample No.	Ag	Cu	Zn	Mo
1896	H - 73	1	58	83	<2
1897	75	1	50	113	<2
1898	76	1	96	94	<2
1899	77	1	45	114	<2
1900	79	1	30	110	<2
1901	80	1	82	139	<2
1902	81	2	86	113	<2
1903	82	1	77	98	<2
1904	83	1	109	104	<2
1905	84	1	72	86	<2
1906	85	1	118	92	<2
1907	86	2	53	112	<2
1908	87	1	118	94	<2
1909	89	1	118	92	<2
1910	90	1	92	90	<2
1911	91	1	72	96	<2
1912	92	1	53	90	<2
1913	94	1	40	96	<2
1914	95	1	68	83	<2
1915	97	1	108	103	<2
1916	99	1	78	87	<2
1917	100	1	82	145	<2
1918	101	1	96	88	<2
1919	102	1	118	93	<2
1920	103	1	62	91	<2
1921	104	1	72	82	<2
1922	105	1	62	66	<2
1923	106	1	68	90	<2
1924	107	1	49	86	<2
1925	109	1	36	112	<2
1926	110	1	72	84	<2
1927	111	2	86	74	<2
1928	112	2	49	57	<2
1929	113	2	53	63	<2
1930	114	2	53	58	<2
1931	115	1	36	29	<2
1932	116	2	45	54	<2
1933	117	1	59	65	<2
1934	119	1	22	42	<2
1935	120	1	30	49	<2
1936	121	1	26	44	<2
1937	122	1	30	31	<2
1938	123	1	53	73	<2
1939	125	2	72	86	<2
1940	126	1	78	70	<2
1941	127	2	82	70	<2
1942	128	1	86	67	<2
1943	129	2	68	66	<2
1944	131	1	82	59	<2
1945	132	1	100	76	<2
1946	134	2	96	61	<2
1947	136	1	82	63	<2
1948	137	1	109	84	<2
1949	138	1	114	64	<2
1950	139	1	109	76	<2
1951	140	1	63	47	<2
1952	141	<1	22	36	<2
1953	143	2	86	94	<2
1954	144	1	178	76	<2
1955	145	1	72	87	<2
1956	146	1	82	84	<2
1957	148	2	82	97	<2
1958	149	1	82	83	<2
1959	150	1	82	87	<2
1960	151	<1	164	64	<2
1961	H - 152	1	36	74	<2
1962	153	1	36	76	<2
1963	154	1	45	55	<2
1964	155	2	25	76	<2
1965	156	1	40	50	<2
1966	157	1	30	55	<2
1967	158	1	30	57	<2
1968	160	2	36	52	<2
1969	161	1	63	81	<2
1970	162	1	40	54	<2
1971	163	1	36	59	<2
1972	164	2	53	64	<2
1973	165	1	25	61	<2
1974	166	1	49	70	<2
1975	167	1	17	70	<2
1976	168	1	25	55	<2
1977	169	1	37	51	<2
1978	170	2	100	57	<2
1979	171	1	74	75	<2
1980	172	2	68	72	<2
1981	173	1	85	74	<2
1982	174	2	86	81	<2
1983	176	2	29	29	<2
1984	178	2	88	82	<2
1985	179	2	76	76	<2
1986	180	2	70	87	<2
1987	181	1	70	81	<2
1988	182	2	75	74	<2
1989	183	2	75	62	<2
1990	184	2	94	75	<2
1991	185	2	70	88	<2
1992	186	1	59	70	<2
1993	187	<1	27	39	<2
1994	188	2	95	80	<2
1995	189	2	79	70	<2
1996	190	1	88	55	<2
1997	192	2	64	64	<2
1998	193	2	91	56	<2
1999	194	2	84	88	<2
2000	195	2	70	46	<2
2001	196	1	59	31	<2
2002	197	2	50	37	<2
2003	198	2	55	81	<2
2004	199	2	72	52	<2
2005	200	2	57	70	<2
2006	202	2	65	77	<2
2007	203	2	58	57	<2
2008	204	2	77	84	<2
2009	206	3	54	53	<2
2010	207	2	55	53	<2
2011	208	2	48	49	<2
2012	209	2	39	77	<2
2013	210	1	37	67	<2
2014	211	<1	41	83	<2
2015	212	<1	39	72	<2
2016	214	2	37	41	<2
2017	215	<1	39	48	<2
2018	216	<1	48	56	<2
2019	218	1	49	48	<2
2020	219	1	32	48	<2
2021	221	<1	56	49	<2
2022	222	<1	35	48	<2
2023	223	2	56	44	<2
2024	224	3	51	49	<2
2025	225	2	39	60	<2
2026	H - 226	1	34	38	<2
2027	227	1	84	66	<2
2028	228	1	92	90	<2
2029	229	3	90	83	<2
2030	230	3	64	55	<2
2031	231	1	64	69	<2
2032	232	3	80	59	<2
2033	233	2	89	64	<2
2034	235	2	80	62	<2
2035	Hi - 1	2	76	129	<2
2036	3	2	39	88	<2
2037	4	3	51	76	<2
2038	5	2	69	93	<2
2039	6	2	77	77	<2
2040	7	2	67	86	<2
2041	8	1	36	87	<2
2042	9	1	58	93	<2
2043	10	1	45	69	<2
2044	11	1	78	105	<2
2045	12	1	64	90	<2
2046	13	1	71	86	<2
2047	14	1	71	97	<2
2048	15	<1	104	68	2
2049	16	1	112	74	<2
2050	17	<1	84	66	<2
2051	19	<1	84	65	<2
2052	20	<1	67	48	<2
2053	21	<1	58	50	<2
2054	23	<1	100	60	<2
2055	25	<1	90	50	<2
2056	26	1	64	105	<2
2057	28	1	73	95	<2
2058	29	-	-	-	-
2059	30	1	74	72	<2
2060	31	1	48	84	<2
2061	32	1	45	125	2
2062	34	<1	71	61	<2
2063	35	1	77	76	<2
2064	37	1	51	84	<2
2065	38	<1	79	76	<2
2066	40	1	80	74	<2
2067	41	1	82	87	<2
2068	42	1	88	96	<2
2069	44	1	77	78	<2
2070	45	1	80	77	<2
2071	46	1	83	115	<2
2072	47	<1	78	97	<2
2073	49	1	84	87	<2
2074	51	<1	100	93	<2
2075	53	1	87	98	<2
2076	54	1	60	87	<2
2077	55	1	80	105	<2
2078	56	1	90	87	<2
2079	57	1	102	89	<2
2080	59	1	35	62	<2
2081	60	2	56	121	<2
2082	61	1	36	91	<2
2083	63	1	31	51	<2
2084	64	1	49	54	<2
2085	65	3	60	74	<2
2086	66	2	73	126	<2
2087	67	2	42	86	<2
2088	68	2	44	91	<2
2089	70	1	42	79	<2
2090	71	1	46	82	<2

(ppm)

Ser.No.	Sample No.	Ag	Cu	Zn	Mo
2091	Hi - 72	1	52	147	< 2
2092	73	1	33	143	< 2
2093	74	1	52	126	< 2
2094	75	1	42	86	< 2
2095	76	1	46	83	< 2
2096	78	1	57	113	< 2
2097	79	1	58	134	< 2
2098	80	1	33	57	< 2
2099	81	2	71	84	< 2
2100	82	1	65	80	< 2
2101	83	1	42	79	< 2
2102	84	1	75	97	< 2
2103	85	1	73	97	< 2
2104	h - 1	1	292	83	< 2
2105	3	1	77	66	< 2
2106	4	1	94	62	< 2
2107	5	1	106	81	< 2
2108	6	1	321	56	< 3
2109	7	1	75	80	< 2
2110	8	1	94	77	< 2
2111	9	1	510	91	< 2
2112	10	1	96	87	< 2
2113	11	1	120	80	< 2
2114	12	1	127	89	< 2
2115	13	1	125	86	< 2
2116	14	1	128	77	< 2
2117	15	1	109	90	< 2
2118	16	1	108	90	< 2
2119	17	< 1	149	70	< 2
2120	18	< 1	135	82	< 2
2121	19	1	115	86	< 2
2122	20	1	130	86	< 2
2123	21	1	125	93	< 2
2124	22	1	123	86	< 2
2125	23	1	125	90	< 2
2126	24	1	92	71	< 2
2127	25	1	85	74	< 2
2128	26	1	78	56	< 2
2129	28	1	33	69	< 2
2130	30	1	75	56	< 2
2131	31	1	73	51	< 2
2132	32	1	62	51	< 2
2133	34	1	82	49	< 2
2134	35	1	83	50	< 2
2135	37	1	81	48	< 2
2136	38	1	61	80	< 2
2137	39	1	31	84	< 2
2138	40	1	49	95	< 2
2139	41	1	53	79	< 2
2140	42	1	64	86	< 2
2141	43	1	51	82	< 2
2142	44	1	55	89	< 2
2143	46	1	69	91	< 2
2144	47	1	66	91	< 2
2145	48	1	66	86	< 2
2146	49	1	66	86	< 2
2147	50	1	81	76	< 2
2148	51	1	61	77	< 2
2149	52	1	59	85	< 2
2150	54	1	63	78	< 2
2151	56	1	48	66	< 2
2152	57	1	29	40	< 2
2153	58	1	55	79	< 2
2154	62	1	64	73	< 2
2155	64	1	55	94	< 2
2156	h - 65	1	56	82	< 2
2157	66	1	102	91	< 2
2158	68	1	104	87	< 2
2159	69	2	41	69	< 2
2160	70	1	95	83	< 2
2161	72	1	29	64	< 2
2162	73	1	89	86	< 2
2163	74	1	29	74	< 2
2164	75	1	158	117	< 2
2165	76	1	127	101	< 2
2166	77	1	124	114	< 2
2167	78	1	31	97	< 2
2168	79	1	44	67	< 2
2169	80	1	31	86	< 2
2170	82	1	31	71	< 2
2171	83	< 1	25	77	< 2
2172	84	< 1	22	77	< 2
2173	85	1	39	86	< 2
2174	86	1	46	91	< 2
2175	87	1	54	74	< 2
2176	88	1	41	63	< 2
2177	89	1	61	80	< 2
2178	91	1	61	66	< 2
2179	93	1	68	73	< 2
2180	94	1	76	83	< 2
2181	95	1	69	74	< 2
2182	96	1	58	75	< 2
2183	97	1	66	60	< 2
2184	98	1	59	85	< 2
2185	101	1	81	84	< 2
2186	103	1	54	74	< 2
2187	104	1	71	63	< 2
2188	106	1	76	63	< 2
2189	108	1	89	74	< 2
2190	109	1	91	70	< 2
2191	110	1	80	69	< 2
2192	111	1	63	88	< 2
2193	113	< 1	38	40	< 2
2194	114	< 1	45	39	< 2
2195	115	< 1	47	34	< 2
2196	116	< 1	62	45	< 2
2197	117	1	36	40	< 2
2198	119	1	45	43	< 2
2199	120	< 1	15	31	< 2
2200	122	1	61	63	< 2
2201	123	1	36	87	< 2
2202	125	1	43	106	< 2
2203	126	1	52	74	< 2
2204	127	1	46	77	< 2
2205	128	1	42	73	< 2
2206	129	1	89	142	< 2
2207	131	1	40	86	< 2
2208	132	1	40	74	< 2
2209	133	1	40	70	< 2
2210	136	1	54	79	< 2
2211	137	1	51	76	< 2
2212	138	1	58	99	< 2
2213	139	1	40	81	< 2
2214	140	1	70	82	< 2
2215	141	1	65	74	< 2
2216	143	1	70	115	< 2
2217	144	1	69	73	< 2
2218	145	1	67	63	< 2
2219	146	1	71	58	< 2
2220	147	1	84	74	< 2
2221	h - 149	1	51	87	< 2
2222	150	1	21	71	< 2
2223	151	1	61	82	< 2
2224	153	1	71	59	< 2
2225	154	1	106	72	< 2
2226	156	< 1	43	89	< 2
2227	157	1	46	92	< 2
2228	158	1	111	89	< 2
2229	161	1	102	97	< 2
2230	162	1	57	66	< 2
2231	163	1	33	66	< 2
2232	164	1	79	62	< 2
2233	165	1	31	96	< 2
2234	166	1	83	69	< 2
2235	167	1	67	69	< 2
2236	168	1	102	89	< 2
2237	169	1	73	73	< 2
2238	170	1	95	84	< 2
2239	172	1	41	70	< 2
2240	173	1	38	75	< 2
2241	175	1	43	61	< 2
2242	176	1	45	75	< 2
2243	178	1	57	105	< 2
2244	180	1	48	84	< 2
2245	181	1	48	95	< 2
2246	182	1	33	80	< 2
2247	183	1	46	82	< 2
2248	184	< 1	46	67	< 2
2249	185	1	46	76	< 2
2250	187	1	52	76	< 2
2251	188	1	45	71	< 2
2252	189	1	50	99	< 2
2253	190	1	50	76	< 2
2254	191	1	50	71	< 2
2255	192	1	35	63	< 2
2256	193	1	33	81	< 2
2257	194	1	48	93	< 2
2258	195	1	45	72	< 2
2259	196	1	33	81	< 2
2260	197	1	50	105	< 2
2261	198	1	48	70	< 2
2262	199	1	38	55	< 2
2263	200	1	36	67	< 2
2264	201	2	50	83	< 2
2265	202	1	55	97	< 2
2266	203	1	29	81	< 2
2267	204	1	48	83	< 2
2268	205	1	48	129	< 2
2269	206	2	48	84	< 2
2270	207	1	30	95	< 2
2271	208	< 1	35	79	< 2
2272	209	1	67	79	< 2
2273	210	1	62	63	< 2
2274	211	1	31	107	< 2
2275	212	1	27	116	< 2
2276	213	2	65	63	< 2
2277	214	1	67	71	< 2
2278	215	2	71	79	< 2
2279	F - 6	1.2	142	134	0.6
2280	25	1.9	100	334	1.0
2281	36	1.2	93	138	1.1
2282	37	0.8	68	170	1.0
2283	43	0.9	739	185	3.5
2284	46	0.3	64	130	2.7
2285	48	1.0	58	73	3.2

(ppm)

Ser.No.	Sample No.	Ag	Cu	Zn	Mo
2286	F - 49	1.0	76	125	1.2
2287	50	0.9	246	104	2.4
2288	51	0.9	165	156	1.4
2289	52	0.3	30	120	2.2
2290	54	1.0	66	1,138	0.7
2291	57	0.8	300	104	0.9
2292	65	0.4	101	68	0.8
2293	68	0.7	68	129	1.2
2294	71	0.3	32	42	1.1
2295	85	0.9	76	205	1.3
2296	96	0.6	67	193	1.0
2297	97	0.2	34	197	1.8
2298	101	2.1	58	24	2.1
2299	104	0.5	31	42	1.7
2300	108	0.6	35	76	0.9
2301	111	0.6	46	17	1.5
2302	113	0.4	59	101	0.8
2303	114	0.8	60	143	0.3
2304	117	0.1	25	10	0.9
2305	118	0.3	78	99	0.7
2306	121	0.4	144	105	0.6
2307	122	0.6	157	282	0.3
2308	126	0.5	196	361	0.3
2309	127	0.3	69	185	0.4
2310	140	1.7	53	107	0.2
2311	147	0.9	41	100	0.0
2312	247	0.1	21	33	1.0
2313	257	0.4	42	12	0.7
2314	309	1.5	85	166	0.4
2315	320	0.7	43	131	0.3
2316	328	0.3	47	86	0.5
2317	335	0.7	43	101	0.3
2318	337	1.0	67	166	0.4
2319	418	0.3	134	56	4.0
2320	426	0.3	62	29	23
2321	435	0.6	71	65	1.9
2322	436	0.2	98	123	1.3
2323	438	0.2	90	15	2.7
2324	443	81.4	44	476	2.0
2325	444	1.2	74	132	0.5
2326	445	0.9	74	164	0.8
2327	448	0.9	74	203	1.9
2328	449	1.2	115	130	0.7
2329	500	0.3	64	129	1.0
2330	504	1.4	120	120	0.7

Ser.No.	Sample No.	Ag	Cu	Zn	Mo
2331	F - 542	1.7	120	235	0.7
2332	544	1.4	81	181	0.6
2333	595	0.8	99	38	0.9
2334	605	0.3	73	20	1.0
2335	616	0.5	26	23	1.2
2336	619	0.4	91	23	2.2
2337	661	0.4	46	23	1.6
2338	666	0.7	100	117	0.2
2339	667	1.1	91	87	0.1
2340	669	1.1	110	175	0.5
2341	675	1.7	151	243	0.2
2342	680	0.6	126	192	0.7
2343	687	0.9	167	215	1.1
2344	688	1.1	333	401	0.9
2345	f - 2	1.2	132	143	0.5
2346	7	1.3	138	161	0.6
2347	8	1.8	135	216	0.7
2348	14	1.3	166	141	0.4
2349	19	1.5	104	327	0.5
2350	27	1.0	87	138	0.6
2351	31	1.6	120	125	0.5
2352	36	0.6	341	85	1.6
2353	37	0.4	321	73	3.3
2354	49	1.0	249	33	1.4
2355	53	0.7	393	111	7.2
2356	54	1.2	334	30	10.2
2357	59	1.4	140	257	4.2
2358	60	0.7	148	246	1.6
2359	65	0.3	101	72	1.3
2360	66	0.4	127	438	2.1
2361	78	1.6	64	412	0.8
2362	79	1.4	218	262	2.7
2363	85	1.5	276	301	1.2
2364	86	0.7	364	222	2.1
2365	93	0.2	55	49	1.2
2366	94	0.2	48	69	1.1
2367	98	0.1	38	50	1.2
2368	103	0.5	40	46	0.8
2369	113	1.0	128	170	0.7
2370	114	0.6	94	118	0.7
2371	173	0.1	45	92	0.9
2372	185	0.4	45	150	1.0
2373	343	0.6	17	10	6.8
2374	478	1.7	50	70	0.1
2375	517	1.4	98	140	0.5

Ser.No.	Sample No.	Ag	Cu	Zn	Mo
2376	f - 567	1.0	133	136	0.6
2377	569	0.8	46	115	0.3
2378	570	1.1	150	375	1.4
2379	572	1.3	148	337	1.6
2380	575	1.4	136	533	2.1
2381	579	0.8	81	232	0.7
2382	607	0.4	71	59	1.0
2383	610	0.1	114	50	0.9
2384	614	0.1	71	62	0.4
2385	617	0.3	237	37	1.9
2386	621	0.1	136	552	0.4
2387	622	0.4	156	23	0.5
2388	625	0.9	159	223	0.5
2389	627	1.4	166	302	0.2
2390	630	1.0	241	203	2.3
2391	638	0.3	121	264	2.3
2392	658	1.1	177	618	1.6
2393	689	1.5	213	312	0.7
2394	698	0.7	193	387	0.9
2395	699	0.1	30	79	0.4
2396	700	0.7	45	143	0.6
2397	701	1.4	117	278	0.9
2398	708	0.7	116	284	1.3
2399	713	1.1	120	281	0.7
2400	719	0.7	57	154	0.5
2401	721	1.3	58	535	0.7
2402	734	0.7	33	109	0.3
2403	736	0.6	30	86	0.6
2404	740	0.3	32	73	1.2
2405	745	0.3	30	103	0.7
2406	747	0.6	29	100	1.0
2407	750	0.6	19	106	0.8
2408	752	0.3	37	109	0.7
2409	753	0.7	90	226	1.0
2410	756	0.9	116	231	0.8
2411	758	0.5	58	114	1.0
2412	759	1.5	67	177	1.5
2413	760	0.3	50	210	1.5
2414	761	0.5	15	63	0.3
2415	762	1.2	84	114	1.2
2416	765	1.5	95	123	1.1
2417	766	0.8	71	153	1.4

(ppm)

Ser.No.	Sample No.	Cu	Pb	Zn	Ba
2418	fB 1000	36	15	96	195
2419	1001	51	160	277	390
2420	1002	34	26	149	542
2421	1003	30	16	103	108
2422	1004	70	147	373	304
2423	1005	28	14	91	87
2424	1006	92	29	186	304
2425	1007	122	43	154	943

Ser.No.	Sample No.	Cu	Pb	Zn	Ba
2426	fB 1008	33	20	143	165
2427	1009	101	167	326	376
2428	1011	84	403	430	329
2429	1012	85	851	582	259
2430	1013	106	1,246	561	1,270
2431	1017	123	100	146	247
2432	1018	174	24	104	282

Ser.No.	Sample No.	Cu	Pb	Zn	Ba

(ppm)

Ser.No.	Sample No.	Ag	Pb	Zn	Ba
2433	F - 154	0.3	27	34	77
2434	168	0.8	43	97	199
2435	f - 116	2.3	61	119	235
2436	117	1.6	20	131	247
2437	118	1.8	31	104	259
2438	119	0.3	16	73	165
2439	120	2.5	18	106	165
2440	121	0.8	25	141	259
2441	f - 122	1.1	24	123	282
2442	127	1.8	23	174	168
2443	128	1.3	20	200	200
2444	130	2.3	24	163	137
2445	131	1.6	22	171	210

(B) Soil (−80-mesh fraction)

(ppm)

Ser.No.	Sample No.	Cu	Zn	Ni	Co
2446	C - 69	8	6	6	8
2447	70	9	8	3	7
2448	71	13	10	10	8
2449	72	3	9	10	7
2450	73	15	10	2	7
2451	74	38	19	8	10
2452	75	3	5	2	7
2453	76	26	12	4	17
2454	77	3	2	4	3
2455	78	9	5	6	9
2456	79	13	22	6	6
2457	80	20	14	4	4
2458	81	34	19	18	5
2459	82	13	10	2	5
2460	83	40	13	6	9
2461	84	34	24	8	10
2462	85	58	30	18	32
2463	86	39	30	47	25
2464	87	43	36	31	18
2465	88	103	38	198	53
2466	89	425	152	38	77
2467	90	98	67	20	69
2468	91	133	158	37	85
2469	92	124	84	26	63
2470	104	432	88	18	44
2471	105	12	12	2	5
2472	106	17	14	6	75
2473	107	46	38	16	25
2474	108	138	30	20	55
2475	109	182	45	19	49
2476	110	89	23	24	48
2477	111	21	73	26	49
2478	112	29	36	34	73
2479	169	21	40	3	13
2480	170	33	43	4	7
2481	171	78	55	21	22
2482	172	67	49	21	16
2483	173	103	57	24	22
2484	174	31	26	8	4
2485	175	14	20	12	4
2486	187	67	56	15	22
2487	188	36	24	10	14
2488	189	18	16	8	13
2489	190	49	20	6	12
2490	191	48	21	18	12
2491	192	47	55	9	23
2492	193	38	39	29	15
2493	217	385	44	30	56
2494	218	205	52	27	59
2495	219	111	48	40	79
2496	C - 220	61	50	66	167
2497	221	85	62	52	123
2498	222	64	56	62	150
2499	223	79	69	58	133
2500	224	59	50	73	166
2501	225	59	38	73	127
2502	226	81	62	48	93
2503	227	90	38	32	75
2504	228	101	38	47	79
2505	229	320	147	31	78
2506	230	503	47	31	63
2507	231	690	38	27	78
2508	232	145	53	24	62
2509	233	242	38	44	56
2510	234	310	50	24	67
2511	235	357	56	24	75
2512	236	414	56	24	81
2513	237	129	145	24	67
2514	238	140	100	16	82
2515	239	149	71	24	59
2516	240	220	57	36	93
2517	241	425	51	28	68
2518	242	340	59	39	82
2519	243	338	75	22	76
2520	244	190	62	34	125
2521	245	116	73	63	48
2522	246	54	90	48	55
2523	247	70	93	30	38
2524	248	102	71	40	70
2525	249	86	55	32	37
2526	250	295	52	40	72
2527	251	255	52	56	96
2528	252	190	57	56	81
2529	260	245	51	32	59
2530	261	142	37	26	56
2531	262	228	52	28	60
2532	263	229	66	32	63
2533	214	235	58	38	77
2534	265	340	38	44	113
2535	266	407	38	40	79
2536	267	382	33	34	68
2537	268	610	60	38	89
2538	269	193	36	19	61
2539	270	190	38	27	60
2540	271	252	38	32	73
2541	272	145	40	50	117
2542	273	48	39	51	69
2543	274	51	39	52	73
2544	275	89	48	40	63
2545	276	43	40	27	32
2546	C - 277	40	28	13	19
2547	278	56	36	22	30
2548	279	125	49	35	40
2549	280	198	90	29	123
2550	281	172	31	39	117
2551	282	202	31	32	81
2552	203	206	21	27	78
2553	284	198	31	29	59
2554	285	124	93	20	60
2555	286	134	84	24	57
2556	287	58	33	6	28
2557	288	23	39	6	14
2558	289	20	39	6	21
2559	290	23	31	8	15
2560	291	24	39	8	22
2561	292	24	41	6	29
2562	293	26	24	8	26
2563	294	29	19	10	18
2564	295	33	24	10	15
2565	296	19	23	10	14
2566	297	29	23	8	21
2567	298	19	20	8	13
2568	299	64	32	16	20
2569	300	18	23	4	14
2570	301	23	19	10	18
2571	302	26	33	10	22
2572	303	37	44	10	24
2573	304	28	24	10	19
2574	305	28	35	12	18
2575	306	32	26	18	20
2576	307	35	31	23	19
2577	308	51	24	23	16
2578	309	25	20	8	16
2579	310	19	24	8	15
2580	311	27	27	12	43
2581	312	30	43	10	27
2582	313	28	19	12	15
2583	314	36	20	19	13
2584	315	36	36	8	25
2585	316	18	18	10	12
2586	317	30	29	16	12
2587	318	22	14	10	14
2588	319	32	24	10	16
2589	320	32	14	12	12
2590	321	96	43	31	24
2591	322	270	19	20	38
2592	323	365	34	27	51
2593	324	470	36	40	71
2594	325	265	36	27	37
2595	326	282	38	47	43

(ppm)

Ser.No.	Sample No.	Cu	Zn	Ni	Co
2596	C - 327	107	58	32	46
2597	328	738	74	36	56
2598	329	231	53	36	62
2599	330	20	45	52	75
2600	331	58	60	63	94
2601	332	74	61	55	87
2602	333	119	49	30	50
2603	334	199	78	33	72
2604	335	262	66	47	67
2605	336	315	56	30	60
2606	337	319	59	47	95
2607	338	284	68	33	60
2608	339	140	91	27	75
2609	340	327	53	46	81
2610	CA - 11	189	58	30	75
2611	12	127	95	33	66
2612	13	66	38	31	80
2613	14	74	28	37	84
2614	15	374	39	37	74
2615	16	36	31	42	87
2616	17	21	45	50	112
2617	18	300	54	44	87
2618	23	129	63	43	87
2619	24	22	21	16	15
2620	25	21	16	21	12
2621	26	23	18	15	5
2622	27	23	29	22	12
2633	28	33	23	22	7
2624	29	17	17	16	4
2625	30	25	29	16	12
2626	32	14	32	11	10
2627	45	67	47	46	37
2628	46	146	114	70	75
2629	47	49	52	33	25
2630	48	38	33	30	21
2631	49	38	30	12	20
2632	68	46	36	30	12
2633	69	75	37	30	12
2634	71	73	42	57	22
2635	72	118	87	33	42
2636	79	154	81	43	80
2637	80	92	92	22	50
2638	81	38	39	33	21
2639	82	46	67	36	37
2640	83	31	42	26	19
2641	84	200	95	22	42
2642	85	214	54	30	62
2643	86	189	63	24	62
2644	87	377	100	40	73
2645	88	228	50	22	52
2646	89	169	50	50	112
2647	91	132	37	45	65
2648	92	34	43	52	50
2649	107	16	47	19	25
2650	108	42	38	22	25
2651	109	42	47	52	94
2652	110	45	72	40	54
2653	111	62	83	44	34
2654	112	248	64	40	84
2655	113	154	35	52	62
2656	114	414	60	28	105
2657	115	338	54	45	88
2658	116	375	73	50	84
2659	117	120	29	43	30
2660	118	36	40	50	52

Ser.No.	Sample No.	Cu	Zn	Ni	Co
2661	CA - 119	240	32	52	33
2662	120	73	25	38	33
2663	121	60	33	34	36
2664	122	85	23	29	33
2665	123	30	32	43	49
2666	124	106	29	37	39
2667	125	112	29	36	44
2668	126	400	63	37	71
2669	127	36	32	22	19
2670	128	93	63	35	30
2671	129	29	32	31	42
2672	130	56	29	33	20
2673	131	22	17	51	12
2674	133	49	42	33	15
2675	135	59	37	33	22
2676	136	27	20	22	15
2677	137	27	21	19	20
2678	CE - 1	18	25	19	21
2679	3	23	20	15	17
2680	4	40	46	26	34
2681	5	205	61	24	37
2682	6	159	41	22	37
2683	7	205	81	28	56
2684	8	232	74	30	62
2685	9	191	63	36	75
2686	10	50	32	31	12
2687	11	22	31	15	12
2688	12	59	65	67	37
2689	13	36	33	41	31
2690	14	36	32	30	15
2691	15	364	45	49	66
2692	16	368	53	52	75
2693	17	198	28	48	62
2694	18	121	59	37	48
2695	19	64	42	37	19
2696	20	25	15	25	12
2697	21	25	26	22	12
2698	22	25	21	15	16
2699	23	57	27	37	16
2700	24	56	44	67	46
2701	25	28	88	56	75
2702	26	27	59	67	97
2703	27	154	66	48	94
2704	28	107	63	46	60
2705	29	100	58	67	41
2706	30	7	13	25	10
2707	31	45	32	30	22
2708	32	66	37	25	40
2709	33	41	37	21	35
2710	35	104	54	9	62
2711	36	125	46	37	72
2712	37	27	29	34	21
2713	38	34	47	45	25
2714	39	40	145	37	50
2715	40	118	38	45	79
2716	41	75	53	45	84
2717	42	105	83	30	75
2718	43	215	65	69	71
2719	44	518	53	63	75
2720	45	243	45	43	50
2721	46	214	34	45	84
2722	47	69	42	52	140
2723	48	109	39	67	100
2724	49	182	38	42	50
2725	50	32	21	43	13

Ser.No.	Sample No.	Cu	Zn	Ni	Co
2726	CE - 51	38	28	57	25
2727	52	68	41	27	17
2728	53	73	48	60	37
2729	54	114	37	49	50
2730	55	33	51	30	31
2731	56	48	54	42	50
2732	57	38	33	57	34
2733	58	157	36	24	29
2734	59	148	59	84	87
2735	60	27	41	63	85
2736	61	32	52	58	62
2737	62	64	63	37	62
2738	66	55	41	19	25
2739	67	57	41	84	25
2740	68	164	71	56	62
2741	69	95	52	93	50
2742	70	144	71	50	62
2743	71	107	53	44	81
2744	72	121	46	50	65
2745	73	177	74	100	100
2746	75	173	47	40	66
2747	82	50	39	27	25
2748	83	44	39	57	25
2749	84	62	46	57	22
2750	85	66	47	28	25
2751	86	244	65	25	42
2752	87	73	56	59	42
2753	88	175	49	76	77
2754	89	283	43	61	81
2755	90	350	51	65	85
2756	91	53	38	48	37
2757	92	67	47	82	37
2758	97	308	47	68	72
2759	98	154	32	79	103
2760	99	354	50	23	75
2761	100	45	47	53	[illegible]
2762	101	145	33	77	14
2763	102	42	39	42	69
2764	103	83	51	59	87
2765	104	82	76	52	75
2766	111	33	71	59	119
2767	112	75	73	76	65
2768	113	406	61	42	50
2769	114	258	76	73	72
2770	115	137	74	33	62
2771	116	150	89	56	50
2772	CN - 17	139	79	150	42
2773	18	102	93	74	16
2774	19	122	50	67	50
2775	20	92	55	69	91
2776	21	348	50	37	37
2777	23	265	53	49	56
2778	24	75	86	59	66
2779	25	237	66	52	50
2780	26	133	137	84	88
2781	27	292	72	34	57
2782	28	221	62	39	62
2783	29	137	65	37	50
2784	30	133	59	37	65
2785	31	108	52	52	66
2786	32	314	59	40	56
2787	47	28	26	52	13
2788	45	23	24	148	13
2789	49	38	45	59	15
2790	50	81	56	74	23

(ppm)

Ser.No.	Sample No.	Cu	Zn	Ni	Co
2791	CN - 51	72	68	52	17
2792	52	42	45	56	29
2793	53	6	13	25	12
2794	54	387	47	50	75
2795	55	150	57	45	85
2796	56	154	53	33	84
2797	57	15	34	67	96
3798	58	63	50	44	85
2799	62	273	122	44	77
2800	77	27	47	24	16
2801	84	18	13	46	10
2802	85	38	27	25	22
2803	86	36	58	50	22
2804	87	33	49	65	19
2805	88	33	52	38	22
2806	96	104	68	42	52
2807	97	75	75	44	75
2808	98	104	54	47	87
2809	99	117	76	35	60
2810	100	86	54	82	59
2811	101	85	38	29	60
2812	102	33	29	15	19
2813	103	20	18	17	9
2814	104	17	16	18	6
2815	105	116	49	33	25
2816	106	33	25	18	12
2817	107	50	31	23	17
2818	108	48	30	39	25
2819	109	32	22	18	10
2820	110	29	23	23	11
2821	111	48	25	23	8
2822	112	48	51	27	30
2823	125	19	65	42	30
2824	126	83	68	23	27
2825	127	82	78	45	37
2826	128	32	26	21	15
2827	129	46	33	23	21
2828	130	56	57	45	33
2829	131	40	61	49	50
2830	134	116	61	27	59
2831	135	177	38	27	77
2832	136	117	38	40	87
2833	137	125	39	40	87
2834	138	168	39	36	94
2835	140	121	49	38	42
2836	141	171	93	45	52
2837	144	70	41	39	50
2838	146	52	40	55	25
2839	147	21	25	34	12
2840	148	31	30	19	10
2841	149	34	33	19	12
2842	150	46	38	21	25
2843	151	38	43	23	37
2844	152	145	43	52	50
2845	153	188	38	21	50
2846	154	315	33	36	47
2847	155	377	39	36	44
2848	156	238	38	32	37
2849	164	123	43	23	50
2850	166	108	38	30	50
2851	167	292	31	24	37
2852	168	25	29	24	20
2853	169	23	36	15	31
2854	170	31	29	15	18
2855	171	23	33	15	12

Ser.No.	Sample No.	Cu	Zn	Ni	Co
2856	CN - 172	14	15	15	27
2857	173	31	32	30	27
2858	174	155	38	45	55
2859	175	135	39	29	50
2860	176	72	37	32	65
2861	177	102	35	30	65
2862	178	119	95	45	86
2863	179	105	59	30	70
2864	180	368	42	23	49
2865	131	55	59	28	74
2866	182	62	58	27	80
2867	183	34	35	25	77
2868	184	91	33	38	145
2869	185	37	43	56	76
2870	186	55	47	42	45
2871	187	93	29	44	87
2872	188	491	34	43	80
2873	189	65	33	44	94
2874	190	115	38	42	96
2875	191	125	49	38	94
2876	192	76	46	36	96
2877	193	37	31	49	95
2878	194	105	62	45	94
2879	195	48	46	36	29
2880	204	99	105	23	65
2881	205	97	72	15	50
2882	206	75	92	23	60
2883	207	75	95	21	59
2884	208	77	79	23	56
2885	209	89	84	30	53
2886	210	73	79	23	50
2887	CU - 24	101	87	30	50
2888	25	79	102	29	75
2889	26	77	80	26	68
2890	27	96	76	28	69
2891	28	79	79	25	50
2892	29	82	65	30	50
2893	30	84	65	34	48
2894	31	30	53	48	87
2895	32	92	67	30	63
2896	33	125	47	25	31
2897	34	113	47	23	33
2898	36	50	42	43	79
2899	37	121	42	53	71
2900	38	125	46	34	63
2901	39	320	53	21	65
2902	40	98	34	30	56
2903	41	50	42	27	37
2904	42	55	35	35	40
2905	43	102	75	30	36
2906	44	93	50	30	45
2907	45	106	52	28	36
2908	46	115	41	32	52
2909	47	32	46	28	46
2910	48	342	51	38	53
2911	PA - 15	70	34	18	16
2912	17	103	63	48	34
2913	19	63	55	27	28
2914	21	112	47	35	32
2915	PB - 33	189	40	40	85
2916	35	192	59	40	73
2917	37	63	34	35	57
2918	41	250	71	44	73
2919	43	92	29	48	75
2920	47	192	57	40	59

Ser.No.	Sample No.	Cu	Zn	Ni	Co
2921	PB - 49	214	48	28	45
2922	51	173	57	36	69
2923	PC - 17	245	57	46	76
2924	19	263	49	31	50
2925	21	390	65	34	50
2926	23	380	96	31	60
2927	PE - 9	41	34	31	32
2928	11	280	62	48	63
2929	15	162	52	40	65
2930	17	70	52	46	105
2931	PF - 9	74	105	87	41
2932	11	228	67	48	80
2933	17	219	64	34	53
2934	19	340	64	31	83
2935	21	72	36	26	63
2936	PG - 11	350	41	25	45
2937	17	140	56	34	61
2938	19	246	64	32	73
2939	21	298	56	18	49
2940	PH - 3	104	68	62	42
2941	5	109	96	198	46
2942	7	82	100	82	30
2943	11	85	71	60	40
2944	15	96	54	198	45
2945	17	255	79	22	50
2946	19	568	50	22	72
2947	21	270	61	40	90
2948	23	318	51	18	68
2949	PI - 1	98	58	31	34
2950	3	61	32	31	24
2951	5	56	31	32	32
2952	7	99	50	104	37
2953	9	125	54	104	48
2954	11	140	55	20	37
2955	15	81	31	34	77
2956	17	88	28	32	75
2957	19	154	75	20	55
2958	PJ - 1	102	63	48	43
2959	3	44	21	16	14
2960	5	278	27	27	24
2961	7	122	66	67	45
2962	11	219	54	26	47
2963	15	140	45	18	45
2964	17	154	51	26	70
2965	PK - 11	162	84	26	54
2966	13	168	91	26	49
2967	15	173	97	26	55
2968	17	125	61	32	50
2969	19	173	65	20	43
2970	21	235	49	32	55
2971	25	184	46	52	77
2972	27	258	64	38	69
2973	29	88	32	32	75
2974	31	320	79	42	77
2975	39	312	105	38	80
2976	41	330	71	58	100
2977	43	191	57	50	95
2978	47	600	60	26	64
2979	49	305	79	20	71
2980	51	230	48	17	70
2981	53	246	44	10	53
2982	55	268	32	14	63
2983	59	147	48	28	75
2984	61	140	38	116	78
2985	63	88	42	32	77

(ppm)

Ser.No.	Sample No.	Ag	Cu	Zn	Mo
2986	P - 40	0.6	398	161	4.4
2987	45	0.9	275	25	7.1
2988	47	1.6	607	78	6.9
2989	69	0.5	55	54	1.3
2990	70	0.5	53	48	1.6
2991	72	0.1	11	4	1.2
2992	74	1.9	204	53	1.1
2993	76	1.6	179	56	1.5
2994	77	0.5	19	12	0.8
2995	80	0.4	48	36	1.1
2996	86	0.4	42	42	1.3
2997	87	0.3	69	39	2.4
2998	91	0.5	10	7	3.5
2999	92	0.7	40	15	2.2
3000	93	0.4	16	7	3.2
3001	94	0.2	6	4	2.3
3002	99	0.1	10	6	2.3
3003	100	25.3	36	11	2.0
3004	109	0.8	15	39	0.4
3005	110	0.5	22	40	1.4
3006	141	1.0	37	19	0.1
3007	142	0.5	37	24	0.2
3008	143	1.2	83	28	0.1
3009	148	0.9	65	43	0.2
3010	149	0.4	40	17	0.4
3011	150	0.7	101	25	2.0
3012	183	1.0	59	35	0.2
3013	208	0.6	48	28	0.8
3014	209	2.4	184	216	2.5
3015	210	0.3	62	31	0.7
3016	211	0.7	29	37	0.1
3017	212	1.3	109	57	1.9
2018	213	0.3	33	25	0.5
3019	214	0.7	126	40	1.5
3020	215	0.3	29	51	0.8
3021	216	0.7	51	75	0.8
3022	217	0.9	81	43	3.1
3023	219	0.6	87	45	1.3
3024	220	0.6	104	84	0.9
3025	221	0.9	69	57	1.7
3026	222	0.7	94	53	1.5
3027	223	0.5	47	64	0.9
3028	224	0.3	57	8	1.7
3029	225	0.6	26	42	1.6
3030	227	1.3	50	22	3.0
3031	228	0.8	13	10	1.6
3032	229	0.8	11	13	1.0
3033	230	0.2	5	6	0.7
3034	231	0.5	147	10	1.9
3035	232	0.3	13	89	1.4
3036	233	0.5	6	6	1.3
3037	234	0.7	13	11	1.8
3038	235	0.8	11	9	2.4
3039	237	0.5	8	10	0.8
3040	238	0.6	18	10	1.1
3041	241	0.6	28	13	1.0
3042	243	0.2	59	42	1.9
3043	244	0.5	40	45	1.4
3044	245	1.0	42	36	1.9
3045	246	0.8	51	48	1.8
3046	247	1.4	193	36	1.5
3047	248	0.3	32	30	1.5
3048	249	1.0	62	39	1.8
3049	250	0.3	36	54	1.3
3050	251	0.1	25	15	1.2

Ser.No.	Sample No.	Ag	Cu	Zn	Mo
3051	P - 253	1.0	34	36	1.2
3052	254	0.1	25	16	0.8
3053	256	0.4	44	28	1.3
3054	258	0.3	35	9	1.1
3055	259	0.3	23	13	1.0
3056	260	0.1	21	15	0.9
3057	264	0.3	11	11	0.8
3058	265	0.6	20	15	0.9
3059	266	1.1	9	13	0.9
3060	267	0.6	14	9	1.0
3061	268	0.6	11	9	0.9
3062	269	0.1	10	9	0.7
3063	272	0.7	54	42	0.6
3064	274	0.3	37	31	0.9
3065	275	1.0	26	36	0.6
3066	276	0.9	26	13	1.2
3067	277	3.1	19	13	2.6
3068	282	1.8	86	53	0.4
3069	351	1.0	172	120	0.5
3070	357	1.4	276	279	0.5
3071	358	1.5	221	139	0.9
3072	361	1.7	197	123	1.2
3073	362	0.5	237	197	1.5
3074	378	0.9	38	36	0.3
3075	384	0.8	183	116	0.5
3076	394	0.9	87	69	0.6
3077	397	0.6	60	57	0.4
3078	398	0.3	153	51	0.5
3079	404	1.5	369	243	1.1
3080	408	0.5	221	36	1.7
3081	409	0.6	209	57	3.8
3082	410	0.3	177	42	2.6
3083	411	1.7	500	44	2.1
3084	414	1.2	118	78	2.7
3085	416	0.3	174	53	3.3
3086	417	0.8	166	38	1.5
3087	419	0.6	126	101	2.3
3088	420	0.5	144	23	2.8
3089	421	0.5	150	51	3.4
3090	423	0.6	158	41	5.4
3091	428	0.9	567	48	4.6
3092	429	0.5	210	27	4.2
3093	430	0.8	438	97	4.8
3094	431	0.8	319	21	3.3
3095	437	1.2	158	15	2.9
3096	438	0.2	213	9	8.4
3097	440	1.2	134	77	9.3
3098	601	1.8	143	48	1.0
3099	603	0.5	120	17	1.7
3100	604	0.3	71	8	1.5
3101	606	0.3	67	11	1.1
3102	607	0.8	170	140	2.4
3103	611	0.3	88	15	1.3
3104	612	0.6	154	40	1.0
3105	614	0.3	209	11	3.6
3106	617	0.3	93	23	2.9
3107	618	0.4	352	14	4.2
3108	622	0.1	136	7	4.1
3109	623	0.4	25	9	2.2
3110	624	1.0	35	9	1.7
3111	625	0.8	21	6	0.5
3112	627	1.0	156	43	1.3
3113	632	0.4	139	32	1.7
3114	635	0.3	24	7	0.6
3115	636	0.3	52	9	0.5

Ser.No.	Sample No.	Ag	Cu	Zn	Mo
3116	P - 637	0.8	97	7	1.1
3117	640	0.8	159	68	0.3
3118	641	0.8	114	28	0.7
3119	644	0.3	135	43	1.0
3120	645	0.5	80	26	1.0
3121	646	0.5	20	30	0.4
3122	647	0.9	16	78	0.3
3123	651	0.9	81	6	1.6
3124	654	0.2	55	4	2.4
3125	659	0.2	86	4	3.4
3126	660	0.2	117	4	5.9
3127	664	0.2	217	20	2.0
3128	676	0.5	90	115	0.5
3129	724	1.1	49	37	0.2
3130	f - 13	0.9	197	118	0.7
3131	36	0.6	456	64	1.6
3132	40	1.5	308	201	2.5
3133	42	0.9	169	65	3.5
3134	45	2.2	570	219	0.8
3135	46	1.5	266	136	2.1
3136	51	1.2	359	190	0.6
3137	53	0.7	295	94	3.6
3138	56	1.3	266	91	4.2
3139	57	1.1	323	55	2.1
3140	59	0.3	306	119	1.7
3141	61	0.5	148	141	1.3
3142	63	2.2	1,095	125	1.0
3143	66	1.6	232	199	0.6
3144	68	1.4	223	566	1.2
3145	72	1.1	139	308	1.0
3146	76	1.6	228	112	1.9
3147	95	0.6	202	56	2.8
3148	97	0.7	122	36	2.7
3149	154	0.9	52	31	0.4
3150	155	8.1	118	73	0.7
3151	156	0.7	89	23	0.4
3152	157	0.4	86	46	0.2
3153	158	0.5	85	35	0.4
3154	159	1.2	80	61	0.5
3155	160	1.0	65	52	0.4
3156	161	0.9	100	29	0.3
3157	162	0.6	272	112	1.4
3158	163	0.7	152	94	0.7
3159	164	0.5	128	61	0.9
3160	165	0.2	165	25	0.7
3161	166	0.5	88	26	1.5
3162	167	0.6	43	21	2.7
3163	168	0.2	33	14	1.6
3164	170	0.4	43	22	0.8
3165	171	0.9	105	51	1.1
3166	172	0.6	38	18	0.9
3167	173	0.1	100	105	1.0
3168	174	0.1	32	25	0.6
3169	175	0.5	34	26	2.0
3170	176	0.4	42	42	1.4
3171	177	0.3	30	43	0.7
3172	180	0.1	18	15	0.9
3173	181	0.1	38	33	0.8
3174	182	0.3	23	21	0.6
3175	183	0.3	33	24	1.2
3176	185	0.4	67	44	0.7
3177	186	0.3	81	52	1.5
3178	187	0.6	31	24	1.8
3179	188	0.3	29	18	0.8
3180	189	0.3	26	19	0.7

(ppm)

Ser.No.	Sample No.	Ag	Cu	Zn	Mo
3181	f - 190	0.7	42	17	0.7
3182	191	0.7	67	28	0.8
3183	192	1.2	89	49	0.7
3184	194	1.0	45	18	1.6
3185	195	1.4	18	14	0.9
3186	196	0.3	15	8	0.9
3187	226	1.4	109	46	0.9
3188	227	1.2	135	42	2.2
3189	228	0.3	128	21	3.8
3190	229	0.5	56	16	1.4
3191	230	0.6	4	45	2.9
3192	233	0.3	99	15	2.6
3193	234	0.3	48	19	0.8
3194	235	1.0	147	60	0.9
3195	236	0.7	110	78	1.1
3196	239	0.2	93	69	1.0
3197	243	0.6	89	98	0.9
3198	244	1.9	114	63	0.5
3199	247	0.3	103	81	0.7
3200	248	1.5	142	82	0.6
3201	254	1.9	129	110	0.7
3202	255	0.6	59	33	0.7
3203	259	1.4	159	61	0.5
3204	262	1.0	160	59	0.6
3205	264	1.4	189	148	2.0
3206	265	1.3	236	85	0.9
3207	268	0.3	208	85	0.8
3208	270	1.9	226	98	0.6
3209	272	1.8	159	73	0.8
3210	275	1.5	186	52	0.6
3211	278	1.2	73	33	0.5
3212	279	0.9	71	27	0.3
3213	282	1.2	92	39	0.4
3214	283	1.2	98	34	0.3
3215	332	2.0	192	92	1.0
3216	338	0.1	24	21	3.9
3217	339	0.1	38	27	2.8
3218	340	0.1	22	13	4.3
3219	344	0.3	21	24	2.1
3220	346	0.1	20	24	1.6
3221	348	0.1	8	11	3.6
3222	351	0.1	11	7	1.7
3223	353	0.1	31	9	1.4
3224	356	1.8	47	27	3.1
3225	359	0.3	43	15	2.1
3226	360	0.3	56	22	1.3
3227	364	0.3	26	23	2.1
3228	365	1.4	153	87	0.7
3229	367	0.9	60	36	2.4
3230	368	0.3	53	35	2.5
3231	369	0.9	69	84	1.1
3232	372	0.3	56	48	1.1
3233	373	0.9	52	33	1.0
3234	374	0.5	43	38	1.5
3235	376	0.8	68	33	1.1
3236	377	0.6	35	30	0.8
3237	380	0.9	70	51	0.9
3238	381	0.3	52	53	0.6
3239	382	0.9	108	68	1.5
3240	405	1.4	697	14	14.0
3241	432	0.9	30	30	2.6
3242	472	0.3	72	7	1.4
3243	473	0.3	75	6	0.7
3244	474	0.5	98	9	1.0
3245	476	0.2	60	7	1.1
3246	f - 478	0.8	86	8	1.6
3247	479	0.9	99	21	1.1
3248	481	1.0	132	23	4.6
3249	482	1.0	57	14	0.7
3250	483	0.3	111	8	0.7
3251	484	0.4	62	11	0.4
3252	488	0.8	89	29	0.4
3253	489	1.1	102	41	0.3
3254	490	0.6	63	28	0.3
3255	491	0.5	45	20	0.4
3256	492	0.6	70	24	0.5
3257	493	0.1	52	16	0.5
3258	994	0.9	45	18	1.0
3259	495	0.4	131	37	0.6
3260	496	0.5	36	20	0.6
3261	497	0.6	88	71	0.5
3262	607	0.4	144	46	3.2
3263	610	0.8	113	59	2.3
3264	612	0.3	103	104	2.7
3265	615	0.1	58	56	1.4
3266	617	0.6	196	26	1.9
3267	618	0.4	24	11	1.3
3268	619	0.8	113	55	2.4
3269	623	0.6	136	131	0.4
3270	624	0.5	199	136	0.4
3271	626	2.1	215	250	0.2
3272	628	0.8	199	126	0.3
3273	629	1.0	297	115	0.4
3274	635	0.9	26	173	0.2
3275	636	0.3	24	53	0.5
3276	637	0.7	30	44	1.6
3277	638	0.9	522	398	10.3
3278	639	0.3	81	36	1.2
3279	640	0.4	118	40	1.9
3280	641	1.0	136	48	1.2
3281	644	0.5	50	60	0.5
3282	645	0.7	146	219	1.0
3283	646	1.0	40	58	0.5
3284	647	0.8	31	54	0.6
3285	649	1.3	187	265	2.2
3286	650	1.0	70	64	0.5
3287	651	1.1	42	55	0.6
3288	652	0.4	41	4	2.2
3289	654	1.0	41	52	0.8
3290	660	1.5	179	73	0.3
3291	661	1.2	105	70	0.8
3292	664	1.5	194	86	0.9
3293	665	0.7	180	60	1.0
3294	666	1.5	107	60	1.0
3295	670	1.5	200	221	1.0
3296	671	2.0	229	43	2.4
3297	672	1.4	345	129	3.6
3298	675	0.9	166	86	1.2
3299	676	1.6	123	43	0.8
3300	677	1.2	156	102	0.3
3301	679	0.5	113	87	1.1
3302	681	1.2	127	107	0.7
3303	684	1.4	174	103	1.4
3304	686	1.1	95	471	0.9
3305	688	1.8	262	286	1.1
3306	690	1.2	286	102	1.1
3307	692	0.8	279	61	3.4
3308	693	0.9	137	93	0.9
3309	695	0.9	302	80	2.0
3310	696	1.2	180	86	0.2
3311	f - 700	0.3	80	117	0.5
3312	701	1.4	127	239	0.8
3313	702	0.8	79	107	0.8
3314	705	0.8	132	57	1.0
3315	706	0.5	134	222	0.6
3316	707	0.8	117	89	1.6
3317	708	0.8	156	129	2.4
3318	712	0.4	366	54	0.7
3319	714	0.7	155	103	0.7
3320	715	0.5	51	86	1.5
3321	716	1.1	68	130	1.0
3322	718	0.9	81	104	0.3
3323	719	1.3	82	91	0.5
3324	720	0.8	78	63	0.3
3325	772	0.8	41	33	0.2
3326	725	1.4	61	63	0.4
3327	727	1.8	119	177	0.6
3328	728	1.8	120	127	0.2
3329	729	0.7	239	37	0.5
3330	730	1.4	131	154	0.6
3331	731	0.8	76	117	0.7
3332	732	0.7	71	486	0.2
3333	733	1.4	89	133	0.4
3334	735	1.4	55	54	0.6
3335	738	0.7	85	123	1.1
3336	741	1.1	92	137	1.1
3337	743	0.6	92	122	1.6
3338	747	0.6	85	122	1.0
3339	749	0.8	97	201	1.0
3340	751	0.4	68	83	0.9
3341	753	1.0	103	200	1.2
3342	755	1.1	155	266	0.7
3343	757	0.5	90	107	1.2
3344	758	2.0	116	149	1.0
3345	759	0.8	90	180	1.8
3346	762	0.3	89	103	1.2
3347	768	0.6	320	26	2.4
3348	769	0.9	168	60	1.9
3349	770	0.9	147	43	1.9
3350	771	0.3	122	34	2.2
3351	773	0.3	116	11	1.7
3352	774	0.5	104	23	4.2
3353	776	0.6	404	74	3.1
3354	777	0.6	204	97	2.1
3355	778	0.6	324	79	0.7
3356	779	0.9	238	94	1.7
3357	780	0.9	324	193	0.8
3358	783	1.2	228	117	0.9
3359	F - 2000	1.2	55	45	0.5
3360	2001	1.9	86	77	0.6
3361	2003	1.5	78	55	0.5
3362	2004	2.0	63	58	0.5
3363	2006	2.0	62	87	0.3
3364	2007	1.7	63	60	0.6
3365	2008	1.9	62	75	0.5
3366	2010	1.2	52	24	0.3
3367	2012	1.0	85	34	0.6
33	2013	1.4	108	58	0.6
3369	2014	1.7	135	71	0.3
3370	2016	1.5	80	29	0.6
3371	2017	0.9	89	32	0.3
3372	2018	1.2	84	33	0.3
3373	2019	0.7	102	95	0.8
3374	2020	1.9	72	33	0.6
3375	2021	1.9	41	40	0.2

(ppm)

Ser.No.	Sample No.		Ag	Cu	Zn	Mo
3376	F -	2022	1.9	56	54	0.3
3377		2023	1.1	226	15	3.2
3378		2024	1.9	81	90	0.6
3379		2025	1.6	86	99	1.5
3380		2026	1.8	95	144	0.6
3381		2027	2.3	69	91	0.5
3382		2028	2.6	58	62	0.5
3383		2029	1.6	196	58	0.4
3384		2030	2.3	82	57	0.6
3385		2031	2.1	258	45	0.7
3386		2032	1.8	209	40	0.6
3387		2033	1.8	179	54	0.9
3388		2035	1.4	59	63	1.0
3389		2036	1.9	96	82	1.3
3390		2037	1.4	74	63	1.0
3391		2039	1.6	108	95	0.9
3392		2040	1.6	63	153	3.7
3393		2042	1.6	12	21	0.3
3394		2043	0.3	16	36	0.3
3395		2044	1.9	11	20	0.2
3396		2045	1.1	12	8	0.1
3397		2046	0.7	13	10	0.2
3398		2047	0.9	9	11	0.1
3399		2048	0.9	3	8	0.1
3400		2049	0.7	4	8	0.1
3401		2050	2.1	46	22	0.2
3402		2051	0.9	38	41	0.3
3403		2052	2.0	94	75	0.4
3404		2053	1.3	15	26	0.1
3405		2054	1.0	13	24	0.2
3406		2055	1.6	9	32	0.2
3407		2056	1.3	16	36	0.2
3408		2057	1.8	40	69	0.3
3409		2059	1.6	30	33	0.5
3410		2060	0.8	25	20	0.4
3411		2061	1.6	127	29	1.0
3412		2063	1.6	243	67	0.7
3413		2064	1.6	120	54	0.6
3414		2065	1.5	92	74	1.1
3415		2066	1.8	76	78	0.7
3416		2068	1.4	75	69	0.6
3417		2069	1.8	136	35	2.7
3418		2070	1.4	178	33	1.4
3419		2072	1.4	110	37	0.7
3420		2073	1.1	98	33	0.9
3421		2074	1.0	81	28	1.1
3422		2075	1.4	76	29	1.0
3423		2076	0.6	49	21	1.1
3424		2077	1.0	88	42	1.2
3425		2078	1.1	30	40	0.6
3426		2079	1.0	27	27	0.5
3427		2080	0.9	18	24	0.4
3428		2081	0.8	46	14	1.6
3429		2083	0.8	28	24	0.7
3430		2084	0.5	26	17	0.8
3431		2085	1.1	10	15	0.2
3432		2086	1.1	11	11	0.3
3433		2087	1.3	12	15	0.2
3434		2088	1.5	17	18	0.3
3435		2089	0.9	17	15	0.3
3436		2090	1.5	17	19	0.4
3437		2091	0.8	50	35	3.7
3438		2092	1.7	58	22	0.3
3439		2093	0.8	60	72	0.8
3440		2094	1.6	85	47	0.8

Ser.No.	Sample No.		Ag	Cu	Zn	Mo
3441	F -	2095	1.6	49	29	0.9
3442		2096	1.5	104	51	0.4
3443		2097	1.2	49	19	0.5
3444		2098	1.2	22	17	0.7
3445		2099	1.2	21	16	0.3
3446		2100	1.3	23	14	0.4
3447		2101	1.1	24	14	0.1
3448		2102	1.5	304	24	11.2
3449		2103	1.3	64	19	0.3
3450		2104	0.7	68	44	0.4
3451		2105	1.1	162	26	0.5
3452		2106	1.6	189	41	0.5
3453		2107	2.3	171	34	0.4
3454		2108	1.6	173	184	0.4
3455		2109	1.3	169	67	0.3
3456		2110	0.9	108	41	0.3
3457		2111	1.3	95	38	0.6
3458		2112	0.8	108	26	1.1
3459		2113	0.5	156	34	0.7
3460		2114	1.1	70	30	0.6
3461		2115	1.1	46	39	0.5
3462		2116	0.9	73	34	0.5
3463		2117	0.9	157	52	0.6
3464		2118	0.9	114	38	0.4
3465		2119	0.9	52	54	0.6
3466		2120	0.9	32	44	0.3
3467		2121	2.0	49	78	0.6
3468		2122	1.9	44	79	0.7
3469		2123	2.4	118	76	1.0
3470		2124	1.3	186	222	0.9
3471		2125	1.5	94	148	1.1
3472		2126	1.2	64	78	0.3
3473		2127	1.6	55	41	0.2
3474		2128	1.1	58	48	0.1
3475		2129	1.3	47	56	0.3
3476		2130	1.3	34	41	0.5
3477		2131	1.6	51	31	0.4
3478		2132	1.3	53	31	0.2
3479		2133	0.9	27	25	0.1
3480		2134	0.8	83	54	0.4
3481		2136	1.1	31	38	0.2
3482		2137	1.4	57	59	0.5
3483		2138	1.1	34	42	0.3
3484		2139	0.9	65	38	0.3
3485		2140	1.6	46	38	0.2
3486		2141	1.6	50	42	0.3
3487		2142	1.4	45	38	0.4
3488		2143	1.2	33	31	0.3
3489		2144	1.8	52	68	0.3
3490		2145	0.7	63	45	0.5
3491		2146	0.8	103	72	0.9
3492		2148	1.8	93	143	0.8
3493		2149	1.5	110	142	1.5
3494		2151	0.9	96	60	1.2
3495		2152	1.1	66	65	0.4
3496		2153	1.4	102	76	0.7
3497		2155	0.9	121	95	1.1
3498		2156	0.9	105	67	1.0
3499		2157	0.9	109	41	1.3
3500		2158	2.8	125	73	1.3
3501		2159	2.0	107	65	0.4
3502		2160	1.6	237	62	1.1
3503		2161	0.8	137	59	0.7
3504		2163	0.3	116	38	1.7
3505		2165	0.4	93	26	2.0

Ser.No.	Sample No.		Ag	Cu	Zn	Mo
3506	F -	2166	0.4	118	32	1.7
3507		2167	0.9	107	29	2.0
3508		2168	0.9	145	34	1.7
3509		2169	1.2	102	124	0.5
3510		2170	0.8	179	67	1.4
3511		2171	0.5	139	67	1.3
3512		2172	1.0	100	70	0.6
3513		2173	0.5	271	101	0.6
3514		2174	0.7	156	100	0.6
3515		2175	0.8	168	99	0.6
3516		2176	0.8	123	78	0.5
3517		2177	0.8	213	81	0.7
3518		2178	0.8	202	68	0.8
3519		2179	1.0	189	96	1.6
3520		2181	1.0	330	81	2.6
3521		2182	0.9	192	77	2.3
3522		2183	1.2	274	64	2.0
3523		2184	0.4	310	52	1.2
3524		2185	1.2	231	72	0.9
3525		2186	1.0	179	176	0.7
3526		2187	1.2	186	52	0.9
3527		2188	0.8	121	57	0.8
3528		2189	0.5	54	26	0.3
3529		2190	0.7	54	29	0.5
3530		2191	0.7	78	31	0.7
3531		2192	0.7	202	29	0.7
3532		2193	1.8	356	248	1.0
3533		2194	1.3	215	186	0.7
3534		2195	1.0	77	278	0.9
3535		2196	0.8	29	75	0.2
3536		2197	1.0	97	40	0.4
3537		2198	1.0	114	41	1.1
3538		2199	1.0	71	42	0.5
3539		2200	0.9	81	23	0.5
3540		2201	0.8	77	74	0.5
3541		2202	1.0	87	63	0.8
3542		2203	1.0	147	98	1.1
3543		2204	0.8	165	63	0.4
3544		2205	0.8	45	32	0.2
3545		2206	0.8	36	27	0.3
3546		2207	0.8	128	39	0.6
3547		2208	0.5	44	14	0.3
3548		2209	0.5	65	13	0.5
3549		2210	0.5	70	17	0.6
3550		2211	0.7	71	24	0.8
3551		2212	0.5	36	27	0.5
3552		2213	0.5	103	54	0.2
3553		2214	0.3	29	9	0.1
3554		2215	0.3	14	13	0.1
3555		2216	0.4	9	11	0.1
3556		2217	0.7	52	98	0.4
3557		2218	1.0	47	23	0.5
3558		2219	1.7	47	30	0.1
3559		2221	0.6	36	22	0.7
3560		2222	0.8	38	18	0.5
3561		2223	0.8	43	22	0.6
3562		2224	0.5	32	15	0.3
3563		2225	0.6	41	13	0.4
3564		2226	0.5	42	12	0.5
3565		2227	0.6	137	27	0.7
3566		2228	1.2	330	43	1.3
3567		2229	0.6	335	55	2.0
3568		2230	1.9	203	33	0.9
3569		2232	1.9	110	28	1.0
3570		2233	1.9	137	34	1.1

(ppm)

Ser.No.	Sample No.	Ag	Cu	Zn	Mo
3571	F - 2234	1.3	346	28	1.8
3572	2235	1.2	167	25	0.8
3573	2236	0.6	39	16	0.2
3574	2237	0.4	5	18	0.1
3575	2238	0.8	13	21	0.2
3576	2239	0.8	39	28	0.4
3577	2240	0.9	197	84	1.3
3578	2241	1.2	159	148	2.0
3579	2242	1.3	225	60	1.6
3580	2243	1.4	306	73	2.2
3581	2244	1.0	124	117	0.9
3582	2245	1.1	161	97	0.7
3583	2246	1.6	198	112	0.5
3584	2247	1.6	120	93	0.9
3585	2248	1.3	85	140	0.4
3586	2249	1.1	108	187	0.5
3587	2250	1.1	244	157	0.5
3588	2251	2.3	355	96	0.8
3589	2252	2.1	287	156	0.8
3590	2253	1.4	219	104	1.9
3591	2254	1.0	181	152	2.7
3592	2255	1.4	263	221	1.3
3593	2256	1.0	642	160	1.4
3594	2257	0.8	87	21	1.4
3595	2258	0.4	47	13	1.7
3596	2259	0.8	72	13	1.9
3597	2260	1.3	248	33	3.3
3598	2261	1.4	464	61	2.3
3599	2262	1.0	173	100	0.8
3600	2263	1.6	222	131	0.8
3601	2264	1.3	422	94	1.0
3602	2265	1.4	290	106	1.5
3603	2266	0.4	385	13	2.3
3604	2268	0.4	120	7	3.6
3605	2269	1.2	98	69	2.0
3606	2270	1.7	138	31	4.5
3607	2271	1.3	468	37	10.7
3608	2272	0.9	165	40	1.5
3609	2273	0.8	80	150	1.8
3610	2274	1.5	50	41	1.2
3611	2275	1.5	54	30	1.7
3612	2276	0.8	105	23	2.1
3613	2278	0.5	126	17	1.5
3614	2279	1.8	141	33	1.7
3615	2280	1.8	331	81	6.6
3616	2281	1.9	345	175	0.7
3617	2282	3.0	412	82	0.7
3618	2284	1.3	158	64	1.0
3619	2285	1.0	120	53	1.3
3620	2286	1.4	208	73	1.8
3621	2287	1.7	165	143	0.7
3622	2288	1.4	218	53	0.8
3623	2289	0.8	113	52	1.2
3624	2290	1.3	169	73	1.2
3625	2291	2.4	139	81	1.3
3626	2292	0.6	268	24	0.9
3627	2293	0.5	119	327	3.5
3628	2294	1.3	257	109	1.5
3629	2295	1.3	225	207	3.5
3630	2296	1.9	191	262	2.0
3631	2297	2.3	167	269	0.6
3632	2298	1.8	182	122	0.8
3633	2300	1.4	81	32	0.9
3634	2301	1.8	98	52	0.7
3635	2302	1.7	125	48	0.6
3636	F - 2303	1.4	235	77	0.5
3637	2304	1.9	244	78	0.7
3638	2305	2.0	263	103	0.4
3639	2306	1.8	348	94	0.3
3640	2307	1.5	229	68	0.3
3641	2308	1.4	224	18	0.5
3642	2309	1.1	437	37	12.9
3643	2310	0.9	345	28	4.5
3644	2311	1.1	398	66	0.5
3645	2312	1.4	793	83	6.2
3646	2313	1.5	333	116	0.7
3647	2314	1.1	251	97	0.7
3648	2315	1.2	265	147	0.3
3649	2316	1.5	212	129	0.6
3650	2317	1.8	307	190	0.4
3651	2318	1.6	216	101	0.6
3652	2319	1.2	210	123	0.3
3653	2320	1.2	205	96	0.3
3654	2321	1.2	121	96	0.4
3655	2322	1.4	285	90	0.7
3656	2323	1.5	91	109	0.5
3657	2324	0.9	112	206	0.6
3658	2326	0.3	44	27	0.5
3659	2327	2.0	169	101	0.5
3660	2328	1.5	145	593	0.1
3661	2329	1.2	84	119	0.3
3662	2330	1.4	140	109	0.6
3663	2332	0.5	134	150	1.0
3664	2333	1.1	802	50	1.1
3665	2334	0.8	264	32	1.4
3666	2335	1.1	422	34	1.1
3667	2336	1.3	53	10	0.4
3668	2337	0.9	109	12	0.7
3669	2338	0.7	81	9	0.6
3670	2339	0.5	65	7	1.3
3671	2340	0.8	108	30	1.5
3672	2341	0.4	78	23	1.4
3673	2342	0.5	123	15	1.1
3674	2343	0.5	62	23	1.1
3675	2345	0.8	110	41	1.4
3676	2346	1.1	106	35	1.4
3677	2347	0.5	75	30	1.3
3678	2348	0.3	53	9	1.3
3679	2349	0.3	52	10	2.4
3680	2350	0.8	187	50	0.5
3681	2351	1.1	151	30	0.9
3682	2352	0.7	36	18	1.3
3683	2353	0.8	52	10	1.4
3684	2354	0.7	72	12	0.7
3685	2355	1.1	84	30	1.0
3686	2356	0.9	213	26	0.6
3687	2357	1.2	171	41	0.4
3688	2358	0.5	82	28	0.3
3689	2359	0.7	167	17	0.5
3690	2360	0.4	42	11	0.6
3691	2361	0.5	81	12	0.6
3692	2362	2.0	142	30	1.5
3693	2363	0.7	167	13	0.5
3694	2364	0.7	88	15	1.1
3695	2365	0.4	53	11	0.7
3696	2366	0.4	168	15	2.9
3697	2367	0.3	105	12	2.3
3698	2368	1.1	95	6	2.2
3699	2369	0.8	126	8	2.3
3700	2370	0.4	94	13	2.9
3701	F - 2371	0.7	41	9	15.8
3702	2372	0.4	41	8	2.2
3703	2373	0.5	61	10	1.2
3704	2374	0.3	143	7	2.2
3705	2375	0.4	126	7	4.3
3706	2376	0.7	199	10	9.6
3707	2377	0.9	158	46	8.8
3708	2378	0.5	144	24	3.6
3709	2379	0.8	52	10	1.5
3710	2380	1.8	225	88	0.7
3711	2381	1.2	106	43	0.4
3712	2382	1.4	115	41	0.7
3713	2383	1.1	131	24	0.8
3714	2384	0.9	70	14	0.9
3715	2385	0.9	64	17	0.8
3716	2386	0.8	104	26	0.7
3717	2387	0.8	81	23	0.8
3718	2388	1.1	94	25	0.7
3719	2389	1.9	322	76	1.0
3720	2390	0.5	50	14	0.6
3721	2391	0.8	46	9	1.0
3722	2392	0.9	116	13	1.2
3723	2393	0.7	99	8	1.9
3724	2394	0.9	86	14	1.0
3725	2395	0.7	167	12	4.0
3726	2396	0.8	139	14	2.7
3727	2397	0.7	172	11	2.4
3728	2398	0.4	185	23	1.9
3729	2399	1.5	204	85	0.6
3730	2400	0.5	74	34	0.9
3731	2401	0.9	134	11	5.0
3732	2402	0.3	56	6	3.1
3733	2403	0.9	83	8	3.5
3734	2404	1.1	93	6	2.1
3735	2405	0.4	93	8	2.2
3736	2406	0.3	93	6	1.9
3737	2407	0.9	102	7	2.0
3738	2408	0.2	104	11	1.8
3739	2409	0.4	108	11	1.7
3740	2410	0.2	111	13	1.8
3741	2411	0.6	171	17	1.6
3742	2412	0.2	39	7	0.4
3743	2414	0.3	42	10	0.2
3744	2415	0.4	62	9	1.3
3745	2416	0.3	197	10	2.6
3746	2417	0.6	64	86	0.2
3747	2418	0.6	139	27	0.6
3748	2419	0.4	93	14	1.2
3749	2420	0.2	81	16	0.9
3750	2422	0.3	107	21	1.1
3751	2423	0.2	133	35	2.5
3752	2424	0.3	242	24	3.5
3753	2425	0.6	124	13	1.6
3754	2426	0.4	88	11	0.8
3755	2427	0.1	88	8	1.9
3756	2428	0.6	133	7	1.7
3757	2429	0.4	69	30	1.1
3758	2430	0.7	75	29	2.1
3759	2431	0.6	88	14	3.0
3760	2432	0.6	57	13	2.3
3761	2433	0.8	51	16	1.1
3762	2434	0.3	57	17	1.3
3763	2435	0.7	53	17	1.1
3764	2436	0.6	221	17	7.7
3765	2437	0.6	140	17	1.9

(ppm)

Ser.No.	Sample No.	Ag	Cu	Zn	Mo
3766	F - 2439	0.2	40	16	0.8
3767	2440	0.3	44	9	1.0
3768	2441	0.2	14	6	1.0
3769	2442	0.6	37	15	0.8
3770	2443	1.1	51	24	0.8
3771	2444	0.3	115	8	3.2
3772	2445	0.5	154	7	3.9
3773	2446	0.3	196	6	4.6
3774	2447	0.1	172	6	6.3
3775	2448	0.5	311	13	7.5
3776	2449	0.6	342	7	10.4
3777	2450	0.5	237	4	8.6
3778	2451	0.5	300	6	36.3
3779	2452	0.5	275	5	29.5
3780	2453	0.2	124	4	14.7
3781	2454	0.2	132	9	1.7
3782	2456	1.4	206	34	2.6
3783	2457	1.3	176	34	2.3
3784	2458	1.2	190	34	1.9
3785	2460	0.9	132	25	2.5
3786	2461	1.2	149	37	1.3
3787	2463	1.5	239	42	1.1
3788	2464	1.7	314	45	2.5
3789	2465	1.4	477	38	3.0
3790	2466	1.4	525	17	5.6
3791	2467	1.4	342	13	2.3
3792	2468	1.0	111	23	11.4
3793	2469	1.0	72	10	1.5
3794	2470	0.5	95	7	8.1
3795	2473	1.4	362	11	0.7
3796	2474	0.9	294	15	1.9
3797	2475	0.4	172	4	2.2
3798	2476	0.5	214	5	5.8
3799	2477	0.5	307	7	1.8
3800	2478	0.6	191	4	1.9
3801	2479	0.7	291	9	2.1
3802	2480	0.4	97	6	1.1
3803	2481	0.5	136	14	0.8
3804	2482	0.5	153	14	5.2
3805	2483	0.7	135	17	2.4
3806	2484	0.7	81	10	2.1
3807	2486	0.1	34	8	1.0
3808	2487	0.2	32	11	0.7
3809	2488	0.2	56	13	0.7
3810	2489	0.1	180	7	1.4
3811	2490	0.6	257	14	0.9
3812	2491	0.2	93	8	1.3
3813	2492	0.1	60	8	1.7
3814	2493	0.1	32	7	1.3
3815	2494	0.1	26	9	3.4
3816	2495	0.5	72	10	12.8
3817	2496	0.6	88	30	3.9
3818	2497	0.5	98	14	1.9
3819	2498	0.2	66	14	3.6
3820	2499	0.4	167	26	3.9
3821	2500	0.4	101	20	1.7
3822	2502	0.3	40	7	3.6
3823	2503	0.8	65	14	2.1
3824	2504	1.5	84	14	1.5
3825	2505	1.1	75	13	1.3
3826	2506	1.1	93	7	0.9
3827	2507	1.1	122	15	1.2
3828	2508	1.0	115	13	1.6
3829	2509	1.0	88	15	0.8
3830	2510	0.4	96	5	3.1

Ser.No.	Sample No.	Ag	Cu	Zn	Mo
3831	F - 2511	0.3	69	4	8.9
3832	2512	0.3	67	4	6.8
3833	2513	0.3	2	3	0.7
3834	2514	0.3	23	9	1.4
3835	2515	0.3	19	6	1.0
3836	2516	0.5	86	54	0.9
3837	2517	0.6	79	68	2.5
3838	2518	1.0	42	54	3.2
3839	2519	0.9	36	19	2.2
3840	2520	0.5	53	18	1.3
3841	2521	1.0	49	10	3.1
3842	2522	0.8	27	5	2.2
3843	2523	0.3	25	6	10.6
3844	2524	0.1	45	8	2.2
3845	2527	0.6	121	8	3.1
3846	2528	0.5	119	16	3.4
3847	2529	0.6	116	10	3.2
3848	2530	0.3	101	26	1.2
3849	2531	0.5	104	28	1.0
3850	2532	0.3	142	15	1.0
3851	2533	1.1	127	15	1.4
3852	2534	0.7	141	9	1.0
3853	2535	1.1	214	9	0.6
3854	2536	0.8	277	10	0.6
3855	2537	1.6	576	22	3.4
3856	2538	1.8	335	32	11.1
3857	2539	1.7	368	34	7.9
3858	2540	1.2	376	51	7.9
3859	2542	1.4	277	61	1.1
3860	2545	1.6	386	9	1.3
3861	2546	2.0	309	11	1.4
3862	2547	1.4	250	14	1.4
3863	2548	1.6	163	12	1.1
3864	2549	2.4	391	61	1.4
3865	2550	1.3	329	21	3.4
3866	2551	1.1	371	17	3.9
3867	2552	1.3	311	15	4.6
3868	2553	1.3	260	14	3.7
3869	2554	1.8	259	37	3.6
3870	2555	1.7	266	29	4.6
3871	2556	1.8	337	44	5.3
3872	2557	1.3	317	28	3.3
3873	2558	1.8	300	21	5.2
3874	2560	1.8	190	104	0.9
3875	2561	1.3	133	88	1.7
3876	2562	1.4	85	59	0.9
3877	2563	1.3	103	76	1.3
3878	2565	1.4	137	112	1.1
3879	2566	1.8	94	69	1.2
3880	2567	1.7	83	56	1.2
3881	2568	1.6	136	112	0.9
3882	2569	1.3	117	71	0.9
3883	2570	0.5	75	53	1.2
3884	2571	0.5	97	104	1.5
3885	2572	0.5	61	24	1.3
3886	2573	0.5	60	20	1.6
3887	2574	0.4	38	14	1.0
3888	2575	0.9	51	20	1.5
3889	2576	0.9	95	50	1.5
3890	2577	0.9	88	43	1.5
3891	2578	0.5	72	26	1.7
3892	2579	1.0	168	42	2.8
3893	2580	0.9	290	62	4.3
3894	2581	0.4	33	7	2.6
3895	2582	1.6	124	28	3.4

Ser.No.	Sample No.	Ag	Cu	Zn	Mo
3896	F - 2583	0.8	217	18	4.9
3897	2585	0.5	53	36	1.1
3898	2586	1.4	1961	71	21.5
3899	2587	1.2	410	6	28.3
3900	2588	0.9	398	10	41.4
3901	2589	1.2	505	24	8.5
3902	2590	1.3	615	69	10.3
3903	2591	1.0	620	25	15.4
3904	2592	0.9	358	79	2.5
3905	2593	1.2	554	50	3.2
3906	2594	0.8	477	20	3.5
3907	2595	1.0	104	6	6.0
3908	2596	0.5	103	7	6.1
3909	2597	0.4	114	8	4.5
3910	2598	0.5	67	6	5.1
3911	2599	0.5	138	6	2.5
3912	2600	0.7	185	21	4.1
3913	2601	1.0	126	11	2.6
3914	2602	0.9	183	10	2.3
3915	2603	0.8	146	6	2.1
3916	2604	0.7	104	6	3.2
3917	2605	0.7	254	16	1.5
3918	2607	0.8	367	28	3.6
3919	2608	0.7	221	41	6.7
3920	2609	0.5	154	14	6.1
3921	2610	0.7	211	27	4.8
3922	2611	0.8	163	43	7.6
3923	2612	1.3	281	36	9.6
3924	2613	0.3	57	5	8.8
3925	2614	0.3	87	9	2.3
3926	2615	0.4	113	8	1.8
3927	2616	0.4	211	7	2.3
3928	2617	0.7	290	12	3.6
3929	2618	0.7	103	11	2.0
3930	2619	0.3	109	7	11.4
3931	2620	1.3	631	32	4.3
3932	2621	1.2	400	56	5.3
3933	2622	1.3	510	27	9.4
3934	2623	1.3	560	38	7.4
3935	2624	1.0	718	38	10.5
3936	2625	1.3	444	43	5.0
3937	2626	1.2	343	36	5.2
3938	2628	1.3	721	26	9.8
3939	2629	1.0	454	16	7.8
3940	2630	1.6	652	91	11.8
3941	2631	1.9	1132	38	26.5
3942	2632	1.7	1154	40	33.4
3943	3633	1.7	2776	63	15.0
3944	2634	0.9	581	11	19.7
3945	2635	0.4	345	3	20.4
3946	2636	0.7	430	15	21.5
3947	2637	0.5	335	5	24.2
3948	2638	1.1	524	8	23.9
3949	2639	1.7	635	8	16.6
3950	2640	0.9	554	10	23.5
3951	2641	1.5	206	22	3.7
3952	2642	0.9	94	22	1.7
3953	2644	1.6	83	44	1.7
3954	2645	0.9	59	21	1.7
3955	2646	0.9	28	11	1.1
3956	2647	0.3	37	21	0.8
3957	2648	0.9	49	30	1.0
3958	2649	1.3	55	43	0.8
3959	2650	0.4	88	82	1.4
3960	2651	0.7	89	82	1.1

(ppm)

Ser.No.	Sample No.	Ag	Cu	Zn	Mo
3961	F - 2652	0.9	75	44	1.6
3962	2653	0.8	144	62	1.4
3963	3654	1.1	52	67	0.7
3964	2655	1.1	35	64	0.8
3965	2656	0.5	91	74	0.5
3966	2657	0.5	84	55	0.7
3967	2658	0.3	28	74	0.7
3968	2660	1.1	44	59	1.3
3969	2661	1.6	122	70	0.6
3970	2662	1.2	94	57	0.5
3971	2663	1.2	259	103	3.0
3972	2664	1.2	368	87	3.9
3973	2665	1.2	122	98	1.3
3974	2666	1.0	145	169	1.2
3975	2667	0.3	132	44	1.7
3976	2668	1.3	129	29	1.6
3977	2669	1.3	132	32	1.6
3978	2670	1.3	134	73	1.0
3979	2671	0.9	172	30	1.6
3980	2673	0.3	123	8	3.3
3981	2674	0.6	172	29	3.0
3982	2675	0.6	378	4	9.3
3983	2676	0.3	233	4	6.4
3984	2677	0.4	134	3	3.0
3985	2678	0.3	107	3	3.3

Ser.No.	Sample No.	Ag	Cu	Zn	Mo
3986	F - 2679	0.6	135	9	5.4
3987	2680	0.1	39	3	4.2
3988	2681	0.9	28	3	2.3
3989	2682	0.4	129	55	3.5
3990	2683	0.1	70	5	5.1
3991	2684	1.2	246	7	7.0
3992	2685	0.9	142	5	3.8
3993	2686	1.5	120	30	4.7
3994	2687	0.9	117	4	7.0
3995	2688	0.1	82	7	15.6
3996	2689	0.1	70	4	13.2
3997	2690	0.3	110	8	16.5
3998	2691	0.4	86	8	7.2
3999	2692	0.3	70	3	1.8
4000	2693	0.4	89	13	4.4
4001	2694	0.3	89	16	2.1
4002	2695	0.6	73	29	1.4
4003	2696	0.9	122	6	0.6
4004	2697	0.3	84	3	0.6
4005	2698	0.3	127	72	2.0
4006	2699	0.9	98	24	3.3
4007	2700	1.0	97	9	1.1
4008	2701	0.3	56	3	1.0
4009	2702	0.7	123	3	2.6
4010	2703	0.7	144	3	4.0

Ser.No.	Sample No.	Ag	Cu	Zn	Mo
4011	F - 2704	0.4	92	4	5.4
4012	2705	0.3	110	11	3.0
4013	2706	0.7	147	20	6.3
4014	2705	0.3	164	30	4.6
4015	2708	0.4	224	48	4.2
4016	2709	1.0	513	140	4.1
4017	2710	1.5	226	48	1.9
4018	2711	1.2	187	40	1.6
4019	2712	1.2	163	58	1.9
4020	2713	1.2	202	46	2.1
4021	2714	1.5	397	17	3.5
4022	2715	1.2	254	13	5.3
4023	2716	1.3	257	9	3.8
4024	2717	0.9	303	20	3.5
4025	2718	0.6	285	37	4.2
4026	2719	1.3	311	37	4.9

(ppm)

Ser.No.	Sample No.	Cu	Pb	Zn	Ba
4027	fB - 1013	183	144	457	106

Ser.No.	Sample No.	Cu	Pb	Zn	Ba

Ser.No.	Sample No.	Cu	Pb	Zn	Ba

(ppm)

Ser.No.	Sample No.	Ag	Pb	Zn	Ba
4028	F - 151	0.4	21	13	44
4029	152	1.0	21	11	132
4030	153	0.8	20	11	110
4031	155	0.8	7	3	44
4032	156	1.0	29	21	121
4033	157	0.3	29	16	44
4034	159	1.0	15	14	55
4035	161	0.5	26	10	33
4036	163	0.3	31	9	33
4037	164	0.3	58	6	44
4038	165	0.5	84	16	66
4039	166	0.3	18	7	33
4040	167	1.6	18	64	77
4041	169	0.3	153	9	66
4042	170	1.8	55	23	110
4043	171	0.4	25	30	66
4044	172	1.3	27	129	166
4045	173	0.5	23	26	132
4046	174	0.4	21	37	88
4047	175	1.3	46	30	88
4048	177	2.0	22	43	199
4049	179	0.5	14	33	88
4050	180	0.5	14	34	188
4051	181	0.3	26	37	132
4052	182	1.3	26	69	199
4053	185	0.3	304	20	110
4054	186	0.5	41	20	99
4055	187	0.8	27	6	55

Ser.No.	Sample No.	Ag	Pb	Zn	Ba
4056	F - 188	0.8	21	13	88
4057	189	0.7	46	73	66
4058	191	0.8	12	4	57
4059	192	0.5	41	10	123
4060	193	1.8	84	14	132
4061	194	1.8	281	11	189
4062	195	1.6	140	20	151
4063	196	1.8	81	15	132
4064	197	0.4	33	87	47
4065	198	0.3	5	4	19
4066	199	0.4	18	32	94
4067	200	0.4	26	32	76
4068	201	0.8	14	48	113
4069	280	1.8	17	68	179
4070	283	1.7	23	64	208
4071	284	1.2	23	68	151
4072	285	1.2	26	55	151
4073	286	0.5	11	39	132
4074	287	0.7	26	41	113
4075	288	1.1	18	111	189
4076	289	1.5	12	44	151
4077	290	0.5	16	31	132
4078	291	0.8	23	48	113
4079	294	1.5	18	51	113
4080	295	1.7	87	70	170
4081	296	0.9	12	36	94
4082	297	1.1	23	60	132
4083	299	1.5	23	36	132
4084	300	1.1	23	163	170
4085	306	2.2	29	73	227

Ser.No.	Sample No.	Ag	Pb	Zn	Ba
4086	F - 307	0.9	25	22	104
4087	308	1.7	17	42	142
4088	f - 116	1.8	16	51	223
4089	117	2.1	18	94	282
4090	118	0.7	27	54	235
4091	119	1.6	27	66	235
4092	120	1.6	99	51	259
4093	123	0.5	16	46	212
4094	124	0.3	18	50	241
4095	125	0.8	20	44	270
4096	131	2.3	24	40	231
4097	132	2.6	22	63	189
4098	134	2.4	21	49	147
4099	135	0.5	15	24	63
4100	136	0.3	16	10	42
4101	137	0.5	23	29	105
4102	138	0.4	12	6	42
4103	139	0.3	16	4	32
4104	140	0.3	7	19	189
4105	141	0.3	66	4	32
4106	143	1.4	18	17	105
4107	147	5.2	48	19	116
4108	148	2.6	61	11	95
4109	149	1.6	86	20	95
4110	150	0.3	29	20	63
4111	151	0.5	40	13	177
4112	152	0.9	20	14	155
4113	153	1.3	205	33	110

Fig. 1 Cumulative frequency distribution

Fig. 1－1 Cumulative frequency distribution of Cu, Zn, Mo and Ag in the I Area
N = 449 (data on －80-mesh fraction)

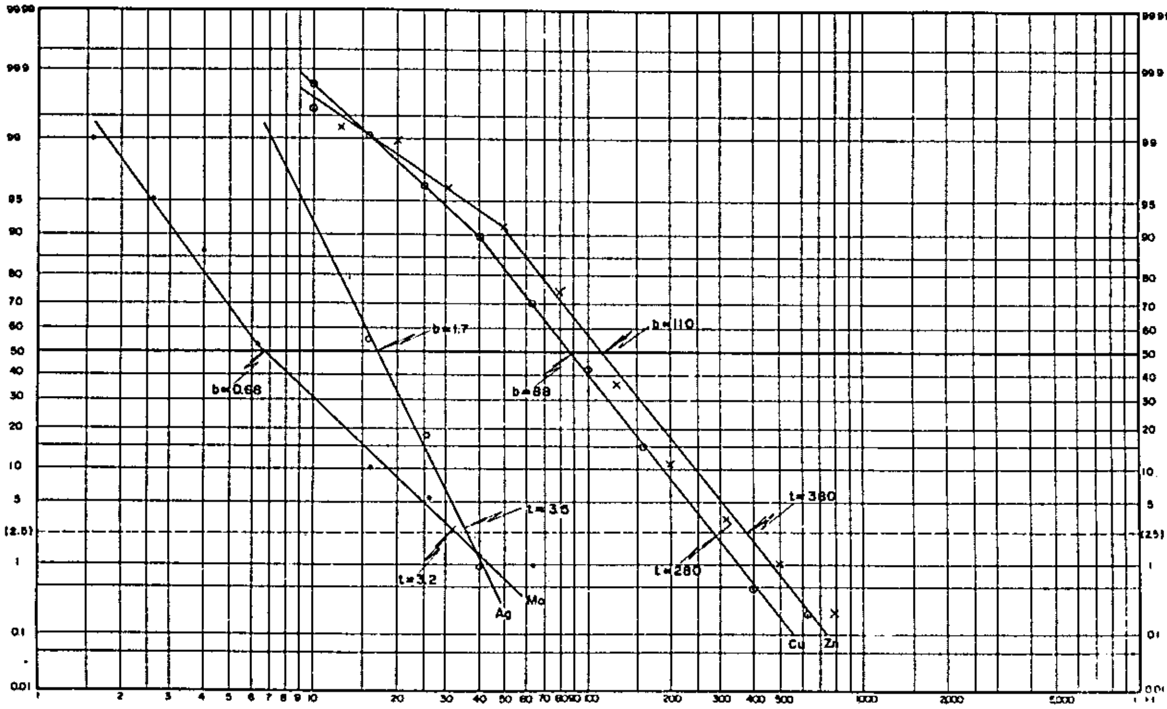

Fig. 1－2 Cumulative frequency distribution of Cu, Zn, Mo and Ag in the II Area
N = 1,046 (data on －80-mesh fraction)

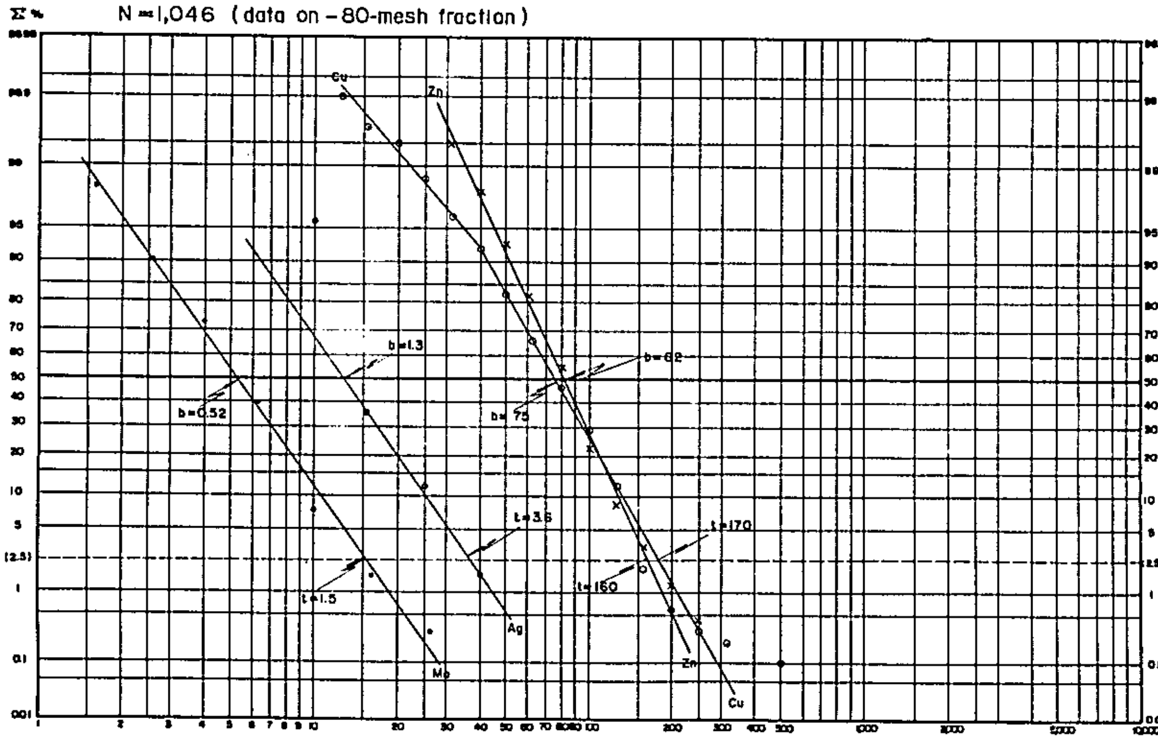

Fig. 1-3 Cumulative frequency distribution of Cu, Zn, Ni and Co in the III Area

Σ% N-552 (data on -80-mesh fraction)

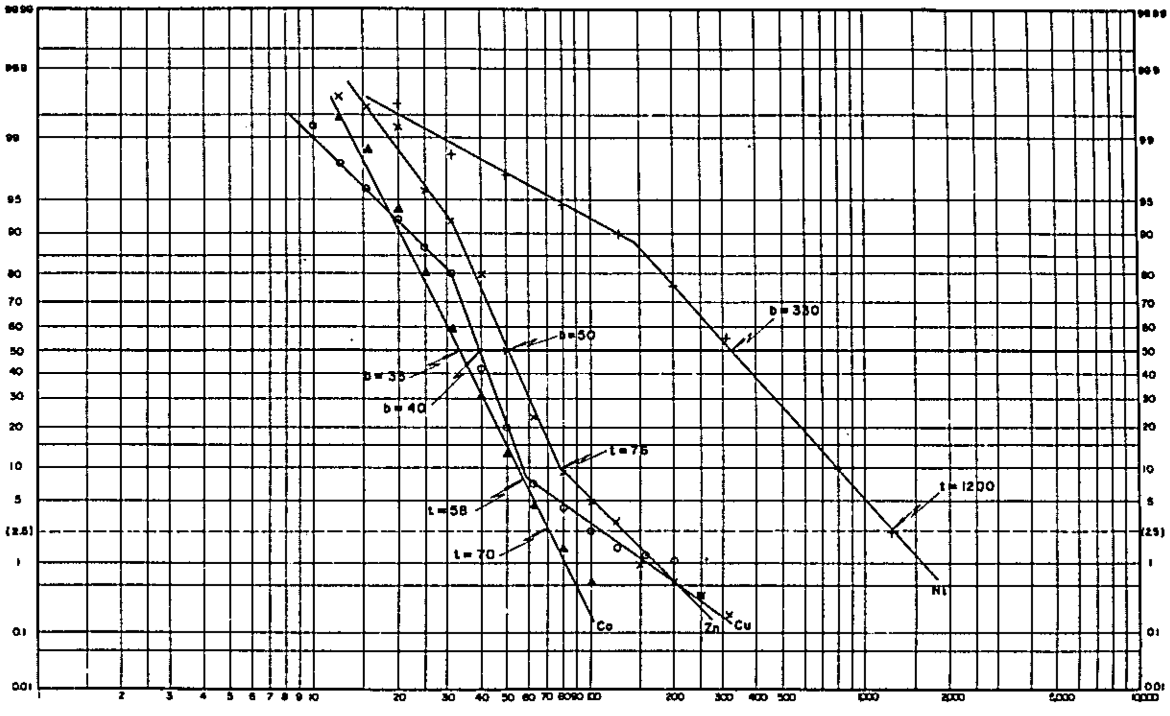

Fig. 1-4 Cumulative frequency distribution of Cu, Zn, Ni and Co in the IV-a Area

Σ% N=157 (data on-80-mesh fraction)

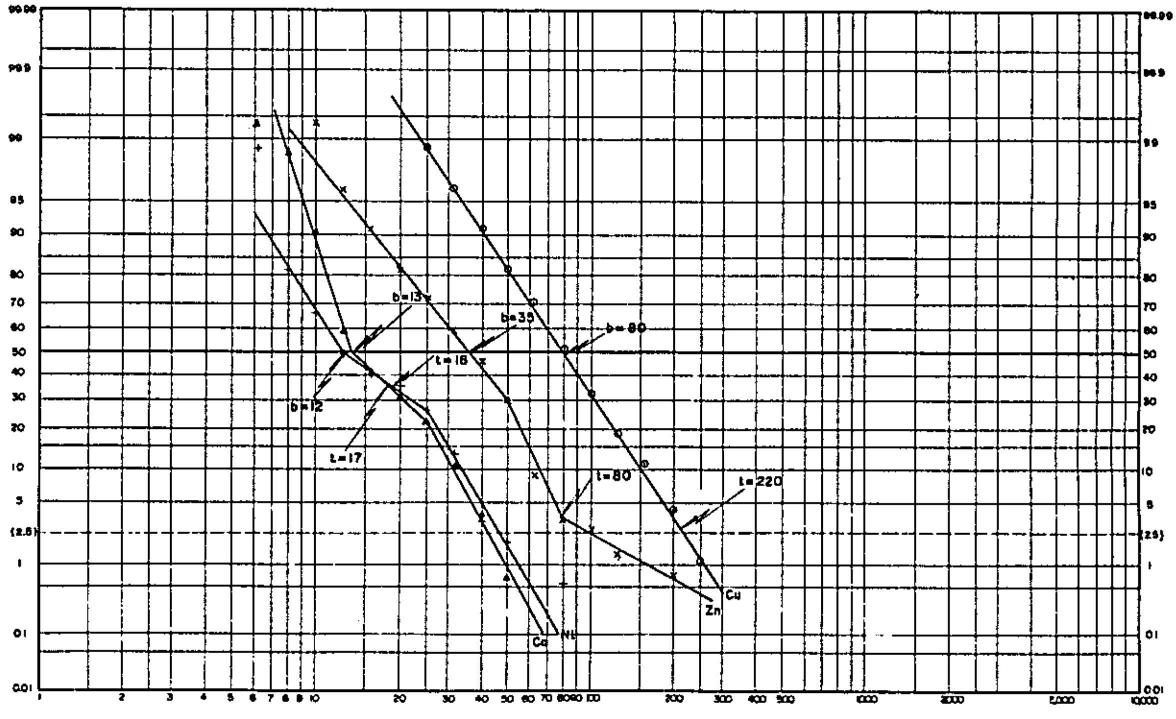

Fig. 1-5 Cumulative frequency distribution of Cu, Zn, Ni and Co in the IV-6 Area

Σ% N = 678 (data on -80-mesh fraction)

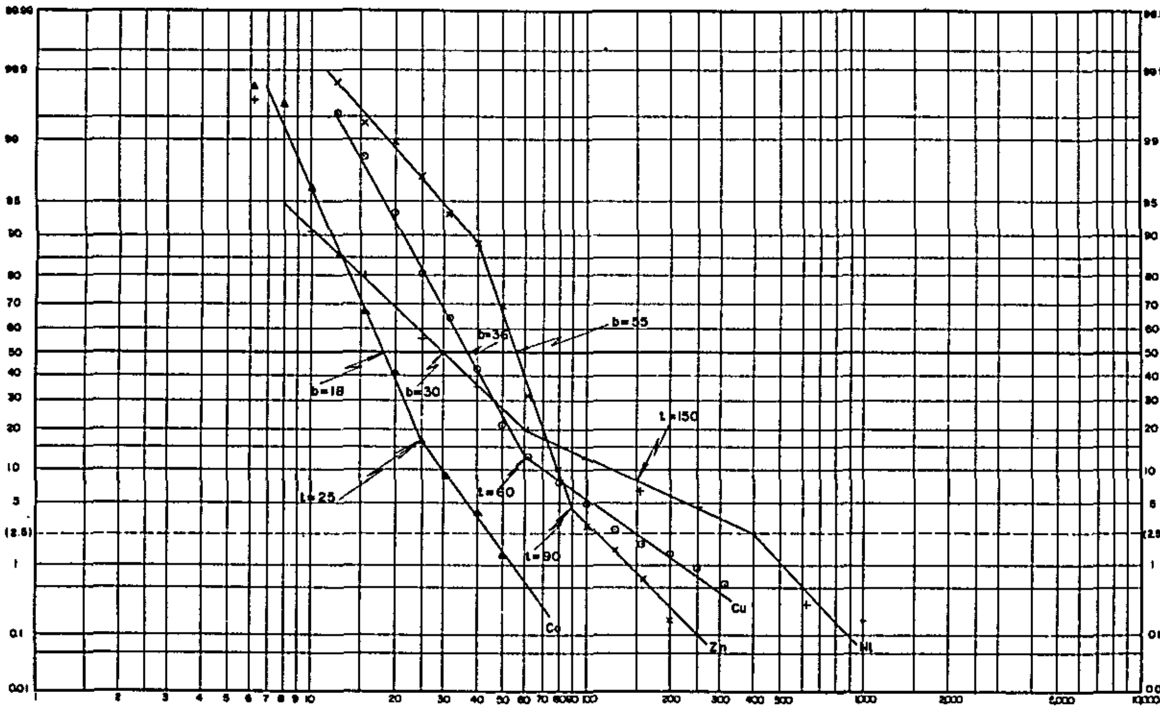

Fig. 1-6 Cumulative frequency distribution of Cu, Zn, Mo and Ag in the Bislig Area

Σ% N = 829 (data on -80-mesh fraction)

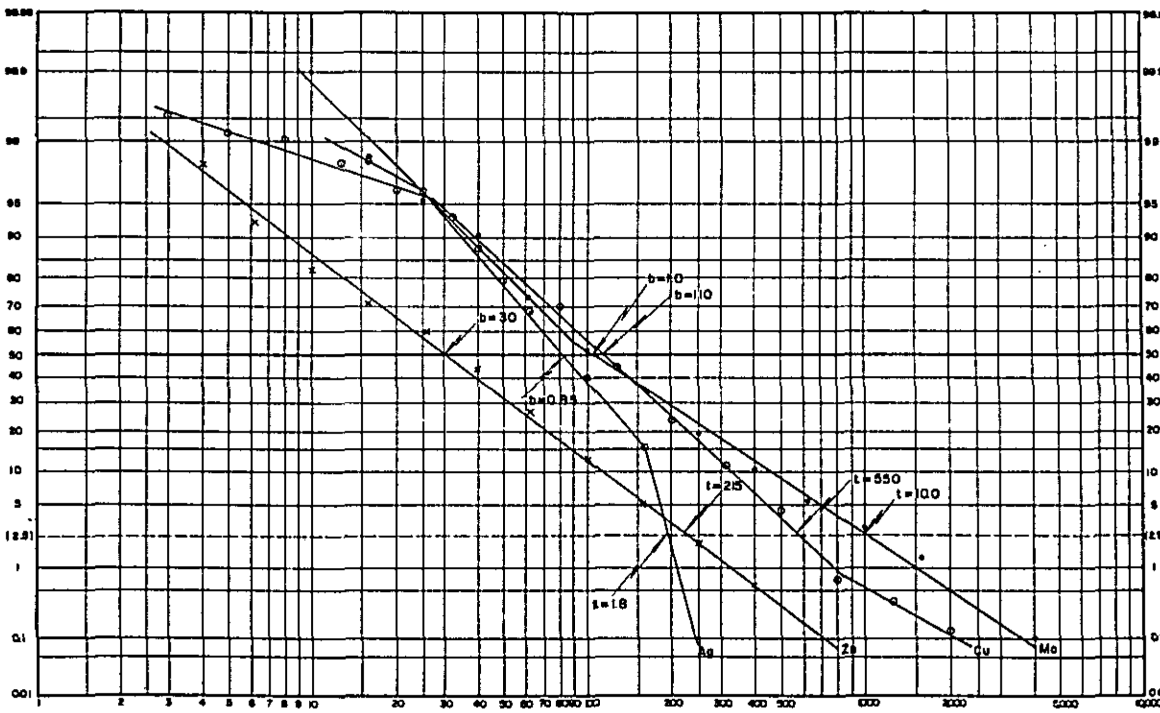

Fig. 1-7 Cumulative frequency distribution of Cu, Zn, Mo and Ag in the Silver belt Mine Area
N = 95 (data on -80-mesh fraction)

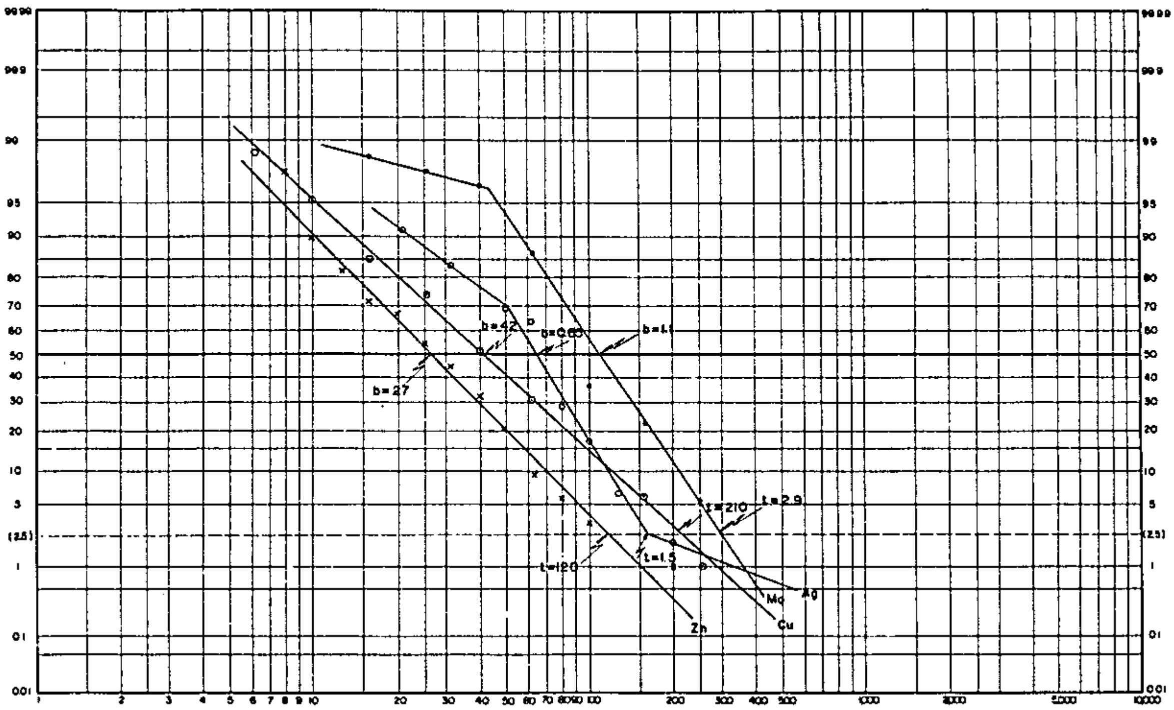

Fig. 1-8 Cumulative frequency distribution of Ag, Pb, Zn and Ba in the Lepanto Mine Area
N = 86 (data on -80-mesh fraction)

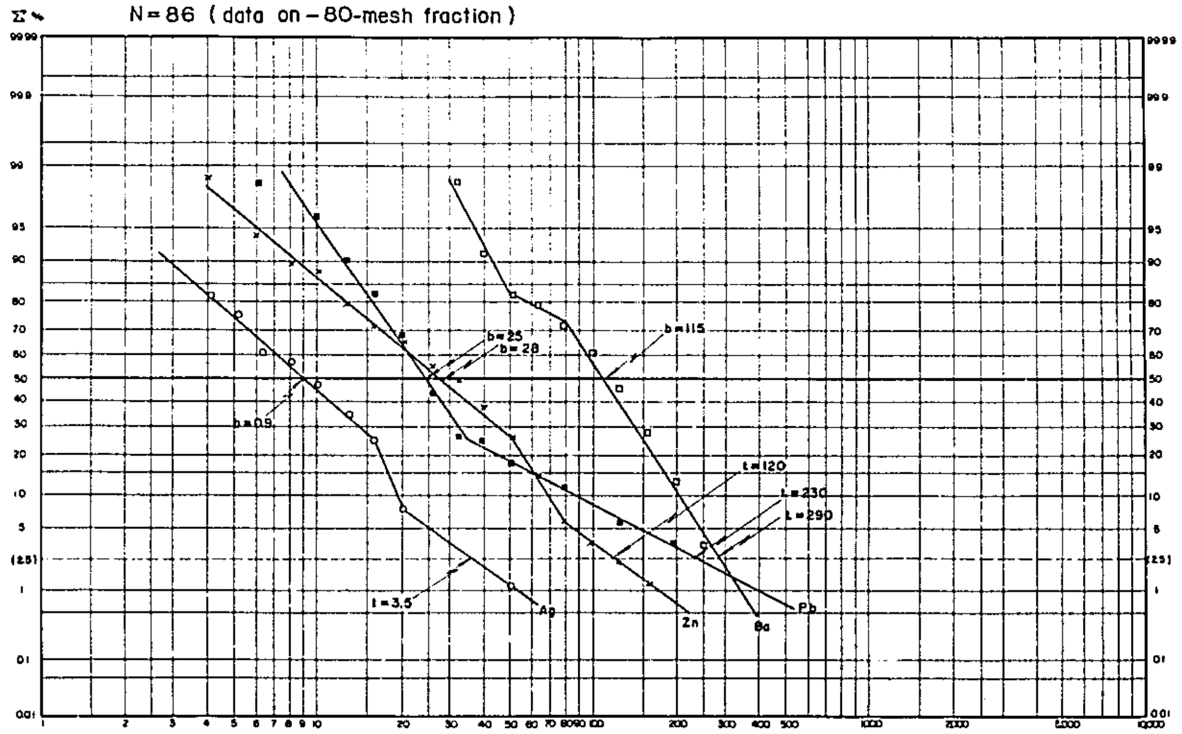

Fig. 1-9 Cumulative frequency distribution of Cu, Zn, Ni and Co in the Tagbiga Area

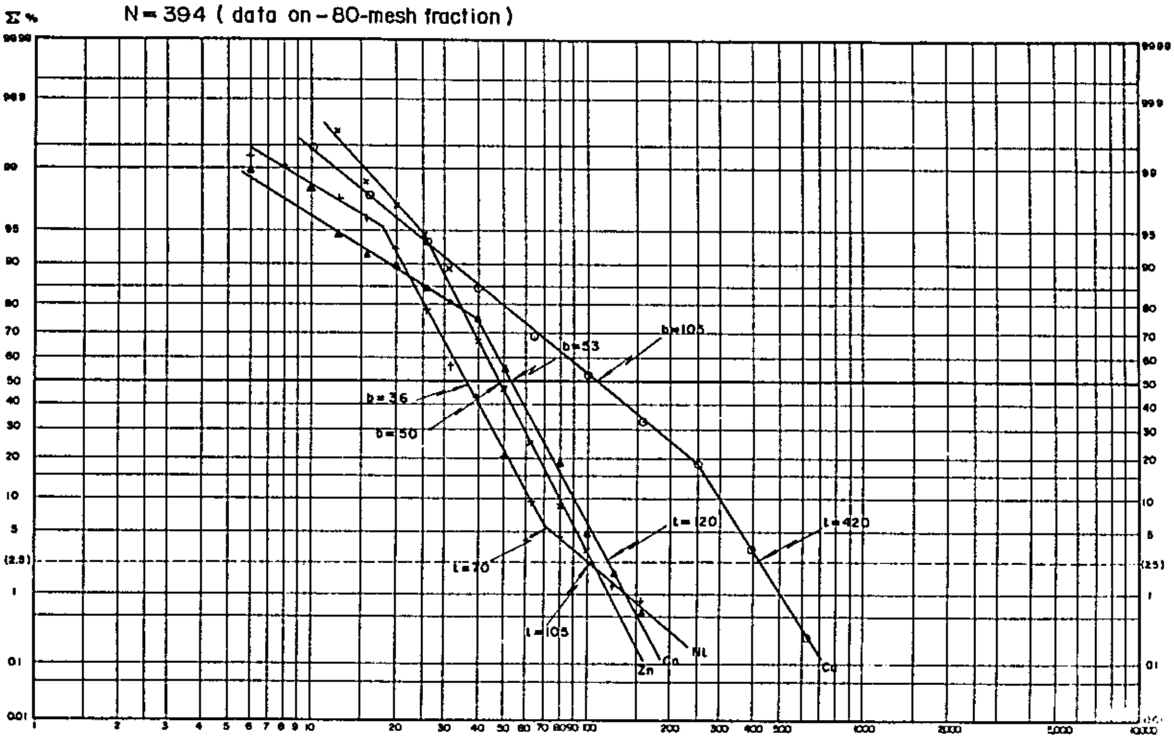

Fig. 2 Correlation diagram

Fig. 2-1 Correlation diagram Zn/Ag, Bislig Area

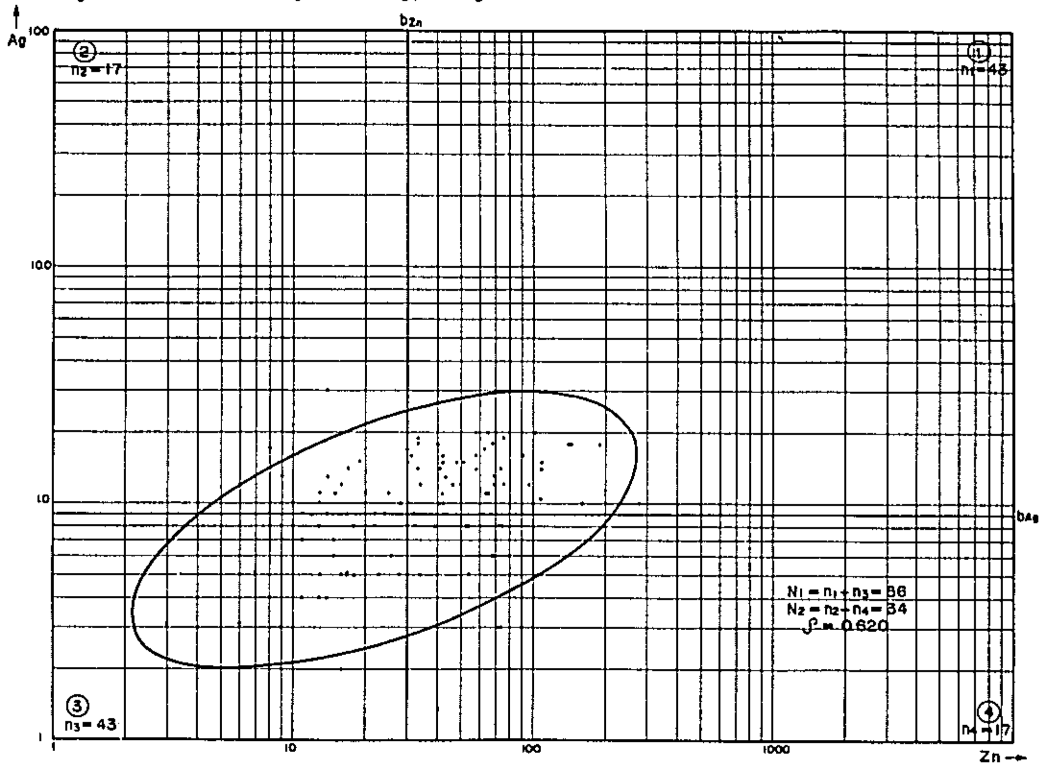

Fig. 2-2 Correlation diagram Mo/Zn, Bislig Area

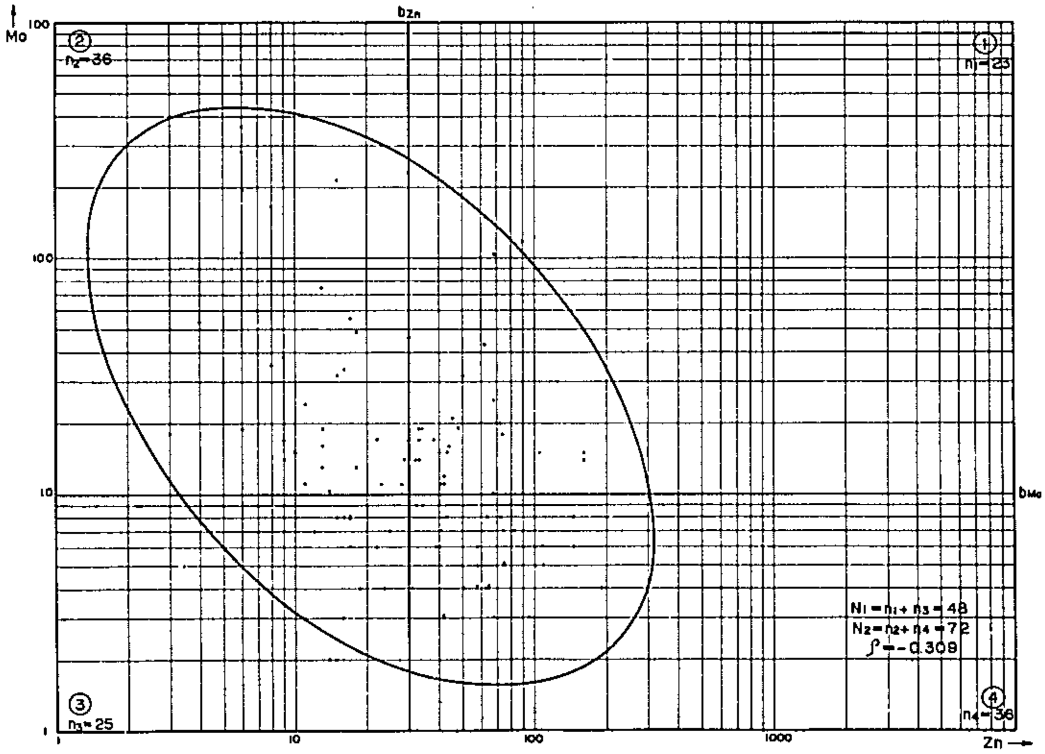

Fig. 2-3 Correlation diagram Co/Cu, Tagbiga Area

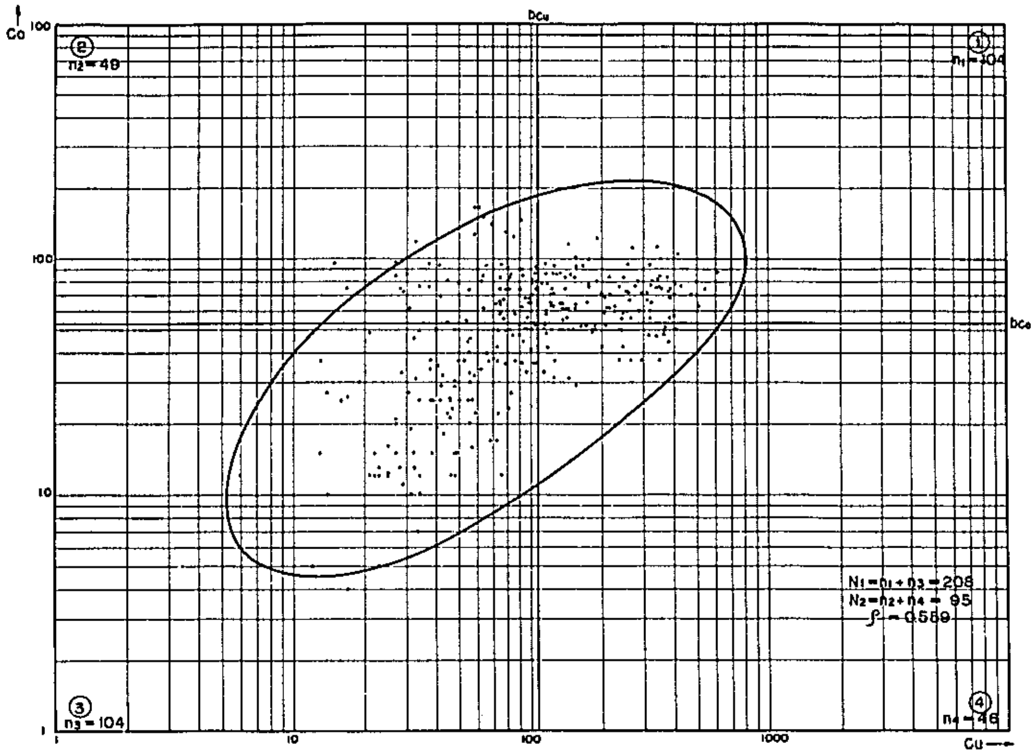

Fig. 2-4 Correlation diagram Ni/Cu, Tagbiga Area